GeoGuide

Peter Kresten
Valentin R. Troll

The Alnö Carbonatite Complex, Central Sweden

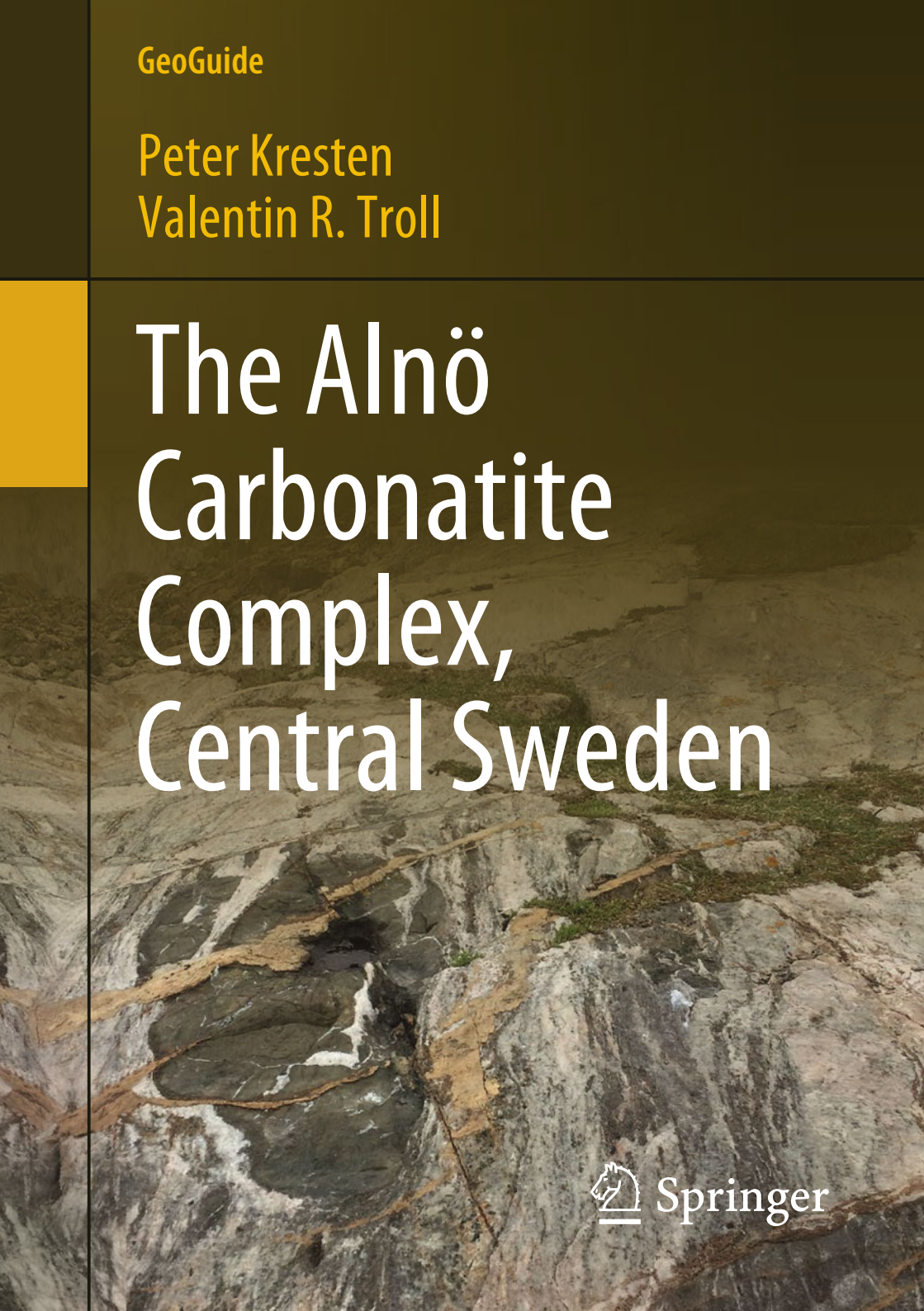

Springer

GeoGuide

The GeoGuide series publishes travel guide type short monographs focussed on areas and regions of geo-morphological and geological importance including Geoparks, National Parks, World Heritage areas and Geosites. Volumes in this series are produced with the focus on public outreach and provide an introduction to the geological and environmental context of the region followed by in depth and colourful descriptions of each Geosite and its significance. Each volume is supplemented with ecological, cultural and logistical tips and information to allow these beautiful and fascinating regions of the world to be fully enjoyed.

More information about this series at http://www.springer.com/series/11638

Peter Kresten · Valentin R. Troll

The Alnö Carbonatite Complex, Central Sweden

Springer

Peter Kresten
Section for Mineralogy, Petrology and Tectonics
Department of Earth Sciences
Uppsala University
Uppsala
Sweden

Valentin R. Troll
Section for Mineralogy, Petrology and Tectonics
Department of Earth Sciences
Uppsala University
Uppsala
Sweden

ISSN 2364-6497 ISSN 2364-6500 (electronic)
GeoGuide
ISBN 978-3-319-90223-4 ISBN 978-3-319-90224-1 (eBook)
https://doi.org/10.1007/978-3-319-90224-1

Library of Congress Control Number: 2018940669

Printed on acid-free paper

This Springer imprint is published by the registered company Springer International Publishing AG part of Springer Nature
The registered company address is: Gewerbestrasse 11, 6330 Cham, Switzerland

Foreword

Carbonatites are by the International Union of Geological Sciences classified as igneous rocks containing more than 50% (modal) of primary (i.e. magmatic) carbonate minerals and less than 20 wt.% SiO_2. Depending on the dominating carbonate mineral(s), the carbonatites can be further subdivided into Ca-rich (calciocarbonatites), Mg-rich (dolomite carbonatites), Fe-rich (ankerite carbonatites) and Na-rich (natrocarbonatites). They occur on all continents on Earth, including Antartica, and range in age from approximately 3 billion years old until the present day (Woolley and Kjarsgard 2008).

Some of the earliest works where a magmatic origin was proposed for carbonatite—alkaline silicate rock associations focused on the Alnön and Fen complexes in the Fennoscandian Shield (Högbom 1895, Brøgger 1921, von Eckermann 1948). Although many early researchers strongly suspected a magmatic origin of carbonatites it was not until in the 1960s that conclusive proof came in the form of experimental petrology (Wyllie and Tuttle 1960), and short thereafter also by eyewitness accounts of eruptions of natrocarbonatitic magma at the Oldoinyo Lengai volcano in northern Tanzania (Dawson 1962). Ample work has since been carried out characterizing the field relationships, petrology, mineralogy and isotope compositions of carbonatites. From field relations, it is clear that carbonatites often occur in close spatial association with various types of silica-undersaturated silicate magmas (e.g. nephelinites, phonolites, melilitites, melilitolites, syenties, lamprophyres and kimberlites). This association implies that there is a petrogenetic link between the carbonatites and the silica-undersaturated alkaline magmas. However, the exact nature of this link is still a matter of intense debate with the prevailing hypotheses involving separation of carbonatites from carbonated silicate parental magmas by liquid immiscibility and/or fractional crystallization, or by a low degree partial melting of carbonated mantle source. Although carbonatites were early on considered as being rare, and rather anomalous rocks, the recent scientific interest has resulted in more than 500 confirmed occurrences worldwide

(Wolley and Kjarsgaard 2008) a today carbonatites and their associated alkaline silicate rocks are one of the main sources of the economically important Rare Earth Elements. In addition to this, the broad spatial and temporal distribution of carbonatites makes them a prime source of information on various petrogenetic processes operating on a global scale, as well as the evolution of the Earth's mantle from the Archaean to the present.

The only currently active carbonatite volcano, Oldoinyo Lengai (Fig. 1a) in the East African Rift System of northern Tanzania, stands out from the other carbonatite occurrences in the world because of its unusually alkali-rich magma compositions (with up to 40 wt.% $Na_2O + K_2O$). The volcano has been active for at least 800,000 years (Sherrod et al. 2013), but carbonatites seem to be a relatively recent feature in the evolution of the volcano (i.e. restricted to the last 10,000 years; Klaudius and Keller 2006). The first unwitting eyewitness observation of natrocarbonatite lava was made by Uhlig (1905). However, as the existence of

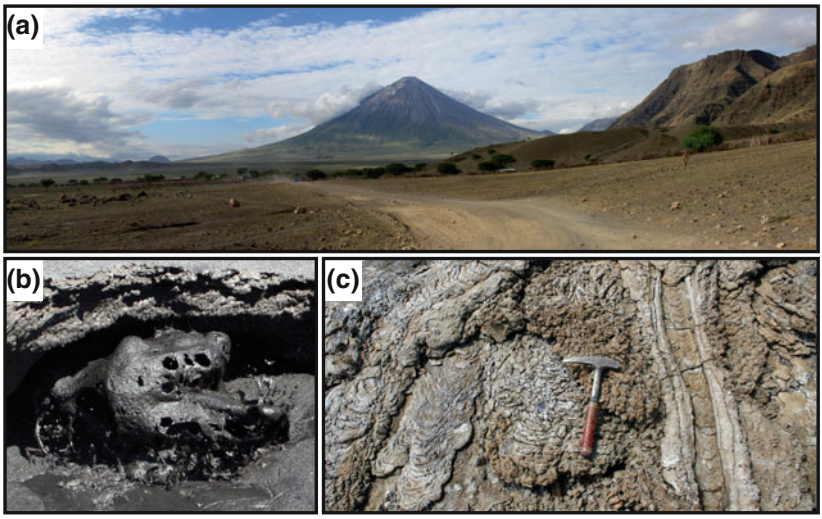

Fig. 1 **a** View of the Oldoinyo Lengai stratovolcano from the north. The volcano is rising 2000 m above its surroundings in the East African Rift in northern Tanzania. The small hills on the left side of the image are monogenetic volcanic vents formed by melilititic–nephelinitic magmas. On the right, the main fault escarpment of the East African Rift is visible. **b** Degassing (boiling) of an active natrocarbonatitic lava lake inside the summit crater. The height of the churning lava is approximately 0.4 m. **c** A few weeks old, slightly altered, natrocarbonatitic lava flows on the upper flanks of the volcano. *Photography* Hannes B. Mattsson

natrocarbonatites was not known at that time, Uhlig described them as "*mud flows*", which were "*covered with efflorescences of a white sodium salt*", and it was not until nearly sixty years later that Barry Dawson recognized them to be of magmatic origin (Dawson 1962). Although famed for its recent carbonatite magmas, they only represent >5% of the volume, and the bulk of the volcanic edifice is composed of different varieties of nephelinitic and phonolitic silicate lavas and pyroclastics (Klaudius and Keller 2006). Seen over the last century, the volcanic activity of Oldoinyo Lengai has been dominated by mildly explosive to effusive eruptions emplacing small-volume natrocarbonatitic lava flows inside the summit crater, eventually causing overflowing from the crater, leaving white streaks on the upper slopes of the volcano (Fig 1a). A characteristic feature of the natrocarbonatites is that they are unstable and rapidly alter in contact with water in the atmosphere to form an array of secondary carbonate minerals (Zaitsev and Keller 2006). Within days of emplacement, the originally pitch black lava (Fig. 1b) is transformed into a white crumbly texture (Fig. 1c). The seasonal rainfall events rapidly remove soluble mineral phases from the natrocarbonatites (Bosshard-Stadlin et al. 2017), and the composition of the remaining rock shifts to be similar to calciocarbonatites (Keller and Zaitsev 2006). Based on this chemical transformation, it has been suggested that alteration of natrocarbonatites ultimately leads to calciocarbonatites, and that most of the calciocarbonatite occurrences in the world may be the remnants of alkaline carbonatites similar to those erupted at Oldoinyo Lengai. In the last 100 years, the "normal" effusive carbonatite activity has been truncated by at least four vigorous explosive eruptions of peralkaline silicate magma (i.e. combeite–wollastonite-bearing nephelinites). This further substantiates the intimate association between carbonatite magmas and alkaline silicate rocks.

For nearly 60 years, following on from the first experimental evidence for a magmatic origin of carbonatites, the general consensus was that the natrocarbonatites produced at Oldoinyo Lengai and the volumetrically much more abundant calciocarbonatites could not be related by fractional crystallization, and that their sources must be different. However, recent results from experimental petrology show that many carbonatite magmas have evolved from a common, moderately alkali-rich, parental magma (Weidendorfer et al. 2017). The chemical variability recorded in carbonatites today is thus largely dependent on the amount of fractional crystallization affecting the magmas in crustal reservoirs and the degree of post-emplacement alteration.

In this respect, the late Proterozoic Alnö igneous complex in central Sweden is one of the most classical localities in carbonatite research, and it holds a wide range of associated silicate rocks (e.g. nephelinites, nephelinesyenites, melilitites and

alnöites). Although the carbonatites at Alnö are Ca-rich, the similarity of the rocks to those found at the currently active Oldoinyo Lengai volcano in Tanzania is striking. A significant difference between the two is that more than 500 million years of post-emplacement uplift and erosion has exposed the deeper levels of the magmatic plumbing system at Alnö. Many of the glacially polished outcrops that can be found along Alnö's northern coastline offer a rare snapshot into the inner workings of the subvolcanic magmatic system of a carbonatite volcano. Combining information retrieved from the active Oldoinyo Lengai volcano with detailed studies of processes occurring at deeper levels of the magma systems (as exposed at Alnö) is the key to unlock the secrets of carbonatite-alkaline silicate magmatic complexes. The present geological field guide offers a comprehensive and up-to-date compilation of the current state of research on the Alnö carbonatite and alkaline igneous complex since the very first descriptions by Högbom in 1895. In the first part of the book, the authors highlight the main characteristics of the different rock types that can be found at Alnö. Relevant scientific publications in the field combined with informative schematic illustrations to explain the emplacement of the different types of magmas. The second part covers the mineralogy of the silicate and carbonatite rocks. It includes in-depth descriptions of how, and where, the most commonly found mineral phases occur within the Alnö complex. A long list of relatively rare minerals can be found here, which are of great interest for the potential mineral collector. The third part is devoted to the geochemistry and economic relevance of alkaline–carbonatite complexes, with special emphasis on Rare Earth Elements and the Alnö rock suite. The section compiles both published and unpublished major and traces element data together with stable and radiogenic isotope data, which are helpful in order to unravel the genetic relationships between the different types of magmas and potential alteration processes. This is followed up by detailed itinerary with carefully suggested excursion stops which focus on the key localities/outcrops on the island. As a whole, the field guide is written in a concise and comprehensible format; it contains up-to-date maps, beautiful high-quality photographs and key geological references on the Alnö igneous complex. It is suitable for both the professional geologist, as well as the interested geotourist visiting the area. This book therefore succeeds in its aim to provide a comprehensive overview of the Alnö igneous complex and its multitude of rock types and minerals, and as such it will undoubtedly serve for quite some time as the main "go-to-book" for this iconic carbonatite locality.

Uppsala, Sweden

Hannes B. Mattsson
Department of Earth Sciences
Uppsala University

References

Bosshard-Stadlin SA, Mattsson HB, Stewart C, Reusser E (2017) Leaching of lava and tephra from the Oldoinyo Lengai volcano (Tanzania): remobilization of fluorine and other potentially toxic elements into surface waters of the Gregory Rift. J Volcanol Geotherm Res 332:14–25

Brøgger WC (1921) Die Eruptivgesteine des Kristianiagebietes. IV. Das Fengebiet in Telemark, Norwegen. Videnskapsselsk. Skr.I, Mat.naturv.Kl. 1920, No. 9

Dawson JB (1962) Sodium carbonate lavas from Oldoinyo Lengai, Tanganyika.—Nature 195: 1075–1076

Högbom AG (1895) Über das Nephelinsyenitgebiet auf der Insel Alnö. Geologiska Föreningen i Stockholm Förhandlingar. 17:100–160, 214–256

Holohan EP, Troll VR, van Wyk de Vries B, Walsh JJ, Walter TR (2008) Unzipping long valley: an explanation for vent migration patterns during an elliptical ring fracture eruption. Geology 36:323–326

Keller J, Zaitzev AN (2006) Calciocarbonatite dykes at Oldoinyo Lengai, Tanzania: the fate of natrocarbonatite. Can Mineral 44, 857–876

Klaudius J, Keller J (2006) Peralkaline silicate lavas at Oldoinyo Lengai, Tanzania. Lithos 91: 173–190

Sherrod DR, Magigita MM, Kwelwa S (2013) Geologic map of Oldonyo Lengai (Oldoinyo Lengai) and surroundings, Arusha Region, United Republic of Tanzania. U.S. Geol Surv Open File Report 2013–1306, 65 p

Uhlig C (1905) Bericht über die Expedition der Otto Winter-Stiftung nach den Umgebungen des Meru. Z. Ges. Erdkunde 1905, 120–123

von Eckermann H (1948) The alkaline district of Alnö Island. Sver Geol Unders Ca 36:176

Weidendorfer D, Schmidt MW, Mattsson HB (2017) A common origin of carbonatite magmas. Geology 45, 507–510

Woolley AR, Kjarsgaard BA (2008) Carbonatite occurrences of the world: map and database. Geol Surv Can, Open File 5796

Wyllie PJ, Tuttle OF (1960) The system CaO–CO2–H2O and the origin of carbonatites. J Petrol 1:1–46

Zaitsev AN, Keller J (2006) Mineralogical and chemical transformation of Oldoinyo Lengai natrocarbonatites, Tanzania. Lithos 91:191–207

Acknowledgements

We are grateful to a large number of individuals that helped shape our views on Alnö's geology and on carbonatite magmatism in general. These include, Alasdair Skelton, Barry Dawson, Bjarne Almqvist, Chris Harris, Georg Troll, Hannes Mattsson, Harry von Eckermann, Jörg Keller, Tom Andersen, Kent Brooks, Barry Dawson, William Griffin, Knut Heier, Brian Robins, Thomas Lundqvist, Barbara Scott-Smith, Herman Zeissink, Magnus Andersson, Volker Lorenz, Alireza Mahlemir, Lutz Kübler, Stefan Kurszlaukis, Acke Rahman, Brian Upton and Henry Emeleus. Special thanks go to Tom Andersen for providing Sr and Nd data and associated discussion and to Christer Wiklund for access to his mineral collection from Alnö and to Sture Österlund for kind help. Länsstyrelsen i Västernorrland (the Västernorrland County administration), in particular John Granbo, has provided boat transport as well as valuable photographs, and we are greatly indebted to him also. Students that worked on Alnö for their undergraduate theses and who contributed material to this publication are Tobias Mattsson and Sherissa Roopnarain and both are thanked warmly for their efforts, scientific advances and contributions to this book on Alnö. Peter Kresten is especially indebted to Jonas Brundin, Ivar Esping, Sven Jonasson, Viorica Morogan, Ingemar Olsson and Folke Wikberg for help during fieldwork. Konstantinos Thomaidis is particularly thanked for his tireless effort and help with preparation of the manuscript for this book and so is Sophie Omidian, who helped with preparing the isotope section. We furthermore thank the Swedish Geological Survey (SGU), the Swedish Mineralogical Society (SMS), and Vetenskapsrådet Sweden (VR) for logistical and financial support of our work. Further, Peter Kresten acknowledges a post-doctoral fellowship by the Norwegian Council for Technical and Scientific Research (NTNF) 1978–1979 at Mineralogisk-Geologisk Museum, Oslo, enabling him to compare

Alnö with the Fen Complex. Subsequently, he organized the “Nordic Carbonatite Symposium”, at Alnö in 1979, supported by a generous grant from Nordic Culture Fund. A special issue of Lithos (Vol. 13, Nr. 2, 1980) contains the proceedings of that symposium.

Contents

About the Authors

Dr. Peter Kresten (born 1945) started off as Precambrian bedrock geologist (Ph.D. 1970, D.Sc. and appointed Assoc. Prof. 1974; Stockholm University). His interest in "unusual rocks" arose after having served as geologist in the United Nations Development Programme (UNDP), where he joined the kimberlite exploration programme in Lesotho in 1972–73. Back in Scandinavia, he began mapping the Alnö Complex in 1974, with support from the Swedish Natural Science Research Council (NFR). Joining the Swedish Geological Survey (SGU) in 1977 as Senior State Geologist, he continued his studies on Alnö as part of the mapping of Västernorrland County. A post-doctorate fellowship to Kresten in 1978–79 by the Norwegian Council for Technical and Scientific Research (NTNF) on the "Petrology of carbonatites and associated rocks" made field work at the Fen Complex possible. The fellowship also supported an extensive electron microprobe investigation and neutron activation analyses of materials from Alnö, Fen, Kalix and Sokli and investigation of reference materials from kimberlites in Finland, southern Africa and India. Parts of these efforts were presented at the Nordic Carbonatite Symposium in 1979, which Kresten co-organized. In the final years before retirement, he was employed as geochemist by the Swedish Central Board of National Antiquities (RAÄ), trying to apply geological knowledge to solve archaeological questions, focusing especially on the so-called vitrified hill forts in Sweden and other parts of Europe. Since 2017, Kresten is a Visiting Professor at Uppsala University where he continues to engage in research on Alnö and the mysteries of vitrified hill forts.

Prof. Valentin R. Troll (born 1971) is an igneous petrologist and volcanologist and is a Chair Professor in the Department of Earth Sciences, Uppsala University, Sweden (since 2008). He is also an Honorary Research Associate at the "Istituto Nazionale di Geofisica e Vulcanologia" (INGV), Rome, Italy, and at the University of Las Palmas, de Gran Canaria, Spain. Prior to his current employment at Uppsala, he served as a Lecturer at Trinity College Dublin, Ireland, for seven years. At Uppsala, he directs the National Microprobe Facility and leads the GPV research group. He supervised 19 Ph.D. students to completion and is an elected Fellow at the Mineralogical Society of UK and Ireland since 2008. He received his Ph.D. from GEOMAR Research Center at the University of Kiel, Germany, in 2001 and his BSc from St. Andrews University, UK, in 1998. He has worked on volcanic phenomena and geochemical processes of alkaline and subalkaline rocks the Canary Islands, the North Atlantic Igneous Province and the Sunda Arc with a focus on magmatic crystals and the information they retain. He was elected the Fellow of Trinity College Dublin in 2009 for "higher academic achievements" and has been presented with the VMSG Award by the Volcanic and Magmatic Studies Group of the Geological Society of London, UK, in 2011 for "significant contributions to our understanding of magmatic processes". Most recently, he has been invited to take up an Honorary Research Associate Position at Padjadjaran University (UNPAD) in Bandung, Indonesia.

List of Figures

List of Tables

An Introduction to Carbonatites and Carbonatite Complexes

1

Abstract

The Alnö igneous complex intruded local migmatites and granite country-rocks of Svecofennian age at ~580 Ma and produced a suite of early alkaline silicate intrusives (e.g., ijolites, nepheline syenites) and dykes (e.g., trachytes, phonolites) and later a suite of carbonatite sheet intrusions for which Alnö is widely known. The Alnö igneous complex displays an older and deformed northern ring complex and the main "southern" ring complex. An explosive carbonatite vent with melilitite lapilli is apparently a late event, as are kimberlitic alnöite dykes. The latter seem not to be diamantiferous.

Carbonatites are rare carbonate-rich magmatic rocks that are usually associated with alkaline silica-undersaturated intrusions. Although they make up a very small portion of the crust's volume, they occur in all continents and from Archaean to the present and are of great relevance for our understanding of crustal and mantle processes. The Alnö complex is one of only several tens of known alkaline and carbonatite ring-intrusions in the world (see Appendix 1) and is the type-locality for the rock type alnöite ("porphyritic trap" of Hisinger 1808; "melilite-basalt" of Törnebohm 1883; and "alnöite" Rosenbusch 1887). The Alnö intrusion was emplaced at 584 ± 7 Ma (Meert et al. 2007) into Palaeoproterozoic country-rock and comprises plutonic and alkaline dyke rocks, carbonatites, and ultramafic lamprophyres. In addition, a carbonatite vent-breccia with accretionary lapilli provides evidence for explosive volcanic activity (von Eckermann 1960b; Kresten 1990). Alnö's deeper plumbing system, and that of most other carbonatite ring-complexes, remains poorly constrained, however, leaving us with considerable uncertainties as to how exactly the plutonic and the volcanic environments in carbonatite centres are connected (see e.g. Andersson et al. 2013).

P. Kresten and V. R. Troll, *The Alnö Carbonatite Complex, Central Sweden*, GeoGuide, https://doi.org/10.1007/978-3-319-90224-1_1

Discussions on the genesis, origin and emplacement of carbonatite have been ongoing for many decades (e.g. von Eckermann 1948, 1960a, 1960b; Le Bas 1977; Kresten 1980, 1990; Treiman and Essene 1985; Gittins 1988; Phipps 1988; Wallace and Green 1988; Keller and Hoefs 1995; Vuorinen and Skelton 2004; Mitchell 2005; Fischer et al. 2009; Rukhlov and Bell 2010). Carbonatites frequently occur in ring-complexes, and have been related to stable cratonic regions, orogenies, rifting and extension within continental margins, and to mantle plumes (Le Bas 1977; Gittins 1988; Phipps 1988; Wallace and Green 1988; Meert et al. 2007; Fischer et al. 2009; Rukhlov and Bell 2010). They have been found in all continents with the Kaiserstuhl volcanic complex in the Rhine graben (Le Bas 1977; Keller 1989) and the Oldoinyo Lengai volcano in the East African Rift Valley (Fischer et al. 2009; Mattsson et al. 2014) being the youngest examples. The latter is the only known active carbonatite volcano, albeit of unique composition (Dawson 1962; Rukhlov and Bell 2010). As most carbonatites are known from plutonic complexes and only a few volcanic examples are available, there is a significant gap in our understanding of the plutonic-eruptive association for this unusual group of rocks as plutonic and eruptive episodes are rarely preserved side by side (Gernon et al. 2012). The plutonic and volcanic occurrence of carbonatites at Alnö (von Eckermann 1948; Kresten 1990) thus provides an opportunity to further our understanding of magma storage and transport in carbonatite ring centres.

Indeed, the discoveries of carbonatite occurrences around the world have gone from 56 to around 530 between 1987 and today, and 49 of them are considered extrusive. They extend back to the Archean and the oldest carbonatites that have been found to date are more than 2000 million years old and are located in South Africa and Finland. About 40 of the extrusive carbonatite occurrences are dominated by calcite, 7 by dolomite and the remaining two are known to be of alkaline natrocarbonatite composition (Mitchell 2005; Jones et al. 2013). Moreover, the number of occurrences of carbonatites has increased with decreasing age, which indicates that carbonate formation has probably become more common with time and that the conditions for carbonatite formation become more widespread (Jones et al. 2013). However, critics of this scheme argue that preservation of old carbonatites may not be too likely, thus implying a possibly continuous amount of carbonatite occurrences through geological time.

The mantle plume model is a popular model but recent discoveries of strong repeated lithospheric controls over the course of carbonatite ages have been made. Newer discoveries of carbonatite-silicate volcanism from the Neogene to the Quaternary, comprising occurrences in France, Spain and Italy allow researchers to further our knowledge about extrusive carbonatite volcanism and its mantle origins

(Jones et al. 2013), although some of these newest localities are heavily contested by some researchers. We note, however, that several relatively young oceanic island basalts show association with carbonatites (e.g. on Fuerteventura in the Canary Islands) and that carbonatite from the volcano Oldoinyo Lengai, and the rest of the East African also appear to link up to a lithospheric or deeper mantle origin and thus mantle-derived carbonatite volcanism seems often to connect to a mantle plume in one way or another (Nelson et al. 1988; Jones et al. 2013).

1.1 The Alnö Nature Reserve

In the years between 1910 and 1970, Sweden formally demarcated a series of nature reserves according to Swedish jurisdiction and available international environmental treaties of that time (Dahlström et al. 2006), which was a trend that was initiated by nature activists like John Muir in the USA in the last decades of the 19th century. Like the US counterparts, the Swedish nature reserves were to be collectively managed, and balanced against the economic and social goals of the surrounding farms, towns or cities (Dasmann 1972; Shafer 1990). A large part of the territory that constitutes Alnö Island, became a fully authorized nature reserve already in the 1940's (Swedish Heritage Archives 2012). Since then, the timber trade, as well as agricultural and fishing livelihoods on the island have all been cultivated within and around this nature reserve and are considered to be part of what symbolises "rural" Sweden (Fig. 1.1). The concept of a nature reserve does therefore not denote "free of humans", but rather it symbolises a 'Hegelian' ethic towards nature, where the human footprint is comparatively small. The nature reserve status is thus not originally connected to Alnö's geology, but geological aspects were later added to the reserve program and certain sites were selected on the island were protection of flora, fauna and geology have now been made a special priority.

Indeed, the timber trade and agricultural and fishing livelihoods still provide much needed employment on Alnö and in the region and brought considerable capital to the island and surrounding districts in the early to late 1800's and into the early 1900's (Fig. 1.2). Then unemployment in the region became remarkably high (Swedish Heritage Archives 2012). A number of sawmills on Alnö itself existed, but have all been dismounted (Fig. 1.3) and presently, employment from tourism plays a strong role on Alnö (Swedish Heritage Archives 2012). This is in part a function of the status as a Nature reserve, providing a sense of rural landscape to tourists, thus boosting the local livelihoods. Although Alnö is separate from the

Fig. 1.1 **a**, **b** Farmhouse with barn and horse meadow, Northern Alnö. Traditional red timber houses at Alnö "hembygdsförbund", next to Alnö kyrka

Fig. 1.2 **a** Timber is one of the biggest economic resources in the region, leading to economic bloom in the 19th century. **b** The Hotel Knaust in Sundsvall is a witness of that time. It is said that the "rich timber barons" were riding up this staircase on horseback after their annual economic meeting (and prior to indulging in a visit to the local casino in Sundsvall)

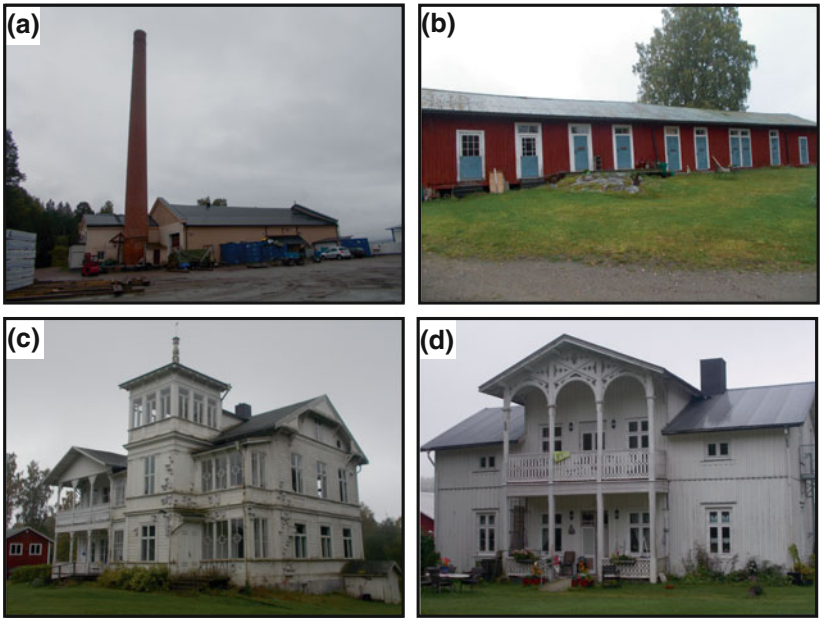

Fig. 1.3 **a** Remnant chimney of an old sawmill on the SW coast of Alnö Island. **b** Eriksdal sawmill ("sågverk") utility buildings and **c** and **d** Eriksdal sawmill office and living houses of the former owners, reflecting the at times extremely successful timber trade of past days

main land, and was up to the 1960s only accessible by ferry (Fig. 1.4), a bridge is now in place that allows quick and easy access, but also brings a rapid influx of commercial trends to Alnö. Repeated commercial interest such as barite, iron, or carbonatite mining in the northern and central parts of the Alnö Complex is at odds with this concept of a rural and traditional use of Alnö's landscape and this aspect is discussed in more detail in the chapter on Geochemistry below.

1.2 The History of Research in the Alnö Area

The Alnö Complex has been the object of geological research since the early 19th century, when the first description of alnöite was published. "Alnöite" was probably first mentioned by Hisinger (1808) in his mineralogical geography (Fig. 1.5). There, Hisinger (from Uppsala University) records a "porphyritic trapp" (dolerite)

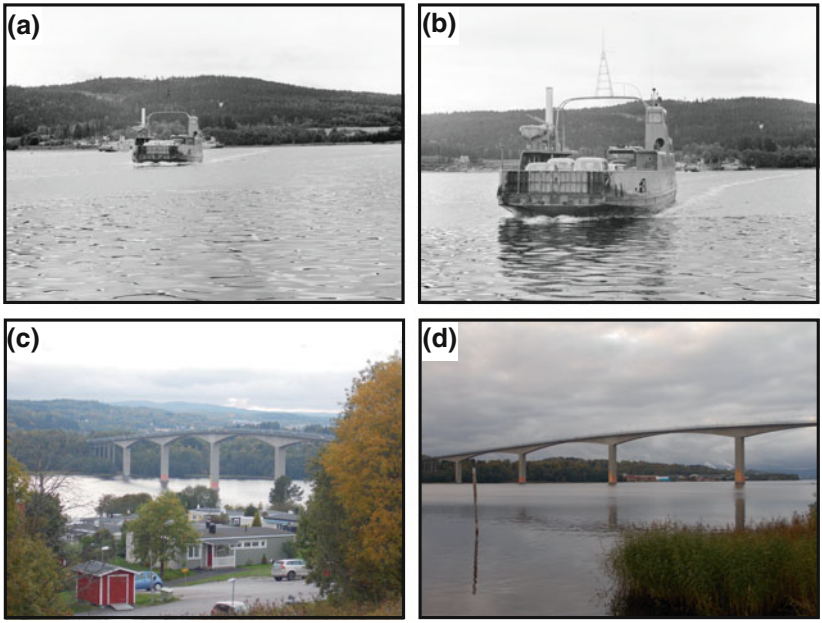

Fig. 1.4 **a**, **b** The Alnö ferry in 1962 (courtesy of Länsstyrelse Västernorrland). **c** and **d** the new Alnö bridge viewed from Alnö. The bridge was erected in 1964. When the bridge was opened, it was the longest bridge in Sweden

with large crystals of dark mica that he found on Alnö, which likely is the present day "alnöite". The unusual geology of the Alnö area was then rediscovered by Lieutenant Hoppe in 1881 (von Eckermann 1948) of the Swedish Geological Survey (SGU). He described a melilite-bearing dyke rock, a detailed description of which was published by Törnebohm (1883), documenting it as melilite-basalt. The term "alnöite" was fully introduced into the catalogue of rock names by Rosenbusch in 1887 as part of a much large nomenclature scheme to explain the systematics of igneous rocks globally (Fig. 1.5). On initiative by Rosenbusch, Berwerth (1893) carried out a very detailed petrographic analysis of alnöite on Törnebohm's samples from the two type localities (Stornäset, Kåtan), including a partial analysis of pyroxene.

Around that time, in 1889, Högbom began a detailed study of the alkaline rocks at Alnö, and later published the monograph: "*Über das Nephelinsyenit-gebiet auf*

Fig. 1.5 **a** Hisinger, **b** Törnebohm, **c** Rosenbusch, **d** Högbom, **e** a young von Eckermann and **f** a senior von Eckermann (images from Wikimedia commons)

der Insel Alnö" (Högdom' 1895). Later still, the Alnö ring complex became internationally well-known due to von Eckermann's research, stretching over a period of more than forty years and resulting in 36 publications, the most famous being the "*Alnö Memoir*" of 1948 (*The Alkaline District of Alnö Island*). Von Eckermann's models on the petrogenesis of fenites, alkaline rocks and carbonatites, as well as his scheme for the emplacement of Alnö dykes all have had a considerable impact upon studies of similar intrusions world-wide and his views are still widely influential in carbonatite geology and petrology up to the present day (Fig. 1.5).

The next person that made substantial contributions to our understanding of the geology and mineralogy of the Alnö area, and one of a new generation of scientists

was Peter Kresten from the Geological Survey of Sweden (SGU). His works include the seminal report and geological map on Alnö "*Beskrivning till Berggrundskartan över Västernorrland*" Kresten (1990), and a series of high-profile scientific papers on structure and composition of the Alnö rock-suite. His popular science report "*Alnöområdets Geologi*" Kresten (1984) published by Västernorrland County, and, in particular, another report with the same title published in the year-book for 1984 of the Swedish Tourist Association (STF) have introduced the geology of the Alnö Complex to a very wide audience and cemented Alnö as an geological icon. Subsequent to these efforts, Alnö has created interest amongst a whole string of workers, resulting in significant publication activity over the last two decade, such as Morogan and Woolley (1988), Morogan and Lindblom (1995), Vuorinen et al. (2005), Haslinger et al. (2007), Meert et al. (2007), Skelton et al. (2007), and Andersson et al. (2013). These more recent studies focus on petrogenesis in the Alnö carbonatite complex, fluid-rock interaction at carbonatite-gneiss contacts, major and trace element variations of Alnö rocks, on fenitization associated with the Alnö carbonatite complex, on rock magnetics and, finally, on the seismic structure of the underlying magmatic system. However, the relationship between carbonatite and silicate magmas, the role of fractional crystallisation versus liquid immiscibility, the controls on metal mobility in carbonatitic magmas and fluids, and the primary sources of carbonatite magmas, still remain incompletely understood. Research into these topics is therefore as exciting as it was in the days when carbonatites were first discovered.

1.3 Geological Overview—Alnö and Surroundings

The Alnö intrusion is famous world-wide and is unique within the Swedish bedrock (von Eckermann 1948; Brueckner and Rex 1980; Kresten 1990; Meert et al. 2007). During the Cambrian, carbonate-rich melts (carbonatites), various alkaline rocks and alnöites (dark dyke rocks) intruded from the depths of the Earth. Today, we see the root zone of that volcano, as erosion has removed 500 to maybe 1000 m of overburden and on Alnö we find minerals and rocks that occur nowhere else in Sweden (Figs. 1.6 and 1.7). Indeed, the island of Alnö hosts the ~580 Ma semi-circular Alnö intrusive complex with a radius of 2.5 km in the northernmost part of the island. It is one of ~500 documented alkaline-carbonatite and carbonatite intrusions in the world and it is one of the larger carbonatite ring-complexes of which only several tens are known (Appendix 1). In addition, Alnö represents a rare case of an intrusive-extrusive carbonatite association (von Eckermann 1960a, 1960b; Kresten 1990; Andersson et al. 2013). The main portion

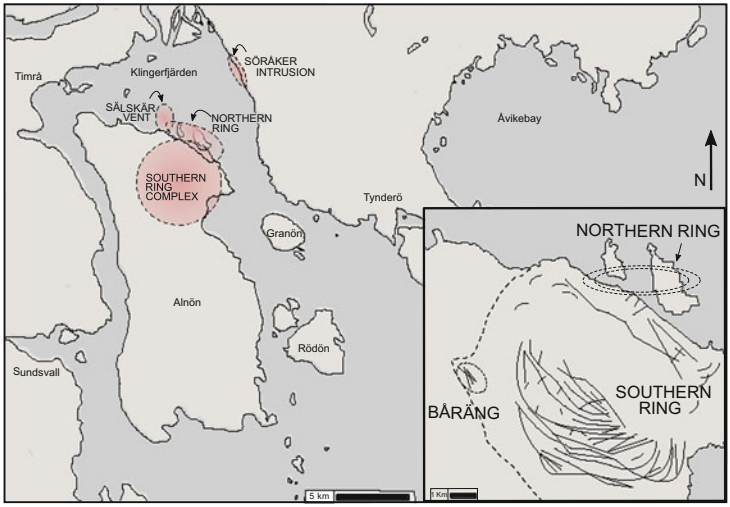

Fig. 1.6 "Alnön" (Alnö Island) and surroundings, with the different parts of the Alnö Igneous Complex marked in pink. Inset shows details of the Complex in the northern parts of Alnö (modified after Kresten 1990)

of the Alnö igneous complex contains a suite of alkaline silicate rocks (ijolite, nepheline-syenite, and pyroxenite) and various sövites and silico-sövites that crop out in a semi-circular pattern (Fig. 1.7) (von Eckermann 1948; Kresten 1980; Le Maitre 2002). Alnöite, an ultramafic lamprophyre, has been named after the island (Rosenbusch 1887). The carbonatites at Alnö occur dominantly as dykes and have been divided into two groups with respect to their size and dip direction (Kresten 1990). The longer and thicker dykes are restricted to the southern part of the intrusion and generally dip outward from the centre (ring-dyke geometry), whereas shorter and thinner dykes dip dominantly inward towards the centre of the complex (cone sheet geometry). A suite of radial dykes is present as well, which from field mapping is thought to be the oldest group of dykes (von Eckermann 1948; Kresten 1980) (Fig. 1.8). Migmatites and gneisses, the country rocks to the magmatic complex (Fig. 1.7), have been locally metasomatised to fenites through fluid-rock interaction in a 500–600 m wide zone (von Eckermann 1948). An overburden of up to 1 km is estimated to have been eroded from the complex since the time of its emplacement (Kresten 1980). The present erosion surface in the Stöde area, about 45 km west of Alnö island, is very close to the sub-Cambrian peneplain (see Fig. 1.7), which gives some perspective on erosion dimensions.

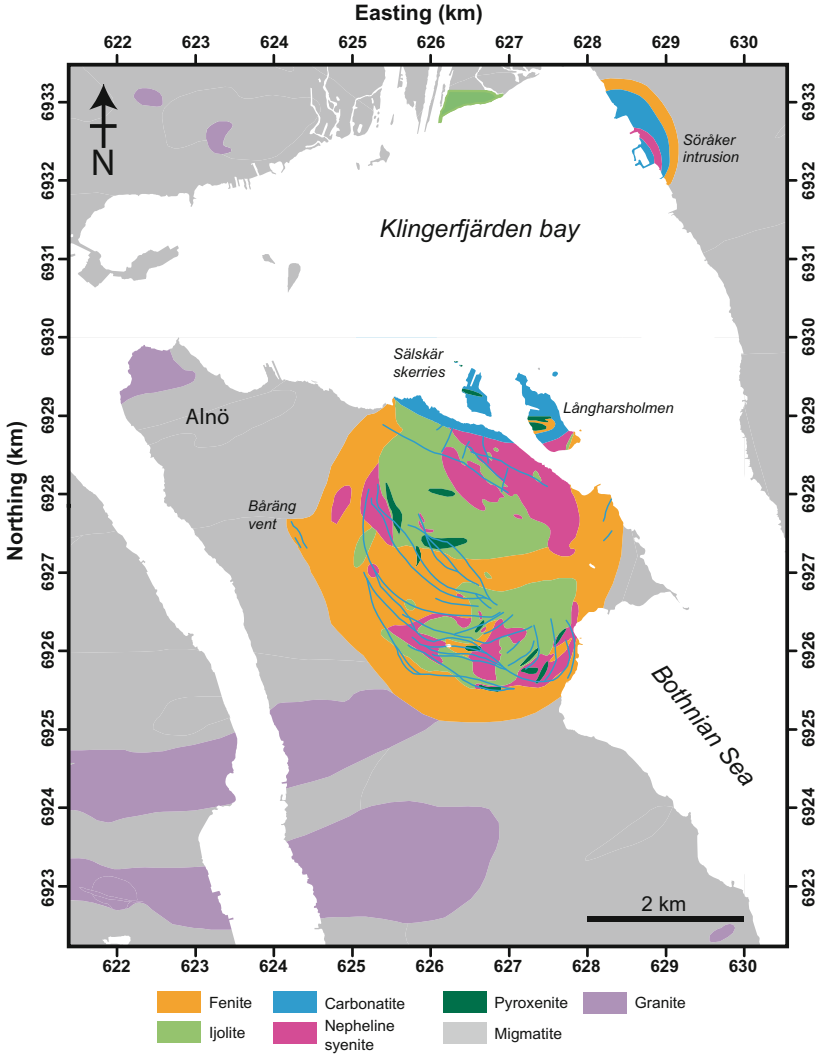

Fig. 1.7 Geological overview map of northern Alnö and surrounding areas (modified after Kresten 1990 and Andersson et al. 2013)

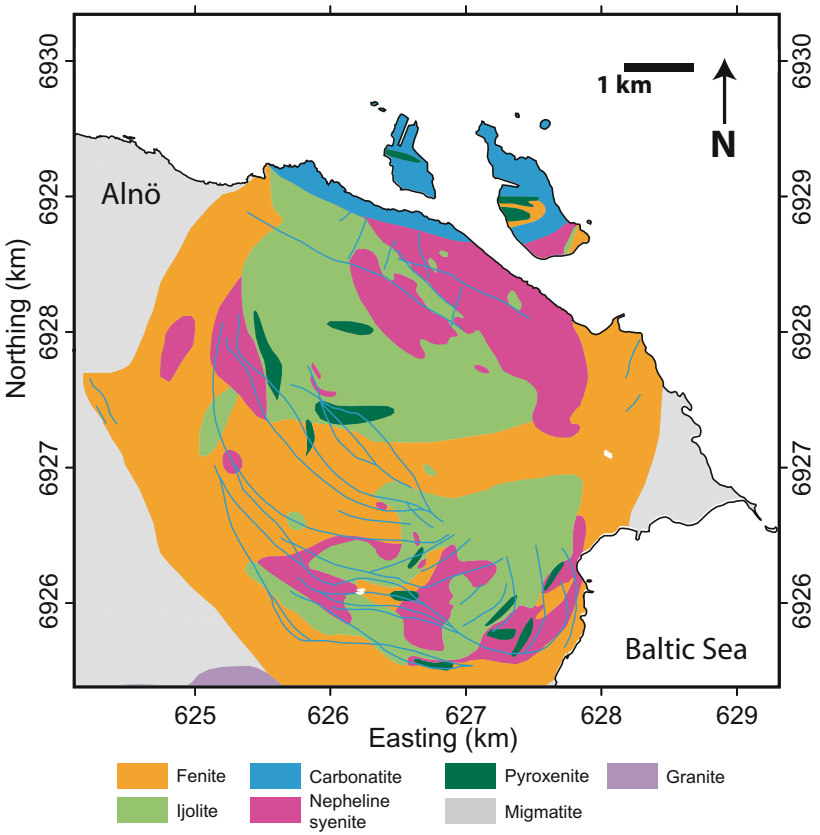

Fig. 1.8 Simplified geological map of northern Alnö (after Kresten 1990 and Andersson et al. 2016)

Evidence of extrusive volcanism in the form of a vent breccia with accretionary melilitite lapilli and fragments of carbonatite in a carbonatite matrix is given by numerous boulders at the Sälskär skerries 700 m north of Alnö Island (Figs. 1.6 and 1.7), documenting an explosive volcanic venting in this region (von Eckermann 1960b; Kresten 1979, 1990). In the 1980s, the diamond potential at Alnö was investigated but without significant results (Kresten and Nairis 1982).

Two scenarios for the emplacement of the Alnö complex and its associated carbonatite dykes are currently available (von Eckermann 1948; Kresten 1980), which we discuss in more details below. Although the complex is relatively poorly exposed, the combination of extensive earlier work and the recent geological and geophysical studies make Alnö one of the best-characterized carbonatite complexes in the world.

1.4 Age of the Alnö Intrusion

The Alnö complex is coeval with the Fen carbonatite complex in southern Norway (583–615 Ma) determined via $^{40}Ar/^{39}Ar$ dating (Meert et al. 1998), although they are some 600 km apart. It has been suggested that they are genetically linked and that a palaeo-rift could also link carbonatites in the Kola Peninsula to Alnö and Fen (Fig. 1.9) (Meert et al. 2007; van Balen and Heeremans 1998; Korja et al. 2001). However, most intrusions in Kola are either younger (380–360 Ma) or older (Palaeoproterozoic) (Rukhlov and Bell 2010; Downes et al. 2005), making it likely that Alnö and Fen belong to a separate event.

In fact, there are a number of alkaline and carbonatite complexes on the Baltic shield and they can be broadly divided into four age groups after when they formed (Doig 1970; Vartiainen and Woolley 1974; Kresten et al. 1977; Roberts et al. 2010). These are (a = alkaline, c = carbonatite, l = lamprophyre):

1. Sveco-Karelian 2500–1850 Ma: Siilinjärvi (c), Laivajoki (c) and Kortejärvi (c) in Finland.
2. Fennoscandian 1580–1560 Ma: Norra Kärr and Almunge (both a) in Sweden.
3. Sveconorwegian 1142 Ma: Kalix (cl) in Sweden.
4. Cambrian to Hercynian ca. 540–240 Ma: Särna (ac) and Alnö (acl) in Sweden; the Kola alkaline province (acl) in Russia; Sokli (cl) and Iivara (a) in Finland; Fen (acl), Ytteröy (l), Söröy-Breivikbotn (ac), Stjernöy-Lillebukt (acl) and Stjernöy–Pollen (c), as well as Seiland-Store Kufjord (ac) in Norway.

Various rocks from the Alnö Complex have been dated to 562 Ma (U–Th-total Pb; von Eckermann and Wickman 1956), 553 ± 6 Ma (Rb–Sr isochron age) and 546–605 Ma (K–Ar determinations) (Brueckner and Rex 1980). These dates indicate a lower Cambrian age (Fig. 1.10). Several K–Ar ages fall outside this time-span, e.g., an age of 668 ± 24 Ma for uncompahgrite of the Söråker intrusion, two ages of about 380 Ma (middle Devonian) for a melilitite dyke, and two ages of about 370 Ma for the Sälskär material and a jacupirangite in contact with

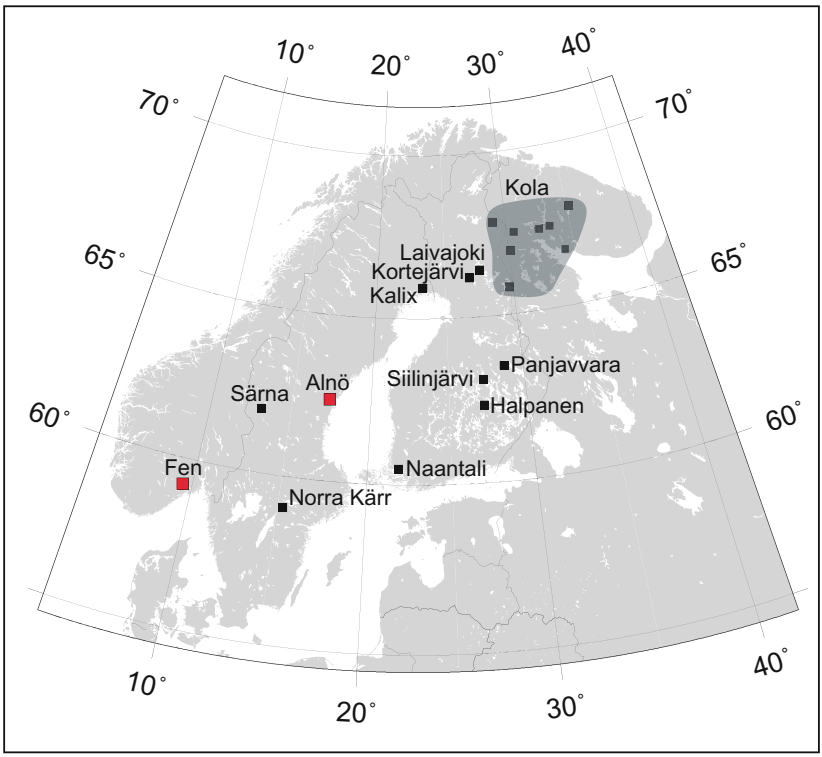

Fig. 1.9 Alnö and Fen carbonatite complexes (red squares) and further Scandinavian carbonatite and alkaline silicate intrusives (compiled from various sources; see text for details)

kimberlitic alnöite, respectively (Brueckner and Rex 1980). These deviating ages still need further confirmation. The latest radiometric dating of Alnö, suggests an age of 584 ± 7 Ma (Meert et al. 2007) determined by feldspar and biotite $^{40}Ar/^{39}Ar$ dating, and which is likely the most reliable radiometric age to date.

Regarding the age relationships of rock units within the Alnö complex, we need to rely on traditional geological methods. From field work, the following chronology of geological events is suggested for the Alnö igneous complex:

(1) Intrusion of melilitolite (uncompahgrite, garnets with kimzeyitic cores) and Ti-andradite bearing sövites in the Söråker area, accompanied by fenitization and intrusion of some dyke rocks.

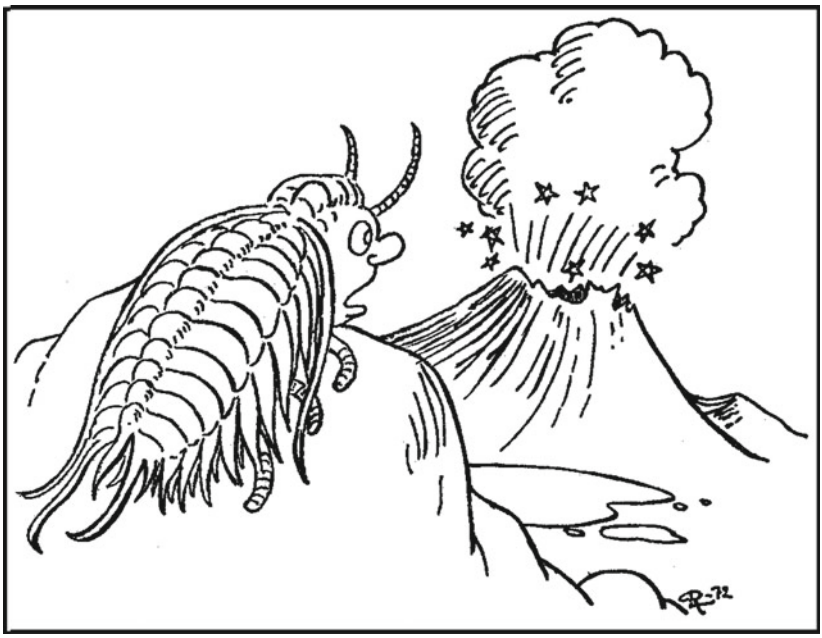

Fig. 1.10 "The formation of the alnöite was witnessed by the trilobite". Cartoon drawing by Rolf Lidberg (1972)

(2) Intrusion of the ring-complex to the north of Alnö island, comprising massive sövite dykes (with perovskite, aeschynite) with layers of pyroxenite. Some nepheline syenite as well as ijolite occurs and an intrusion of younger (cross-cutting) ijolite is recorded (Kresten 1990).
(3) Intrusion of the main complex at Alnö (the southern ring complex), with pyroxenite, ijolites, and nepheline syenites. The southern ring complex emplacement was accompanied by widespread fenitization. Later veining by sövite is recorded, which only rarely reaches major sizes, (see Smedsgården for exceptions though). The sövites contain fersmite and pyrochlore minerals and even formed a separate intrusion at Båräng.
(4) The Sälskär extrusive vent, with melilitite lapilli and carbonatite and melilitite fragments (plus pyrochlore) appears the youngest event and was likely accompanied by occasional melilitite dykes in the northern parts of Alnö Island.

Dykes have most plausibly intruded during the whole period. Possibly, alkaline silicate dykes (trachytes, phonolites, nephelinites) may be rather early, as they appear in an orthogonal intrusion pattern (N30°W–N60°E), thereby completely differing from carbonatite and lamprophyre dykes that show generally a radial dyke—cone sheet pattern (see also below). The kimberlitic alnöites are probably quite late, as they have so far not been found cross-cut by any other dykes.

1.5 Regional Geology and Emplacement Models for the Alnö Complex

The bedrock of the Alnö area is dominated by Early Proterozoic complexes formed during and after the Svecofennian or Svecokarelian orogeny. These complexes consist of supracrustal (metasedimentary) gneisses and migmatites as well as intrusions of early and late orogenic granitoids. Younger than these are an orogenic rapakivi granite (Rödö granite) and major dolerite sheets (Fig. 1.7). Dyke intrusions of the area comprise late Svecofennian pegmatites and aplites, granite porphyries and dolerite porphyries associated with the Rödö granite, and dolerite dykes related to the sheets. In the following, only brief information is given on the major crustal rock types. For more details the reader is referred to the description of the geology of Västernorrland County by Lundqvist et al. (1990).

1.5.1 Supracrustal Gneisses and Migmatites

Gneisses of greywacke origin prevail, made up of dominating arenitic layers composed of quartz, oligoclase and biotite, and more subordinate argillitic layers composed of biotite, plagioclase, quartz and sometimes muscovite. Occasionally, garnet, cordierite and/or sillimanite occur in the latter. The gneisses have been extensively transformed into migmatites, in part as veined gneisses, but largely also as raft migmatites. Subordinate intercalations of meta-basalts transformed into amphibolites are found. The age of the greywackes is probably about 1880 Ma (Lundqvist et al. 1990). The general trend of foliation in the Alnö area is ENE to NE (Fig. 1.7), while south and south-west of Sundsvall the trend is mostly E-W or ESE-WNW.

1.5.2 Early Orogenic Granitoids

Early orogenic intrusions occupy vast areas south to west of Sundsvall. They also occur e.g. on southernmost Alnö and in the northern parts of the area shown in Fig. 1.7. Usually these intrusions form variably gneissic and migmatized granites, granodiorites and tonalites, with only minor gabbro, diorite and ultramafites. They are intrusive into the metagreywackes, and were folded and metamorphosed along with these during the Svecofennian or Svecokarelian orogeny. Their radiometric age is about 1880–1870 Ma (Lundqvist et al. 1990).

1.5.3 Late Orogenic Granites and Pegmatites

Late orogenic intrusions of granite and pegmatite occur as small, scattered plugs over the whole Sundsvall area. Typically the granites are greyish white or reddish, fine- or medium-grained rocks, in which lath-shaped microcline megacrysts are sometimes found. They are associated with abundant pegmatites. The late orogenic intrusions postdate the regional Svecofennian migmatization. However, they predate some late Svecofennian movements, and may thus in cases display a distinct foliation. The age of the granites, according to a U–Pb age determination on monazite from a minor intrusion in the southern part of the Sundsvall area, is 1822 ± 5 Ma (Claesson and Lundqvist 1990).

1.5.4 Anorogenic Rapakivi-Type Granite (Rödö Granite)

The Rödö granite occurs on the island of Rödön east of Alnö, and on some small skerries in the vicinity (Fig. 1.7). It shows several typical rapakivi features such as potasium feldspar of orthoclase or mixed orthoclase-microcline structure, plagioclase mantling of potasium feldspar. Also, rare pegmatites and miarolithic cavities filled with calcite, quartz and feldspar occur. The Rödö granite has been dated at 1497 ± 6 Ma (Ahl et al. 1997).

Closely associated with the Rödö granite are numerous dykes of granite porphyry and dolerite porphyrite. They occur in the Rödö granite itself as well as within an area of about 16 km diameter surrounding Rödön. The dykes, which have been studied by Holmquist (1899) and by von Eckermann (1945), display beautiful examples of magma mingling.

1.5.5 The Åvike Sandstone

Orthoquartzitic sandstone of undetermined age (Lundqvist et al. 1990) occurs in an outcrop at the western shore of Åvike Bay. Together with a nearby dolerite, it is severely crushed and brecciated, a feature that was taken by Henkel et al. (2005) as argument for the bay being possibly an impact crater.

1.5.6 Dolerite

Dolerite occurs as flat-lying sheets in the northern parts of Åvike Bay, and throughout the area as commonly steeply dipping dykes that range in width between some centimetres and up to ten metres. Preferred strike directions are E-W, but also N-S. Their age is 1215 Ma (Welin and Lundqvist 1975; recalculated values by Welin 1979), i.e., post-Jotnian.

1.5.7 Palaeozoic and Younger Rocks

The distribution and extension of Palaeozoic sedimentary rocks on the bottom of the Gulf of Bothnia has been investigated by Axberg (1980). According to this study, Palaeozoic rocks extend to a line just off the coast of the area discussed. Boulders of Ordovician limestone are found on the shores from Härnön in the north and southward across the Alnö area (see Lundqvist et al. 1990).

West of Stöde village, about 45 km west of Sundsvall along route E14, fissures in the migmatite have been filled with gravel, sand and silt, all of which are cemented by calcite. The infillings are devoid of microfossils (A. Nyers, pers. comm.), but can in all probability considered to be Palaeozoic. This would imply that the present erosion surface at Stöde is close to the sub-Cambrian peneplain, in harmony with e.g. Lidmar-Bergström (1986).

Axberg (1980) reports a possible post-Ordovician dyke on the bottom of the Gulf of Bothnia east of the Alnö area. The reflections received by seismic investigations in an area with Ordovician limestone may indicate a dyke of Permian age, or possibly a late dyke related to the Alnö igneous activity.

Along the northern shore of Alnö island, at Hörningsholmen, and along the shore of the mainland at Söråker, scattered boulders of Cretaceous rocks—mainly flint—are found. They have been the ballast of timber vessels from England. Other "ballast imports" include various shales and phyllites (see also Lundqvist et al. 1990).

1.5.8 Major Tectonic Lineaments

The Alnö area is located near the intersection of a number of major lineaments. The great majority of these probably represent steep faults, although the displacement is generally hard to determine due to the nature of the bedrock (migmatites and granites).

First it should be noted that the Alnö complex as well as other centres of igneous activity (the sub-Jotnian rapakivi massif at Nordingrå and some post-Jotnian dolerite sheets) are situated on the mega-lineament (the "Norrland line") defined by the fairly straight, NNE-running coast line of central Sweden. Along this mega-lineament, extensive deposits of Jotnian sandstones in the Gulf of Bothnia have according to all evidence been down-faulted (Axberg 1980; Ahlberg 1986).

The most important lineament, the "Alnö Fault", runs N-S along the Mjällån valley. It appears to be displaced by a younger fault in the Timrå region north-west of the Alnö complex and from there continues southward in Alnösundet, which separates the Alnö island from the mainland in the west.

Another important lineament runs NW-SE in the Indalsälven river valley and possibly continues along the northern shore of Alnö island. A more NNW-striking lineament is found along the shore of Söråker and extends northward to the vicinity of Ljustorp. From Stavreviken, about 10 km north of Alnö island, a NE-SW-running lineament extends some 50 km to the north-east, to the southern part of the Nordingrå rapakivi massif. In addition to these major lineaments there are numerous less extensive ones, especially in directions between E-W and NW-SE.

It should also be noted that movements, probably along existing faults and fissures, still take place in the Alnö-Sundsvall region. Forming part of a larger region along the coast of the Gulf of Bothnia, it is known as one of the seismically more active regions in Sweden (Lundqvist et al. 1990). The reasons are either to be sought in post-glacial uplift or in release of stress set up by recent plate movements (Skordas et al. 1991).

1.5.9 Regional Setting for the Emplacement of the Alnö Igneous Complex

The Baltic Sea area was developing in the Mid Proterozoic and again in the Late Proterozoic due to intra-cratonic lithospheric rifting, the latter episode being related to the eventual breakup of the supercontinent Rhodinia (Torsvik et al. 1996).

Rifting was associated with thermal doming in the Vendian and led to crustal subsidence and basin formation in the Baltic area once the thermal domes declined (Torsvik et al. 1996; Korja et al. 2001). Lateral crustal extension, was probably limited. Basin subsidence is recorded for the Early Cambrian to Late Ordovician period (ca 580–430 Ma) forming the Bothnian Bay basin and the main Baltic basin (van Balen and Heeremans 1998). Three hypotheses have been put forward to explain the rifting and associated thermal uplift followed by basin formation (van Balen and Heeremans 1998); (i) symmetrical asthenospheric diapirism with subsequent evolution/development of dominant figures or "upwelling" that explain the temporal evolution of the Bothnian and Baltic basins. (ii) a deep mantle plume that is either stationary but feeds different migrating lithospheric regions, or, a "migrating" plume that may be exploit crustal weaknesses. (iii) lithospheric delamination, where cold and dense sub-continental mantle material detaches and sinks into the deeper mantle. This will cause a filling in of the space with ambient upper mantle that will likely support the initial lithospheric uplift associated with such a process (e.g. van Balen and Heeremans 1998; Korja et al. 2001). However each of these hypotheses has a drawback, being in case of (i) that the basins are not simultaneous as would be expected in case of symmetrical upwelling, even though their relative magnitude may differ. For (ii) not independent evidence for a mantle plume exists, and for (iii) that the model predicts replacement of sub-crustal lithosphere beneath Archean crust, which is not consistent with the available seismic evidence (Torsvik et al. 1996; van Balen and Heeremans 1998).

The Alnö carbonatites, intruded in the region of the later Bothnian basin at 584 Ma (see above), i.e. during the peak of thermal uplift and the breakup of Rodinia and just prior to basin subsidence. In case of (i) the signal recorded by isotopes should be that of an upper mantle reservoir MORB-type, which would also be the case for hypothesis (iii), while hypothesis (ii) should record an ocean island geochemical signal in case of a plume origin. Noteably, recent isotope data (e.g. Roopnarain 2013) support an "ocean island-type" character of the investigated Alnö samples (see Chap. 3), which argues for e.g. plume fingers that caused the thermal uplift in the region at the end of the Vendian period and which fed e.g. the Alnö and possibly also the Fen complex. We can speculate that this may have been analogous to active plume fingers in the East African rift valley or the Rhine graben, where young carbonatites volcanoes are found today.

The Alnö complex intruded into *ca.* 1.9 Ga migmatitic gneiss. The intrusions have locally imprinted intense contact metasomatic reactions on the country rock, producing a range of lateral contact facies (fenites) for which Alnö, after Fen in Norway, is famous (e.g. Morogan and Woolley 1988; Morogan and Lindblom

1995). Similar to the Fen complex, the Alnö complex has the shape of a concentric stock with coarse-grained calcite carbonatite, ijolite and nepheline syenite in the core (Figs. 1.7 and 1.8). The surrounding migmatite country rocks grade in composition from quartz syenitic to (nepheline) syenitic closest to the plutonic rocks of the complex and it is apparent that the Alnö intrusion altered the composition of the migmatites to different grades, a process that is common around alkaline and some carbonatite intrusions and is named "fenitization" after the Fen complex in Norway. This fenitization can be seen hundreds of meters from the intrusive rocks, yet original migmatites features may still be locally present as isolated remnants even in heavily fenitized rock (von Eckermann 1948, 1966; Morogan and Lindblom 1995; Kresten 1988, 1990).

There is, however, an important difference between the complexes at Fen and Alnö. As is evident from the rock names given at Fen (sövite, rauhaugite, melteigite) and Alnö (alnöite, alvikite, beforsite), Fen is dominated by plutonic rocks, while dykes and hypabyssal rocks are abundant at Alnö. Therefore, we are probably looking at a deeper section at Fen, and at a more shallow level (near-surface) section at Alnö.

1.6 The Plutonic Rocks of the Alnö Intrusions and associated Fenites

The same rock types occur both in the Northern Ring Complex (NRC) and in the Main Intrusion on Alnö Island (Figs. 1.6 and 1.8), although with differences in proportions and appearance. The sövites of the NRC are quite wide flow-banded ring-dykes, intercalated with (sheeted) layers of pyroxenite, or flow-layered melteigite and ijolite. The rocks appear to have been intruded simultaneously. Boudination of the pyroxenites in sövite is quite common. Nepheline syenites play a minor role within the NRC and fenites occur mainly as components of complicated breccias together with dominant alkaline plutonic rocks. One reason for this apparent lack of a fenite in the NRC may be that the contact to the migmatite wall-rock is not exposed. Importantly, the rocks of the NRC have been intruded by younger ijolite.

Within the Main Intrusion (or Southern Ring Complex), pyroxenites, melteigite-ijolite rocks, nepheline syenites and sövites form major intrusives, and anostomosing dykes of sövites are common. All that is surrounded by a fenite aureole, grading from very weakly affected wall-rock to leucocratic fenites with syenitic compositions that are rheomorphic, i.e., the show intrusive behaviour close to and within the main complex. The chronological sequence implies that the earliest intrusions in the Alnö complex were pyroxenite and ijolite-series rocks,

followed by nepheline syenites and eventually by the sövites. No younger ijolites (as in the NRC) have been encountered within the main southern intrusion, implying that the NRC is older than the main complex (see also above).

To the west of the main intrusion, the Båräng vent is a small satellite intrusion consisting of sövite, up to 40 m wide and alkaline silicate intrusives emplaced into mainly high-grade fenites of syenitic compositions (von Eckermann 1948).

1.6.1 The Fenites

The term "fenite" has been coined by Brøgger (1921) for metasomatic alteration products caused by "magmatic solutions" at Fen, Norway, which he assumed emanated from ijolite-melteigite-magmas (Brøgger 1921). He distinguished several types of fenites and realized that composition changes with distance from the igneous rocks exist.

At Alnö, the migmatite country rocks that surround the complex show a fairly constant strike direction of about N80°E, with usually steep to vertical dips. When approaching the igneous complex, the strike directions of the outer fenite zone (i.e. within the quartz-bearing fenites) gradually changes and becomes eventually parallel with the outlines of the igneous complex, indicating plastic deformation of the fenitized wall-rock around the complex. Also, the structure of the original migmatite becomes increasingly blurred until it is locally completely wiped out. Typical signs include reddish colouration in patches, or along cracks, and an increased presence of feldspar.

Along with the signs for structural deformation, changes in mineral parageneses occur in the fenite aureole. Specifically, plagioclase and potassium-feldspar become increasingly sericitisized when approaching the igneous complex, and quartz contents decrease. Biotite breaks down, while newly formed minerals include various alkali amphiboles such as richterite and arfvedsonite, alkali feldspar, and aegirine (acmite). Notably, zircon, commonly regarded as a refractory phase, is often among the first minerals to disappear, with Zr being incorporated into aegirine. This implies that zircon, like quartz, reacts intensely with aggressive CO_2-rich fluids (cf. Donaldson and Henderson 1988).

The boundary between quartz-bearing and quartz-free fenites (Kresten 1990) is sometimes marked by a narrow zone of intense crushing (the "thermodynamic shock zone" of von Eckermann, 1948). Minerals that have been affected by the crushing include quartz, biotite, alkali amphibole and acmitic clinopyroxene. Crushing must have occurred in association with fenitization and implies ductile behaviour that grades into brittle parts of the aureole in combination with rapid and

intense fluid- or gas-driven deformation. A fluid front is indicated by this boundary type, and mylonitic shattering appears to have occurred. After that zone, the fenites here are often massive in appearance and quartz contents are low to nil, although remnants of the original structure of the rock are sometimes locally preserved e.g. at the end of Hartungvägen (see Chap. 4).

The quartz-free "syenitic fenites" are dominated by alkali feldspar and clinopyroxenes, commonly aegirine-augites, while most original mineral phases of the migmatite wall-rock have been eradicated. In addition, some mica and accessory magnetite, calcite, apatite, andradite and wollastonite are found. The quartz-free fenites have been mobile to a certain extent, probably being dragged along with the intruding alkaline rocks. This mobility has apparently caused a separation between leucocratic mobilisates and melanocratic restites. This can be observed at a local scale in form of a rather narrow dyke-like body of pyroxenite that is found close to a cottage about 800 m NE of Alnö church. The pyroxenes in the rock are of the same composition as those in high-grade fenites, i.e., acmitic. Accordingly, this pyroxenite is likely not a plutonic rock of the Alnö complex but a "rest-fenite". A similar body was uncovered during road-works near Nedergård (there even with relict quartz crystals), and several more have been indicated by ground magnetometric surveys (Kresten 1976b), suggesting extensive but selective fenite mobilization (rheomorphism) within the Alnö complex. On a small scale, mobilization and differentiation into leucocratic and melanocratic parts can be seen, for instance, near Ås jetty (see Chap. 4).

Brøgger (1921) believed the ijolite-melteigite intrusions to have caused fenitization. Only a brief glance at the geological map of Alnö (Kresten 1979, 1990) shows that this must be true for Alnö as well. Indeed, local fenitization can be intense when found in connection with sövite and carbonatite intrusions, as well as with alnöite dykes. However, large-scale fenitization around the complex must have been caused by the dominantly alkaline plutonic rocks of the Alnö. During the intrusion of the alkaline plutonic rocks (pyroxenites, melteigite and ijolite series) the migmatites wall-rock responded with plastic deformation, and compositional changes (low-grade to intense fenitization). Plastic deformation was probably caused by the displacement of 'heated' rock masses by intrusion of magma at depth and by dykes and cones sheets. The intruding magmas did probably constitute partial mushes and were likely not a fully molten phase at the current exposure level. At some point, the mechanical stability of the wall-rock within the central part of the complex was exceeded, which led to roof rupture and deformation. The country rock broke in many places in the periphery, while within the inner fenite zone, the country rock showed increasingly ductile behaviour (see e.g. Kresten 1990).

At the Fen complex, Kresten and Morogan (1986) studied fenites associated with ijolite-melteigite rocks, and those close to sövites. From each group, low-, medium- and high grade fenites could be distinguished. The fenitizing fluids emanating from the alkaline plutonic rocks had high activities of Si, Na, K, and Mg, while fluids emanating from silico-sövite had high activities of Na, Ca, and Fe with low activity of Si. A rather pure (magnesian) sövite was associated with high activities of Ca, K, and Mg. Even with the same fenitizing agents, the resulting fenite types could be rather different.

Gittins (1989) has argued that aqueous solutions produced by silicate magma (e.g., ijolite) can generally be eliminated as causing fenitization, being relatively rich in silica. All evidence, not only at Fen or Alnö, shows that this statement does not hold true. Kresten (1994) has shown that ijolite-induced fenites show small gains in silica and have lower REE contents, features that both contrast carbonatite-induced fenites.

Kresten (1988) divided the fenites of the Fen complex into aureole, contact and vein fenites, with petrographic grades as above. In order to achieve some quantification of the process, he applied the equation of Gresens (1967) for the relationship between composition and mass transfer of metasomatic rocks. Based on the assumption that the total mass change during fenitization would be at minimum (±5%), the mass transfer for fenites from the various areas could be calculated. In addition, a "fenitization index" (F.I.) was suggested as the sum of all major element gains. It could be shown that this index corresponded very well with petrographic grade.

That approach was followed up by Morogan (1989) for Alnö fenites, while Kresten (1994) even included various trace elements. Again, ijolite-related fenites are predominantly potassic, while sövite-related fenites are sodic to intermediate (Stornäset) or intermediate to potassic (the latter at higher F.I.s, e.g. at Båräng).

However, rare cases of sodic fenites (with nepheline) have been reported near sövites (Morogan and Woolley 1988), with fenitization caused by sövite overprinting pre-existing fenite caused by ijolite. It might be surprising to find newly formed quartz in fenites. At Fen, many low to medium grade fenites show positive SiO_2 balance (Brøgger 1921; Kresten 1988) and even at Alnö, newly formed quartz crystals have been found in both low and high grade fenites. Morogan and Woolley (1988) conclude that nepheline is found only in contact fenites to sövites, and that fenite nephelines are distinguished from magmatic nephelines by equilibration temperatures of 500–700 °C for the former, and 700–775 °C for the latter.

1.6.2 Alkaline Silicate Plutonic Rocks

Pyroxenites usually occur as minor intrusions, commonly lenticular in geometry (see Figs. 1.7 and 1.8) and according to field relationships, three types of pyroxenites are found (i.e. a rock with >90% of modal pyroxene). These comprise: (i) Independent intrusions of pyroxenites, older than the melteigite/ijolite series; (ii) Pyroxenites closely associated with, and grading into rocks of the melteigite/ijolite series; (iii) Minor pyroxenite intrusions within the fenite aureole, which are, however, not to be confused with pyroxenite lenses within the fenite aureole that are "restites" in the fenite and were left behind by the mobilised leucocratic components (Fig. 1.11).

Principal constituents of the intrusive pyroxenites are titanian augites, often associated with variable amounts of amphibole (titanian edenite/hastingsite), biotite, apatite, calcite, and nepheline. There are variations of these pyroxenites, which include nepheline, pyroxene and titanium-rich magnetite (*jacupirangite*), or with dark andradite garnet (*cromaltite*). Some of the pyroxenites on Alnö have been mined sporadically for iron from the 17th to the 19th century (see Statens industriverk 1980; Kresten 1990).

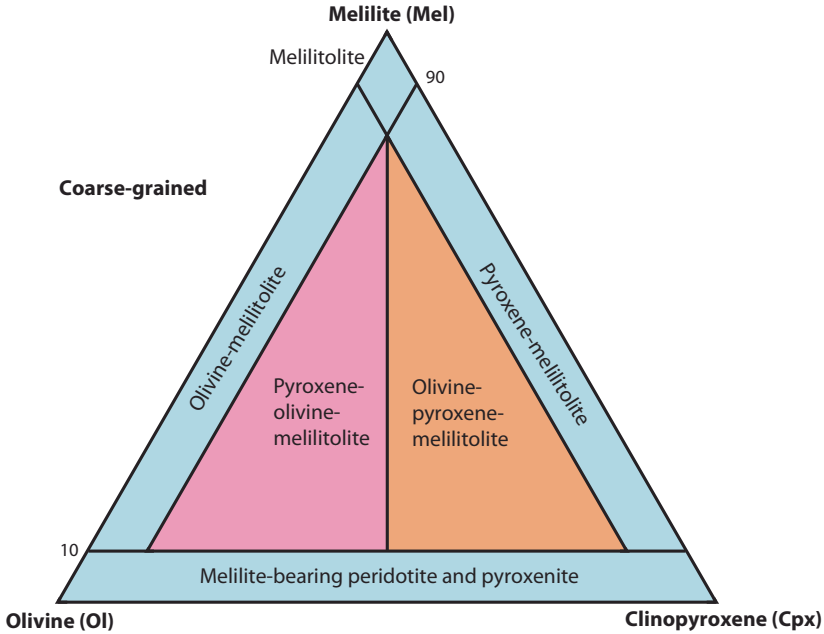

Fig. 1.11 Classification of rocks from the pyroxenite to melteigite-urtite series

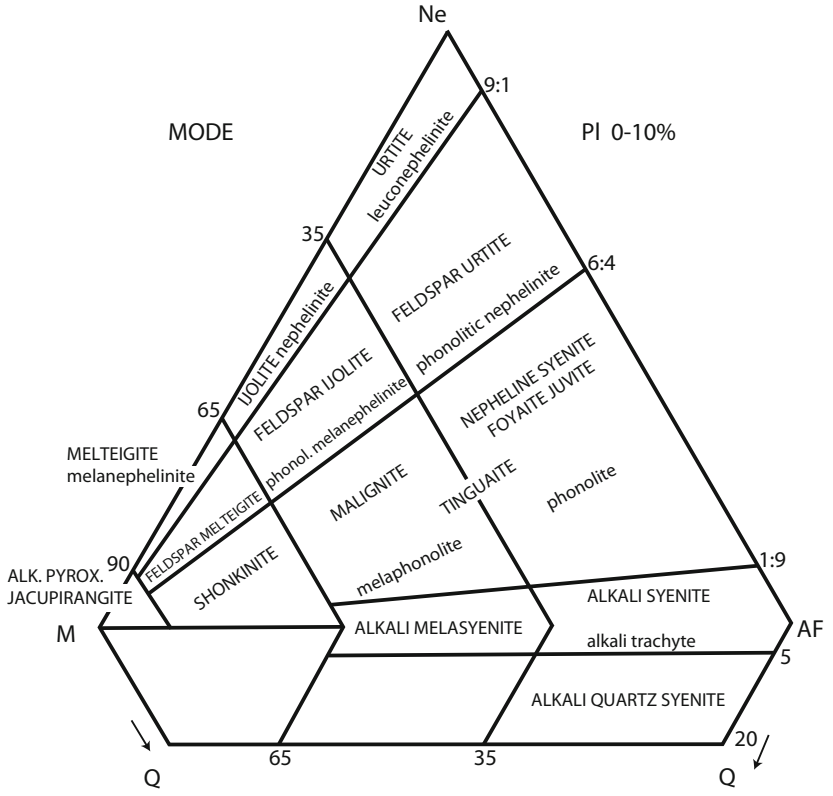

Fig. 1.12 Nomenclature of alkaline rocks in the system nepheline-mafics-alkali feldspar-quartz (after Kresten 1979). Plutonic rock names are capitalized

Narrow dyke-like bodies of pyroxenite (type iii) that occur within the fenite aureole, preferentially at the boundaries to the mobile leucocratic fenites, are not plutonic rocks but "restites" as discussed above. Their pyroxene is aegirine-augite; in addition, amphibole, feldspar and/or apatite are found.

Rocks of the *melteigite/ijolite/urtite* series (Figs. 1.12 and 1.13) are the most prominent alkaline silicate plutonic rocks of the complex. The rocks in the ijolite series are distinguished after nepheline content: *Urtite* contains >70% of nepheline, *ijolite* 30–70%, and *melteigite* contains <30% of nepheline. They are usually medium-grained, equigranular rocks but coarse-grained varieties with large needles

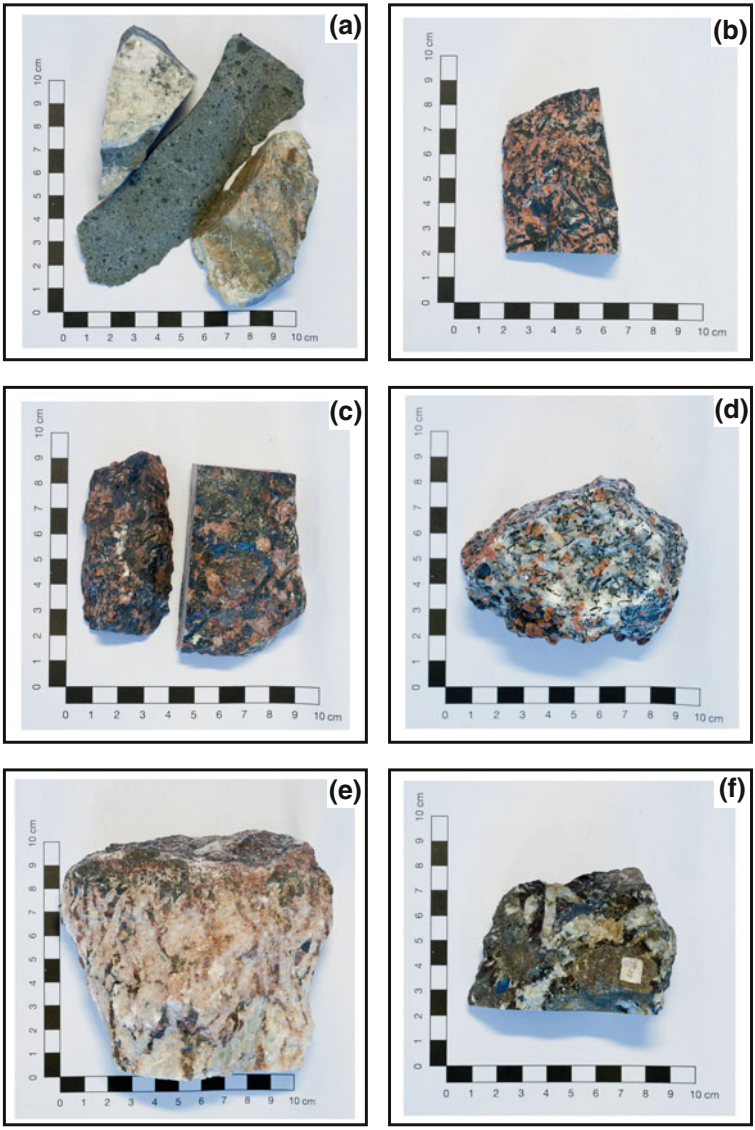

Fig. 1.13 Representative rock types from Alnö (Uppsala University petrological collection). **a** sövite vein (top left), alnöite (middle) and migmatite country rock (bottom right), **b** ijolite, **c** nepheline-syenite, **d** nepheline-pegmatite, **e** sövite-pegmatite, **f** syenite pegmatite with calcite. These specific samples were collected by Prof. von Eckermann and Prof. Collini in 1948 (photos from Roopnarain 2013)

of clinopyroxene are occasionally found. In some outcrops, flow-layering is seen with layers ranging for example from pyroxenite to urtite in composition and xenoliths of pyroxenites and/or fenites can be common. The rocks of the melteigite/ijolite series are composed of nepheline (often hydrated) and clinopyroxene in variable proportions (titanium augite, augite, aegirine augite). Smaller mineral constituents include biotite, sphene, apatite, andradite or melanite, titanomagnetite, wollastonite, pectolite and calcite.

Nepheline syenites usually cross-cut pyroxenites and melteigites/ijolites and often contain xenoliths of these rocks and also of the fenite suite. The nepheline syenites are commonly massive and medium-grained rocks, but very fine-grained as well as rather coarse-grained varieties are occasionally found (Fig. 1.13). Flow-structures are sometimes indicated by semi-parallel arrangements of tabular feldspar and/or by preferred orientation of the entrained xenoliths. Nepheline syenites contain <10% feldspathoids (F = 0 − 10) and P/(A + P) is 10–35 in the QAPF classification after Streckeisen (1976). The major constituents are Na-orthoclase and nepheline, together with clinopyroxene (augite to aegirine augite), biotite, cancrinite, natrolite, calcite, andradite and apatite in variable amounts. Accessory minerals include pyrite, brookite and pyrochlore.

1.6.3 Sövites and Silico-Sövites

Sövite is named after a quarry near Söve within the Fen complex, Norway (Brøgger 1921). Sövite is commonly a plutonic carbonatite rock, despite their common appearance as dykes within the Alnö complex. Sövites are here defined as containing more than 70% carbonate by volume, while silico-sövites have carbonate contents in the range of 50–70% (cf. Roopnarain 2013). Sövites and silico-sövites are coarse-grained at Alnö and calcite is the predominant carbonate mineral (Fig. 1.13). Small amounts of dolomitic or ankeritic carbonates occur only on occasion. Other major constituents include phlogopite or biotite mica and clinopyroxene (diopside to augite). Apatite and notably magnetite, pyrite, sphene and andradite/melanite are common minor constituents.

The pattern of sövite intrusions varies in different parts of the Alnö complex. Along the northern shore of Alnö island and on the small islands to the north (the Northern Ring Complex), sövites form a broad ring-dyke pattern with thin intrusions dominating (see Fig. 1.7). In the South, individual sövite sheets display widths that can exceed 100 m (e.g. at Smedsgården). Unfortunately, outcrops are often poor in this area and the overall ring-dyke structure is to some degree inferred. A typical feature of the “northern sövites” is the occurrence of perovskite

type minerals as accessory phases (perovskite, dysanalyte, aeschynite). Further, the "northern sövites" are intruded by later ijolites (e.g. seen Chap. 4) and a generation of younger sövite dykes. In addition, the sövite ring dyke pattern is accompanied by a similar pattern for mainly pyroxenites (see Fig. 1.8), indicating that their intrusion was probably more or less simultaneous to the sövites here.

Within the main (southern) ring intrusion, sövite dykes are narrower than in the north and frequently form anastomosing veinlets when found in the alkaline plutonic rocks, although a vague indication of a ring-dyke pattern can be inferred (Fig. 1.8). The sövites in this central area are generally younger than the alkaline plutonic rocks and they do not contain perovskite type minerals as accessory constituents, but pyrochlore instead (including fersmite and columbite). Also, the sövites of the Båräng vent form a ring-like pattern, but show several minor off-shoots. They carry pyrochlore minerals and seem to thus more closely related to the sövites of the southern type.

Field evidence, as well as the mineralogical differences between the "northern" and "southern" sövites indicates that the northern sövites, together with alkaline plutonic rocks, might have once formed a separate intrusive (ring-dyke) complex. This northern centre appears nevertheless related to the main activity on Alnö Island in that the intrusions of the southern portion of the complex appears to have deformed the northern ring complex. This deformation style appears very similar to the deformation of the fenite wall-rock, resulting in a bend ellipsoidal shape of the northern ring-dyke complex (Fig. 1.8). We therefore speculate that the time between the northern and southern ring intrusions was probably geologically short.

Sövite pegmatites: This term has been coined by von Eckermann (1948) describing a coarse-grained and oriented intergrowths between calcite and clinopyroxene, with accessory apatite and spinel. The rock roughly corresponds to the "Hollaite pegmatite" at Fen described by Brøgger (1921). Sövite pegmatite dykes occur at a few localities only e.g. at Hörningsholm (see Chap. 4). It seems evident that they have been formed by late-stage pegmatitic crystallization of the sövite magmas in pods and sheets and may have grown at high growth rates as inferred from pegmatites elsewhere.

Sometimes, such as at Stugholmen islet, flow-layered sövite contains blebs or pods of recrystallized material vaguely resembling sövite pegmatite. There, one can see the progressive stages from the beginning of crystallization to the advanced stage of pure coarse-grained radial calcite growth with all of the mafic minerals having been pushed to the margins. These blebs or pods appear to have formed by late stage in situ, possibly hydrothermal (re-)crystallization (see Chap. 4).

1.7 The Söråker Intrusion

At Söråker, on the mainland north of Alnö island (Fig. 1.8), a satellite intrusion is found, measuring about 1 × 2 km (based upon magnetometric measurements, (Kresten 1976b). Only very few outcrops are available (see Chap. 4). The plutonic rocks of the Söråker intrusion contrast those of the Alnö complex in that coarse-grained melilite-rich rocks (uncompahgrites) are found, as well as some rich in melanite, phlogopite, apatite and wollastonite. Kimzeyitic garnet (about 10% ZrO_2) is also identified as a common core phase of garnets at Söråker. One outcrop discloses a rock composed of 70% garnet (again, kimzeyitic cores) and 30% phlogopite. A now due to construction no longer available outcrop near the shore showed sövite made up of calcite, apatite, biotite and abundant melanite, the latter forming idiomorphic dodecahedrons several centimetres across, but see also Chap. 4. The Söråker intrusion is probably surrounded by a fenite aureole that can be inferred from the few outcrops available.

1.8 The Sälskär volcanic Vent

Boulders of volcanic breccia are found at the Sälskär skerries north of Alnö island (Fig. 1.14), indicating the existence of a volcanic vent. The Sälskär breccia consists of fragments of sövites and melilitite lapilli in a carbonatite matrix composed of calcite, apatite, phlogopite, magnetite and pyrochlore, and with abundant xenocrysts of olivine. The fragments in the breccia range in size from less than a millimetre up to several centimetres across. Accretionary lapilli occur and typically they show a nucleus of magnetite or olivine, surrounded by up to ten consecutive shells of very fine-grained melilitite. At very low water, Peter Kresten recovered a boulder between Ö:a Sälskär and Hörningsholmen showing the breccia in contact with fine-grained melilitite. The contact surface showed "sand-blasting" features.

The mineral paragenesis of the melilitite component is melilite, magnetite, perovskite, monticellite $\pm$ olivine $\pm$ diopside. The shells of the accretionary lapilli show similar composition, but are more fine-grained, with laths of melilite paralleling the shape of the magnetite or olivine cores. The formation of accretionary lapilli is commonly interpreted as being the result of explosive venting, while the mineral paragenesis of the melilitite is interpreted as being derived from a CO_2-rich ultramafic magma (olivine + diopside) (e.g. Schumacher and Schmincke 1995; Gernon et al. 2012). Carbonatite-melilitite volcanism and volcanic vents have been

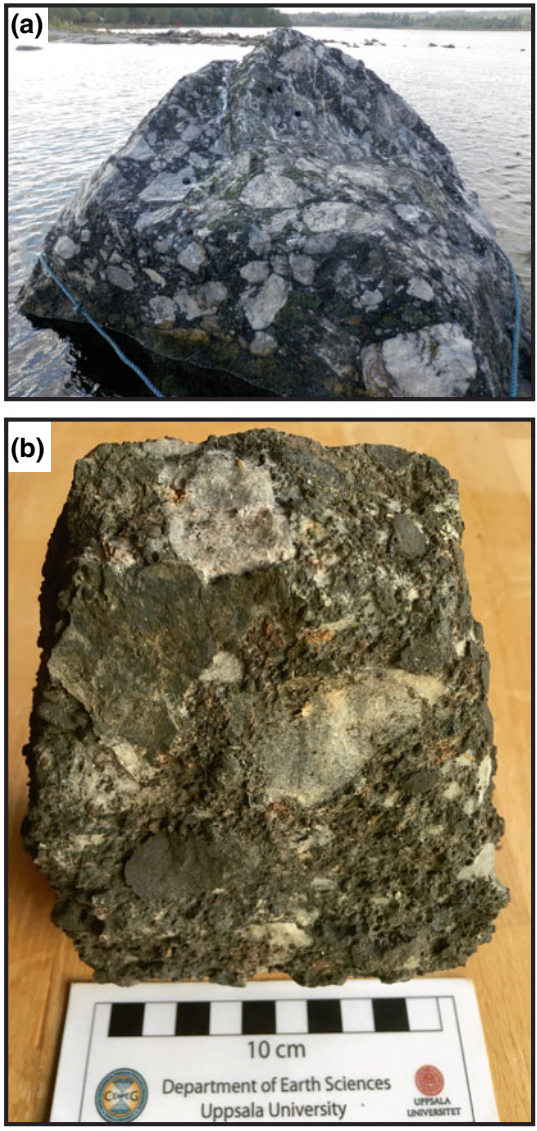

Fig. 1.14 **a** Sälskär breccia; photo courtesy of Magnus Andersson. **b** Rock specimen from Sälskär showing a typical Sälskär breccia (see text for details)

recorded from other carbonatite occurrences, for instance in the African Rift Valley (Hay 1978; Dawson 2012).

Despite considerable efforts, the breccia has not been found in outcrop. Magnetometric measurements (Kresten 1976b; SGU 1997) indicate an area north-west of the skerries as the probable site of the volcanic vent. An oval-shaped roughly area with a diameter of about 1000 × 1500 m, with a total field intensity of up to 1000 gammas above the background of 51600 gammas has been noted, which would indicate an estimated depth of up to 700 m.

1.9 Indications of other Intrusions

A possible intrusion within the Åvike Bay has been suggested by Söderström (Tallbacka) (1966), based upon the fracture pattern in the area, the frequent occurrence of various dykes as well as the presence of breccia boulders containing "Åvike sandstone" (Tallbacka 1968a, 1968b). The semi-circular shape of the bay (Fig. 1.6) is intriguing, but not proof of any volcanic activity. Aeromagnetic data (see below) do not support the concept of an central intrusion within the bay.

Loose boulders along the shore of the bay comprise alnöites, alnöite breccias (with sövite fragments), fenites (with abundant melanite and/or wollastonite) and ijolites. Indeed, along the shore, numerous dykes of alnöite and carbonatite are found, as well as some sövite dykelets. Much of this can be explained by good exposure conditions. The sövite fragments in alnöite breccias show the paragenesis calcite, biotite, apatite, magnetite, calzirtite and zirconolite—the latter two minerals being completely unknown from other parts of the Alnö area (Kresten 1990). This indicates that sövite of unusual composition exists somewhere at depth, but despite the dyke rocks here, there is no strong argument for a separate "Åvike Intrusion".

By contrast, Henkel et al. (2005) argue that the bay is a possible impact structure. Their arguments comprise the fracture pattern but also, the occurrence of a submarine central mound, and the (scarce) occurrence of monomict and polymict breccias with possible planar deformation features.

1.10 The Dyke Rocks

Since 1974, Peter Kresten has mapped the dyke rocks of the area around Alnö Island. Within about 1200 sq. km, about 1200 dykes of various geometries were registered. Fortunately, the motorway northwards from Sundsvall was under construction at the time and a fair number of dykes, many of which are nowadays

beneath the tarmac, were temporarily exposed. Most of the dykes registered in the region are not very wide, as shown by the following statistics: width <2 cm: 10.8%; 2–10 cm: 38.8%; 10–20 cm: 24.9%; 20–100 cm: 18.6%; 1–2 m: 5.1%; >2 m: 1.7%.

1.10.1 Alkaline Silicate Dykes

Alkaline dykes of the Alnö area comprise pyroxenite dykes, nephelinite dykes, phonolite dykes and trachyte dykes. In total, 76 alkaline silicate dykes have been registered.

Pyroxenite dykes on the mainland north of Alnö, in the Söråker area (two observations), show augitic pyroxene as principal constituent. Possibly, three parallel dykes in a railway cutting north of the delta (N62°32'54.4"—E17°26'50.6"), the "stavrites" of von Eckermann (1948) fall into this group as well. Their composition is, however, altered into amphibole and chlorite mineralogy.

Nephelinite dykes have been found north of Hartung on Alnö (by now in a "disappeared" geological locality, N62°28'10.3"—E17°25'39.9"), and at Fagervik on the mainland north-west of Alnö (von Eckermann 1948). They are porphyritic, with megacrysts of nepheline and often melanite garnet in a matrix composed of nepheline, melanite and clinopyroxene (aegirine-augite). Their matrix is often hydrated or carbonated.

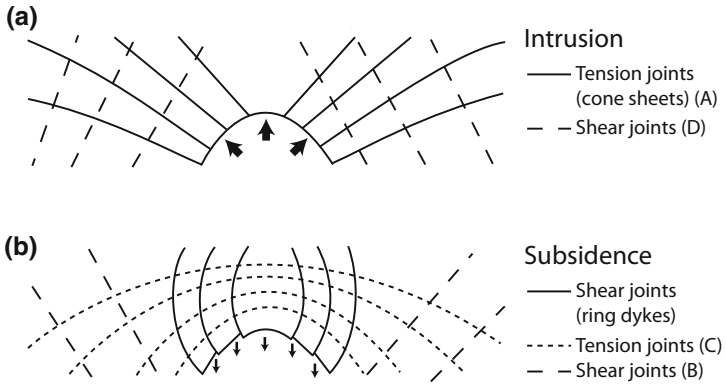

Fig. 1.15 Proposed model for the emplacement of Alnö dykes during **a** updoming and intrusion of magma and **b** during subsequent subsidence. Relative frequency of occurrece is: A (most frequent)-C-B-D (least frequent). After Kresten (1980)

Phonolite dykes are characterized by reddish grey colour, usually with laths of nepheline set in a fine-grained matrix composed of alkali feldspar, nepheline and some clinopyroxene (sodic augite). Quite often they have the "sound quality" that their name indicates. They are the most common alkaline dykes with some thirty observations recorded. They are notably also common in the Fagervik area (von Eckermann 1948). On Alnö, they can, for example, be found in outcrop some 150 m south of the jetty at Ås (see Chap. 4).

Trachyte dykes have a brick-red to brownish red colour and commonly display a fine-grained matrix. The trachytes are frequently aphanitic with occasional phenocrysts of alkali feldspar. Many trachytes contain blebs of violet, greenish or grey fluorite and/or calcite e.g. at the type occurrence of "borengite" at Båräng; an aphanitic trachyte (von Eckermann 1960a) (see Chap. 4).

The intrusion pattern of nephelinite, phonolite and trachyte dykes is quite specific and distinct from the other dykes of the region. They appear in an orthogonal pattern of N30°W and N60°E, dipping from ~60° to vertical. All three lithological types can occur in the same fracture zone, such as within the dyke swarm stretching from Röde via Närsta to north of Hartung, often arranged "*en echelon*". This pattern, contrasting the ones for carbonatite or alnöite dykes, could be interpreted as following pre-existing fractures in the wall-rocks, especially as these dykes have so far been almost exclusively recorded to occur within the wall-rock (e.g. Fagervik, NW Alnö) or in the low-grade fenites of the aureole. This realisation implies that the alkaline silicate dykes have probably been amongst the earliest dykes to intrude at Alnö.

1.10.2 Carbonatite Dykes

Alvikites (called after "Alvik" on Alnö; von Eckermann 1948) are calcite carbonate dykes. They are commonly very fine-grained and their colour varies from white, grey, greyish brown to almost black, reflecting the variable mineral composition. This comprises, besides dominating calcite (>70 vol.%), also biotite, apatite, magnetite and pyrite. Alvikites proper are represented by 148 recorded field occurences.

With increasing contents of mainly biotite they grade into lamprophyric compositions, and some workers speak of "silico-alvikites", "alvikitic alnöites", but many use simplified terminology such as "*carbonatite dykes*". These are the most common dykes of the area, with 601 recorded observations. Remarkably, an alvikitic alnöite dyke near a motel N of Sundsvall (N62°24'47.9"—E17°20'39.2") contained xenocrysts of chromium-rich pyrope garnets (Kresten 1976a).

Beforsites, named after Bergeforsen on the mainland (von Eckermann 1948), are carbonatite dykes with dominating dolomite (more rarely, ferrodolomite), being the hypabyssal counterpart of the rauhaugites of Fen (Brøgger 1921), a rock which has not been found within the Alnö complex. Besides dolomite, the beforsites contain a variety of exotic minerals, rich in barium, the rare earths, or thorium. One could further distinguish between "apatite beforsites" with up to 40 vol.% of apatite, and those with up to 10 vol.% barite, and 5% REEs. These are obviously very highly evolved rocks and common constituent is potassium feldspar, as there seems to be to some extent a gradation between beforsites and trachytes via "carbonated trachytes". Beforsites occur subordinate to calcite carbonatites with 78 observations (compared to the >600 calcite-dominated carbonatite dykes). However, what they lack in number, they compensate by size: the widest carbonatite dykes are beforsites, spanning up to several metres, e.g., the dyke at the road cutting near Töva (N62°22'35.1"—E17°07'33.1"), about 12 km west of Sundsvall. Another wide beforsite dyke is found at Bänkåsviken (N62°21'40.0"—E17°28'29.2") on the southern coast of Alnö. Why these massive dykes occur at greater distance from the supposed centre of magmatic activity has not yet been resolved.

1.10.3 Alnöites

Alnöite is an ultramafic lamprophyre (UML; Rock 1991), a term originally coined by Kresten et al. (1981) for the Kalix dykes. The term replaces Streckeisen's (1979) "melilitic lamprophyres" because melilite-rich and melilite-free lamprophyres commonly coexist (Rock 1986). Within the UML group, we even find the damkjernite, a nepheline-bearing ultramafic lamprophyre of the Fen area (Brøgger 1921).

Alnöites of Alnö are usually composed of large phenocrysts of phlogopitic mica, magnetite and, more rarely, clinopyroxene or amphibole (hastingsite), in a fine-grained dark to medium grey to sometimes reddish-grey matrix. The matrix is made up of mica, magnetite, calcite ($\leq 30\%$), perovskite, apatite, melanite and, in some cases, melilite. The original definition of alnöite as being a melilite-bearing lamprophyre (Rosenbusch 1887) is just one rock among several similar types that occur on Alnö. Some alnöite dykes are carrying abundant xenoliths (fenites, sövites, wall-rocks, deep crustal granulites and eclogite) and are then called alnöite breccias (e.g. see at Hovid Chap. 4). Note that alnöites may give rise to contact fenites, as opposed to kimberlitic alnöites, which do usually not display this type of contact reaction.

Aeromagnetic maps (17H, SGU 1997) show several small positive anomalies particularly in the area north and north-east of Söråker. Some of the small anomalies have been investigated and have turned out to be alnöite "pipes", measuring some 10 m across. Attempts to recover diamonds from those rocks have failed (see Chap. 2).

1.10.4 Kimberlitic Alnöites (Parakimberlites)

Kimberlitic alnöites have phenocrysts of olivine and phlogopite in a matrix of olivine, phlogopite, serpentine, perovskite, diopside, amphibole, ilmenite, chromite, magnetite, Ti-andradite, apatite, little calcite and occasional melilite. Some samples even indicate the presence of diatreme- or crater-facies rocks in the area (Scott-Smith 1985).

An important feature that separates these rocks from alnöites proper is the frequent occurrence of ultramafic xenoliths (Griffin and Kresten 1987), measuring 5–25 cm along the longest, 2–10 cm along the shorter axis. Most of them have dunitic composition and granoblastic texture. Some are wehrlites with 5–20 vol.% of Cr-diopside. All of the nodules contain spinel (picotites, Cr-pleonastes, Ti-magnetites) and most of them contain picroilmenite (4–12% MgO). Phlogopite, with Cr_2O_3 contents in the range of 0.2–1.3% is found in subordinate amounts in most xenoliths. Sulphides with compositions very near FeS are common accessories. They are interpreted as re-equilibrated pyrrhotite or troilite solid solutions. Contacts between xenoliths and host rock are often sharp. In some cases, however, re-equilibration within a crustal magma chamber is indicated by abundant melilite in the matrix, and dunite xenoliths that are rimmed by monticellite, and wehrlites by monticellite and melilite (Griffin and Kresten 1987). Equilibration conditions as deduced from spinel-ilmenite exsolutions range from 760 °C, log f_{O2} = −13.5 bar, to 1100 °C, log f_{O2} = −9 bar, using the Buddington and Lindsley (1964) calibration. Oxygen fugacities are thus slightly above the FMQ buffer.

As opposed to alnöites proper, and most other Alnö rocks, no dykes have been found cross-cutting the kimberlitic alnöites. Thus, they appear to be among the youngest rocks in the area. Most of the kimberlitic alnöites have been found in the form of glacial boulders. These are common along the shore of Ås bay and Ås jetty (see Chap. 4). A particularly large boulder, measuring some 2 m across, was found in the bay about 200 m south of Ås jetty. Many of the boulders from there, however, have been consumed when investigating the rocks here for their diamond potential (see Chap. 2).

1.10.5 Melilitite Dykes

Melilitite dykes seem not directly related to the alnöites, and occur occasionally in the northern parts of Alnö Island. They resemble the melilitites of the Sälskär vent in composition, but with much higher melilite contents (up to 80% by volume). The matrix contains ample spinel minerals (e.g., picotite). In the field, they appear as greyish black, fine-grained dykes that usually cross-cut both fenites and pyroxenites (e.g., von Eckermann 1948). In their appearance they may easily be confused with the dolerite dykes of the area. Notably, the melilitite dykes are commonly not intersected by other dykes and rank thus also amongst the youngest sheet intrusions in the Alnö complex.

1.10.6 Miscellaneous Dykes and Veins

Barite deposits, originating from late hydrothermal dykes, are found at Pottäng and Hartung. Coarse flaky, white to pinkish barite makes up most of the rock there. Other phases present, but in smaller quantities are calcite, fluorite (white, yellow, greenish, and violet), pyrite, chlorite and goethite. At Pottäng, movements in connection with the deposition of barite are indicated by slickensides (horizontal) and mylonitic zones (vertical). Both deposits have been mined during WWII and at Pottäng, over 6300 tonnes of barite have been extracted according to the existing records. Minor barite veins are also found near Röde and on the mainland near Söråker. In addition, another major barite dyke was recently discovered by members of the Sundsvall Geological Society.

In the fenite aureole at the old sövite quarry near Smedsgården, a narrow dyke composed of magnetite and some mica occurs (Kafkas 1976). Near Stavsätt, an apatite-rich dyke occurs (about 27% P_2O_5), with some sphene and natrolite. The dyke is slightly radioactive.

Hydrothermal veins would have formed during a late stage in the history of the complex. Calcite veins occur sporadically. Fluorite-rich dykelets or veins, some are botryoidal with Fe-rich carbonates, have been found along the east coast of Alnö, e.g. near Grönviken.

Somewhat surprising might be the occurrence of quartz veins in the Alnö environment. Near Stolpås, colourless quartz crystals, radiating goethite needles and aragonite occupy cavities in high-grade fenite. Along the road from Släda to Nedergård, along the boundary between quartz-free and quartz-bearing fenites, frequent cracks have been filled with (smoky) quartz, aragonite, calcite and

goethite. Although at a distance to the main complex, late horizontal movements here are indicated by slickensides.

1.11 Mode of Emplacement

1.11.1 Emplacement of Carbonatite Dykes and Lamprophyres

The classic model for the emplacement of Alnö dykes was created by von Eckermann (1939). At a meeting of the Geological Society in Stockholm, he reported that "basic dykes" (alnöites, nephelinites, melilite basalts) commonly occupy vertical, from the eruptive centre radiating joints, and alvikite dykes define cone-sheets that show progressively increased dips closer to the centre. Beforsites occur both as radial dykes and cone-sheets but with steeper dips than alvikites. He also suggested a stratification of the magma chamber which he changed some years later (von Eckermann 1942) to a magma column with increasing density (top: calcitic carbonate; bottom: alnöite). In this paper, he also introduced the "central sövite core" (located off the northern coast of Alnö).

In his *Alnö Memoir* (von Eckermann 1948), he slightly revised the cone sheet pattern with the alvikites having a more distinct focus at about 2 km depth, while the beforsites intersections scatter at around 7 km depth. He omitted several dykes shown in the previous version, e.g., all beforsites at distances greater than 8 km.

The projection of the dykes from the Fagervik and Östrand tunnels were later additions (von Eckermann 1958) and define apparent foci at 2, 3.5, and 6–7 km depth, the second focus being more subordinate. They are interpreted as foci for alvikites, magnesian alvikites, and beforsites (von Eckermann 1966) and include two sets of radial dykes related to the foci at 2 and $\sim$7 km depth, distinguished by the presence of ankerite in radial dykes related to the deeper focus. In his last contribution to the subject (von Eckermann 1974), he presented his dyke centres and the "central sövite core" in a comprehensive and very convincing manner.

Von Eckermann's model has found many followers (e.g. Garson 1965, 1966; Le Bas 1977). The increased complexity of his model is superseded by those he inspired, like the spiral structure of cone sheet emplacement proposed for Homa Mountain, Kenya (Flegg et al. 1977), where a series of suggested foci are represented by as little as 3–6 cone sheets each. Mathematical models for the cone sheet intrusion pattern have been devised (cf. Bahat 1979) and experimentalists have

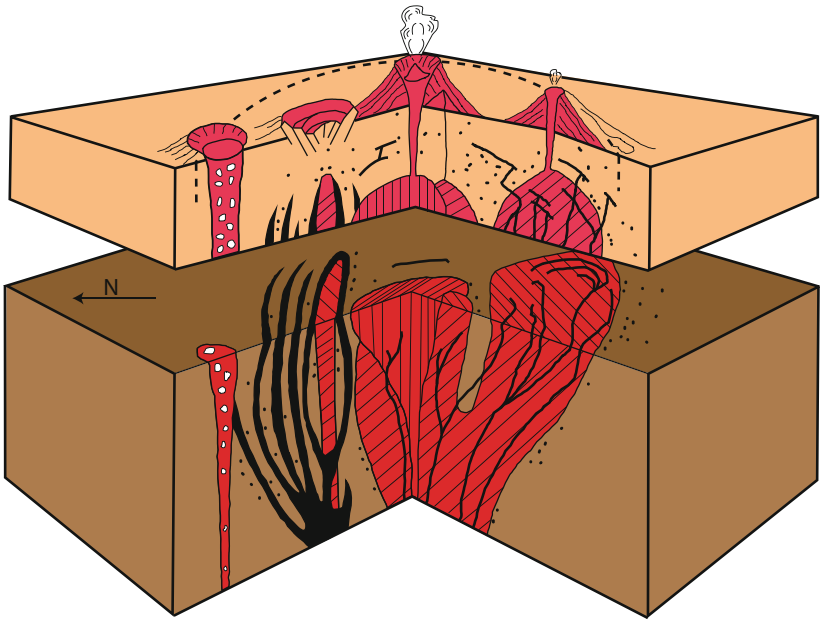

Fig. 1.16 Block diagram of the Alnö complex and satellite intrusions after Kresten (1990)

tried to reproduce the cone sheet pattern, either with nitro-glycerine in Plexiglas (Tallbacka 1968a), or with air blown into sand (Mulugeta 1982), but in both cases with limited success.

Remapping of the Alnö Complex and its surroundings commenced in 1974 by Peter Kresten and assistants. It became soon evident that von Eckermann's model and what could be seen in nature was not strictly identical. Ground magnetometric measurements (Kresten 1976b) revealed that the suggested "centre" was actually outside of the complex. Many dykes that appeared not to fit the model had been omitted and all dykes that were outward dipping from the "centre" were not considered for one reason or another. The need for a revised model was pressing.

An alternative emplacement model was eventually presented by Kresten (1979, 1980, 1990) (Fig. 1.15). The dykes were considered to emanate from the complex

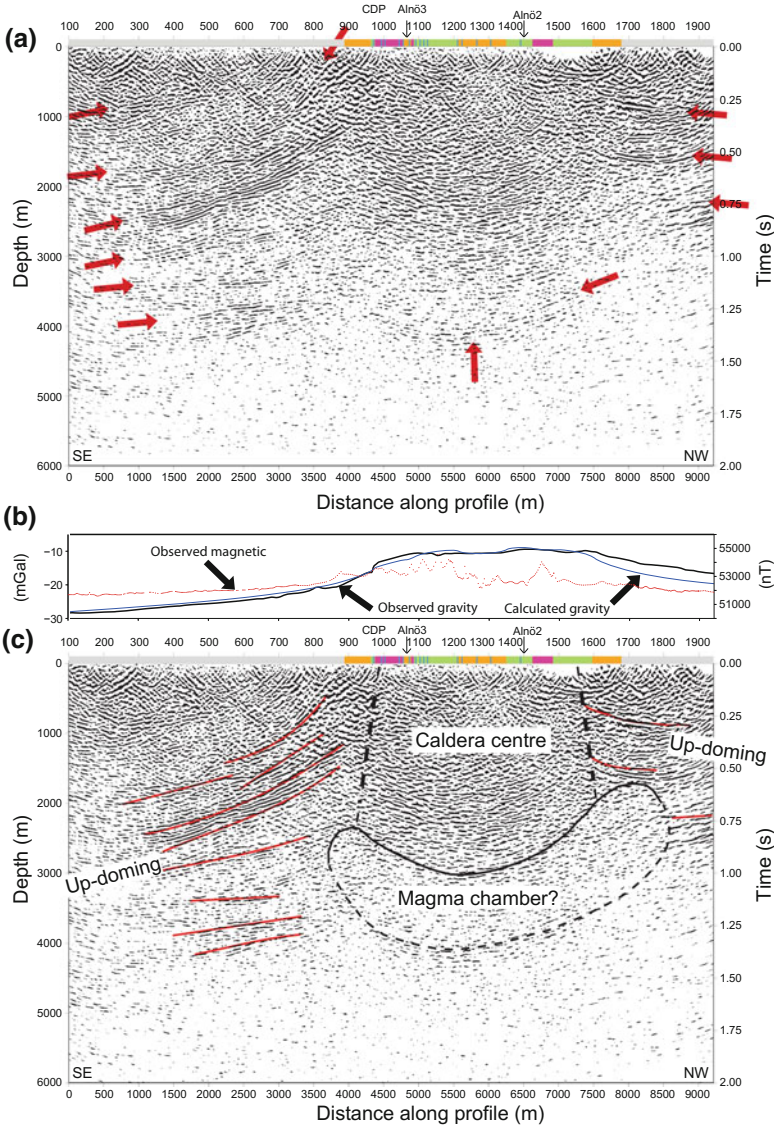
(a)
CDP
Alnö3
Alnö2
Depth (m)
Time (s)
SE
NW
Distance along profile (m)
(b)
(mGal)
(nT)
Observed magnetic
Observed gravity
Calculated gravity
(c)
Caldera centre
Up-doming
Up-doming
Magma chamber?
Depth (m)
Time (s)
SE
NW
Distance along profile (m)

◀ **Fig. 1.17** Seismic section over Alnö after Andersson et al. (2013), with an indication of supporting gravity and magnetic data **a** uninterpreted; **b** gravity and magnetic data; **c** interpreted. Surface geology (as in Fig. 1.8) is shown along the top of the seismic profile. A complex reflectivity pattern extends down to a depth of about 3 km. The transparent zone below this depth represents the likely location of the magma chamber from which carbonatite dykes were fed. Gently to steeply dipping reflections observed in the southern and northern parts of Alnö represent up-doming structures (solid red lines in **c**) associated with a saucer-shaped magma chamber. The boundary between the dipping reflectors outside the igneous complex and the chaotic interior is marking the position of a ring-fault system (steep dashed black lines). The gravity modelling along the seismic profiles (below) is consistent with the seismic interpretation that the main intrusion (former magma chamber) has a maximum vertical extent of ~1 km and resides at depth of about 3–4 km

as a whole and not from specific "foci". For geometric projections, an arbitrary centre was selected. Within the cone-sheet system, four groups were distinguished:

(1) Inward-dipping dykes with shallow to moderate dips (<45°). True cone-sheets in tension joints during intrusive phase.
(2) Inward-dipping dykes with steep dips (about 60–80°). True cone-sheets in shear joints during subsidence phase.
(3) Outward-dipping dykes with shallow dips (<30°). Tension joints during subsidence phase.
(4) Outward-dipping dykes with steeper dips (>45°). Shear joints during intrusive phase.

This emplacement model (Fig. 1.16) postulates initial up-doming followed by caldera subsidence caused by a single magma chamber that underlies Alnö at shallow depth, and which was the main source of the Alnö ring-complex (Fig. 1.16). It was postulated that the roof of the magma chamber during time of intrusion was less than 2 km deep. Renewed studies of the Alnö dykes have refined these initial views and latest field evidence suggests that early radial dykes do not strictly emanate from a discrete centre, but likely from the complex as a whole (Kresten 1990; Mattsson et al. 2014). Also, alkaline silicate dykes show locally a different pattern of emplacement (see Sect. 1.10.1).

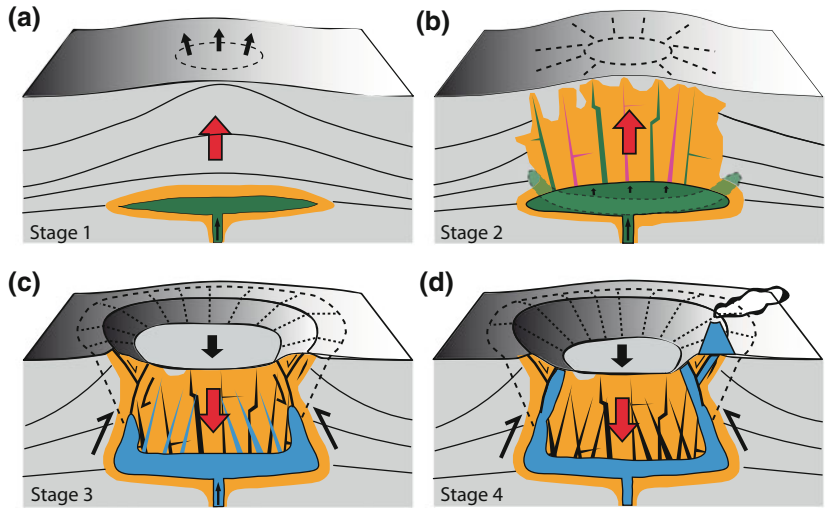

Fig. 1.18 Schematic model of the emplacement of the Alnö complex after Andersson et al. (2013). **a** A low-viscosity silicate magma rich in CaCO3 ascended and was trapped at about 4–5 km depth below the Earth's surface. There, it formed a laterally extensive sill-shaped magma chamber. This initiated up-doming and a surface bulge and caused early radial dykes to intrude. **b** Growth and inflation of this magma chamber increased tumescence of the overburden. Radial dykes and increasingly inward dipping cone-sheets were intruded into the country-rock above the chamber. **c** Magma, now with a significant carbonatite component was progressively evacuated from the magma chamber via dykes, which presumably led to a pressure drop due to material withdrawal, causing the central part of the roof to subside. **d** Concentric outward dipping fractures formed and were intruded to make ring-dykes during subsidence of the central block/roof (caldera collapse). This likely caused the edges of the main chamber to migrate upwards, at which point further carbonatite dykes were intruded into reverse and normal faults in the caldera periphery, likely represented by eruption of carbonatite vent breccias to the north of Alnö Island (e.g. Sälkär breccia, Fig. 1.14)

1.11.2 Emplacement of the Complex as a Whole

Alnö was recently investigated with seismic methods (Andersson et al. 2013) which confirmed that it is characterized by a ring-type structure associated with a central collapse domain that subsided into a shallow, low-viscosity, likely saucer-shaped magma reservoir (Figs. 1.17 and 1.18). The seismic study by Andersson et al. 2013 inferred a main magma reservoir at ~3 km depth and outwards dipping dykes require collapse of a central area as in the ring-dyke model

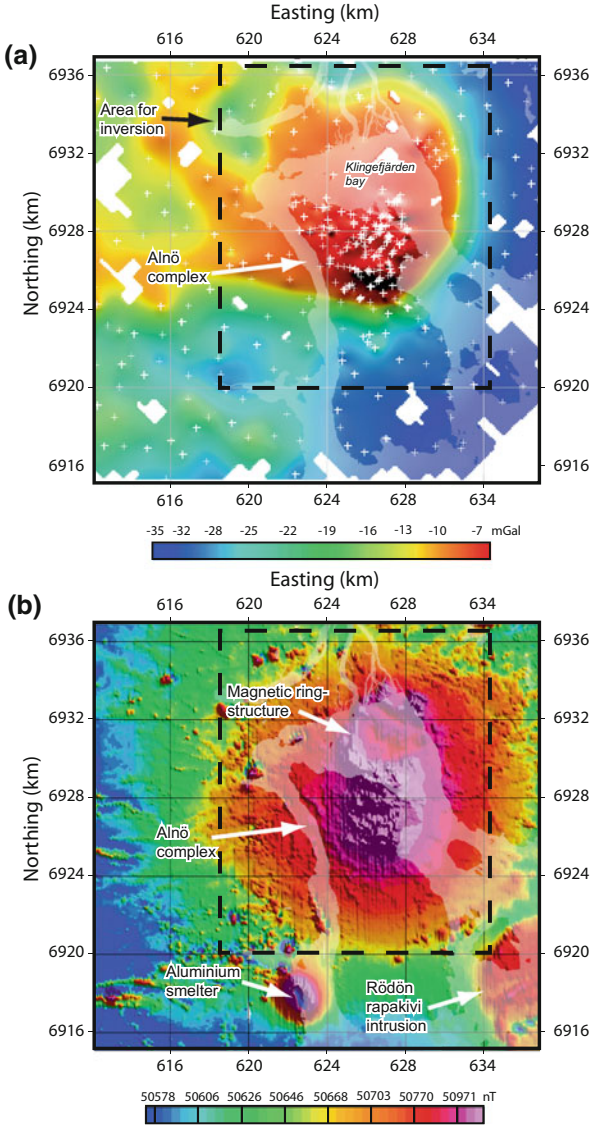
(a)
Easting (km)
616
620
624
628
634
Northing (km)
6936
6932
6928
6924
6920
6916
Area for inversion
Klingefjärden bay
Alnö complex
-35 -32 -28 -25 -22 -19 -16 -13 -10 -7 mGal
(b)
Easting (km)
Magnetic ring-structure
Alnö complex
Aluminium smelter
Rödön rapakivi intrusion
50578 50606 50626 50646 50668 50703 50770 50971 nT

◀ **Fig. 1.19** Gravity and total-field magnetic maps of the Alnö area from Andersson (2015). **a** Bouguer anomaly map showing a major positive gravity anomaly associated with the Alnö igneous complex. "Plus" signs in the map indicate the locations of gravity stations. **b** Total field aeromagnetic map (flight lines 200 m apart in north-south directions and 60 m flight-height) show a major positive magnetic anomaly associated with the Alnö complex. The magnetic anomaly in the south-eastern corner of the map is related to a c. 1.5 Ga rapakivi granite intrusion on Rödön Island (Welin 1994; Andersson 1997). A semi-circular anomaly with about 2 km extent (low magnetic inside high-magnetic area) in the southern part of the map is related to an aluminium smelter. In both maps water surfaces are indicated with pale colour. The rectangle with a dashed line shows the area of the geological map in Fig. 1.8. The colour transition from red to yellow in (**b**) may give an idea of the dimensions of the former Alnö volcano at this depth level

(Figs. 1.17 and 1.18) and a collapsed caldera maybe interpreted from seismic sections. However, no clear relationship between dyke composition and depth of origin is found, but rather a series of centres or magma reservoirs and pockets may have existed throughout Alnö's active time (see also Mattsson et al. 2014).

Figure 1.19a shows a Bouguer anomaly map of the Alnö area. "Plus" signs indicate the locations of gravity stations employed. The gravity stations are about 100 m apart inside and about 1 km apart outside the intrusion area. Figure 1.19b, in turn shows an aeromagnetic map of the area, the flight lines run north-south with 200 m distance between profiles, at a nominal flight-height of 60 m (from Andersson 2015). The magnetic anomaly in the south-eastern corner of the map is related to a rapakivi granite intrusion at Rödön Island (see above). For the Alnö complex a semi-circular anomaly with about 2 km extent (low-magnetic inside high-magnetic area) is indicated. The anomaly in the southern part of the map is related to an aluminium smelter. In both maps water surfaces are indicated with pale colour. Constructed from this data, Fig. 1.20 provides an oblique 3D view of the surface geological map of Northern Alnö and depth slices extracted from the 3D inversion models in Andersson (2015) and in (a) density and in (b) magnetic susceptibility models are shown. Both the gravity and the magnetic inversion models indicate that the main northern and southern intrusions merge at $\sim$1 km depth and that it is unlikely that the intrusion continues below 3.5 km depth. For the area under the bay, the magnetic model is more reliable than the density model because there are no gravity data points in the centre of the bay. The magnetic inversion model delineates a circular low-susceptibility body with a high-susceptibility rim. The low-susceptibility body extends down to about 2 km depth where a higher susceptibility region appears. This may represent a collapse structure (a caldera) with intense ring-intrusions. The density model indicates that

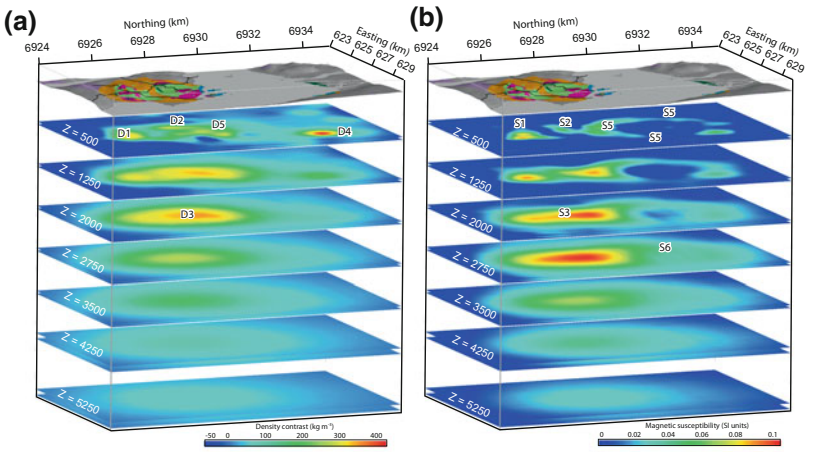

Fig. 1.20 Oblique 3D view from Alnö surface downward using depth slices extracted from the 3D inversion models after Andersson (2015), showing **a** density and **b** magnetic susceptibility. Both the gravity and the magnetic inversion models indicate that the main northern and southern intrusions begin to merge at ~1 km depth (D1/S1 and D2/S2) and that it is unlikely that the intrusion continues below 3.5–4 km depth (D3/S3). For the area under the bay the magnetic model is more reliable than the density model because there are no gravity data points in the centre of the bay. The magnetic inversion model delineates a circular low-susceptibility body with a high-susceptibility rim (S5). The low-susceptibility body extends down to about 2 km depth where the higher susceptibility region (S6) begins to appear. The density model indicates that the satellite-intrusion in Söråker (D4) does not extend as deep as the main intrusion on Alnö Island

the satellite-intrusion in Söråker may not connect with the main intrusion beneath Alnö Island.

Integrating these geophysical data with the latest petrological efforts on the emplacement of the Alnö complex, we believe activity began with an alkaline silicate magma rich in dissolved $CaCO_3$ and associated with CO_2-bearing hydrous fluids (Vuorinen and Skelton 2004). From Sr-, Nd-, and O-isotope data, the mantle source for the Alnö magmas was suggested to have been OIB-like in character (see Chap. 3). The magma likely ascended via a weak zone within the migmatite country- rocks, e.g. a fault-zone in an extensional rift setting (Dahlgren 1994; van Balen and Heeremans 1998; Korja et al. 2001), which may have acted as a conduit

to allow formation of a sill-like magma chamber at some shallow level in the crust (2–4 km depth below the palaeo-surface; see Kresten 1990; Andersson et al. 2013). The complex is encircled by fenite that formed from the transformation of the wall rock with the help of volatiles with high CO_2 content from the intruding carbonatites and alkaline silicate rocks. It is believed that about ≥ 500 m of overburden have been removed by erosion since the time of emplacement (Kresten 1990). Growth and inflation of this crustal magma chamber resulted in considerable up-doming at the land surface and initially produced radial tensile and shear fractures around the central intrusion (e.g. Kresten 1980) (Fig. 1.16). Magma emplacement was associated with intense fenitization of the country rock and ijolites, nepheline-syenites, and pyroxenites intruded initially. The geometry of the magma chamber at this stage may have been already "lopolithic" (Figs. 1.17 and 1.18), but it is also possible that a saucer shape was attained during later collapse, as suggested on the basis of the latest seismic data (e.g. Andersson et al. 2013). Much of the fenitization around the complex also occurred at this stage. Following the initial emplacement, probably due to magma immiscibility of silicate and carbonatite liquids or fractional crystallization, Alnö produced a volumetrically relevant portion of separate carbonatite magma that are likely derived from the alkaline parent liquids (Treiman and Essene 1985; Gittins 1988; Vuorinen and Skelton 2004) and a first generation of alnöites and carbonatites intruded the early radial fractures and the cone-sheet fractures during advanced stages of up-doming. The large concentration of carbonatite dykes in the southern part of the complex (Fig. 1.7), suggests that the magmatic focus lay ultimately beneath this part of the intrusive complex. Progressive dyke intrusions into initially radial and subsequently cone-sheet type fractures led to a pressure drop in the magma reservoir due to chamber evacuation and associated degassing and subsidence along steep to outward dipping concentric faults set in to form a caldera-like structure (cf. Anderson 1937; Kresten 1980; Walter and Troll 2001) (Figs. 1.16 and 1.18). A new generation of carbonatite dykes, longer and thicker in nature, then intruded from the margin of the magma chamber into these steep to outward dipping ring-faults to form the ring-type structure of the Alnö complex exposed today (cf. Kresten 1980; Figs. 1.7, 1.16). Syn-collapse migration of magma from the main magma reservoir into caldera periphery structures led to satellite intrusions around Alnö Island and may have triggered the eruption of carbonatite about 700 m north of Alnö Island in form of the Sälskär vent (Figs. 1.14 and 1.18). If is this plausible that subsidence of the roof of the magma reservoir probably connects the explosive vents in the northern part of the complex with the 'seismically' shattered central region below Alnö (Fig. 1.17), and with the possibly saucer-shaped main magma reservoir at depth, hence linking magma storage,

magma transport and eruption at Alnö (e.g. von Eckermann 1948; Kresten 1980, 1990; Andersson et al. 2013).

Alnö thus evolved through a major caldera cycle, involving up-doming and subsequent subsidence of a shallow crustal magma chamber roof leading to a complex intra-caldera rock association (cf. Kresten 1980; Andersson et al. 2013). A deep seated magma chamber some 10 km below the palaeo-land surface as the origin of the carbonatite dykes and volcanism (von Eckermann 1948) has not been verified so far. Alnö is thus best explained by processes similar to those observed in silicic caldera-type environments where caldera structures are controlled by shallow (<5 km) and frequently sill-like magma chambers (see e.g. Walter and Troll 2001; Troll et al. 2002; Holohan et al. 2008), but in the Alnö case with an unusual (alkaline and carbonatitic) composition. However, the unusual composition seems not to have affected the fundamental volcano-tectonic processes or the broad geometry of traditional caldera volcanism. This geometry may not be unique to Alnö, but instead may be common to carbonatite ring-complexes elsewhere (see Appendix 1). On a more local level, a long-lived shallow magma chamber at Alnö would unfavourably have dissolved diamonds as their survival in kimberlite-type magmas is thought to be a function of very rapid ascent (Russell et al. 2012; Gernon et al. 2012), hence offering an explanation for the unsuccessful diamond exploration at Alnö (see Chap. 2). The Alnö carbonatites may, in the future, perhaps qualify as a viable source rock for REEs, due to their enriched alkaline chemistry, but at present they are likely not an economically viable target (see Chap. 3).

1.12 Late Tectonic Movements

Evidence of late tectonic movements have been found at the Pottäng barite quarry. Immediately south-east of the open pit, a minor barite vein (with goethite and chlorite) is found in the extrapolated extension of the deposit. The small barite vein is heavily slickensided indicating flat outward (from the centre of the main intrusion) and downward movements (340°–05°) as would be expected in connection with the regional subsidence that has been postulated above.

At the south-eastern edge of the complex, similar observations have been made along the road from Släda to Nedergård, in trenches dug for water supply pipes. The pyroxenite and the adjacent fenite are heavily jointed - the open cracks are coated with crystals of (smoky) quartz, needles of goethite and late covers of aragonite. Slickensides again indicated a flat outward movement (350°–05°), and the western block was apparently displaced to the south, thus mirroring the

observations at Pottäng. Lastly, near Stolpås, quartz crystals (with some goethite) have been found in horizontally slickensided quartz-free fenite. These observations are taken as indications of late (based on the mineral paragenesis) shallow outward sliding that probably relates to the final subsidence of the complex.

References

Ahl M, Andersson UB, Lundqvist T, Sundblad K (eds) (1997) Rapakivi granites and related rocks in central Sweden. SGU Forskningsrapporter, Ca87, 99 pp

Ahlberg P (1986) Den svenska kontinentalsockelns berggrund. Sammanfattning av tillgängliga undersökningar. Sver Geol Unders Rapp Medd 47

Anderson EM (1937) Cone-sheets and ring-dykes: the dynamical explanation. Bull Volc 1:35–40

Andersson M, Almqvist B, Burchardt S, Troll V, Malehmir A, Snowball I, Kübler L (2016) Magma transport in sheet intrusions of the Alnö carbonatite complex, central Sweden. Sci Rep 6(1)

Andersson M (2015) 3D structure and emplacement of the Alnö alkaline and carbonatite complex, Sweden. Academic Dissertation (PhD), Uppsala University

Andersson M, Malehmir A, Troll VR, Dehghannejad M, Juhlin C Ask M (2013) Carbonatite ring-complexes explained by caldera-style volcanism. Sci Rep 3(1)

Andersson UB (1997) Petrogenesis of some Proterozoic granitoid suites and associated basic rocks in Sweden (Geochemistry and Isotope Geology). Sveriges Geol undersökning Rm 91:1–216

Axberg S (1980) Seismic stratigraphy and bedrock geology of the Bothnian Sea, northern Baltic. Stockh. Contrib. Geol. XXXVI(3): 153–213

Bahat D (1979) Interpretation on the basis of Hertzian theory of a spiral carbonatite structure at Homa Mountain, Kenya. Tectonophysics 69:235–246

Berwerth F (1893) Ueber Alnöit von Alnö. Annalen des Naturhist Museums Wien 8(H. 3–4):440–454

Brøgger WC (1921) Die Eruptivgesteine des Kristianiagebietes. IV. Das Fengebiet in Telemark, Norwegen. Videnskapsselsk. Skr.I, Mat.naturv.Kl. 1920, No 9

Brueckner HK, Rex DC (1980) K–Ar and Rb–Sr geochronology and Sr isotopic study of the Alnö alkaline complex, northeastern Sweden. Lithos 13:111–119

Buddington AF, Lindsley DH (1964) Iron titanium oxide minerals and synthetic equivalents. J Petrol 5(310):357

Claesson S, Lundqvist T (1990) Svecofennian granites in the Bothnian Basin, Central Sweden. Abstract, 19. Nordiske Geologiske Vintermöte, Stavanger

Dahlgren S (1994) Late Proterozoic and Carboniferous ultramafic magmatism of carbonatitic affinity in southern Norway. Lithos 31:141–154

Dahlström A, Cousins SA, Eriksson O (2006) The history (1620–2003) of land use, people and livestock, and the relationship to present plant species diversity in a rural landscape in Sweden. Environment History 12:191–212

Dasmann RF (1972) Towards a system for classifying natural regions of the world and their representation by national parks and reserves. Biol Cons 4:247–255

Dawson JB (2012) Nephelinite-melilitite-carbonatite relationships: evidence from Pleistocene-recent volcanism in northern Tanzania. Lithos 152:3–10
Dawson JB (1962) Sodium carbonate lavas from Oldoinyo Lengai, Tanganyika. Nature 195:1075–1076
Doig R (1970) An alkaline rock province linking Europe and North America. Can J Earth Sci 7(1):22–28
Donaldson C, Henderson C (1988) A new interpretation of round embayments in Quartz crystals. Mineral Mag 52(364):27–33
Downes H, Balaganskaya E, Beard A, Liferovich R, Demaiffe D (2005) Petrogenetic processes in the ultramafic, alkaline and carbonatitic magmatism in the Kola Alkaline Province: a review. Lithos 85:48–75
Fischer T, Burnard P, Marty B, Hilton D, Füri E, Palhol F, Sharp Z, Mangasini F (2009) Upper-mantle volatile chemistry at Oldoinyo Lengai volcano and the origin of carbonatites. Nature 459(7243):77–80
Flegg AM, Clarke MCG, Sutherland DS, Le Bas MJ (1977) Homa Mountain II: The main carbonatite centre. In: Le Bas MJ (ed) Carbonatite-Nephelinite volcanism. Wiley, pp 222–232
Garson MS (1966) Carbonatites in Malawi. In: Tuttle OF, Gittins J (eds) Carbonatites. Interscience Publishers, pp. 33–71
Garson MS (1965) Carbonatites in southern Malawi. Geol Surv Malawi Bull 15, 128 p
Gernon TM, Brown RJ, Tait MA, Hincks TK (2012) The origin of pelletal lapilli in explosive kimberlite eruptions. Nature Commun 3(832):1–7
Gittins J (1989) The origin and evolution of carbonatite magmas. In: Bell K (ed) Carbonatites. Genesis and evolution, Unwin Hyman, London, pp. 580–600
Gittins J (1988) The origin of carbonatites. Nature 335:295–296
Gresens RL (1967) Composition-volume relationships in metasomatism. Chem Geol 2:47–65
Griffin WL, Kresten P (1987) Scandinavia—the carbonatite connection. In: Nixon PH (ed) Mantle Xenoliths. Wiley, pp 101–108
Haslinger E, Ottner F, Lundstrom US (2007) Pedogenesis in the Alnö carbonatite complex, Sweden. Geoderma 142:127–135
Hay RL (1978) Melilitite-carbonatite tuffs in the Laetolil Beds of Tanzania. Contrib Mineral Petrol 67:357–367
Henkel H, Puura V, Flodén T, Kirs J, Konsa M, Preeden U, Lilljequist R, Fernlund J, (2005) Åvike Bay a 10 km diameter possible impact structure at the Bothnian Sea Coast of Central Sweden. In: Koeberl C, Henkel H (eds) Impact tectonics. Springer, Heidelnerg, pp 323–340
Hisinger W (1808) Samling till en mineralogisk geografi öfver Sverige. H. A. Nordström, Stockholm
Högbom AG (1895) Über das Nephelinsyenitgebiet auf der Insel Alnö. Geol Fören Stockh Förh 17(100–160):214–256
Holmquist PJ (1899) Om Rödöområdets rapakivi och gångbergarter. Mit einem Resumé in deutscher Sprache. SGU C181
Holohan EP, Troll VR, van Wyk de Vries B, Walsh JJ, Walter TR (2008) Unzipping long valley: an explanation for vent migration patterns during an elliptical ring fracture eruption. Geology 36:323–326

Jones AP, Genge M, Carmody L (2013) Carbonate melts and carbonatites. Rev Mineral Geochem 75(10):289–322
Kafkas Y (1976) A magnetite dyke in the Alnö complex. Geol Fören Stockh Förh 98:362–363
Keller J (1989) Extrusive carbonatites and their significance. In: Bell K (ed) Carbonatites: genesis and evolution. Unwin Hyman, pp 70–88
Keller J, Hoefs J (1995) Stable isotope characteristics of recent natrocarbonatites from Oldoinyo Lengai. In: Bell K, Keller J (eds) Carbonatite volcanism: Oldoinyo Lengai and the petrogenesis of natrocarbonatites. Springer, Heidelberg, pp 113–123
Korja A, Heikkinen P, Aaro S (2001) Crustal structure of the northern Baltic Sea palaeorift. Tectonophysics 331:341–358
Kresten P (1994) Chemistry of fenitization at Fen, Norway and Alnö, Sweden. In: Meyer HOA, Leonardos OH (ed) Proceedings of the fifth international kimberlite conference on Kimberlites, Related Rocks and Mantle Xenoliths, Araxá, Brazil 1991, pp 252–262
Kresten P (1990) Alnöområdet. In: Lundqvist T, Gee D, Kumpulainen R, Karis L, Kresten P (eds) Beskrivning till berggrundskartan över Västernorrlands län. Sveriges geologiska undersökming, ser Ba, 31, 238–278
Kresten P (1988) The chemistry of fenitization: examples from Fen, Norway. Chem Geol 68:329–349
Kresten P (1984) Alnöområdets geologi. Svenska Turistforeningens Årsskrift 1984:208–221
Kresten P (1980) The Alnö complex: tectonics of dyke emplacement. Lithos 13:153–158
Kresten P (1979) The Alnö complex: discussion of the main features, bibliography and excursion guide. Nordic Carbonatite Symposium, Alnö
Kresten P (1976a) Chrome pyrope from the Alnö complex. Geol Fören Stockh Förh 98:179–180
Kresten P (1976b) A magnetometric survey of the Alnö complex. Geol Fören Stockh Förh 98:361–362
Kresten P, Morogan V (1986) Fenitization at the Fen complex, southern Norway. Lithos 19:27–42
Kresten P, Nairis HJ (1982) Alnö diamonds. Geol Fören Stockh Förh 104, 210
Kresten P, Åhman E, Brunfelt AO (1981) Alkaline ultramafic lamprophyres and associated carbonatite dykes from the Kalix area, northern Sweden. Geol. Rundsch 70:1215–1231
Kresten P, Printzlau T, Rex DC, Vartiainen H, Woolley A (1977) New ages of carbonatite and alkaline ultramafic rocks from Sweden and Finland. Geol Fören Stockh Förh 99:62–65
Le Bas MJ (1977) Carbonatite-Nephelinite volcanism. Wiley
Le Maitre RW (2002) Igneous rocks. A classification and glossary of terms. In: Recommendations of the international union of geological sciences subcommission on the systematics of igneous rocks, 2nd edn. Cambridge University Press, New York
Lidmar-Bergström K (1986) Tolkning av kartan "Sveriges relief" (1:2000000). Lantmäteriverket, Gävle
Lundqvist T, Gee DG, Kumpulainen R, Karis L, Kresten P (1990) Beskrivning till Berggrundskartan över Västernorrlands Län. SGU Ba 31

Mattsson T, Burchardt S, Troll V, Kresten P (2014) The sub-volcanic structure of the Alnö carbonatite complex, Sweden. In: Geophysical Research Abstracts, vol 16, EGU2014-16633

Meert GJ, Torsvik TH, Eide EA, Dahlgren S (1998) Tectonic Significance of the Fen Province, S. Norway: constraints from geochronology and paleomagnetism. J Geol 106:553–564

Meert JG, Walderhaug HJ, Torsvik TH, Hendriks BWH (2007) Age and paleomagnetic signature of the Alnø carbonatite complex (NE Sweden): Additional controversy for the Neoproterozoic paleoposition of Baltica. Precambr Res 154:159–174

Mitchell RH (2005) Carbonatites and carbonatites and carbonatites. Canadian Mineralogist 43:2049–2068

Morogan V (1989) Mass transfer and REE mobility during fenitization at Alnö, Sweden. Contrib Mineral Petrol 103:25–34

Morogan M, Lindblom S (1995) Volatiles associated with the alkaline-carbonatite magmatism at Alnö, Sweden: a study of fluid and solid inclusions in minerals from the Långarsholmen ring complex. Contrib Miner Petrol 122:262–274

Morogan V, Woolley AR (1988) Fenitization at the Alnö carbonatite complex, Sweden: distribution, mineralogy and genesis. Contrib Miner Petrol 100:169–182

Mulugeta G (1982) Experimental test models, simulating cone-sheet, radial and ring-type fractures, UUDMP research report (Uppsala universitet. Mineralogisk-petrologiska avdelningen), no. 32

Nelson DR, Chivas AR, Chappell BW, McCulloch MT (1988) Geochemical and isotopic systematics in carbonatites and implications for the evolution of ocean-island sources. Geochim Cosmochim Acta 52:1–17

Phipps SP (1988) Deep rifts as sources for alkaline intraplate magmatism in eastern North America. Nature 334:27–31

Roberts RJ, Corfu F, Torsvik TH, Hetherington CJ, Ashwal LD (2010) Age of alkaline rocks in the Seiland Igneous Province, Northern Norway. J Geological Soc 167:71–81

Rock NMS (1991) Lamprophyres. Blackie and Son Ltd

Rock NMS (1986) The nature and origin of ultramafic lamprophyres: alnöites and allied rocks. J Petrol 27:155–196

Roopnarain Sherissa (2013) Petrogenesis of carbonatites in the Alnö complex, Central Sweden. Master thesis, Uppsala University, p 108

Rosenbusch H (1887) Mikroskopische Physiographie der Minerialen und Gesteine. II. Massige Gesteine. Schweizerbart, Stuttgart

Rukhlov AS, Bell K (2010) Geochronology of carbonatites from the Canadian and Baltic shields, and the Canadian cordillera: clues to mantle evolution. Miner Petrol 98:11–54

Russell JK, Porritt LA, Lavallée Y, Dingwell DB (2012) Kimberlite ascent by assimilation-fuelled buoyancy. Nature 481:352–357

Schumacher R, Schmincke H-U (1995) Models for the origin of accretionary lapilli. Bull Volcanol 56:626–639

Scott-Smith BHS (1985) Brief petrography of some parakimberlites from Alnö, Sweden. Report No. SSP-85-7 (unpublished)

SGU (1997) Aeromagnetic map 17H Sundsvall

Shafer CL (1990) Nature reserves: Island theory and conservation practice. Smithsonian Institution Press, Washington, p 189

Skelton A, Vuorinen JH, Arghe F, Fallick A (2007) Fluid-rock interaction at a carbonatite-gneiss contact, Alnö, Sweden. Contrib Miner Petrol 154(1):75–90
Skordas E, Meyer K, Olsson R, Kulhanek O (1991) Causality between interplate (North Atlantic) and intraplate (Fennoscandia) seismicities. Tectonophysics 185:295–307
Söderström (Tallbacka) L (1966) The kimberlites of Åvike Bay, on the Bothnian coast of Sweden. Geol Fören Stockh Förh 88:351–360
Statens industriverk (1980) Berg och malm i Västernorrlands län. SIND PM 1980:18
Streckeisen A (1979) Classification and nomenclature of volcanic rocks, lamprophyres, carbonatites and melilitic rocks. N. Jb. Mineral Abh 134:1–14
Streckeisen A (1976) To each plutonic rock its proper name. Earth Sci Rev 12(1):1–33
Swedish Local Heritage Federation (Swedish Heritage Archives) (2012) History of Alnö: the Alnö rural museum archives. Sveriges Hembygdsförbund, Stockholm, 112
Tallbacka L (1968a) A tectonic study of the Alnö Island Åvike Bay region, northern Sweden. Lic. thesis, Dep. Mineral., Univ. Stockholm
Tallbacka L (1968b) A petrographic and mineralogic study of the carbonatitic kimberlitic occurrences within the Åvike Bay region, northern Sweden. Lic. thesis, Dep. Mineral., Univ. Stockholm
Törnebohm AE (1883) Mikroskopiska bergartsstudier; XVIII Melilitbasalt från Alnö. GFF 76: 240–251
Torsvik TH, Smethurst MA, Meert JG, van der Voo R, McKerrow WS, Brasier MD, Sturt BA, Walderhaug HJ (1996) Continental break-up and collision in the Neoproterozoic and Palaeozoic—a tale of Baltica and Laurentia. Earth Sci Rev 40(3–4):229–258
Treiman AH, Essene EJ (1985) The Oka carbonatite complex, Quebec: geology and evidence for silicate-carbonate liquid immiscibility. Am Miner 70:1101–1113
Troll VR, Walter TR, Schmincke HU (2002) Cyclic caldera collapse: piston or piecemeal subsidence? Field and experimental evidence. Geology 30:135–138
van Balen RT, Heeremans M (1998) Middle Proterozoic–early Palaeozoic evolution of central Baltoscandian intracratonic basins: evidence for asthenospheric diapirs. Tectonophysics 300:131–142
Vartiainen H, Woolley R (1974) The age of the Sokli carbonatite, Finland, and some relationships to the North Atlantic alkaline igneous province. Bull Geol Soc Finl 46:81–91
von Eckermann H (1974) The chemistry and optical properties of some minerals of the Alnö alkaline rocks. Arkiv Mineral Geol 5(8), 93–210
von Eckermann H (1966) Progress of research on the Alnö carbonatite. In: Tuttle OF, Giltins J (eds) Carbonatites, Interscience, Publication, Wiley, pp. 3–31
von Eckermann, H. (1960a) Borengite. A new ultra potassic rock from Alnö Island. Arkiv Mineral Geol 2(39), 519–528
von Eckermann H (1960b) Boulders of volcanic breccia at the Sälskär shoals north of Alnö Island. Arkiv Mineral Geol 2(40):529–537
von Eckermann H (1958) The alkaline and carbonatitic dikes of the Alnö formation on the mainland north-west of Alnö Island. Kungliga Svenska Vetenskapsakademiens Handlingar IV, 7, Nr 2. 61 pp
von Eckermann H (1948) The alkaline district of Alnö Island. Sver Geol Unders Ca 36:176
von Eckermann H (1945) Contributions to the knowledge of the jotnian rocks of the Nordingrå-Rödö Region. IV-X. Geol Fören Stockh Förh 67:54–66

von Eckermann H (1942) Ett preliminärt meddelande om nya forskningsrön inom Alnö alkalina område. Geol Fören Stockh Förh 64:399–455
von Eckermann H (1939) De alkalina bergarternas genesis i belysning av nya forskningsrön från Alnön. Geol Fören Stockh Förh 61:142–151
von Eckermann H, Wickman FE (1956) A preliminary determination of the maximum age of the Alnö rocks. Geol Fören Stockh Förh 78:122–124
Vuorinen JH, Hålenius U, Whitehouse MJ, Mansfeld J, Skelton ADL (2005) Compositional variations (major and trace elements) of clinopyroxene and Ti-andradite from pyroxenite, ijolite and nepheline syenite, Alnö Island, Sweden. Lithos 81:55–77
Vuorinen JH, Skelton ADL (2004) Origin of silicate minerals in carbonatites from Alnö Island, Sweden: magmatic crystallization or wall rock assimilation? Terra Nova 16:210–215
Wallace ME, Green HG (1988) An experimental determination of primary carbonatite magma composition. Nature 335:343–346
Walter TR, Troll VR (2001) Formation of caldera periphery faults: an experimental study. Bull Volcanol 63:191–203
Welin E (1994) The U–Pb zircon age of the Rödön rapakivi granite, central Sweden. Gff 116:113–114. https://doi.org/10.1080/11035899409546169
Welin E (1979) Tabulation of recalculated radiometric ages published 1960–1979 for rocks and minerals in Sweden. Geol Fören Stockh Förh 101:309–320
Welin E, Lundqvist Th (1975) K–Ar ages of Jotnian dolerites in Västernorrland County, central Sweden. Geol Fören Stockh Förh 97:83–88

Alnö Minerals

2

Abstract

Alnö is famed for its unusual richness in rare minerals that often occur in collector quality within and around the Alnö igneous complex. This chapter provides a list of all major mineral phases found in N-Alnö and offers descriptions where important mineral deposits occur and in which rock association they are expected. In addition, the exploration efforts for diamond are summarised. The legendary mineral knopite that was found on Alnö some 100 years ago is also discussed, but remains a matter of debate to the present day.

The great diversity of rocks that occurs within the Alnö area accounts for the multitude of unusual minerals that are found (Table 2.1). Harry von Eckermann's last publication "*The chemistry and optical properties of some minerals of the Alnö alkaline rocks*" was posthumously published in 1974 and gives chemical and optical data on some 35 minerals species and varieties, being the result of "more than 40 years of intermittent labour". Although not complete, he deemed it prudent "on account of old age to publish the investigation as it now stands". The number of analyses presented is 83, which does nowadays not seem too overwhelming, but it has to be remembered that all of those were accomplished using wet-chemical techniques, and much of the costs were carried by von Eckermann himself.

Today, about 130 minerals have been identified in the rocks from Alnö. In the chapter below, the reported minerals are listed and some minerals and mineral groups are subsequently discussed, including both rare and also common phases (Table 2.1, Fig. 2.1).

P. Kresten and V. R. Troll, *The Alnö Carbonatite Complex, Central Sweden*, GeoGuide, https://doi.org/10.1007/978-3-319-90224-1_2

Table 2.1 Minerals reported from Northern Alnö

Mineral	Formula
Elemental occurrence	
Graphite	C
Sulfides	
Arsenopyrite	FeAsS
Chalcopyrite	$CuFeS_2$
Galena	PbS
Gersdorffite	NiAsS
Marcasite	FeS_2
Molybdenite	MoS_2
Pentlandite	$(Fe, Ni)_9S_8$
Mackinawite	$(Fe, Ni)S_{0.9}$
Pyrite	FeS_2
Pyrrhotite 11H, 4C	$Fe_{0.85-1}S$
Troilite	FeS
Sphalerite	ZnS
Valleriite	$4(Fe, Cu)S * 3(Mg, Al)(OH)_2$
Violarite	$Fe^{2+}Ni_2^{3+}S_4$
Halides	
Fluorite	CaF_2
Halite	NaCl
Sylvite	KCl
Oxides	
Aeschynite-(Ce)	$(Ce, Ca, Fe, Th)(Ti, Nb)_2(O, OH)_6$
Anatase	TiO_2
Brookite	TiO_2
Knopite	$(Ca, Ce, Na)(Ti, Fe)O_3$
Perovskite	$CaTiO_3$
Dysanalyte	$(Ca, Ce, Y, Na)(Ti, Nb, Fe)O_3$
Rutile	TiO_2
Columbite group minerals	
Columbite-(Fe)	$Fe^{2+}Nb_2O_6$
Fersmite	$(Ca, Ce, Na)(Nb, Ta, Ti)_2(O, OH, F)_6$
Periclase	MgO
Pyrochlore	$(Ca, Na)_2Nb_2O_6(OH, F)$

(continued)

Table 2.1 (continued)

Mineral	Formula
Ilmenite group minerals	
Ilmenite	$Fe^{2+}TiO_3$
Picroilmenite	$(Mg, Fe)TiO_3$
Hematite	Fe_2O_3
Pyrophanite	$MnTiO_3$
Corundum	Al_2O_3
Spinel group minerals	
Chromite	$FeCr_2O_4$
(Ti-) Magnetite	$(Fe, Ti)_3O_4$
Picotite	$(Fe, Mg)(Al, Cr)_2O_4$
Cr-Pleonaste	$Mg(Al, Cr)_2O$
Spinel	$MgAl_2O_4$
(Ti-) Maghemite	γ-$(Fe,Ti)_2O_3$
Zirconium oxides	
Baddeleyite	ZrO_2
Calzirtite	$Ca_2Zr_5Ti_2O_{16}$
Tazheranite	$(Zr, Ti, Ca)O_{2-x}$
Zirkonolite	$(Ca, Ce, Y, Th)Zr(Ti, Nb, Ta, Fe)_2O_7$
Hydroxides	
Brucite	$Mg(OH)_2$
Goethite	$FeO(OH)$
Portlandite	$Ca(OH)_2$
Carbonates	
Ankerite	$Ca(Fe, Mg)(CO_3)_2$
Aragonite	$CaCO_3$
Calcite	$CaCO_3$
Dolomite	$Ca, Mg(CO_3)_2$
Kalicinite	$KHCO_3$
Nahcolite	$NaHCO_3$
Strontianite	$SrCO_3$
Synchysite	$Ca(Ce, La)(CO_3)_2F$
Sulfates	
Aphthitalite	$(KNa)_3Na(SO_4)_2$
Barite	$BaSO_4$
Celestite	$SrSO_4$

(continued)

Table 2.1 (continued)

Mineral	Formula
Gypsum	$CaSO_4 * H_2O$
Hanksite	$KNa_{22}(SO_4)_9(CO_3)_2Cl$
Thenardite	Na_2SO_4
Phosphates	
Apatite-(CaF)	$Ca_3(PO_4)_3F$
Brockite	$(Ca, Th, Ce)(PO_4) * H_2O$
Monazite-(Ce)	$(Ce, La, Nd, Th)PO_4$
Vivianite	$Fe_3^{2+}(PO_4)_2 * 8H_2$
Nesosilicates	
Garnet group minerals	
Almandine-Pyrope	$Fe_3^{2+}Al_2(SiO_4)_3 - Mg_3Al_2(SiO_4)_3$
Andradite-Schorlomite	$Ca_3Fe_2^{3+}(SiO_4)_3 - Ca_3Ti_2^{4+}\left(Fe^{3+}Si\right)_3O_{12}$
Kimzeyite	$Ca_3(Zr, Ti)_2^{4+}\left(Si, Al, Fe^{3+}\right)_3O_{12}$
Chrome Pyrope	$Mg_3(Al, Cr)_2(SiO4)_3$
Hydroandradite	$Ca_3Fe_2^{3+}(SiO_4)_{3-x}(OH)_{4x}$
Hydromelanite	
Spessartine	$Mn_3Al_2(SiO_4)_3$
Olivine group minerals	
Fosterite-Fayalite	$\left(Mg, Fe^{2+}\right)_2SiO_4$
Monticellite	$CaMgSiO_4$
Thorite	$(Th, U)SiO_4$
Auerlite	$Th(Si, P)O_4$
Titanite (Sphene)	$CaTi(SiO_4)O$
Zircon	$(Zr, Hf)(SiO_4)$
Sorosilicates	
Fersmanite	$(Ca, Na)_8(Ti, Nb)_4Si_4O_{22}(F, OH)_4$
Wöhlerite	$NaCa_4Zr(Nb, Ti)Si_2O_7(O, F)_4$
Melilite Group minerals	
Åkermanite-Gehlenite	$Ca_2MgSi_2O_3 - Ca_2Al(SiAl)O_7$
Inosilicates	
Pyroxenes	
Aegerine	$NaFe^{3+}Si_2O_6$

(continued)

Table 2.1 (continued)

Mineral	Formula
Aegerine-Augite	$\left(Na_aCa_bFe_c^{2+}Mg_d\right)\left(Fe_e^{3+}Al_fFe_g^{2+}Mg_h\right)Si_2O_6$
Ti-Augite	$(Ca,Na)(Mg,Ti,Fe,Al)(Si,Al)_2O_6$
Enstatite	$MgSiO_3$
Diopside	$CaMgSi_2O_6$
Cr-Diopside	$Ca(Mg,Cr)Si_2O_6$
Amphiboles	
Arfvedsonite	$Na_3\left(Fe^{2+},Mg\right)_4Fe^{3+}Si_8O_{22}(OH)_2$
Ferrorichterite	$Na_2Ca\left(Fe^{2+},Mg\right)_5Si_8O_{22}(OH)_2$
Hastingsite	$Na_2Ca\left(Fe^{2+},Mg\right)_4Fe^{3+}AlSi_6O_{22}(OH)_2$
Hornblende	$Ca_2Fe_4^{2+}\left(Al,Fe^{3+}\right)AlSi_7O_{22}(OH,F)_2$
Kearsutite	$Na_2Ca(Mg_4Ti)(Si_6Al_2)O_{22}O(OH)$
Pargasite	$Na_2Ca(Mg_4Al)Si_6Al_2O_{22}(OH)_2$
Pectolite	$NaCa_2Si_3O_8(OH)$
Richterite	$Na_2Ca\left(Mg,Fe^{2+},Mn\right)_5Si_8O_{22}(OH)_2$
Tremolite	$Ca_2Mg_5Si_8O_{22}(OH)_2$
Wollastonite	$CaSiO_3$
Xonolite	$Ca_6Si_6O_{17}(OH)_2$
Phyllosilicates	
Antigorite	$\left(Mg,Fe^{2+}\right)_6Si_4O_{10}(OH)_8$
Dalyite	$K_2ZrSi_6O_{15}$
Mica Group minerals	
Annite	$KFe_3^{2+}Si_3AlO_{10}(F,OH)_2$
Biotite	$K(Mg,Fe)_3Si_3AlO_{10}(F,OH)_2$
Illite	$(K,H_3O)Al_2(Si_3Al)O_{19}(H_2O,OH)_2$
Muscovite	$KAl_2(Si_3Al)O_{10}(OH,F)_2$
Phlogopite	$KMg_3Si_3AlO_{10}(F,OH)_2$
Chlorite group minerals	
Clinochlor	$\left(Fe^{2+},Mg,Mn\right)_2Al_4Si_2O_{10}(OH)$
Talc	$Mg_3Si_4O_{10}(OH)_2$
Tectosilicates	
Nepheline	$(Na,K)AlSiO_4$
Quartz	SiO_2

(continued)

Table 2.1 (continued)

Mineral	Formula
Feldspar group minerals	
Albite-Anorthite	$NaAlSi_3O_8 - CaAl_2Si_2O_8$
Anorthoclase	$(Na, K)AlSi_3O_8$
Cancrinite	$Na_6Ca_2Al_6Si_6O_{24}(CO_3)_2{*}2H_2O$
Orthoclase	$KAlSi_3O_8$
Sodalite	$Na_8Al_6Si_6O_{24}(Cl, OH)_2$
Zeolite Group minerals	
Analcime	$NaAlSi_2O_6 * H_2O$
Harmotome	$Ba_2(Al_4Si_{12})O_{32} * 12H_2O$
Natrolite	$Na_2Al_2Si_3O_{10} * 2H_2O$
Thomsonite-Sr	$Na(Sr, Ca)_2Al_5Si_5O_{20} * 6 - 7H_2O$

2.1 A Search for Diamond

Kimberlite-type rocks may carry diamonds and intense efforts have been made towards finding them on Alnö. Von Eckermann (1967b) reported "diamond-like crystals" from a thin section of a tuffitic breccia boulder found in the gravel pit of Fillanberget north of Sundsvall. He states: "*they are surrounded by light-coloured reaction zones, indicating a chemical reduction reaction. By the Fedoroff method the refractive index was determined on the universal stage and found to correspond to that of diamond, 2.40 ± 0.05. The crystals are isotropic, so the possibilities of them being some other mineral are of course limited*". After his death, the thin section in question was handed to the Geological Survey of Sweden, where it was investigated in detail by Henno Nairis. The section was remounted, the cover glass removed, and a polished section was prepared. Subsequent microprobe analyses of the three largest grains proved them to be pyralspite garnets (see Table 2.1), with rather high contents of the spessartine molecule. This result corresponds well with garnets found in the pegmatites and granites of the Sundsvall area. The supposed "reduction zones" turned out to be thin kelyphitic shells.

In 1981, a large bulk sample made up from a series of kimberlitic alnöites from northern Alnö was analysed in order to evaluate a possible diamond potential of these rocks. With the exception of samples from the Hartung kimberlitic alnöite dyke, all other samples were from boulders, mainly from Ås bay and surroundings

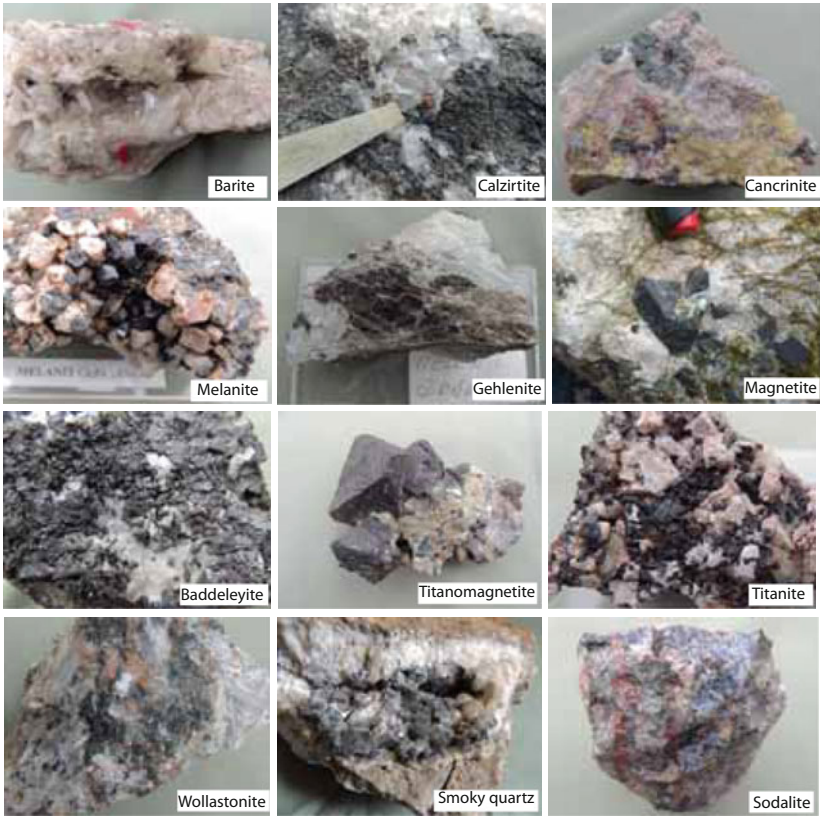

Fig. 2.1 Selected Alnö minerals from the personal collection of Christer Wiklund (Njurunda)

(see Chap. 4). The sample, amounting to 11.5 metric tonnes in total, was processed by SSAB Mineralprocesser, Stråssa, Sweden. Unfortunately, extensive contamination with a wide range of foreign materials appears to have occurred during the processing. The analysed material comprised dolomite, lead-, copper-, zinc- and iron ores as well as ferrochromium slag, highlighting the concept that contamination of a sample with one's processing equipment or outside materials can be an important factor. A rough estimate of the total amount of contaminant exceeded 10% by weight. In addition, only about 10–15% by weight of the total sample (including contaminant) was suitable for treatment following grinding, milling and

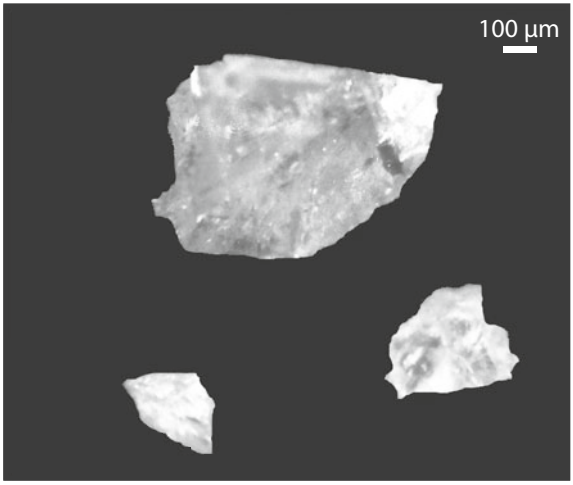

Fig. 2.2 Diamonds recovered from the non-magnetic, heavy, acid-insoluble residue of a bulk sample of kimberlitic alnöite (see text for details)

magnetic separation. Thus, of the original 11.5 tonnes (11.500 kg), less than two tonnes (<2000 kg) reached the final processing stage (shaking table) at the plant. Since diamond is hydrophobic, petroleum jelly was used in the hope for some results. Final concentration was carried out at the Geological Survey of Sweden (Kresten and Nairis 1982). The list of mineral phases identified was very long and contained frequent natural and synthetic contaminants. However, from the "sulphide concentrate" obtained from Stråssa (produced with petroleum jelly on the shaking table), which was heavily contaminated with various sulphides and oxides, three fragmental diamond crystals were recovered (Fig. 2.2). They were type IIa diamonds and slightly different fluorescence indicated at least two different original crystals. With regard to the extensive contamination of the sample, the question as to whether or not the diamonds were authentic, i.e., were derived from the original kimberlitic alnöites or not, was over-shadowing the investigation. An authenticity could not be excluded in a concentrate containing various "kimberlitic" phases, such as chrome diopside, enstatite and picroilmenite. Still, the source of some of the contaminants e.g., silicon carbide, could not be determined. Since, diamond drill-cores were among the materials used at Stråssa, it is possible that an external source of diamonds could have been involved. The study, despite the enormous scope, therefore remained inconclusive.

Subsequent investigations of samples by other mineral processing laboratories (e.g. 145 kg at De Beers; Ashton Mining in 1985) have not resulted in any microdiamonds. For some years, the hopes for diamonds at Alnö have prevailed,

however. Previous finds of chrome pyrope (Kresten 1976), with a composition typical for garnets associated with diamonds, might have contributed to this euphoria, although the host in that case was an alvikitic alnöite. The matter gathered renewed interest recently as SGU's aeromagnetic map of the Sundsvall area indicated a number of circular anomalies on the mainland north of Alnö that might possibly represent "kimberlitic pipes". Kresten visited some of them, classifying them as alnöitic (sensu lato) breccia pipes, accompanied by contact fenites, but no detailed investigation for diamonds was carried out for these intrusions as of yet.

2.2 The "Knopite" Mystery

In 1891, Högbom (1895) sampled various sövite boulders in the Långharsholmen and Stugholmen area, one of which (from Långharsholmen) contained shiny dark grey to black crystals shaped as cube-octahedrons. They were studied in detail by Holmquist (1894), who introduced them as a new mineral "knopite", a perovskite with about 5 weight% REE. Based on their crystallography, type I and type II knopite was distinguished.

Knopite type I occurs as cube-octahedrons with subordinate ikositetrahedrons and tetrakishexahedrons (Fig. 2.3). Polished sections showed pronounced lamellae (Fig. 2.4). Type II occurred as cubes, with rare octahedral combination, showing no obvious macroscopic lamellae.

Type I knopite has so far only been encountered in the boulder originally discovered by Högbom. The mineral has been the subject of a brisk trade (von Eckermann 1974) and still is today (see Figs. 2.3 and 2.4). Small pieces of the original boulder can be purchased from different private sources in Sweden for over several hundred SEK a piece. Despite considerable efforts to find new occurrences of "knopite type I" at Alnö over the last decades, no further boulder turned up, nor was the phase found in outcrop. The occurrence of "knopite type I" in a single boulder only remains one of the unresolved mysteries of Alnö's mineralogy to this day.

Chemical analyses of "knopite type I" single crystals clearly show deficiency in A-site, and excess in B-site cations, as was discussed by von Eckermann (1974). He concluded that "two different types of dysanalyte and knopite exist in the Alnö sövites, one of the normal perovskite formula ABO_3 and one of the abnormal $A_{1.80}B_{0.70}O_3$" (see also Fig. 2.5). It is apparent from the discussion and the analyses that the "abnormal perovskite" (commonly knopite type I) has the structural formula $A_{1.20}B_{0.70}O_3$ instead of the one given (obviously a typing/printing error). That formula, based on complete analyses, is most likely

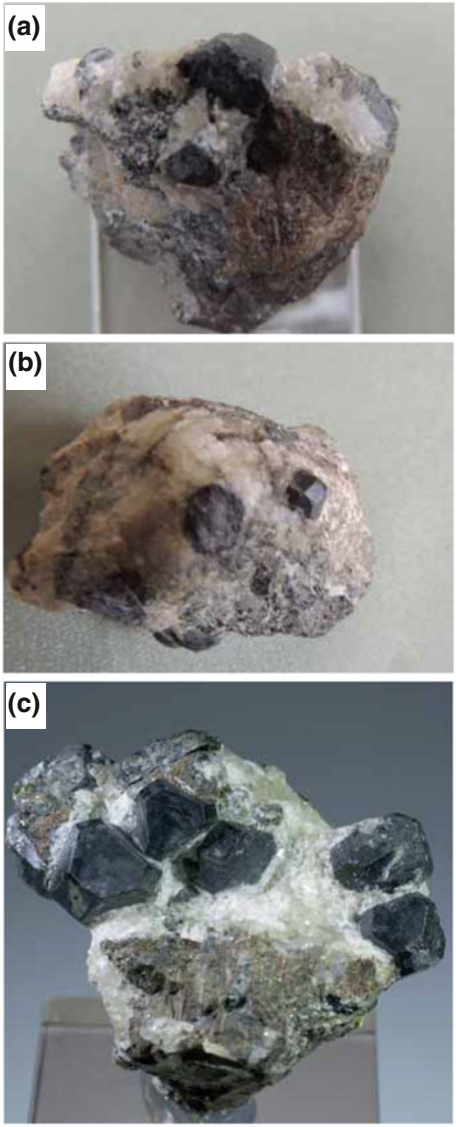

Fig. 2.3 Knopite (type I) from Alnö. All are parts of Högbom's (1895) original sample. **a** from the collection of Christer Wiklund. **b** from the collection of Peter Kresten; **c** Crystals of grey-black perovskite of the variety knopite. This specimen was part of the former Leif Engman collection (#En 216/76) and later the former Axel R. Andersson collection. Photo: courtesy of Conny Larsson, Uppsala University

neither “abnormal” nor “perovskite”, but probably represents a mixture of different phases (see also below).

Holmquist (1894, 1896) discussed the lamellation of knopite type I in detail, particularly their crystallographic orientation. Although noting different appearances of the lamellae, particularly “light lamellae in a darker groundmass”, he never questioned the composition of the lamellae but believed them to be polysynthetic twin lamellae as found in perovskite proper. Kresten (1979) demonstrated that “knopite type I” was a multiphase assemblage consisting of perovskite, titanium oxides (anatase) with or without sphene and ilmenite/pyrophanite. Differential thermal analysis showed a distinct endothermic peak at 622 °C, tentatively identified with dissolution of one of the phases involved (Kresten 1993).

Microprobe analyses of “knopite type I” verified the multiphase assembly, with the “twin lamellae” being different phases. One sample was found to be composed of perovskite, manganoan ilmenite and anatase (Figs. 2.4 and 2.5); another sample consisted of titanite and anatase set in a perovskite matrix. X-ray diffraction patterns of five samples confirmed the complex mineralogy. Heat treatment of the samples (800 °C, vacuum, 36 and 70 days) did not result in any homogenization but in more pronounced perovskite reflections on XRD with less splittings,

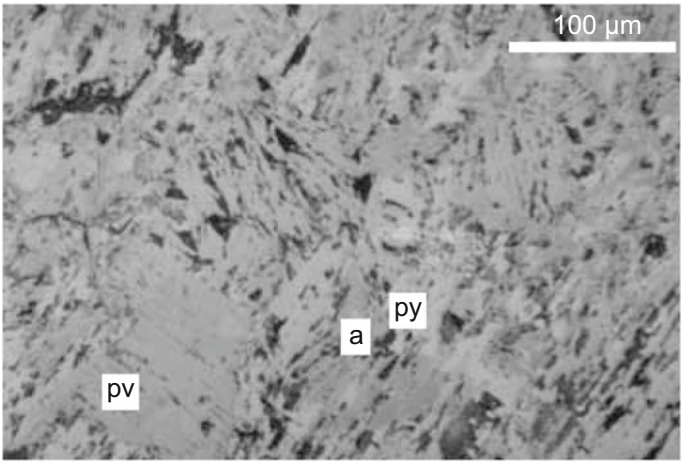

Fig. 2.4 Reflected light photomicrograph of knopite type I, showing intergrowths between perovskite (pv), pyrophanite (py) and anatase (a)

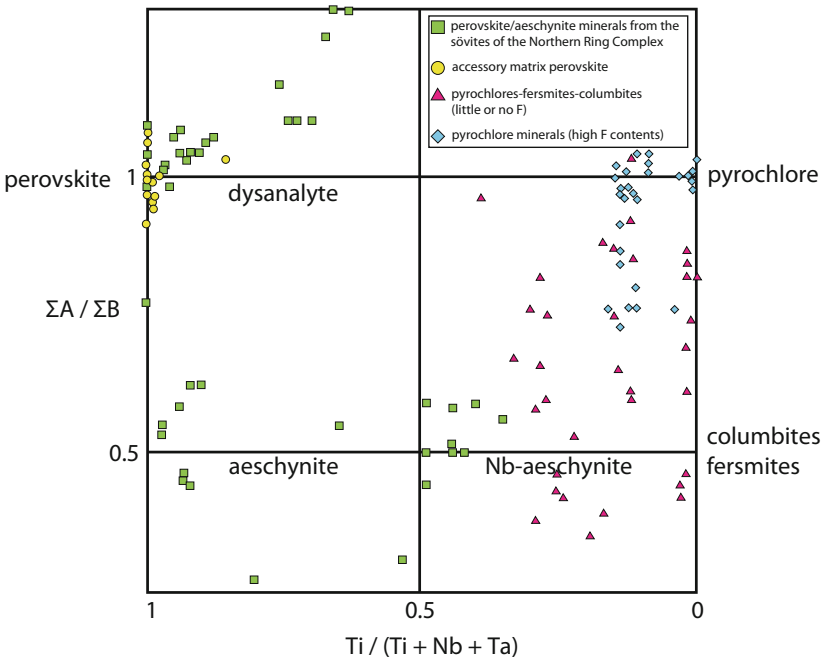

Fig. 2.5 Compositions of perovskite-aeschynite and pyrochlore-fersmite minerals in terms of A- and B- site cation ratios and Ti/(Ti + Nb + Ta) ratios (after Kresten (1990))

indicating a possible transition towards a cubic phase. In addition to perovskite, titanite, and anatase, XRD also identified rutile.

We proposed that "Knopite type I" has to be regarded as a homogeneous mineral from start, which by later reactions became unstable, and is unmixing into several different phases. Assuming that the original phase was of perovskite-chemistry (ABO_3), leaching of A-site cations, and decalcification, would lead to "knopite type I" bulk compositions. A similar decalcification of perovskite to anatase has been recorded from Tapira, Minas Gerais, Brasil (Mariano 1989). Thus, the mineral believed to be found exclusively at Alnö is most likely only a mixture today. "Knopite type II" does not help either in this case, analyses show the crystals to be either aeschynite, or perovskite.

2.3 Spinel Minerals

Maghemite seems to be a rather widespread constituent in Alnö rocks, although it is easily overlooked. It occurs at the grain boundaries of magnetite, and along cracks in magnetite from mainly sövites and pyroxenites (jacupirangites). In some cases, discrete grains completely composed of maghemite have been recovered. If dispersed in a rock matrix, it is not easily found during routine microscopy.

Low-temperature oxidation of primary magnetite produces maghemite with similar contents of minor elements than found in the primary mineral. Maghemite formed at the expense of low-titanium magnetite has fairly low titanium contents, while oxidation of titanomagnetite results in titanomaghemite with up to 10% TiO_2 (see Kresten 1990).

Magnetite and titanomagnetite are the spinels most commonly encountered in Alnö rocks. The following principal types of (titano-)magnetite occurrences are distinguished:

(1) Magnetites and titanian magnetites forming discrete grains or segregations (layers) in sövites.
(2) Titanomagnetites of pyroxenites and plutonic nephelinites, often concentrated in layers.
(3) Megacrysts of titanomagnetite in ultramafic lamprophyres and ultramafic nodules.
(4) Secondary magnetite in lamprophyres, formed during serpentinization of olivine.
(5) Magnetite in magnetite "dykes" (see above and Chap. 4).

Exsolution lamellae of ilmenite are particularly frequent in the titanomagnetites of ultramafic nodules and the titanomagnetite megacrysts (in part xenocrysts) in the groundmass of various ultramafic lamprophyres (for equilibration conditions, see ilmenite). No exsolution lamellae have been found in the titanomagnetites of pyroxenites, plutonic nephelinites, and sövites (c.f. Prins 1972).

Chrome spinel is a characteristic accessory phases in beforsites, melilitites, and ultramafic lamprophyres (including kimberlitic alnöites). These matrix spinels usually form well-crystallized small (to 1 mm) octahedra. Chrome spinel is found as well in a number of ultramafic nodules, commonly being anhedral grains. According to their compositions, they are chromite, chrome hercynite, (titanian) pleonaste, chrome picotite and titanian picotite. Transitions to the (titano-)magnetite suite are sometimes encountered.

Spinel has been found in the heavy mineral concentrate of the tuffbreccia from Oxåsen, on the mainland north of Söåker (Kresten 1990). The mineral forms colourless octahedral forms and analysis showed an almost pure Mg–Al-spinel, with very low contents of silica, titanium and chromium.

Spinel compositional trends: Ever since the theory and applications of spinel compositional variations for solving petrological problems have been outlined by Irvine (1965, 1967), the study of spinels has become a routine when investigating ultramafic and related rocks. Three trends are recognised at Alnö:

Trend 1, magnesiochromite—spinel trend, embracing spinels from beforsites, melilitolites, and from some ultramafic nodules. The spinels of alnöitic rocks, is characterized by titanian magnesiochromites, and possibly grades into titanian pleonaste of trend 3.

Trend 2, chrome picotite—picotite trend, comprises most spinel from ultramafic nodules in kimberlitic alnöites and includes titanian picotite/pleonaste from some ultramafic nodules.

Trend 3, titanian pleonaste—titanomagnetite trend, is defined by spinel from alnöitic rocks, ultramafic nodules, melilitolites, uncompahgrite, pyroxenite, plutonic nephelinites, sövites and fenites.

For kimberlite spinel, two magmatic trends have been defined (Mitchell 1986): subtrend 1, the magnesian ulvöspinel trend, and subtrend 2, the titanomagnetite trend. Of these two, kimberlite subtrend 1 seems to correspond to the Alnö subtrend 2, while kimberlite subtrend 2 appears not represented on Alnö.

2.4 Baddeleyite

Hussak (1898) reported baddeleyite in jacupirangite from Alnö. He verified the identification by optical and crystallographic characteristics, as well as qualitative chemical tests. The jacupirangite was found to contain 0.38 wt% of baddeleyite. The occurrence of baddeleyite was challenged by von Eckermann (1939), who suggested that Hussak could have mistaken melanite garnet for baddeleyite. He maintained this standpoint in his final mineralogy paper (von Eckermann 1974). Indeed, it has not been possible to verify Hussak's original observation, especially because no locality was detailed by the author, but now, however, baddeleyite was found to be a common accessory component of many Alnö rocks. It has been found in sövite, beforsite, alnöite and kimberlitic alnöite. Whenever a fair-sized samples of these rocks was processed, baddeleyite was recovered in the heavy, non-magnetic and acid-insoluble fraction. In several cases, baddeleyite was also found in thin section. There, baddeleyite occurs typically as brownish or dark

brown, irregular (or kidney-shaped) grains up to 3 mm across. The mineral shows brownish to greenish brown pleochroism, and strong birefringence. In sövite, baddeleyite overgrown by zircon was found, indicating that the oxide phase formed first, and the silicate later, when silica activity had reached sufficiently high levels. In kimberlitic alnöites, by contrast, baddeleyite forms reaction rims around zircon, indicating late oxidizing reactions, most likely with carbonate. Similar observations have been made for zircons in kimberlites (Kresten et al. 1975; Raber and Haggerty 1979). X-ray diffraction analysis showed that only the monoclinic, but not the tetragonal phase is present (Kresten 1973; Kresten et al. 1975). Finally, beautiful euhedral crystals of baddeleyite, of up to 2 mm length, have been reported by Sandström et al. (2010) from sövite at the abandoned magnetite mines at Stavsätt.

2.4.1 Ca–Ti–Zr-Oxide Minerals

Ca–Ti–Zr-oxide minerals are a group of rare minerals sometimes found in alkaline rocks and related carbonatites with complex chemical compositions. The principal members of this mineral group have the following simplified formulae:

Tazheranite, $CaTiZr_2O_7$
Calzirtite, $CaTiZr_3O_9$
Zirconolite, $CaTi_2ZrO_7$
Zirkelite, $CaTiZrO_5$

Both the formulae and the nomenclature of the members of this group has been debated (Busche et al. 1972), and it has been suggested that "zirconolite" and "niobozirconolite" should be discredited and replaced by "zirkelite" (Nickel and Mandarino 1987). The mineral formulae can be generalized as $AB_xC_yO_z$, where:

A = Ca, Fe^2, Mg, Mn, U, Th, Y, REE, Al
B = Ti, Fe^3, Nb, Ta, Si
C = Zr, Hf

In respect to composition, there are two compositional clusters; one between the compositions of zirconolite and zirkelite, the other between the compositions of calzirtite and tazheranite. In the following, all four mineral names are retained. Tazheranite and calzirtite, although similar in composition, have different crystal structures (cubic and tetragonal, respectively) and tazheranite has been described as containing trivalent titanium (Konev 1978).

Tazheranite was found in thin section of a kimberlitic alnöite boulder south of Hartung. A fist-sized piece of the rock was crushed and a heavy oxide phase was obtained by separation with heavy liquids and repeated magnetic separations. The X-ray diffraction pattern revealed the material to be tazheranite, contaminated with

some baddeleyite. On Alnö, the mineral is dark brown to black and in thin section, it is dark reddish brown.

Calzirtite. Several grains of calzirtite have been found in a sövite fragment included in an alnöite breccia boulder found within the Åvike Bay area. The paragenesis includes calcite, apatite, phlogopite, (niobian) zirconolite, ilmenorutile and titanian magnetite. The mineral is chestnut-brown in thin section, uniaxial (+), sometimes zoned and/or twinned. Often, the mineral is overgrown by niobian zirconolite, which is metamict and almost opaque in thin section. Niobian zirconolite is also found along cracks in calzirtite.

Zirconolite and niobian zirconolite. Zirconolite has been found in the same sövite fragment that contained the calzirtite. It is reddish brown in thin section and obviously metamict, as is indicated by the isotropic character.

A related phase with much higher (>20%) niobium contents is found in the same sample, forming composite grains with zirconolite and/or surrounding zirconolite or calzirtite. It appears to be completely metamict, and is almost opaque in thin section. In reflected light, it has much lower reflectivity than zirconolite, which in turn is lower than calzirtite.

2.5 Pyrochlore-Fersmite Type Minerals

Pyrochlore is a typical constituent of the sövites from the main intrusion at Alnö, particularly those in the Smedsgården—Stavsätt area, and the sövites from the Båräng vent, where pyrochlore is abundant (Fig. 2.6). Pyrochlore is also found in sövite-impregnated fenites at Båräng, in nepheline syenite west of Hörningsholm, in the matrix of the Sälskär breccia, and in beforsite dykes.

Within the sövites of the Northern Ring Complex, pyrochlore is rare. Boulders collected in the Stugholmen—Långharsholmen area, however, contain pyrochlore (Holmquist 1893; Högbom 1895). At Stugholmen, a fersmite- and apatite-rich concretion in the sövite outcrop occurs. Pyrochlores often contain elevated amounts of thorium and uranium, which makes them readily detected in outcrops with a scintillometer. Some of the minerals, often fersmites or fersmitic pyrochlores, are metamict (Kresten 1992b).

Fersmitization of pyrochlore from Alnö was first described by van der Veen (1963). It leads to A-site deficiency (Fig. 2.5), a result of low-temperature to hydrothermal leaching (van der Veen 1963) leading first to fersmitic, then to columbitic compositions. The process mirrors the relationship between perovskite and aeschynite, the main difference being that the transition from pyrochlore to

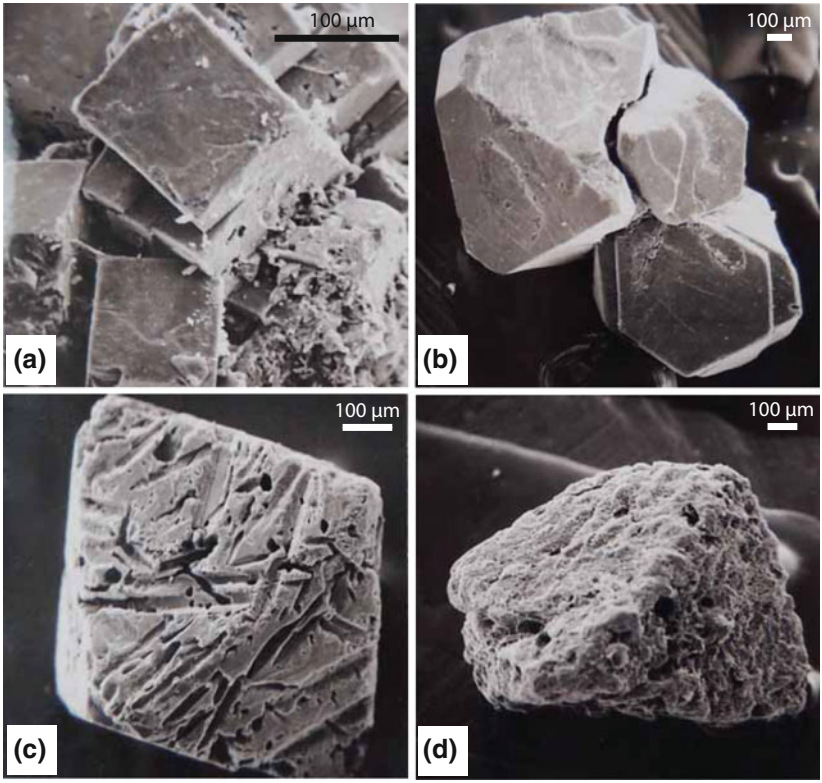

Fig. 2.6 Scanning electron micrographs (SEMs) of perovskite and pyrochlore minerals from Alnö. **a** Dysanalyte in sövite, Prickskär. **b** Clear brown pyrochlore (type 3) in sövite at Stavsätt. **c** Dark brown "fersmitic" pyrochlore (type 4) in the matrix of the Sälskär breccia. Intergrown apatite has been dissolved by treatment with diluted HNO_3. **d** Brownish black "spongy pyrochlore" (type 5) in sövite from quarry north of Smedsgården (treated with diluted HNO_3 to dissolve calcite and apatite). See text for further details

fersmite (columbite) seems to be gradual (Fig. 2.5). According to colour and habit, the following types are distinguished:

(1) *Clear yellow octahedra of pyrochlore*, commonly less than 1 mm across. Observed in the sövites at Båräng.
(2) *Light brown, zoned octahedra* with repeated narrow zones of pyrochlore (light brown) and fersmitic pyrochlore or fersmite (dark brown to black),

measuring up to 5 mm across. Found in sövites and fenites at Båräng, sövites and nepheline syenites at Hörningsholm, and in the matrix of the Sälskär breccia.

(3) *Brown, unzoned octahedra of pyrochlore*, vitreous to resinous lustre, measuring 0.5–8 mm, sometimes in combination with the cube (Fig. 2.6b). Found in sövites at Stavsätt, in sövite boulders at Långharsholmen (Holmquist 1893), in the matrix of the Sälskär breccia, and in beforsite dykes.

(4) *Dark brown octahedra of fersmitic pyrochlore*, again up to 8 mm, with dull resinous to greasy lustre. Sometimes zoned, often intimately intergrown with apatite (Fig. 2.6c). Found in sövites at Båräng and Stavsätt, and in the Sälskär breccia.

(5) *Dull dark brown to brownish black "spongy" pyrochlore/fersmite*, usually less than 1 mm across, occurs as late-stage mineral crowded with inclusions, irregular or with octahedral habit (Fig. 2.6d). Highly radioactive and metamict. Found in sövites at Smedsgården (northern quarry), at Båräng, in the apatite-rich layer at Stugholmen, and in the Sälskär breccia.

(6) *Pitch-black octahedral fersmitic pyrochlore*, up to 10 mm across, with dull resinous lustre. Highly radioactive and metamict. Abundant in the Båräng sövites.

Types 1–3 usually show X-ray diffraction patterns of pyrochlore, with or without some additional reflections. Types 4–6 are more or less metamict; either they show no reflections at all, or else show broadened lines ascribed to pyrochlore or fersmite. On heating, a fersmite-dominated diffraction pattern is obtained. Differential thermal analyses (Kresten 1992b) illustrated the pyrochlore to fersmite transition by increasing exothermic reactions between 450 and 490 °C and gradual appearance of an exothermic peak between 670 and 700 °C. Chemical changes during the pyrochlore to fersmite transition involves the decrease in the $\Sigma A/\Sigma B$ cation ratios from 1 (pyrochlore) to 0.5 (fersmite). REE's were not included in routine microprobe analyses and hence, several of the analyses plot below a site ratio of 0.5 (Fig. 2.5; Kresten 1990).

One may find it difficult to envisage fersmite formation by low-temperature leaching of pre-existing pyrochlore. Only one of the morphological types, the "spongy" type 5 (from above), is clearly late-stage. Other fersmites and "fersmitic pyrochlores" have probably formed contemporaneously with pyrochlore proper e.g., the zoned pyrochlores/fersmites of type 2. These features are most readily accounted for by assuming formation of pyrochlore and fersmite by precipitation from volatile phases with varying activities of calcium, iron, manganese, REE, uranium, thorium as well as titanium, niobium, tantalum and fluorine. Local

equilibria and disequilibria conditions will cause minerals with different chemistry and stoichiometry to develop, which is what we see in thin sections. Not only is compositional zoning abundant, but also wide variations between individual grains. These volatiles must have acted during a wide span in pressure and temperature. Early magmatic fluids have given rise to type 3 pyrochlores, while types 1, 2, 4 and 6 likely crystallized from more evolved fluids. It has been suggested by Kresten (1979) that type 5 represents precipitates of niobium oxide hydrate gels from a low-temperature late-stage fluid. The gel would act as powerful ion-exchange resin, accumulating in a seemingly haphazard manner cations and anions, depending in prevailing p^H-conditions and activities/fugacities.

2.6 REE-Fluoro-Carbonates

Bastnäsite, synchisite and parisite minerals occur in many carbonatites (Hogarth 1989) and may reach economically important concentrations. At Alnö, however, they have so far been identified in two dyke rocks only.

Synchisite-(Ce) is found in a ferro-carbonatite dyke in NW Stornäset. It forms irregular grains, brownish in thin section, often crowded with opaque to semi-opaque inclusions, of probably iron oxides.

"*Ferrosynchisite*". A fluorite-rich alvikite boulder in contact with a trachyte, collected along the shores of Söråker by von Eckermann contains fluorite, pale purple in thin section, crowded with almost opaque discoloration zones that resemble radioactive halos. In reflected light, a somewhat heterogeneous mineral assembly is identified as nuclei. Scanning electron microscopy and energy dispersive analyses revealed: (1) a Ca–Fe-RE phase with considerable amounts of Th; (2) exsolution lamellae which contain slightly higher amounts of Fe than the matrix, and (3) discrete granular exsolutions which are identified as thorite. Small amounts of ferro synchisite have been separated using heavy liquids. The specific gravity of the mineral appears to be about 4 (roughly equal to that of Clerici's solution). It is yellowish brown, flaky, with well-developed basal cleavage.

2.7 Monazite, Brockite and Auerlite

Monazite is occasionally found in the wall-rock, forming the nuclei of radioactive halos in biotite. Monazite persists through low-grade fenitization. When separating sample "ferrosynchisite" (see above), two greenish yellow fragments of monazite were recovered from the same sample. One was used to confirm the mineral with

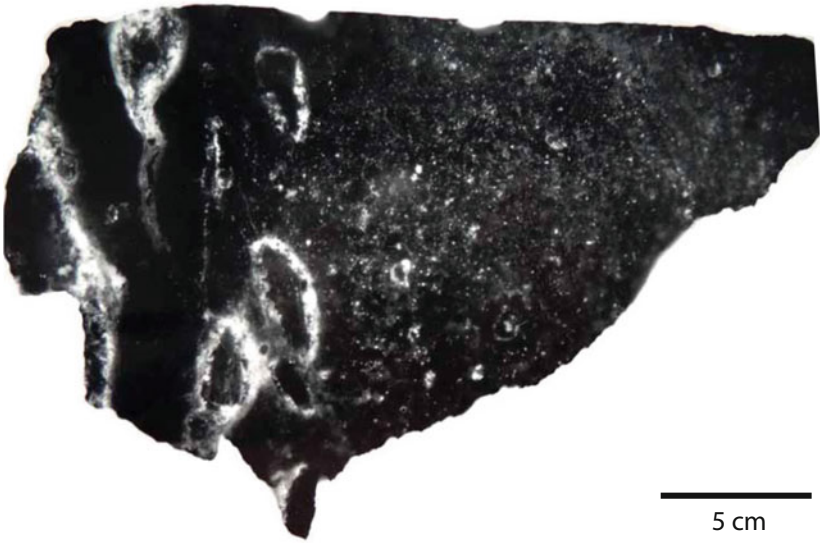

Fig. 2.7 Autoradiograph (positive image) of a polished slab of the thorium-rich beforsite dyke rock from Töva, showing areas of elevated radioactivity (white), along the contact with the migmatic greywacke (left) and around wall-rock fragments in the dyke. The principal radioactive mineral is "auerlite", the necessary silica is supplied by the wall-rock. Image courtesy Gustav Åkerblom

X-ray diffraction, the other was analysed and found to be rich in both Ce and Nd, with rather moderate La contents, and low Th contents. The Alnö monazite seems to be intermediate between monazite-(Ce) and monazite-(Nd), similar to monazite reported from the Fen complex (Andersen 1986).

Brockite, is one of the main carriers of the high thorium contents in the beforsite dyke at Töva (see Chap. 1). It occurs along the contact between beforsite and migmatitic greywacke gneiss, or surrounding gneiss fragments in the beforsite dyke (Fig. 2.7). In thin section, the mineral is bright lemon to orange coloured and forms hexagonal platelets or irregular grains, often dusted with hematite inclusions. The brockite is accompanied by another phase, yellow in thin section and similar to brockite in appearance, but optically isotropic (most plausibly metamict). Chemical analyses reveal the phase to be a silico-phosphate of Ca, Th and U, probably with both REE and H_2O (the latter not determined). The closest similarity is to "auerlite" (Hidden and Mackintosh 1888), which contains more thorium and less calcium and iron than the Töva sample. "Auerlite" is considered to be a variety of

thorite rich in phosphorous (replacing silica). The mineral is more abundant than brockite and the silica required for its formation was obviously provided by the wall-rock (Fig. 2.7).

2.8 Garnets

Pyralspite garnets: On Alnö, pyralspite garnets are rare. The most frequent occurrence is in the alnöite breccia at Hovid, where both discrete garnets (xenocrysts) and garnet-bearing nodules have been found. In the MgO–MnO-plot (Fig. 2.8), garnet compositions range from low-Mn, high-Mg to high-Mn, low-Mg garnets (disregarding one analysis of grossularite in a metasediment). The following compositional groups are distinguished:

I. *Pegmatite garnets* from the wall-rock are all characterized by high (>10%) MnO contents with low to very low MgO contents. Some of the garnets obtained from concentrates of Alnö dykes have similar compositions and are thus clearly derived from a pegmatite of the wall-rock.
II. *Garnets from metasediments* show a wide range in MnO with fairly constant and moderate MgO contents. The group includes also all the garnets from early and late orogenic intrusions, as well as some garnets recovered from concentrates of Alnö dykes. The "diamond-like crystals" of von Eckermann (1967b) are garnets with compositions intermediary between groups I and II and may be derived from either one of those sources.
III. *Granulite garnet in alnöite* from the Hovid breccia show MgO contents of about 10% with fairly low MnO contents. The same type of garnet is found in discrete garnets at the site, indicating that they represent xenocrystal phases derived from disintegrated granulites.
IV. *Lower crust/upper mantle garnets* have high magnesium contents and low manganese contents. The same characteristics apply to garnets from a scyelite nodule and a garnet-serpentine nodule, both from the Hovid breccia and to the xenocrystal garnets found in an alvikitic alnöite dyke north of Sundsvall (Kresten 1976a).

The scyelite nodule that was contained in the Hovid breccia is composed of roughly equal parts garnet, sodian augite and pargasite. The Fe–Mg partitioning between garnet and clinopyroxene indicates a temperature of equilibration at 940 °C, according to the calibration by Råheim and Green (1974). For the Fe–Mg partitioning between garnet and amphibole, the equilibration temperature is 900 °C,

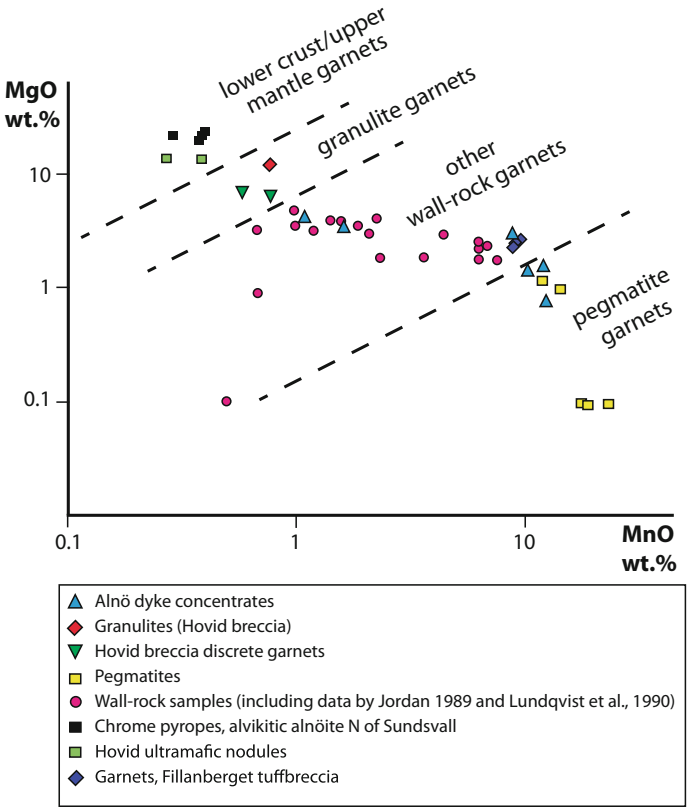

Fig. 2.8 Magnesium versus manganese for pyralspite garnets (note logarithmic scale)

using the calibration of Perchuk (1967b). These consistent results suggest that both pargasite and sodian augite are "primary" phases and that the nodule has not been re-equilibrated during the intrusion of the alnöite but is a sample of an ultramafic granulite, probably from the lower crust or uppermost mantle. The presence of pargasite and sodian augite indicates a rather extensive metasomatism of this part of the crust/mantle.

The chrome-pyrope xenocrysts of the dyke north of Sundsvall are very similar to garnets found in kimberlites. They classify within the G9 and G10 fields (Gurney 1984; Nowicki et al. 2007), i.e., they have the characteristics of peridotite

garnets from kimberlites (G9) or garnet inclusions from diamonds (G10). Thus, they are evidently xenocrysts of upper mantle rocks.

Andraditic garnets are common constituents of many Alnö rocks. They are usually titanian andradites, with TiO_2 ranging between 1.2 and 14.8 weight%. Zirconium is present in several analyses in small amounts; kimzeyitic titanian andradites found in some samples may contain up to 12.7% ZrO_2. The fenites of the Alnö and Söråker intrusion and fenite boulders found along the southern shore of Åvike Bay occasionally contain titanian andradites. At Alnö and within the Åvike Bay area, these garnets are mainly restricted to high-grade fenites. At Söråker, garnets are more widespread. There, a garnet-phlogopite rock is found with megacrysts of euhedral, zoned titanian andradites with decreasing TiO_2-contents towards the rims of the crystal, set with phenocrystal phlogopite in a matrix of essentially phlogopite and calcite. The uncompahgrite at Söråker contains abundant garnet which is strongly zoned. Almost opaque cores rich in titanium and zirconium are surrounded by successive shells which at the rims are rather poor in titanium. A nearby occurrence of sövite, now "eroded" (mainly by mineral collectors), contained about 20% by volume of euhedral titanian andradite garnets that were up to three centimetres in size, and almost invariably showed dodecahedra (110) combined with trapezohedrons (211). Other constituents include calcite, phlogopite, and apatite.

The garnets of the plutonic alkaline rocks of the Alnö complex are titanian andradites ("melanites") to schorlomitic garnets (to about 16% TiO_2), with only trace amounts of zirconium (Kresten 1990). Garnets from sövites have similar compositions, with no detectable zirconium contents.

Garnet megacrysts in nephelinite dykes are schorlomitic andradites (to 13% TiO_2), whereas matrix garnets have substantially lower TiO_2 (about 3%). Titanian andradite, sometimes with high zirconium contents, has been identified in the matrix of some alnöites and kimberlitic alnöites, as well as in the late ferro-carbonatite dyke NW of Stornäset. The latter often show appreciable amounts of niobium, up to 0.36% Nb_2O_5. Niobium, not included in routine analyses, may be present in several other garnets, as is indicated by fairly high tantalum contents of some samples (Kresten 1990).

"*Hydro-melanites*" have been described by von Eckermann (1974) from nepheline syenite. Water contents are up to 1.35% H_2O, corresponding to 1.080–1.525 OH^- in the formulae based on 24 (O, OH), thus confirming the existence of hydro-melanite on Alnö.

"*Hydroandradite*" (name not approved by IMA) was described by Kresten et al. (1982) from cavities in kimberlitic alnöite boulders taken during the bulk sampling (see under diamond). They occur in a paragenesis including xonotlite, natrolite,

chlorite and pyrrhotite. The crystals, commonly twinned rhombdodecahedra, are up to one millimetre in size. Zoning is common, with dull whitish cores surrounded by clear yellowish green margins. The mineral is isotropic with anomalous birefringence (0.005–0.007). Refractive indices vary from 1.81 (cores) to 1.85 (margins of grains). X-ray diffraction analyses showed cubic symmetry, space group *Ia3d*, with unit cell edges of 12.12(8) Å for the cores and 12.21(0) Å for the margins.

The hydrous garnet andradite compositions are characterized by fairly high contents of both alumina and ferric iron in the cores, and by very low alumina contents and very high ferric iron contents of the margins. The presence of water in the structure was confirmed by thermogravimetric analyses, which showed weight losses of about 1% between 700 and 800 °C, and an additional loss of about 5% between 800 and 1000 °C. The parageneses indicate a formation during late-stage deuteric alteration of the kimberlitic alnöite matrix.

2.9 Zircon and Dalyite

Zircon was first reported by Holmquist (1893) from pyrochlore-bearing boulders from the small islands north of Alnö. Högbom (1895) describes zircon crystals measuring up to five millimetres from cavities in a nepheline syenite at the shore of Ås Bay, along with calcite and pyrite. He also published an analysis of the mineral (weight%): SiO_2 29.68, ZrO_2 64.94, FeO 1.15, MnO 0.28, H_2O 3.86, total 99.91. By contrast, von Eckermann (1948a) stated that zircon does not occur in Alnö rocks and that Högbom's sample was either misidentified as a mineral, or else the zircon came from a place other than Alnö. Zircon has, however, been found in several thin sections and in many heavy mineral concentrates and to our knowledge, zircon occurs in fenites, sövites, (kimberlitic) alnöites, alnöite breccias, and in carbonatite dykes.

In the wall-rock, zircon is a common accessory phase (Kresten 1990). In the metagreywackes, it is found as small euhedral or subhedral grains, often embedded in biotite and then surrounded by "radioactive halos". Notably, during the very initial stages of fenitization, when alkali amphiboles are formed at the expense of biotite, zircon remains stable. In a slightly more advanced stage, when aegirine-rich clinopyroxene is formed, zircon disappears. Biotite, although corroded, is still present but as clear flakes without zircon or halos. In one sample, a remnant grain of zircon was found with lowered Zr/Hf ratio, indicating leaching processes. It is surrounded by a shell of a colourless phase which on the basis of qualitative data may be *dalyite* ($K_2ZrSi_6O_{15}$), which appears to be an intermediate phase in the reaction between zircon and alkaline solutions. The instability of

zircon in alkaline solutions is further illustrated by the absence of the mineral in medium to high-grafe fenites, but not in very low grade ones, alkaline plutonic rocks and in alkaline dykes. The only other established relationship with other mineral phases, except dalyite, is to baddeleyite, which is occasionally overgrowing zircon or being overgrown by it.

2.10 Clinopyroxene

Clinopyroxene is a characteristic constituents of most Alnö rocks. The mineral is a major phase in many fenites, in all alkaline plutonic rocks, in some alkaline dykes, some sövites, and most ultramafic lamprophyres and their associated nodules.

2.10.1 Clinopyroxene in Fenites

Clinopyroxene is stable throughout the whole fenite aureole and medium- to high-grade aureole fenites as well as contact fenites commonly contain clinopyroxene. Aegirine-rich pyroxene is among the first distinct fenite minerals in the outermost parts of the fenite aureole, derived from the breakdown of biotite or amphibole. Pyroxene occurs forming narrow veinlets in low-grade fenites (on Alnö, and also at Fen, Norway), with or without alkali feldspar. Most alkaline rocks and many carbonatites—the suggested source rocks of the fenitizing fluids—carry clinopyroxenes, often as dominant or major constituent. Studies of clinopyroxene compositional trends are highly useful when discussing fenite petrogenesis (Kresten 1979, 1988; Kresten and Morogan 1986; Morogan and Woolley 1988; Andersen 1989; Morogan 1989). At Alnö, fenite clinopyroxenes evolve along different trends:

Trend 1, aegirine—aegirine-augite trend, covers clinopyroxene from the fenites north of Hartung, in the northwestern part of the fenite aureole. Morogan and Woolley (1988) state that this trend reflects the "equilibration with an oxidizing, Na-rich fluid, probably emanating from the ijolitic magma", as this area is virtually devoid of carbonatites (Kresten 1986).

Trend 2, aegirine-augite—diopside trend, includes clinopyroxene from the central and southern parts of the complex, from fenites formed in the proximity of sövite dykes and is explained as being the result of "equilibration initially with a fluid emanating from ijolite followed by a contact type re-equilibration" (Morogan and Woolley 1988). The most diopside-rich clinopyroxenes are from fenites in contact with sövite (e.g. in the Ås and Smedsgården areas in the south of the complex).

Trend 3, aegirine-augite—aegirine trend, is reversed with respect to trends 1 and 2. It covers clinopyroxenes from the Stornäset area. Typically, low- to medium-grade fenites suffered late overprinting and a new, aegirine-rich clinopyroxene forms overgrowths on older aegirine-augite or replaces it completely (Jordan 1989). The same trend also covers the fenites of the Båräng area, which is dominated by sövite intrusions.

Rheomorphic fenites at Pottäng have clinopyroxene compositions bridging between trends 1 and 2. Clinopyroxene from leucocratic mobilisates shows successive enrichment in iron, while the melanocratic restile fenite contains the mobilisates.

It may thus be possible to use trend 1 (Morogan and Woolley 1988; Kresten and Morogan 1986) to discriminate ijolite-induced fenites from those which have been regarded as carbonatite-induced fenites. Alnö trend 2, in turn, has been interpreted as being the result of double fenitization (Morogan and Woolley 1988), first by ijolite, then by sövite. Fenites in contact with sövite contain fairly pure diopsides. Most likely, the Pottäng rheomorphic fenites, bridging between trends 1 and 2, are examples of double fenitization as well, with a late carbonatite-type (contact) fenitization triggering rheomorphism. This model explains the decrease in aegirine component in both mobilised and restite clinopyroxenes due to generally lower oxygen fugacities in volatiles emanated from sövites (Morogan and Woolley 1988). Samples evolving along the reversed trend 3 show aegirine-rich clinopyroxenes replacing aegirine-augite, and mesoperthite rimmed by K-rich feldspar. The formation of trend 3 samples has been explained by Morogan and Woolley (1988) as result of equilibration with a supercritical CO_2-rich fluid that initially had a high oxidizing power. This, together with the instability of the albite component in a hot CO_2-rich fluid (c.f. Rubie and Gunter 1983), generated optimal conditions for the formation of sodic pyroxene and amphibole.

2.10.2 Compositional Trends of Clinopyroxene from Plutonic Rocks

For the plutonic rocks of the Fen complex, Mitchell (1980) has given a number of clinopyroxene compositional trends, evolving from diopsidic compositions to aegirine-augitic or more hedenbergitic ones. The Fen trends resemble those for Alnö plutonic clinopyroxene and clinopyroxenes from Alnö plutonic rocks show the following detailed trends:

Trend Ia, diopside—aegirine-augite trend, represents clinopyroxene from sövites and silico-sövites. Starting with diopsidic compositions, they increase in

sodium until reaching aegirine-augitic compositions. Clinopyroxenes from sövites of the Northern Ring Complex have strictly diopsidic compositions. Therefore, they appear less evolved than the sövites from the main complex. *Trend Ib* embraces clinopyroxenes from sövite pegmatites, fine- to coarse-grained lamellar intergrowths between calcite and clinopyroxene, with mica, titanomagnetite, apatite and other components.

Trend II comprises clinopyroxenes from pyroxenites, melteigites, ijolites and nepheline syenites, including the diopsidic clinopyroxene of the Söråker uncompahgrite. It parallels the sövite trend Ia but at higher iron contents.

The brecciated melteigite at Hartung illustrates changes in clinopyroxene compositions caused by late post-magmatic (perhaps metasomatic or autohydrothermal) alterations. The melteigite broke up and, possibly by a combination of solutions from outside and migration from within, pyroxene-rich rims form around the melteigite blocks, the space between which is filled with pyroxene, nepheline and alkali feldspar (i.e., a nepheline syenite composition).

2.10.3 Clinopyroxene in Dykes and Nodules

The clinopyroxene from alkaline dykes is sodian augite to aegirine-augite, similar to the clinopyroxenes in alkaline plutonic rocks. Clinopyroxene is rare in carbonatite dykes (alvikites, beforsites). Clinopyroxene, however, occur in most ultramafic lamprophyres, in the groundmass, as phenocryst, or in nodules included in the lamprophyres. In several parageneses, e.g. that of alnöite, clinopyroxene is not a stable phase and is frequently coated by reaction rims. The composition of the clinopyroxenes is often diopside to salite, with more sodic varieties occurring sporadically, while fassaitic clinopyroxene occurs in an alnöitic tuffbreccia at Oxåsen. Pyroxene in kimberlitic alnöites, in particular in the ultramafic nodules, are more magnesian than in alnöites. Assuming equilibration with orthopyroxene and garnet, maximum temperatures obtained for ultramafic nodule assemblages in kimberlitic alnöite are at about 1100 °C, which is broadly consistent with the temperature obtained for the magnetite-ilmenite equilibration in these nodules (c.f. Kresten and Persson 1975).

2.11 Amphibole

2.11.1 Amphibole in Fenites

The appearance of bluish stringers in brick-red contact fenites (e.g. at Hovid) indicates the presence of alkali amphiboles. In thin section, alkali amphibole fringing biotite flakes is among the first signs of fenitization. Although typical for low- to medium-grade fenites, the alkali amphiboles persist to high-grade and contact samples. In the various parts of the fenite aureole, the following species have been found (e.g. Morogan and Woolley 1988):

Main complex, east: (ferro-)richterite
Main complex, west: richterite, (magnesio-)arfvedsonite
Main complex, central: edenitic hornblende
Söråker: (manganoan) richterite, arfvedsonite

According to Morogan and Woolley (1988), richterite is in the western part of the main complex restricted to fenites cut by sövite dykes. In other, probably ijolite-induced fenites, magnesio-arfvedsonite is found. In the Söråker area both amphibole species are found, although no ijolite intrusion is known from that area. Edenitic hornblende occurs together with abundant biotite in medium-grade fenite at Stolpås, adjacent to a major sövite dyke, which seems to have supplied the calcium necessary for hornblende formation.

2.11.2 Amphibole in Plutonic and Dyke Rocks

Amphibole is only rarely found in Alnö alkaline plutonic rocks. Högbom (1895) mentions a probable inclusion of titanium-rich magnesio-hastingsite in nepheline syenite. In pyroxenites, (ferroan) pargasite occurs, some of which could be primary. Amphibole may also be present in the matrix of the Sälskär breccia and nagnesio-hastingsite is the main phase in altered pyroxenite dykes at Stavreviken. Alkali amphibole, mainly (magnesio-)arfvedsonite, occurs in alvikite and beforsite dykes (e.g. von Eckermann 1974). In contrast, pargasite is the principal amphibole species found in alnöite dykes. In some cases, such as in the Hovid alnöite breccia, they are considered xenocrystal phases, although other alnöites carry amphibole as primary megacryst mineral. Amphibole seem to be absent in kimberlitic alnöites, save for one fist-sized xenocryst which was found in a glacial boulder at the shore of Ås Bay. Pargasite is also an essential primary phase in granulite nodules in alnöite. Most likely secondary in origin are pargasite to edenite found in ultramafic nodules in some kimberlitic alnöites.

2.12 Micas

2.12.1 Biotite and Phlogopite

Biotite is a common major constituent of the metagreywackes surrounding the Alnö intrusions and most micas in these rocks are likely relicts of the original wall-rock mineral assemblage. Increasing fenitization results in a new mica population, characterized by higher silica, ultimately arriving at phlogopite compositions. This second group represents mica formed during fenitization. Only in rare cases are both "wall-rock mica" and "fenite-mica" present in the same sample. In the phlogopite-garnet rock at Söråker, groundmass mica is phlogopite while megacrysts are biotite, which is interpreted in terms of late megacryst formation. Similarly, the garnets are enriched in iron and depleted in magnesium towards the rims.

Pyroxenites, ijolites and nepheline syenites all contain biotite that in most cases is the product of secondary alteration of primary clinopyroxene. Mica from sövite shows considerable variation, but the most magnesium-rich clinopyroxene occurs in the sövites of the Northern Ring Complex. All micas from Alnö dykes and contained nodules are phlogopites, irrespective of host rock composition. Reverse zoning is common in mica in ultramafic lamprophyres. Chromium was detected in mica from kimberlitic alnöite and associated ultramafic nodules. Muscovite and/or paragonite occurs frequently as alteration products of feldspar and nepheline.

2.13 Quartz

Quartz in beforsite and alvikite dykes, with maximum contents of about 28% by volume, has been described by von Eckermann (1948a) and in all cases, quartz occurs as a late interstitial phase, or as spherulitic quartz. In addition, a chalcedony-bearing alnöite dyke has been found near Korsta, on the mainland NE of Sundsvall. Quartz as side-product of the serpentinization of primary olivine is also mentioned by von Eckermann (1974).

Several of the sövite dykes investigated for acid-insoluble minerals were also found to contain quartz. The quartz in the Båräng sövites could perhaps be derived from disintegrated wall-rock fragments. In contrast, quartz found in the pyrochlore-rich dyke at Stavsätt is most certainly authentic and is easily found in hand specimen. It forms rounded grains, up to 1 mm in diameter, water-clear, without undulatory extinction. The most spectacular occurrences of quartz on Alnö

are those in late fractures, however. At Stolpås, clear quartz crystals, up to 6 mm in length, are coated by aragonite, calcite and chalcedony. Goethite is found as spherulitic aggregates within and between the quartz crystals, causing discolouration of the quartz in the former case. Along the Slädaviken road, up to 3 cm tall crystals of smoky quartz can be found, again together with goethite and calcite.

2.14 Feldspars

2.14.1 Plagioclase Feldspars

Plagioclase occurs in the wall-rock metagreywackes and granites and contains between 20 and 40% of the anorthite molecule (Fig. 2.9). Plagioclase is a relict phase in low-grade fenites, disappearing rapidly with increasing fenitization since plagioclase is not stable in more high-grade fenites, nor in many alkaline rocks, carbonatites and ultramafic lamprophyres.

A main occurrence of plagioclase is in granulite nodules of the alnöite breccia at Hovid (See Chap. 4). They are oligoclases on the boundary to andesines, with high contents of the orthoclase component (Fig. 2.9).

2.14.2 Alkali Feldspars

The original alkali feldspar of the wall-rock is a cross-hatched microcline with about 10% of the albite molecule and little or no anorthite (Fig. 2.9). In addition, some exsolutions of almost pure albite from the plagioclase are known.

With the onset of fenitization, the original microcline is replaced by other alkali feldspars, which may be pure orthoclase, perthite, mesoperthite, albite, or any combination of these. Under the microscope, the newly formed feldspars are most often readily distinguished by texture, freshness, and optical properties. Difficulties may arise only for samples subjected to double (or multiple) fenitization by volatiles from different sources, in which case alkali feldspar formed during previous events may became clouded or replaced. Most feldspars formed during fenitization contain variable amounts of barium, by contrast to feldspars in the wall-rock, which are barium poor.

Fenites from the eastern part of the fenite aureole at Alnö contain almost pure orthoclase, perthite, and albite (Fig. 2.9). Morogan and Woolley (1988) state that "In most examples from the eastern aureole the feldspar is orthoclase, which

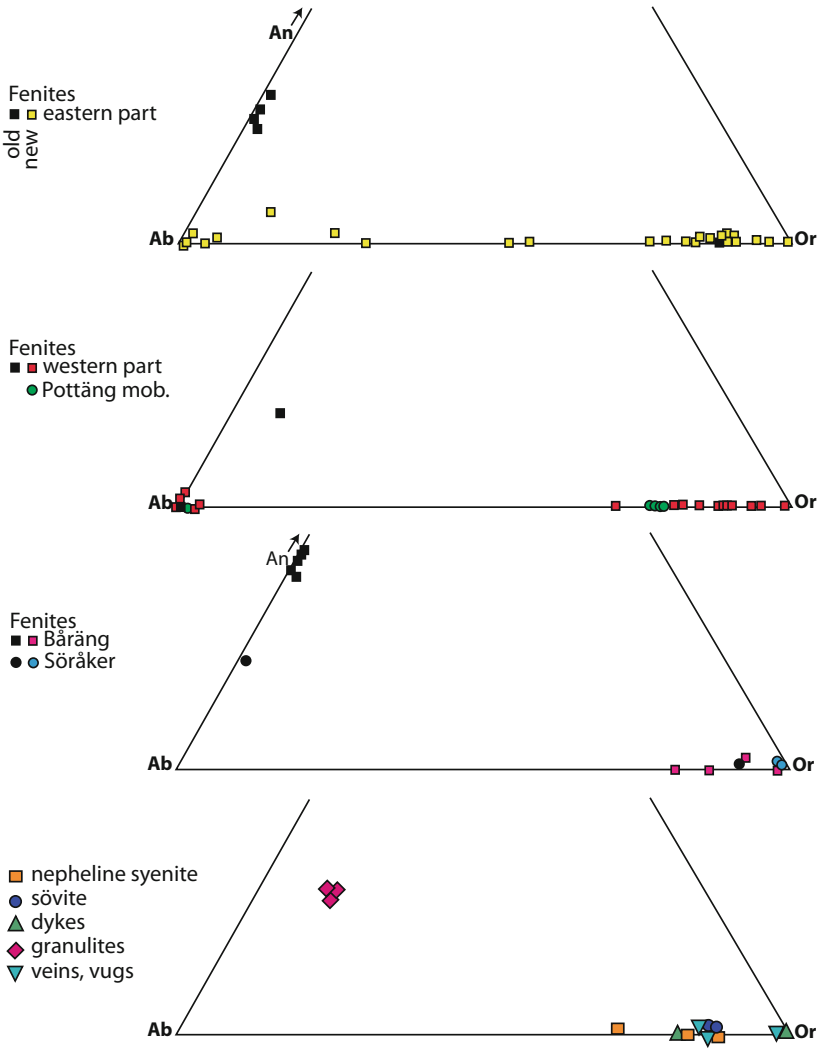

Fig. 2.9 Composition of Alnö feldspar in terms of the albite, orthoclase and anorthite components (after Morogan and Woolley (1988) and Kresten (1990))

becomes pure (95% Or) next to the contact with sövitic dykes, but albite occurs, in association with orthoclase, in some high-grade fenites". Fenites from the western part of the aureole again show a potassic feldspar (Or > 72%) and an albitic phase (Fig. 2.9). The former seems restricted to high-grade fenites and sövite contact fenites (Morogan and Woolley 1988).

Fenites from Båräng and Söråker carry orthoclases; no albite or intermediate phase has been recorded (Fig. 2.9) as both sites most certainly are sövite-induced fenites only, without significant previous ijolite-induced fenitization. The view of Rubie and Gunther (1983) that feldspars that forms by equilibration with super-critical CO_2-rich fluids would be high-K orthoclase seems thus verified. At both, the eastern and western sector of the main intrusion at Alnö, a source of fenitization additional to carbonatite (=sövite), has to be assumed, causing the formation of intermediate feldspars and albites, and the most likely choice is volatiles that emanated from ijolite intrusions.

The Pottäng rheomorphic fenites show three different types of alkali feldspars (Fig. 2.9) Cloudy orthoclase perthite with about 21 mol% albite and low (0.4–0.6) contents of the celsiane. (2) fresh orthoclase perthite with about 20% of the albite molecule and 1.8–2.7% of celsiane. (3) Fresh albite exsolved from perthite type (2). Feldspar phases (2) and (3) yield equilibration temperatures of 550 °C at 1 kbar pressure for sanidine equilibration using the two-feldspar geothermometer of Whitney and Stormer (1977). The estimated equilibration temperatures for Hartung fenites is about 600 °C. The most plausible model for the formation of the rheomorphic fenites, from field evidence, is a double fenitization—first by fluid emanated from ijolite, then by fluids emanated from sövite. Based on the similarities in composition between the two perthite generations—the main difference being the barium contents, a model of double fenitization by volatiles emitted from the same parent is also possible, and could initially produce less evolved (low Ba), then more evolved (high Ba) compositions.

Feldspars from nepheline syenites are perthitic orthoclases and, those from sövites have higher Or contents (Fig. 2.9). Trachyte dykes carry perthites, while carbonatite dykes contain pure orthoclase. Late veins usually also contain fairly pure orthoclase. Adularia (Or 98.5) has been found in vugs in the Oxåsen tuffbreccia.

2.15 Nepheline

Nepheline occurs in some pyroxenites and is a major constituent of melteigite-ijolite-urtite rocks, nepheline syenites, and nephelinite or phonolite dykes. Prone to alterations, nepheline is often altered into cancrinite, white mica and zeolites. Fresh nepheline contains variable amounts of potassium.

Starting off proposing the concept of true magmatic rocks at Alnö (von Eckermann 1942), their area and relative importance was successively diminished (von Eckermann 1948a, 1948b, 1960a) increasingly favouring "nephelinization processes" (von Eckermann 1974). Since then, it has been proven that the pyroxenites, ijolites, and nepheline syenites are true magmatic rocks (Brueckner and Rex 1980; Vuorinen 2005; Vuorinen and Hålenius 2005). Nepheline in fenites are very rare, however, and Morogan and Woolley (1988) conclude that nepheline is found only in contact fenites to sövites (i.e., double-fenitized rocks), and that fenite nephelines are distinguished from magmatic nephelines by equilibration temperatures of 500–750 °C for the former, and 700–775 °C for the latter. The diagram comprising available data (Fig. 2.10) shows that nephelines from fenites plot usually at lower equilibration temperatures than most nephelines from nepheline syenites. Fenite nephelines are similar to nephelines from ijolites and a phonolite. Particularly, many ijolites seem to have been affected by late re-equilibration and/or alteration processes.

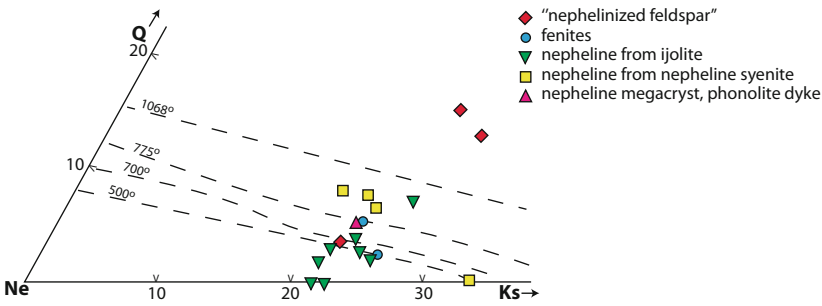

Fig. 2.10 Alnö nepheline compositions in part of the system nepheline-kalsilite-quartz (weight%), with the limits of nepheline solid solution according to Hamilton (1961)

References

Andersen T (1986) Compositional variation of some rare earth minerals from the Fen complex (Telemark, SE Norway): implications for the mobility of rare earths in a carbonatite system. Mineralog Magaz 50:503–509

Andersen T (1989) Carbonatite-related contact metasomatism in the Fen complex, Norway: effects and petrogenetic implications. Mineral Mag 53:395–414

Brueckner HK, Rex DC (1980) K-Ar and Rb- Sr geochronology and Sr isotopic study of the Alnö alkaline complex, northeastern Sweden. Lithos 13:111–119

Busche FD, Prinz M, Keil K, Kurat G (1972) Lunar zirkelite: a uranium bearing phase. Earth Planet Sci Lett 14:313–321

Gurney JJ (1984) A correlation between garnets and diamonds in kimberlites. In: Glover JE, Harris PG (eds) Kimberlite occurrence and origin: a basis for conceptual models in exploration. University of Western Australia, Publication No. 8, pp 143–166

Hamilton DL (1961) Nephelines as crystallization temperature indicators. J Geol 69:321–329

Hidden W, Mackintosh (1888) On a new thorium mineral, auerlite. Am J Sci, s3-36(216): 461–463

Hogarth DD (1989) Pyrochlore, apatite and amphibole: distinctive minerals in carbonatite. In: Bell K (ed) Carbonatites genesis and evolution. Unwin Hyman, London, pp 105–148

Högbom AG (1895) Über das Nephelinsyenitgebiet auf der Insel Alnö. Geol Fören Stockh Förh 17:100–160

Holmquist PJ (1893) Pyrochlor från Alnön. Geol Fören Stockh Förh 15:588–606

Holmquist PJ (1894) Knopit, ett perowskit närstående, nytt mineral från Alnön. Geol Fören Stockh Förh 16(73):95

Holmquist PJ (1896) Synthetische Studien über die Perowskit und Pyrochlormineralien. Thesis. Bull Geol Inst Univ Uppsala III:181–260

Hussak E (1898) Ueber ein neues Vorkommen von Baddeleyit als accessorischer Gemengtheil der jacupirangitähnlichen basischen Ausscheidungen des Nephelinsyenites von Alnö, Schweden. N Jahrb Mineral 2:228–229

Irvine TN (1965) Chromian spinel as a petrogenetic indicator. Part I theory. Can J Earth Sci 2(648):672

Irvine TN (1967) Chromian spinel as a petrogenetic indicator. Part II petrologic applications. Can J Earth Sci 4:71–103

Jordan MM (1989) The Alnö alkali complex, North East Sweden: a field and geo-chemical study of a carbonatite intrusion and the accompanying process of fenitization. MS thesis, University of Glasgow

Konev AA (1978) Les minéraux de titane et de zirconium dans les skarns du massif alcalin de Tagérane (Baïkal, Sibérie). Bull Mineral 101:387–389

Kresten P (1986) The Alnö alkaline area. In: 7th IAGOD symposium excursion guide No. 9/10. Swedish Geological Survey 67, 20–22

Kresten P, Morogan V (1986) Fenitization at the Fen complex, southern Norway. Lithos 19:27–42

Kresten P, Nairis HJ (1982) Alnö diamonds. Geol Fören Stockh Förh 104:210

Kresten P, Persson L (1975) Discrete diopside in alnöite from Alnö Island. Lithos 8 (187):192

Kresten P (1979) The Alnö complex: discussion of the main features, bibliography and excursion guide. Nordic Carbonatite Symposium, Alnö
Kresten P (1973) Kimberlitic zircons. Ext abstr., Int. Kimberl. Conf. Cape Town, pp 191–194
Kresten P (1976) Chrome pyrope from the Alnö Complex. Geol Fören Stockh Förh 98:179–180
Kresten P (1988) The chemistry of fenitization: examples from Fen, Norway. Chem Geol 68 (329):349
Kresten P (1990) Alnöområdet. In: Lundqvist T, Gee D, Kumpulainen R, Karis L, Kresten P (eds) Beskrivning till berggrundskartan över Västernorrlands län. Sveriges geologiska undersökmingar, ser Ba, 31, 238–278
Kresten P (1992b) Identification of metamict minerals by X-ray diffraction and thermoanalytical techniques. Geol Fören Stockh Förh (Submitted)
Kresten P (1993) Identification of metamict minerals by X-ray diffraction and thermoanalytical techniques. Geol Fören Stockh Förh 115:77–91
Kresten P, Fels P, Berggren G (1975) Kimberlitic zircons a possible aid in prospecting for kimberlites. Mineral Depos 10:47–56
Kresten P, Nairis HJ, Wadsten T (1982) Hydroandradite from Alnö Island Sweden. Geol Fören Stockh Förh 104:240
Mariano, A.N., (1989) Nature of economic mineralization in carbonatites and related rocks. In: Bell K (ed) Carbonatites. Genesis and evolution. Unwin Hyman, pp 149–176
Mitchell RH (1980) Pyroxenes in the Fen alkaline complex, Norway. Am Mineral 65:45–54
Mitchell RH (1986) Kimberlites: mineralogy, geochemistry and petrology. Plenum Press, New York and London, p 442
Morogan V, Woolley AR (1988) Fenitization at the Alnö carbonatite complex, Sweden: distribution, mineralogy and genesis. Contrib Mineral Petrol 100:169–182
Morogan V (1989) Mass transfer and REE mobility during fenitization at Alnö Sweden. Contrib Mineral Petrol 103:25–34
Nickel EH, Mandarino JA (1987) Procedures involving the I.M.A. Commission on new minerals and mineral names, and guidelines on mineral nomenclature. Schweiz Mineral Petrogr Mitt 67:185–210
Nowicki TE, Moore RO, Gurney JJ, Baumgartner MC (2007) Diamonds and associated heavy minerals in kimberlite: a review of key concepts and applications. Developments Sedimentology 58:1235–1267
Perchuk, L.L., (1967b) Analysis of thermodynamics of equilibria in amphibole garnet rocks. Izv Akad Nauk SSSR 1967, 3, 57–83. (In Russian)
Prins P (1972) Composition of magnetite from carbonatites. Lithos 5:227–240
Raber E, Haggerty SE (1979) Zircon oxide reactions in diamond bearing kimberlites. In: Boyd FR, Meyer HOA (eds) Kimberlites, diatremes and diamonds. AGU, Washington, pp 229–240
Råheim A, Green DH (1974) Experimental determination of temperature and pressure dependence of the Fe Mg partition coefficient for coexisting garnet and clinopyroxene. Contrib Mineral Petrol 48:179–203
Rubie DC, Gunther WD (1983) The role of speciation in alkaline igneous fluids during fenite metasomatism. Contrib Mineral Petrol 82:165–175
Sandström F, Binett T, Wiklund C, Vikström J (2010) Alnöområdets geologi och mineralogi. Litofilen. 27(2):14–42

van der Veen AH (1963) A study of pyrochlore. Verh Kon Nederlands Geol Mijnbouw Gen, Geol Ser 22, 188
von Eckermann H (1942) Ett preliminärt meddelande om nya forskningsrön inom Alnö alkalina område. Geol Fören Stockh Förh 64(399):455
von Eckermann H (1948) The alkaline district of Alnö Island. Sver Geol Unders Ca 36, 176
von Eckermann H (1948b) The genesis of the Alnö alkaline rocks. Int Geol Congr 18th Sess. III, 3–10
von Eckermann H (1939) The "baddeleyite from Alnö" an error. Mineral Mag 25(413):414
von Eckermann H (1960a) Borengite. a new ultra potassic rock from Alnö island. Arkiv Mineral. Geol. 2(39): 519–528
von Eckermann H (1967b) A comparison of Swedish, African and Russian kimberlites. In: Wyllie PJ (ed) Ultramafic and related rocks. Wiley, pp 302–312
von Eckermann H (1974) The chemistry and optical properties of some minerals of the Alnö alkaline rocks. Arkiv Mineral. Geol 5(8): 93–210
Vuorinen JH (2005) The Alnö alkaline and carbonatitic complex, east central Sweden—a petrogenetic study. PhD Thesis, Stockholm University, 130
Vuorinen JH, Hålenius U (2005) Nb-Zr and LREE-rich titanite from the Alnö alkaline complex: crystal chemistry and its importance as a petrogenetic indicator. Lithos 83:128–142
Whitney JA, Stormer JC Jr (1977) Two-feldspar geothermometry, geobarometry in mesozonal granitic intrusions: three examples from the Piedmont of Georgia. Contrib Mineral Petrol 63:51–64

Geochemistry and Alnö as an Economic Reserve

3

Abstract

The compositional spectrum of Alnö rocks is discussed in respect to major, and trace elements as well as for stable and radiogenic isotopes (O, Sr, Nd). The evidence points to a deep mantle, possibly OIB, origin of the Alnö igneous rocks, bearing similarity to "rift-related" plumlets (plume fingers) that typically penetrate such settings. Although a possible source for REE, Alnö is at present not economically viable. Its status as a Nature Reserve is thus currently not threatened, but a changing economic situation in the coming decades could bring a reversal of this fragile balance. The weathering behaviour and the former use of Alnö carbonatites as fertilizer is briefly outlined.

3.1 Major and Trace Element Geochemistry

Only a short glance at the list of minerals occurring within the Alnö complex (see Chap. 2), in particular the non-silicates, shows that much of the periodic system of elements is present at Alnö, including some of the usually less common elements. Notably, there are substantial variations in the contents of what we usually call major and trace elements, as their role is sometimes reversed at Alnö, with some trace elements of "ordinary" rocks becoming rock-forming components in the Alnö suite, whereas others that are common in sub-alkaline igneous complexes elsewhere are less crucial at Alnö. These variations make it almost impossible to quote "representative analyses", but Table 3.1 shows an attempt to provide semi-representative compositions for the main rock types that occur on and near Alnö.

P. Kresten and V. R. Troll, *The Alnö Carbonatite Complex, Central Sweden*, GeoGuide, https://doi.org/10.1007/978-3-319-90224-1_3

Table 3.1 Representative chemical analyses of Alnö rocks (after Kresten 1990)

ppm	1	2	3	4	5	6	7	8	9	10
	YK167	LHH1	PK141	LHH28	LHH41C	TL69:142	PK75:326	PK75:293	TL69:139	PK75:251B
SiO_2	62.8	48.7	25.9	41.2	46.6	3.31	17.1	7.0	32.9	39.0
TiO_2	0.39	0.36	0.84	1.04	0.66	0.21	1.10	1.0	2.72	0.38
Al_2O_3	14.0	18.8	5.0	16.1	20.6	0.32	5.6	9.0	5.4	1.3
Fe_2O_3	1.0	2.2	9.4	5.4	3.5	3.17	1.72	2.0	8.5	2.5
FeO	2.9	2.8	5.5	4.6	–	2.34	3.22	4.3	–	9.6
MnO	0.07	0.21	0.45	0.35	0.21	0.21	–	0.43	0.15	0.21
MgO	1.54	1.15	3.8	2.5	0.91	3.54	8.4	14.0	7.5	38.5
CaO	1.70	5.8	30.5	12.3	6.5	46.5	34.3	24.6	17.8	2.6
Na_2O	3.4	0.80	1.6	10.0	9.1	0.12	0.13	0.20	3.2	0.2
K_2O	4.2	10.5	0.7	2.8	4.8	0.13	1.30	0.40	3.1	0.8
H_2O	0.9	2.00	1.6	0.6	–	0.20	0.70	0.9	0.4	2.9
P_2O_5	0.23	0.48	6.9	1.30	–	6.2	4.15	1.03	1.49	0.10
CO_2	0.70	4.6	3.5	2.6	–	31.3	22.1	36.3	14.1	0.22
F	–	–	0.29	–	–	0.29	–	0.11	–	0.06
S	0.10	0.38	1.6	0.06	–	–	–	0.55	–	0.29
BaO	0.38	0.85	0.0	0.48	0.97	0.09	0.16	1.80	0.11	0.03
SrO	0.03	0.11	0.41	0.15	0.29	0.52	0.46	0.24	0.12	0.01
Total	99.74	99.74	98.17	101.48	94.14	98.45	100.44	97.36	97.49	99.02
ppm										
Zn	55	125	–	130	160	90	95	35	140	–
Rb	174	145	17	90	95	4.8	60	–	91	12

(continued)

Table 3.1 (continued)

ppm	1	2	3	4	5	6	7	8	9	10
	YK167	LHH1	PK141	LHH28	LHH41C	TL69:142	PK75:326	PK75:293	TL69:139	PK75:251B
Nb	40	500	450	300	280	820	750	–	–	40
La	35.5	530	1650	170	199	510	380	875	166	18.3
Ce	52.7	804	1900	347	332	1300	1200	1990	360	34.0
Eu	1.5	6.3	39	6.7	3.3	14.8	14	14.4	5.9	0.5
Yb	2.3	1.8	19.5	3.2	1.4	3.1	3.5	14.3	1.2	–
Hf	3.3	1.7	48	5.6	6.0	8.0	8.0	–	1.7	1.8
Ta	<1	29	9.8	31	43	320	50	–	7.4	15
Th	8.4	28	39	25	15	570	80	15700	54	6.3
U	19.0	52	–	8.6	–	540	480	58	56	–

1. Weakly fenitized migmatite, east of Stornäset
2. High-grade fenite, south-eastern part of Långharsholmen
3. Uncompahgrite (melilitolite), Söråker. Analysis includes 0.18% ZrO_2
4. Ijolite, intrusion into sövite-pyroxenite layers, northwestern Långharsholmen
5. Nepheline syenite, small skerry east of Långharsholmen
6. Sövite, quarry north of Smedsgården
7. Sälskär volcanic breccia, matrix, boulder south of Östra Sälskär
8. Radioactive beforsite dyke, Töva
9. Matrix of the alnöite breccia at Hovid
10. Ultramafic fragment in kimberlitic alnöite boulder, Rödön. Analysis includes 0.32% Cr_2O_3

The process of fenitization is illustrated by analyses 1 and 2 in Table 3.1, showing a weakly fenitized wall-rock (greywacke migmatite) and high-grade (syenitic) fenite, respectively. Increased fenitization results in drastic lowering of silica and sodium, while calcium, potassium, phosphorous, carbon dioxide, barium and many trace elements increase in concentration due to fluid-rock interaction and the loss of silica. As fenitization is caused mainly by the alkaline silicate rocks such as ijolites, silica would have begun to have been driven off already prior to the intrusion of the sövites. Hence, "silification" of sövites due to fenitization, as claimed by some workers, may not always apply at Alnö. Instead, we find that the silica that was driven off now forms (peripheral) veins and vugs. Uptake of silica-rich materials (e.g. silicate crystals) by later sövites from earlier silicate rocks (e.g. Möller et al. 1980; Vuorinen and Skelton 2004) is not contradicted by this consideration.

The melilitolite (uncompahgrite) at Söråker has a peculiar composition (analysis 3 in Table 3.1), with low silica and high calcium due to high contents of the mineral melilite. Apatite is elevated in P_2O_5 and garnet shows elevated contents of zirconium and hafnium (i.e. kimzeyitic garnet). Rare earth elements are thus at a high level in this rock, but also in general on Alnö (see below).

Alkaline plutonic rocks (analyses 4 and 5 in Table 3.1) show common compositions for such rock types and lack the extreme compositional values of the carbonatites (sövites). The sövite, on the other hand, (analysis 6 in Table 3.1) shows relatively high contents of Nb, Ta, the REE, as well as Th and U. Similar data have been obtained for the matrix of the Sälskär breccias (analysis 7 in Table 3.1), although Th contents are much lower than U contents. A beforsite dyke outcropping on the main road 12 km west of Sundsvall (see above) has a yet more remarkable composition (analysis 8 in Table 3.1). The barium content is high (harmotome), as are the REE, and Th shows percentage values due to the presence of brockite. Using a scintillometer, one can't miss the dyke; the apparatus goes right beyond scale. By contrast, alnöite (analysis 9 in Table 3.1) shows no extreme values, with the exception of a dunite nodule (analysis 10 in Table 3.1) that is almost exclusively composed of Mg-rich olivine and chrome spinel.

As for most alkaline and carbonatite complexes, the geochemistry of Alnö rocks is characterized by relatively high concentrations of various trace elements, such as Ba, Cs, Nb, Zr, Hf, U, Th and the rare earth elements (REE) (see Table 3.1 and Fig. 3.1). There are considerable variations in the contents of these elements in the various rock types, but generally the Alnö carbonatites are enriched relative to regular sub-alkaline igneous rocks (Figs. 3.1 and 3.2). Notably, however, the Alnö carbonatites are not above the REE concentrations that are currently considered

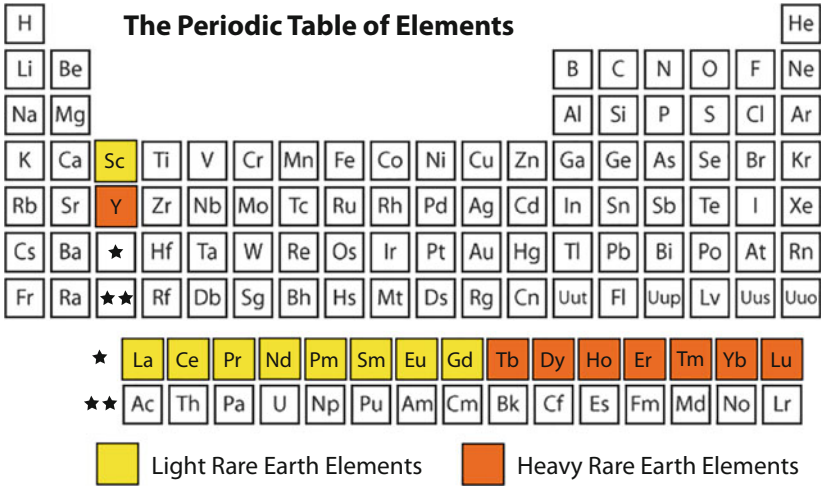

Fig. 3.1 Periodic table of elements with the light rare earth elements (LREE) marked in yellow and the heavy rare earth elements (HREE) in orange

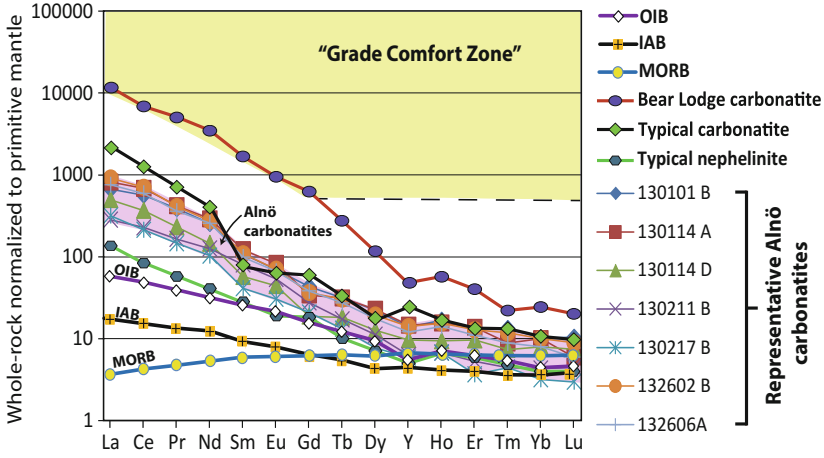

Fig. 3.2 Normalized REE concentrations (after Sun and McDonough 1989) of Alnö carbonatite samples compared to typical carbonatite and nephelinite compositions and to the highly economic Bear Lodge carbonatite in the USA (after Chakhmouradian and Zaitsev 2012). The Alnö carbonatites are not particularly enriched relative to other carbonatites and immediate economic viability is not apparent, at least not in the current economic climate (OIB=Ocean Island Basalt, IAB=Island Arc Basalt, MORB=Mid Ocean Ridge Basalt)

economically viable, i.e. the Alnö carbonatites plot below the "grade comfort zone" of Chakhmouradian and Zaitsev (2012) (Fig. 3.2).

Although, the concentrations for heavy rare earth elements (HREEs) are less pronounced in Alnö carbonatites than those of the LREEs (Fig. 3.2), all REEs are enriched relative to average crust and also relative an array of alkaline complexes throughout the world (Vuorinen and Hålenius 2005). The minerals that bear these high concentrations in the sövites are calcite, apatite, magnetite, titanite, pyrochlore, phlogopite, amphibole, melilite and olivine (cf. Loubet et al. 1972; Hogarth 1989), but especially bastnäsite and monazite (Morogan and Lindblom 1995; see also Chap. 2). These constituents may be regarded as 'economic minerals' and are highly sought after in many volcanic alkaline provinces (Evans 1993; Goodenough 2014; Goodenough et al. 2016). The high concentrations of REE are generally attributed to the enriched nature of carbonatite magmas (Kresten 1980; Andersen 1987; Eriksson 1989; Schleicher et al. 1990; Mitchell 2005), but we note that the REE distributions in the sövites of the Alnö Complex are heterogeneous. Overall, however, the Alnö sövites have similar REE distribution patterns to most silicate rocks from the complex (Möller et al. 1980; Vuorinen and Hålenius 2005) and then common REE distribution patterns imply a common and likely magmatic origin (Möller et al. 1980; Kresten 1986; Viladkar and Pawaskar 1989; Lottermoser 1990). Provided that the parental melts of the carbonatites and alkaline rocks were originally related, the carbonatite melts probably separated through fractionation or liquid immiscibility and the REEs were thus distributed between magmas with a preference of REE to stay in the carbonatite (Möller et al. 1980; Kjarsgaard 1998). Although the REE distribution pattern is shared, the carbonatite liquid would hold a higher capacity to concentrate REE than the silicate liquid, resulting in the carbonatites having often somewhat higher REE concentrations than the associated alkaline silicate rocks (cf. Balashov and Pozharitskaya 1968; Chakhmouradian and Zaitsev 2012).

In addition to REE, kimberlite-type magmas that originate deep in the mantle, may carry peridotite xenoliths and xenocrystals such as garnets and possibly even diamonds (Wyllie and Huang 1975; Dawson 1980; Sparks et al. 2007; Mitchell 2008). Such magmas bear remarkably high densities and volatile reactions between carbon dioxide (CO_2), water (H_2O) and magma/source rock need to occur to promote ascent from the mantle to the crust (Sobolev and Chaussidon 1996; Patterson et al. 2009). For instance, carbonatite magma can mix with silicate mantle melts to make kimberlite magma, which creates a remarkably high potential to ascend at relatively high speed from depth (Russell et al. 2012). Although circumdancial, the late occurrence of the carbonatites at the Alnö Complex, together with the likely existence of a shallow magma chamber (e.g. Andersson

et al. 2013) implies late stage liquid immiscibility of kimberlite-type magmas to produce the Alnö carbonatites (cf. Kresten 1990; Andersson et al. 2013). Thus, if present, diamond survival may have been compromised during upper crustal magma storage and evolution prior to final ascent and eruption (e.g. Andersson et al. 2013).

3.2 Radiogenic Isotopes

Using major and trace elements to assess magmatic source compositions can be difficult due to modal mineral variations or variable degrees of fractionation. Isotopic tracers, in turn, may be more reliable, because radiogenic isotopes are insensitive to physical changes such as temperature, pressure or crystallisation conditions, but reflect the various source compositions involved in petrogenesis (Ellam and Stuart 2004). Carbonatites have long been considered to carry information on the chemical and isotopic evolution of the Earth's interior (e.g. Bell et al. 1982; Nelson et al. 1988; Mitchell 2005; Jones et al. 2013) and radiogenic isotopes are frequently used to evaluate the evolution of the mantle and the contributions of mantle versus crustal components to carbonatite petrogenesis. Igneous rocks emplaced within continental crust do often include crustal components and the Fen complex in Norway is a prime example of a carbonatite intrusion whose radiogenic isotope characteristics reflect interaction with the local bedrock it intruded (e.g. Andersen 1987; Andersen and Taylor 1988). It is therefore imperative to identify crustal additions before interpretation of isotope data for mantle source compositions.

Sr isotope data on the Alnö carbonatite complex have been published by Bell and Powell (1970), Blaxland (1978) and Brueckner and Rex (1980). An initial $^{87}Sr/^{86}Sr = 0.7035 \pm 0.0001$ was obtained by Blaxland (1978), while Brueckner and Rex (1980) reported whole-rock initial $^{87}Sr/^{86}Sr$ of up to 0.70437 ± 0.00017 from alkaline dyke rocks from the main complex. The variation in initial Sr isotopic composition observed by Brueckner and Rex (1980) was interpreted as a result of crustal assimilation of the intrusive silicate rocks. The sövite samples analysed by Brueckner and Rex (1980), in turn, have very low $^{87}Rb/^{86}Sr$, and $^{87}Sr/^{86}Sr$ ratios down to 0.70363 ± 0.00003. These low $^{87}Sr/^{86}Sr$ values agree with the $^{87}Sr/^{86}Sr$ ratio of 0.7032 reported by Bell and Powell (1970) for an Alnö sövite.

Here we present a set of Sr–Nd data from 13 Alnö rock samples that shed further light on these aspects. The samples comprise of carbonatites, apatite-rich rocks and silicate rocks from the Main Complex (including the Båräng vent), the

Northern Ring Complex and the Söråker intrusion. These latest Sr and Nd isotopic compositions were determined by T. Andersen (Oslo University) in the isotope laboratory of the Mineralogical-Geological Museum of Oslo, using methods for separation and mass spectrometry described by Mearns (1986). The data are summarised in Vuorinen (2005) and are presented here with permission from T. Andersen. Sr was run on single Ta filaments, Nd on triple Ta–Re filaments, both in a VG 354 5-collector mass spectrometer. Multicollector peak-switching methods were used for the measurements. Results obtained for the NBS 987 (Sr) and Johnson and Matthey Nd_2O_3 (batch S819093A) standards were similar to those reported earlier from the same laboratory (Mearns 1986; Andersen 1987). The Nd isotope ratios were normalized to $^{146}Nd/^{144}Nd = 0.721900$. Sm, Nd, Rb and Sr concentrations were determined by standard isotope dilution methods using mixed Rb–Sr and Sm–Nd spikes. The Sm and Nd loads were run on the VG 354 instrument, using the triple filament method, whereas a single collector VG Micromass 30 mass spectrometer was used for Sr and Rb determinations (single filament technique). Analytical data are presented in Table 3.2, together with calculated initial $^{87}Sr/^{86}Sr$ and $^{143}Nd/^{144}Nd$ ratios (at 584 Ma) and their corresponding ε-values. The initial $^{87}Sr/^{86}Sr$ and $^{143}Nd/^{144}Nd$ isotopic ratios were recalculated to εSr and εNd values using the bulk earth parameters proposed by Jacobsen and Wasserburg (1984).

All of the above samples, except one, plot in the "depleted mantle" sector in a plot of εNd versus εSr (Fig. 3.3). The Söråker uncompahgrite and the sövites from the Northern Ring Complex have the most depleted character ($\varepsilon Nd > +2.5$, $\varepsilon Sr < -11$). These samples are significantly less radiogenic than the alkaline silicate intrusions reported by Blaxland (1978) and Brueckner and Rex (1980). One of the sövite samples from the Main Complex has a low εSr, similar to the sövites of the Northern Ring Complex, whereas the other samples analysed from the main complex have higher εSr (>−9) and lower εNd (<2.0).

To evaluate the implications for the petrogenesis of the Alnö complex, it is necessary to first characterize possible contamination effects from local upper and/or lower crust before considering possible mantle sources. The Alnö complex has been emplaced into Proterozoic metasedimentary gneisses and migmatites of the Svecocarelian orogenic belt (Lundqvist 1979; Lundqvist et al. 1990). The data in Table 3.2, and additional unpublished data by Vuorinen (2005) show that most Alnö samples fall into the depleted Nd- and Sr-isotope sector, which is common for many carbonatites world-wide. In particular, some ijolite and pyroxenite close to the margins of the main intrusion have slightly enriched Sr-isotopic signatures, which Vuorinen (2005) attribute to magma-crust interaction of intruding magmas with hydrothermally leached fluids from the surrounding crustal rock compositions (e.g. during

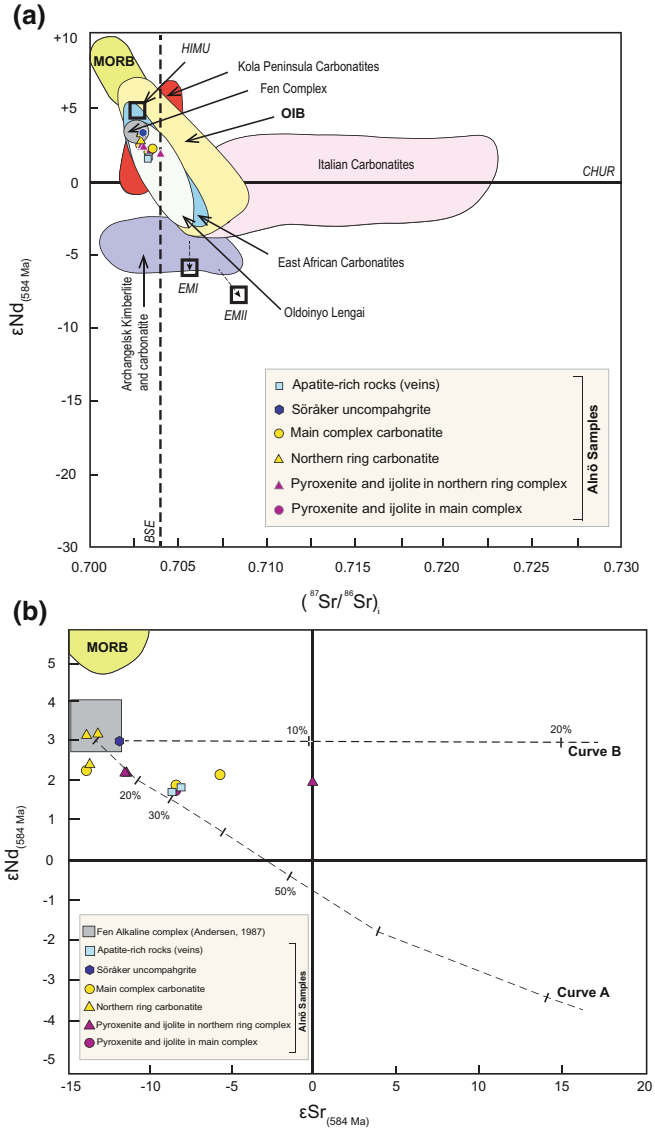

Fig. 3.3 **a** Radiogenic isotope diagram for Alnö samples analyzed by Andersen (see text for details). Most Alnö samples plot in the "depleted" sector of the diagram, implying a depleted mantle to be involved in the petrogenesis of the Alnö rocks. However, their enriched trace element character implies a metasomatically modified mantle source. **b** Crustal additions are frequently observed in carbonatites suites worldwide and the Alnö rocks reflect crustal assimilation of up to 30% for the most affected samples (see text for details)

fenitization). Apart from theses marginal samples, however, there is overlap between the carbonatites and ijolites and nepheline syenites, implying a direct genetic relationship between the silicate and carbonatite igneous rocks from Alnö.

The variation towards enriched initial Sr and Nd isotope compositions in some Alnö samples may reflect a contribution from a component with high εSr and low εNd, such as may be found in old, Rb and LREE-enriched continental crust (see Table 3.2). The effect of contamination on the Sr and Nd isotopic systems is likely pronounced due to the large differences in values (especially for Sr) between Alnö silicate magmas and wall-rock. This is because bulk contamination processes are strongly dependent on the initial Sr and Nd concentrations in the magma and in the contaminant. Carbonatite magmas, in turn, have high initial concentrations of Sr and Nd, and their Sr- and Nd-isotope compositions are thus less sensitive to crustal additions, whereas the associated silicate rocks may more directly reflect open system behaviour due to their lower Sr and Nd concentrations. Indeed, Vuorinen and Skelton (2004) have suggested that considerable amounts of ijolitic and high-grade fenitized wall-rock (sometimes up to 50%) are incorporated into some Alnö carbonatites, making careful assessment of all the available data necessary.

In order to evaluate the possibility of crustal additions as the cause of the elevated Sr-isotope compositions shown by some samples, isotopic mixing calculations after Faure (1986) were carried out, using mixtures between the primitive Alnö composition and the local crust data (Table 3.2). Mixing curve A has been constructed assuming 100 ppm Nd, 10000 ppm Sr in the primary magma, whereas model B assumes 1000 ppm Nd and 1000 ppm Sr. The starting concentrations in the mixing models have been chosen to resemble the Alnö sövite (A) and the uncompahgrite (B). All but two carbonatite samples fall between the two mixing curves. In addition, Vuorinen (2005) also calculated mixing trajectoring using crustal values from Brueckner and Rex (1980) and Claesson (1987) and a melilitite-like starting melt. The results suggest that contamination with an enriched, crustal component of 10–30% bulk contamination with local crustal material can explain the ranges seen in initial Sr and Nd isotopic compositions. However, radiogenic initial Sr-isotopic signatures appear concentrated along the edges of the main intrusion on Alnö, i.e. the contaminated isotope signature may be geographically restricted and Vuorinen (2005) suggested that element exchange may have occurred as a result of fenitization and hydrothermal leaching of surrounding bedrock at late- to post-magmatic stages of crystallization (cf. Morogan and Woolley 1988; Dunworth and Bell 2001).

In the εSr–εNd diagram, most Alnö data plot in the depleted mantle field, a feature common for many carbonatite-alkaline complexes (Andersen 1987; Dunworth and Bell 2001). Vuorinen (2005) argued that the most depleted isotope signatures from Alnö Island can be used to provide some constrain of the isotope

Table 3.2 Sr, Nd, and Pb isotopic data for Alnö rocks

Sample nr	PK141	LHH26	LHH7	JB124	LHH28	PK77:447	PK77:446	FW1	PK74:99	PK324	YK74:138	YK307	PK77:445	
Rock type	uncomp	pyrox	ijolite	ijolite	ijolite	sövite	sövite	sövite	sövite	sövite	sövite	ap-vein	ap-lens	Local
Intrusion	SÖ	N	N	M	PN	N	N	B	M	N	M	M	N	crust
Rb ppm	17.0	13.0	92.0	33.0	54.0	14.0	1.7	8.1	7.9	12.0	95.0	7.4	71.3	166
Sr ppm	3478.0	821.0	2644.0	1083.0	1133.0	7070.0	6773.0	8931.0	9014.0	4192.0	4994.0	4894.0	3683.0	167
$^{87}Rb/^{86}Sr$	0.014	0.046	0.101	0.088	0.138	0.006	0.001	0.003	0.003	0.008	0.055	0.004	0.056	2.891
$^{87}Sr/^{86}Sr$	0.703284	0.703564	0.704827	0.704153	0.704333	0.703076	0.703079	0.703617	0.703045	0.703107	0.703862	0.703423	0.703867	0.7790
2σ	0.000012	0.000012	0.000012	0.000012	0.000010	0.000012	0.000010	0.000011	0.000012	0.000012	0.000012	0.000018	0.000020	
$(^{87}Sr/^{86}Sr)_i$	0.703167	0.703185	0.703995	0.703424	0.703193	0.703029	0.703073	0.703595	0.703024	0.703039	0.703407	0.703387	0.703404	
$\varepsilon Sr_{(584\ Ma)}$	−11.8	−11.5	0.0	−8.1	−11.4	−13.8	−13.1	−5.7	−13.8	−13.6	−8.4	−8.7	−8.4	723
Sm ppm	127.4	32.5	27.7	73.3	25.4	13.3	43.9	29.8	40.8	78.9	40.6	316.8	121.1	4.1
Nd ppm	871.3	240.0	174.7	502.7	175.0	108.2	366.0	266.4	339.8	635.3	310.5	2457.4	848.0	21
$^{147}Sm/^{144}Nd$	0.089054	0.082455	0.096383	0.088736	0.088354	0.074590	0.073119	0.068131	0.073181	0.075631	0.079633	0.078491	0.086971	0.115
$^{143}Nd/^{144}Nd$	0.512392	0.512326	0.512360	0.512330	0.512348	0.512342	0.512338	0.512267	0.512292	0.512310	0.512298	0.512284	0.512318	0.5144
2σ	0.000008	0.000008	0.000008	0.000008	0.000008	0.000008	0.000008	0.000008	0.000008	0.000008	0.000008	0.000008	0.000008	
$(^{143}Nd/^{144}Nd)_i$	0.512051	0.512010	0.511991	0.511990	0.512010	0.512057	0.512058	0.512006	0.512012	0.512021	0.511993	0.511984	0.511985	
$\varepsilon Nd_{(584\ Ma)}$	3.06	2.26	1.89	1.87	2.25	3.16	3.20	2.18	2.29	2.46	1.93	1.74	1.77	−17.3

SÖ Söråker intrusion, *N* Northern Ring complex, *PN* Postdating main intrusive phase in N, *M* Main complex, *B* Båräng vent

composition of the mantle source. Employing the most "depleted" of the Alnö samples, with $\varepsilon Sr < -13$, $\varepsilon Nd > 3.1$, as the most reasonable estimate for the composition of the Alnö mantle source (Fig. 3.2), the full spectrum of isotope ratios observed at Alnö should then be regarded as a result of magmatic differentiation, including crustal assimilation.

An important feature for the "primitive" rocks from Alnö is that, although having depleted signatures with respect to their radiogenic isotope compositions, they are enriched with respect to trace elements (see above). This is similar in character to many Ocean Island Basalts (OIB) and the Alnö complex is similar in this respect to many carbonatites world-wide, being characterized by lower initial $^{87}Sr/^{86}Sr$-ratios and higher εNd than the bulk earth at the time of their formation. Isotopic compositions with $\varepsilon Nd > 0$ and $\varepsilon Sr < 0$ in mantle derived rocks are generally explained by early removal (depletion) of incompatible trace components by partial melting. Experimental studies of melting processes have demonstrated that carbonates are among the earliest phases to melt in mantle lherzolite assemblages (Olafson and Eggler 1983) and that CO_2 is a strongly incompatible component in the uppermost mantle. It is thus highly unlikely that any primeval CO_2 or solid carbonate can survive in mantle lherzolite during depletion event. Subsequent metasomatic introduction of CO_2 into the depleted mantle source seems to be a necessary condition for the formation of carbonatite and a cause for inducing such metasomatism in earlier depleted mantle may be a fluid expelled from a rising astenospheric mantle plume (e.g. Fig. 3.3; Menzies and Wass 1983; Andersen 1987; Bell and Blenkinsop 1987; Griffin et al. 1988; Verhulst et al. 2000; Bell and Tilton 2001; Dunworth and Bell 2001; Vuorinen 2005).

For the Fen complex, Andersen (1987) suggested that percolation of a CO_2–H_2O phase through the upper mantle may selectively remobilize the LREE on a local scale and redeposit them in metasomatic amphibole-phlogopite-carbonate parageneses. These may subsequently melt and form an initial carbonated nephelinite melt. Further LREE enrichment was suggested to occur through volatile transfer into the magma after its formation (Andersen 1987). Such a model may apply to Alnö complex too (see Vuorinen 2005). Notably, the Sr-isotope compositions of alkaline silicate rocks from Alnö Island is similar to that reported from e.g. Greenland, East Africa, Italy and from the Turiy and Kovdor massifs in Russia, most likely reflecting mixing trends between depleted and enriched mantle and crustal components, respectively (e.g. Andersen 1997; Stoppa and Woolley 1997; Harmer 1999; Verhulst et al. 2000; Bell and Tilton 2001; Dunworth and Bell 2001; Antonini et al. 2003; Halama et al. 2003; Wagner et al. 2003; Vuorinen 2005).

3.3 Stable Isotope Geochemistry

Although the mantle is not homogenous (e.g. Hofmann 1997), rocks from the upper mantle usually show a $\delta^{18}O$ ratio of 5.7 ± 0.3 and a $\delta^{13}C$ of −6.5 ± 2.5 (e.g. Taylor et al. 1967; Exley et al. 1986; Ito et al. 1987; Eiler et al. 1996; Hoefs 2009). In turn, OIB has a range of 4.8 to 8‰ for $\delta^{18}O$ and −7 to −5‰ for $\delta^{13}C$ (Kyser 1986; Deines 1989; Keller and Hoefs 1995), while "primary carbonatites" range in $\delta^{18}O$ from ~6 to 10‰ and for $\delta^{13}C$ from −8 to −4‰ (Taylor et al. 1967; Deines and Gold 1973; Deines 1989; Keller and Hoefs 1995; Demény et al. 1998; Dasgupta et al. 2013). The natrocarbonatites from Oldoinyo Lengai in Tanzania (see foreword by Hannes Mattsson) are a key example in this respect and define a restricted field within the 'primary carbonatite' domain, spanning from 5.8 to 6.7‰ for $\delta^{18}O$ and from −7.1 to −6.3‰ for $\delta^{13}C$ (Keller and Hoefs 1995).

Indeed, most of the available Alnö samples fall into the field of "primary carbonatites" and very few values of Alnö carbonatites exceed the primary carbonatite field in carbon and oxygen isotopic compositions. Moreover, the Alnö carbonatite samples available do not follow high-temperature or low-temperature alteration trends (Fig. 3.4; e.g. Demény et al. 1998). Specifically, the combined stable isotope data available suggest that low-temperature interaction with hydrothermal fluids derived from meteoric water has not been a prominent process at Alnö. Moreover, the majority of the isotope values in Fig. 3.4 plot close to or within the primary calcite domain of Skelton et al. (2007), while their "secondary" (remobilised) calcite samples show more scatter, but still plot in the field for "primary carbonatites" defined above.

Modification of primary magma though interaction with its surrounding is indeed plausible as the migmatite around the Alnö complex originates from greywacke-type marine sediments (von Eckermann 1948; Kresten 1979), consistent with a sedimentary signal in some of the $\delta^{18}O$ and $\delta^{13}C$ data (Fig. 3.4). This then likely reflects modest magma-crust interaction (cf. von Eckermann 1948, 1966; Demény et al. 2010). Some data points, in turn, are consistent with the notion of silicate assimilation from e.g. the igneous lower crust or from the basement migmatites (e.g. Russell et al. 2012), which seems to confirm Vuorinen and Skelton (2004) who argued for of locally intense assimilation of silicate minerals by the originally mantle-derived carbonatites at Alnö. Therefore, the various trends (Fig. 3.4) indicate that magma genesis in the Alnö carbonatite system involved both mantle and crustal components (cf. Taylor et al. 1967; Savin and Epstein 1970; Deines 1989; Keller and Hoefs 1995; Demény et al. 1998; Hoefs 2009), thus supporting the available radiogenic isotope data (see above). Various

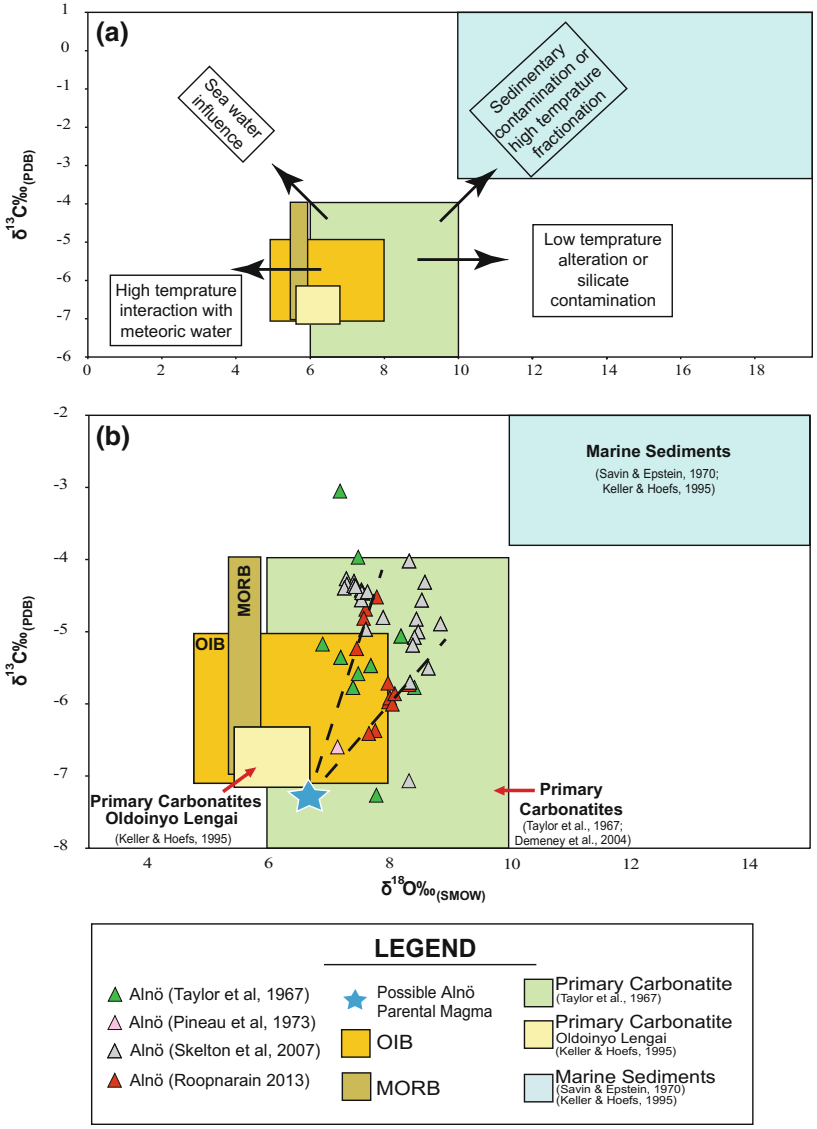
(a)
Sea water influence
Sedimentary contamination or high temprature fractionation
Low temprature alteration or silicate contamination
High temprature interaction with meteoric water
δ13C‰(PDB)
(b)
Marine Sediments
(Savin & Epstein, 1970; Keller & Hoefs, 1995)
MORB
OIB
Primary Carbonatites Oldoinyo Lengai
(Keller & Hoefs, 1995)
Primary Carbonatites
(Taylor et al., 1967; Demeney et al., 2004)
δ18O‰(SMOW)
LEGEND
Alnö (Taylor et al, 1967)
Alnö (Pineau et al, 1973)
Alnö (Skelton et al, 2007)
Alnö (Roopnarain 2013)
Possible Alnö Parental Magma
OIB
MORB
Primary Carbonatite (Taylor et al., 1967)
Primary Carbonatite Oldoinyo Lengai (Keller & Hoefs, 1995)
Marine Sediments (Savin & Epstein, 1970) (Keller & Hoefs, 1995)

◀ **Fig. 3.4** **a** Isotopic variations (O, C) in carbonatites, after Demény et al. (1998). The $\delta^{18}O$ and $\delta^{13}C$ of Mid-Ocean Ridge Basalt (MORB), the ocean island field (OIB) and the 'primary carbonatite' field of 'unaltered' primary magmatic carbonatites are shown. **b** Oxygen-Carbon isotope plot for Alnö carbonatites. Red triangles symbolise the most recent isotopic data (Roopnarain 2013), grey are data by Skelton et al. (2007), green are data by Taylor et al. (1967) and pink are data by Pineau et al. (1973). A prospective projection towards the ultimate Alnö parental magma is also shown (after Roopnarain 2013). Reference fields are after Taylor et al. (1967), Savin and Epstein (1970), Andersen (1987), Exley et al. (1986), Deines (1989), Eiler et al. (1996), Keller and Hoefs (1995), Demény et al. (1998), Melezhik et al. (2003), Skelton et al. (2007), Hoefs (2009), Bouabdellah et al. (2010) and Casillas et al. (2011)

crustal components were likely assimilated *en route* to the surface (Fig. 3.4b), and this realisation now allows us to use the available data to reconstruct the original mantle source (e.g. Roopnarain 2013).

Since the majority of the $\delta^{18}O$ and $\delta^{13}C$ ratios for the Alnö complex also overlap with the OIB field, in addition to the primary carbonatite field, the combined Alnö data support a mantle origin, and taking crustal processes in account, likely an "ocean island-type" character of the investigated samples (cf. Taylor et al. 1967; Keller and Hoefs 1995). This is especially so, because using the most recent $\delta^{18}O$ and $\delta^{13}C$ data from carbonate separates only (red triangles in Fig. 3.4b), a projected "common parent" magma plots at the lower intersection of OIB and primary carbonatite fields (Roopnarain 2013).

We then compare the Alnö carbonatite data with data from other areas (Figs. 3.5 and 3.6), including the Fen complex (Norway), Shombole (Kenya), Spitzkop complex (South Africa), Tamazert Eocene Alkaline complex (Morocco), Khibina Alkaline complexes of the Kola-Kandalaksha Peninsula (Russia), Tororo and Napak Ring complexes (Uganda) as well as with Loolmurwak centre, near Oldoinyo Lengai in Tanzania. Calciocarbonatites, magnesiocarbonatites, siderite-carbonatites and ankerite-carbonatites have been observed in these sites, and akin to the Alnö carbonatites, they have all characteristically intruded alongside nepheline-syenite, ijolite, melteigite and urtite lithologies (Strauss and Truter 1950; Rankin 1977; Kjarsgaard and Peterson 1991; Zaitsev and Bell 1995; Demény et al. 1998; Zaitsev et al. 1998; Harmer 1999; Bouabdellah et al. 2010). Notably the available Alnö data are consistent with previous $\delta^{18}O$ values reported for carbonatites from the Fen complex, from Fuerteventura, from the Kola Superdeep Drillhole in Russia, as well as with the data from the Eocene Tamazert carbonatite complex (Andersen 1987; Demény et al. 1998; Melezhik et al. 2003; Bouabdellah et al. 2010) (Fig. 3.5). Specifically, Fuerteventura in the Canary Islands and the Tamazert complex in Morocco show a very similar spread in isotope composition (Demény et al. 1998; Bouabdellah et al. 2010) and, moreover,

the likely parent magma of the Alnö carbonatites bears similar $\delta^{18}O$ and $\delta^{13}C$ isotopes traits to the primary carbonatite magma(s) of the Oldoinyo Lengai volcano, in Tanzania in the East African rift (Keller and Hoefs 1995). Recent gas chemical work indicates that the origin of Oldoinyo Lengai natrocarbonatites involves carbonatite and nephelinite magmas that separated through liquid immiscibility from an originally mafic and carbonated sub-continental mantle source (Fischer et al. 2009). The Fuerteventura carbonatites, in turn, are clearly plume-related and probably represent low-degree partial melts from OIB-type and ambient upper mantle components (Demény et al. 1998, 2004; de Ignacio et al. 2006). Although some Fuerteventura carbonatite and syenitic magmas were stored in shallow-level magmatic chambers and variably interacted with local crust, including some sedimentary limestone (Hoernle et al. 1991; Demény et al. 1998; Casillas et al. 2011), magmatic carbonatite petrogenesis in Fuerteventura has been attributed to interactions between an ancient and formerly subductioned plume component (HIMU) and the ambient upper mantle (DM) (e.g. Hoernle and Tilton 1991). Primitive isotope ratios from Fuerteventura, Kola and also the Tamazert carbonatites are in close proximity to the primitive Alnö ratios on the plot (Fig. 3.5), thus reflecting a deep magmatic, likely plume-related carbonatite magma that experienced an element of crustal differentiation (cf. Bouabdli et al. 1988; Kjarsgaard and Hamilton 1989; Lee and Wyllie 1994, 1998). In contrast, the calcite value from a vein in migmatite (Roopnarain 2013) is compatible with values from carbonatites of the "continental" Kola Peninsula in Russia and the extreme end of data from the "continental" Tamazert complex in Morocco as well as the rarer crustally affected metacarbonatites from Fuerteventura that also plot partially in the marine sediment region (Fig. 3.6) (Demény et al. 1998; Melezhik et al. 2003; Bouabdellah et al. 2010; Casillas et al. 2011).

Remarkably, the Tamazert carbonatites, have been recently suggested to relate to the plume in the Canary Islands which could have possibly fed magmatic material through a sub-lithospheric channel from beneath the Canary Island to north-west Africa (Marks et al. 2008; Duggen et al. 2009; Bouabdellah et al. 2010). Such a theory corresponds to the petrogenetic framework suggested for the Alnö and the Fen complex by e.g. Andersen (1987, 1988) and the primary magma of the Alnö and Fen complexes may have been connected to a larger lithospheric structure (cf. Andersson et al. 2013). In this respect, the origin of the Alnö carbonatite parental magma can perhaps be explained by a parental magma that originated beneath a plume-fed rift setting, tapping melt from a metasomatised and thus somewhat enriched sub-continental mantle. Plume fingers may have been the cause for thermal uplift in the Bothnian region at the end of the Vendian, likely in a fashion analogous to active plume fingers beneath the Rhine graben or the East

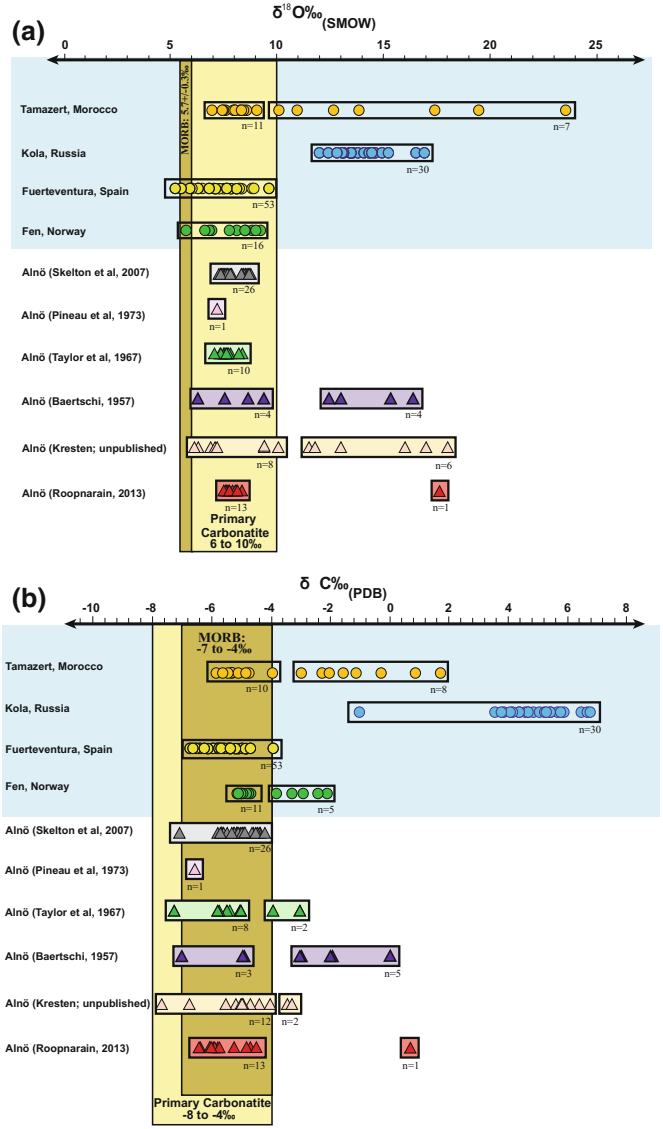

Fig. 3.5 Oxygen and carbon isotope bar charts for samples from Alnö are compared to $\delta^{18}O$ and $\delta^{13}C$ values from carbonatite occurrences elsewhere. Assuming all values are valid, the combination of pristine and metasomatised calcite suites from the comparative data overlap with the broad trends seen in the Alnö suite

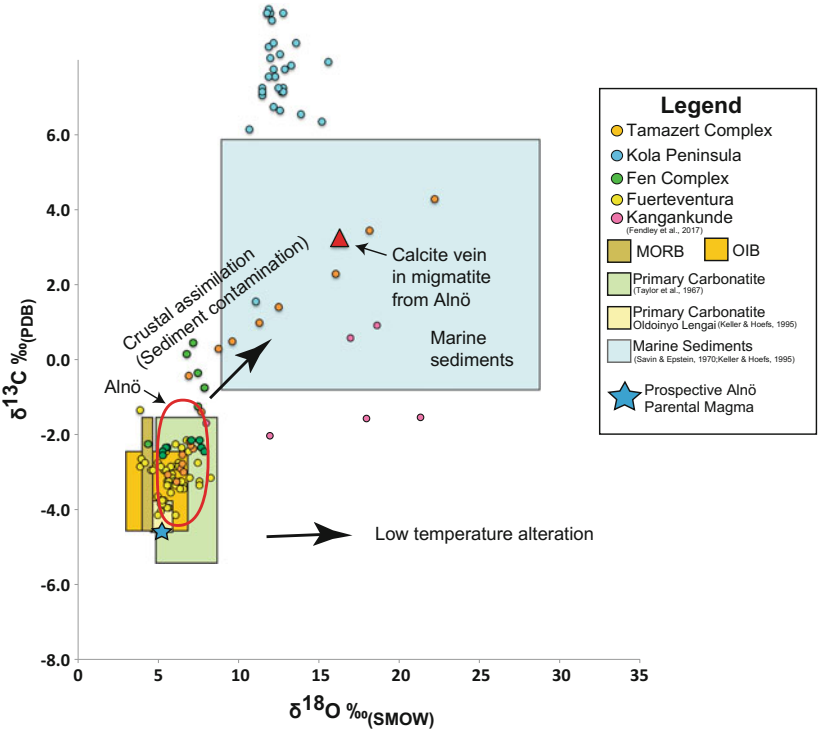

Fig. 3.6 Comparative, stable isotope (O, C) plot for calcite separates from the Alnö carbonatites indicated by red circle and other carbonatites elsewhere. Mantle and crustal domains are indicated. Reference data from Andersen (1987), Demény et al. (1998), Melezhik et al. (2003), Bouabdellah et al. (2010), Casillas et al. (2011), Broom-Fendley et al. (2017). Reference fields after Taylor et al. (1967), Savin and Epstein (1970), Deines (1989), Keller and Hoefs (1995), Hoefs (2009) Andersen (1987), Ito et al. (1987), Eiler et al. (1996), Demény et al. (1998), Melezhik et al. (2003), and Parente et al. (2007)

African rift valley today. Individual centres like Alnö or Fen may then represent piercing points of such plume fingers, ultimately fed by an OIB-type mantle source (cf. van Balen and Heeremans 1998; Korja et al. 2001). Modern day analogues to Alnö may thus be the Kaiserstuhl volcano in the Rhine graben in SW-Germany or the Oldoinyo Lengai volcano in the African Rift Valley in Tanzania (cf. Keyser et al. 2002; Dawson 2012). In respect to the Late Proterozoic thermal upgift in the Baltic region, it now appears possible that plume activity along rift systems was a

relevant factor, and may be comparable to e.g. the situations in parts of present day Europe, with active plume fingers present in the Rhine, the Rhone, and the Eger graben as well as in the Pannonia basin (Schmincke 2004).

3.4 Alnö as an Economic Reserve

Small-scale minings have been carried out for barite e.g. at Pottäng (see Chap. 4), magnetite (e.g. at Släda) and calcite (e.g. at Smedsgården), but were usually not economical over the last two centuries. Moreover, finds of apatite-rich boulders around Söråker created an interest by e.g. Norsk Hydro Agri, to satisfy the growing fertilizer demand. Some of the carbonatites at Alnö were previously exploited as fertiliser in the 1950's and 1960's due to their high P and K content. The effort was eventually terminated due to the also rather high radioactive element concentrations (e.g. thorium and uranium) that were eventually identified as agricultural ecotoxins (Rosén 1994). In that context, the area might ultimately be of interest for REE (Fig. 3.1). However although the calciocarbonatites (sövites) from the Alnö Complex are enriched in REE and especially light rare earth elements (LREE) relative to average continental crust (e.g. Kresten 1979; Möller et al. 1980), they would not be economically viable at present (Fig. 3.2). The unusual composition and high REE concentrations in many Alnö rocks nevertheless begs the question of Alnö as a natural resource for REE in the future.

Increased demand, rising prices and concerns on supply security have recently resulted in a surge in global exploration for REE and other critical metals. In 2010, China reduced their export by 40% compared to the numbers from 2009, which led to the huge increase in global demand and thus in international prices (Chakhmouradian and Wall 2012). Within Europe, Scandinavia and Greenland are key areas in the hunt for these mineral deposits, as these regions contains major areas of alkaline igneous rocks which are, widely held as the main hosts for a range of critical metals. Carbonatites are usually enriched in incompatible elements, critical metals, REE and niobium (Nb). Specifically, seventeen metallic elements constitute the rare earth elements (Fig. 3.1). Today they are an essential commodity for production of mechanical, electronic, and high-tech technology, including green energy, medical and aerospace industries, and in electronic equipment such as industrial and automotive engines or as alloy substance in the steel industry (Wall 2013). For instance, the vibration unit in an iPhone consists of 0.25 grams of the element dysprosium (Hart 2013). Rare earth oxides are moreover vital components in the production of magnetic materials that tolerate high

temperatures with resistant magnetic fields, such as those within hard disk drives and electric motors (Chakhmouradian and Wall 2012; Hatch 2012a). Another noteworthy application is the development of green technologies and REEs have by now become an integral part of wind and water turbines, automotive catalytic converters, as well as of hybrid and electric cars (Eliseeva and Bünzli 2011; Alonso et al. 2012).

Although the fifteen lanthanides, along with scandium and yttrium, are relatively abundant in the Earth's crust, they are often in need of highly specialised extraction and refinement techniques, which is the real reason these elements so 'scarce' (Gupta and Krishnamurthy 2005). While many REEs were actually discovered in Sweden in the early nineteenth century (at Ytterby near Stockholm), Sweden has never sourced its own REEs on a large scale (Chakhmouradian and Wall 2012). China currently dominates the market with the largest REE mine in the world, Baiyun Obo in Mongolia and China has developed a complex network of relationships with the international community regarding the REE export-import relationships (Chen 2011). Notably, more than 77% of the world's rare earth production stems from Baiyun Obo mine in Mongolia and another 20% comes from smaller mines in China (Jones 2010). The remaining 3% in supply originate from mines in Russia, Malaysia, India and Brazil (Lifton 2013). China's increasing export restrictions (Ng 2012), means rare earth mines are being opened in various other parts of the world. The mines of Mountain Pass in the United States and Mount Weld and Dubbo Alkaline Complex in Australia are expected to soon be at the helm of large scale rare earth mining production, but smaller reserves in Vietnam, Indonesia, Thailand, Mauritania, Burundi, Namibia, South Africa, Canada, Kyrgyzstan, Kazakhstan and possibly Norway and Sweden will likely contribute to the global REE supply in the future (Negishi 2012). Although, these mines would still not equal the Baiyun Obo Mine in terms of the rate of supply and efficiency costs involved in REE extraction, separation and refinement (Hatch 2012b), these new mines may help at least to modify the severe imbalance in global supply-demand indices (Bourzac 2011). Industry is therefore increasingly considering REE mining projects in underexplored regions, such as Greenland or the seabed beneath the Arctic Ocean (Goodenough et al. 2016). Ongoing geological explorations reveal a substantial number of as yet untapped rare earth reserves in such regions, which could satisfy up to a quarter of the global market demands for the next fifty years (Komnenic 2013). While environmental concerns have been raised regarding REE being dredged from the enriched seabed beneath the Pacific Ocean, the future REE supply potential of the Pacific Ocean is estimated as very high (Kato et al. 2011; Currie 2013) and some authors argue that the combined reserves of the Greenland, and the Arctic and Pacific regions could

topple China's monopoly in the REE market (Komnenic 2013). For the above reasons, the European Union (EU) now emphasises internal sourcing of REEs through a directive on raw materials (EC 2010; Moss et al. 2011; Jonsson et al. 2012), which in turn, will impact the mining activities in Sweden and might place the Alnö Complex on the list of possible REE targets. Conflicts may then arise on whether Alnö, the Swedish national park icon of rural landscape and heritage, should be preserved, or if it should be exploited for its natural resources. REE extraction and purification may become necessary to meet the growing demands of modern society, whilst it is also necessary to safeguard the environment, possibly creating a complicated dilemma in the not so distant future (cf. Sneddon et al. 2006).

3.5 Environmental Aspects on Alnö Rocks

3.5.1 Weathering

Many Alnö rocks are very prone to rapid weathering. Calcite, is readily attacked by acid fluids, and is the principal component of sövite and a major mineral in many dyke rocks. The calcite in the Alnö sövites often contain minute gas/liquid inclusions, which render it even more open to weathering. Another contributing factor is the presence of pyrite, or sometimes other sulphides, in carbonatite dykes, particularly beforsites. As the pyrites commonly occur as minute grains (<0.5 mm), their highly reactive surface enables swift interaction with water and oxygen. The reaction products, with sulphuric acid among them, then promote the progressive dissolution and consequent disintegration of the rock.

Problems could arise during tunnelling or other construction projects when human activity is exposing various dykes to air and water. In connection with various tunnels being constructed in the Bergeforsen—Fagervik area on the mainland NW of Alnö, Prof. Harry von Eckermann (1958) was called upon as the expert. He noted that some dykes turned from solid rock into plastic clay after a few months of exposure, while other dykes just crumbled away. On the contacts to the surrounding gneissic granite, argillaceous material formed, according to analyses a mixture of montmorillonite and metahalloysite. Hence, the walls of the tunnels had to be reinforced to prevent collapse. It is thus important to bear in mind that a newly exposed sövite outcrop on Alnö undergoes quite dramatic changes due to weathering within just a few month (see von Eckermann 1948, 1958).

3.5.2 Fertilizer

The rapid weathering of Alnö sövite produces mineral soils rich in e.g. iron, calcium, potassium, and phosphorous. This is very much appreciated by the plant live, covering many beautiful outcrops on Alnö with lush vegetation (see also Chap. 4). This realisation might have been the impulse for selling "Alnö limestone" as fertilizer. Råsjö Kross AB opened up a quarry within the Båräng sövite vent in the late 1970s. Everything went as planned, the analysis of a general sample (average of about 10 metric tonnes) showed about 50% CaO, 0.3% each of MgO and K_2O, and 3.5% of P_2O_5. However, the sövite carries various types pyrochlore (yellow, brown, black), and the rock has 3200 ppm Nb, 30 ppm Th, and 185 ppm U and is thus radioactive. Because of the radioactivity, the fertilizer project was abandoned. Also, the timing of the effort was perhaps unfortunate as few years prior, the Swedish people had voted for abandoning nuclear power, thus everything with "uranium" was highly unpopular at the time.

3.5.3 Radioactivity

The Båräng sövite is in fact not highly radioactive. Sövite from the abandoned quarry north of Smedsgården (opposite the Nature Reserve; see Chap. 4) shows 570 ppm Th and 540 ppm U. The matrix of the Sälskär breccia has 80 ppm Th and 480 ppm U. Beforsites seem different and appear to act as a sink for strange elements with contents ranging up to 1900 ppm Th and up to 890 ppm U, always in combination with high REE contents. A wide beforsite dyke on the main road (E14) near Töva, west of Sundsvall, trumps them all with an average concentration of 1.5 wt% ThO_2.

References

Alonso E, Sherman AM, Wallington TJ, Everson MP, Field FR, Roth R, Kirchain RE (2012) Evaluating rare earth element availability: a case with revolutionary demand from clean technologies. Environ Sci Technol 46:3406–3414

Andersen T (1987) Mantle and crustal components in a carbonatite complex, and the evolution of carbonatite magma: REE and isotopic evidence from the Fen complex, Southeast Norway. Chem Geol 65:147–166

Andersen R (1988) Evolution of peralkaline calcite carbonatite magma in the Fen complex, Southeast Norway. Lithos 22:99–112

Andersen T (1997) Age and petrogenesis of the Qassiarsuk carbonatite-alkaline silicate extrusive complex, Gardar Rift, South Greenland. Mineral Mag 61:499–513
Andersen T, Taylor PN (1988) Pb isotope geochemistry of the Fen carbonatite complex, SE Norway: age and petrogenetic implications. Geochim Cosmochim Acta 52:209–215
Andersson M, Malehmir A, Troll V, Dehghannejad M, Juhlin C, Ask M (2013) Carbonatite ring-complexes explained by caldera-style volcanism. Sci Rep 3(1)
Antonini P, Comin-Chiaramonti P, Gomes CB, Censi P, Riffel BF, Yamamoto E (2003) The early Proterozoic carbonatite complex of Angico dos Dias, Bahia State, Brazil: geochemical and Sr–Nd isotopic evidence for an enriched mantle origin. Mineral Mag 67(5):1039–1057
Baertschi P (1957) Messung und Deutung relativer Häufigkeitsvariationen von O^{18} und C^{13} in Karbonatgesteinen und Mineralien. Schweiz. Mineral. Petrogr. Mitt. 37:73–152
Balashov YA, Pozharitskaya LK (1968) Factors governing the behaviour of rare earth elements in the carbonatite process. Geochem Int 5:271–288
Bell K, Blenkinsop J (1987) Nd and Sr isotopic composition of East African carbonatites: implications for mantle heterogeneity. Geology 15:99–102
Bell K, Powell JL (1970) Strontium isotopic studies of alkalic rocks: the alkalic complexes of Eastern Uganda. Geol Soc Am Bull 81:3481–3490
Bell K, Tilton GR (2001) Nd, Pb and Sr isotopic composition of East African carbonatites: evidence for mantle mixing and plume inhomogeneity. J Petrol 42(10):1927–1945
Bell K, Blenkinsop J, Cole TJS, Menagh DP (1982) Evidence from Sr isotopes for long-lived heterogeneities in the upper mantle. Nature 298:251–253
Blaxland AB (1978) Rb–Sr isotopic studies of plutonic agpaitic and miaskitic complexes: a key to the origin of alkaline magmatism. Fortschr Mineral 56(1):9–10
Bouabdellah M, Hoernle K, Kchit A, Duggen S, Hauff F, Klügel A, Lowry D, Beaudoin G (2010) Petrogenesis of the Eocene Tamazert continental carbonatites (Central High Atlas, Morocco): implications for a common source for the Tamazert and Canary and Cape Verde Island carbonatites. J Petrol 51:1655–1686
Bouabdli A, Dupuy C, Dostal J (1988) Geochemistry of Mesozoic alkaline lamprophyres and related rocks from the Tamazert massif, High Atlas (Morocco). Lithos 22:43–58
Bourzac K (2011) MIT technology review online article: the rare earth crisis. www.technologyreview.com. Accessed 19 Apr 2011
Broom-Fendley S, Wall F, Spiro B, Ullmann C (2017). Deducing the source and composition of rare earth mineralising fluids in carbonatites: insights from isotopic (C, O, $^{87}Sr/^{86}Sr$) data from Kangankunde, Malawi. Contrib Mineral Petrol 172:96
Brueckner HK, Rex DC (1980) K–Ar and Rb–Sr geochronology and Sr isotopic study of the Alnö alkaline complex, northeastern Sweden. Lithos 13:111–119
Casillas R, Demény A, Nagy G, Ahijado A, Fernández C (2011) Metacarbonatites in the Basal Complex of Fuerteventura (Canary Islands). The role of fluid/rock interactions during contact metamorphism and anatexis. Lithos 125:503–520
Chakhmouradian AR, Wall F (2012) Rare earth elements: minerals, mines, magnets (and more). Elements 8:333–340
Chakhmouradian AR, Zaitsev AN (2012) Rare earth mineralisation in igneous rocks: sources and processes. Elements 8:347–353
Chen Z (2011) Global rare earth resources and scenarios of future rare earth industry. J Rare Earth 29:1–6

Claesson S (1987) Nd isotope data on 1.9–1.2 Ga old basic rocks and metasediments from the Bothnian Basin, Central Sweden. Precambrian Res 35:115–126
Currie A (2013) Rare earth investing news online article: the Pacific dream: an underwater rare earth behemoth. www.rareearthinvestingnews.com. Accessed 1 Apr 2013
Dasgupta R, Mallik A, Tsuno K, Withers AC, Hirth G, Hirschmann MM (2013) Carbon-dioxide-rich silicate melt in the Earth's upper mantle. Nature 493:211–215
Dawson JB (1980) Kimberlites and their xenoliths. Springer Verlag, Heidelberg
Dawson JB (2012) Nephelinite-melilitite-carbonatite relationships: evidence from Pleistocene-recent volcanism in northern Tanzania. Lithos 152:3–10
de Ignacio C, Muñoz M, Sagredo J, Fernández-Santín S, Johansson A (2006) Isotope geochemistry and FOZO mantle component of the alkaline-carbonatitic association of Fuerteventura, Canary Islands, Spain. Chem Geol 232:99–113
Deines P (1989) Stable isotope variations in carbonatites. In: Bell K (ed) Carbonatites—genesis and evolution. Unwin Hyman, London, pp 301–359
Deines P, Gold DP (1973) The isotopic composition of carbonatite and kimberlite carbonates and their bearing on the isotopic composition of deep seated carbon. Geochim Cosmochim Acta 37:1709–1733
Demény A, Ahijado A, Casillas R, Vennemann TW (1998) Crustal contamination and fluid/rock interaction in the carbonatites of Fuerteventura (Canary Islands, Spain): a C, O, H isotope study. Lithos 44:101–115
Demény A, Vennemann TW, Ahijado A, Casillas R (2004) Oxygen isotope thermometry in carbonatites, Fuerteventura, Canary Islands, Spain. Mineral Petrol 80:155–172
Demény A, Dallai L, Frezzotti ML, Vennemann TW, Embey-Isztin A, Dobosi G, Nagy G (2010) Origin of CO_2 and carbonate veins in mantle-derived xenoliths in the Pannonian Basin. Lithos 117:172–182
Duggen S, Hoernle KA, Hauff F, Klügel A, Bouabdellah M, Thirlwall MF (2009) Flow of Canary mantle plume material through a subcontinental lithospheric corridor beneath Africa to the Mediterranean. Geology 37:283–286
Dunworth EA, Bell K (2001) The Turiy Massif, Kola Peninsula, Russia: isotopic and geochemical evidence for multi-source evolution. J Petrol 42:377–405
Eiler JM, Farley KA, Valley JW, Hofmann AW, Stolper EM (1996) Oxygen isotope constraints on the sources of Hawaiian volcanism. Earth Planet Sci Lett 144:453–468
Eliseeva SV, Bünzli JCG (2011) Rare earths: jewels for functional materials of the future. New J Chem 35:1165–1176
Ellam RM, Stuart FM (2004) Coherent He–Nd–Sr isotope trends in high $^3He/^4He$ basalts: implications for a common reservoir, mantle heterogeneity and convection. Earth Planet Sci Lett 228(3–4):511–523
Eriksson SC (1989) Phalaborwa: a saga of magmatism, metasomatism and miscibility. In: Bell K (ed) Carbonatites—genesis and evolution. Unwin Hyman, London, pp 221–254
European Commission (EC) (2010) Critical raw materials for the EU: report of the Ad-hoc working group on defining critical raw materials. European Commission, Brussels. (140)
Evans AM (1993) Ore geology and industrial minerals: an introduction. Blackwell Scientific Publications, Oxford, p 339
Exley RA, Mattey DP, Clague DA, Pillinger CT (1986) Carbon isotope systematics of a mantle "hotspot": a comparison of Loihi Seamount and MORB glasses. Earth Planet Sci Lett 78:189–199

Faure G (1986) Principles of isotope geology, 2nd edn. Wiley, New York
Fischer T, Burnard P, Marty B, Hilton D, Füri E, Palhol F, Sharp Z, Mangasini F (2009) Upper-mantle volatile chemistry at Oldoinyo Lengai volcano and the origin of carbonatites. Nature 459(7243):77–80
GEOROC (http://georoc.mpch-mainz.gwdg.de/georoc/)
Goodenough K (2014) Critical metals. Geoscientist 24:20–22
Goodenough K, Schilling J, Jonsson E, Kalvig P, Charles N, Tuduri J, Deady E, Sadeghi M, Schiellerup H, Müller A, Bertrand G, Arvanitidis N, Eliopoulos D, Shaw R, Thrane K, Keulen N (2016) Europe's rare earth element resource potential: an overview of REE metallogenetic provinces and their geodynamics setting. Ore Geol Rev 72:838–856
Griffin WL, O'Reilly SY, Stabel A (1988) Mantle metasomatism beneath western Victoria, Australia: II. Isotopic geochemistry of Cr-diopside lherzolites and Al-augite pyroxenites. Geochim Cosmochim Acta 52:449–459
Gupta CK, Krishnamurthy N (2005) Extractive metallurgy of rare earths. CRC Press, Florida, p 484
Halama R, Marks M, Markl G (2003) NdO isotopic and trace element constraints on the petrogenesis of the Grönnedal-Ika carbonatite-syenite complex in the Gardar Province, South Greeenland. 4th Eurocarb Workshop, Canary Islands, Spain, 16–21 Sept 2003. Abstract volume, pp 63–64
Harmer RE (1999) The petrogenetic association of carbonatite and alkaline magmatism: constraints from the Spitskop complex, South Africa. J Petrol 40:525–548
Hart MT (2013) Evaluating United States and world consumption of neodymium, dysprosium, terbium and praseodymium in final products. Academic Dissertation (PhD), Colorado School of Mines, United States of America. (309)
Hatch GP (2012a) Dynamics in the global market for rare earths. Elements 8:341–346
Hatch GP (2012b) Technology metals research online article: 2012 Chinese rare earth export quota allocations, an update. www.techmetalsresearch.com. Accessed 17 May 2012
Hoefs J (2009) Stable isotope geochemistry, 6th edn. Springer, Berlin, pp 1–296
Hoernle K, Tilton GR (1991) Sr–Nd–Pb isotope data for Fuerteventura Basal Complex and subaerial volcanics: application to magma genesis. Schweiz Mineral Petrogr Mitt 71:5–21
Hoernle K, Tilton GR, Schmincke H-U (1991) Sr–Nd–Pb isotopic evolution of Gran Canaria: evidence for shallow enriched mantle beneath the Canary Islands. Earth Planet Sci Lett 106:44–63
Hofmann AW (1997) Mantle geochemistry: the message from oceanic volcanism. Nature 385:219–229
Hogarth DD (1989) Pyrochlore, apatite and amphibole: distinctive minerals in carbonatite. In: Bell K (ed) Carbonatites—genesis and evolution. Unwin Hyman, London, pp 105–148
Ito E, White WM, Göpel C (1987) The O, Sr, Nd and Pb isotope geochemistry of MORB. Chem Geol 62:157–176
Jacobsen SB, Wasserburg GJ (1984) Sm–Nd isotopic evolution of chondrites and achondrites, II. Earth Planet Sci Lett 67:137–150
Jones R (2010) Daily mail online article: inside China's secret toxic unobtainium mine. www.dailymail.co.uk. Accessed 10 Jan 2010
Jones AP, Genge M, Carmody L (2013) Carbonate melts and carbonatites. Rev Miner Geochem 75:289–322

Jonsson E, Högdahl K, Troll VR (2012) Grön teknik slukar sällsynta metaller. Forsk Framsteg 7:34–37
Kato Y, Fujinaga K, Nakamura K, Takaya Y, Kitamura K, Ohta J, Iwamori H (2011) Deep sea mud in the Pacific Ocean as a potential resource for rare earth elements. Nat Geosci 4:535–539
Keller J, Hoefs J (1995) Stable isotope characteristics of recent natrocarbonatites from Oldoinyo Lengai. In: Bell K, Keller J (eds) Carbonatite volcanism: Oldoinyo Lengai and the petrogenesis of natrocarbonatites. Springer, Berlin, pp 113–123
Keyser M, Ritter J, Jordan M (2002) 3D shear-wave velocity structure of the Eifel plume, Germany. Earth Planet Sci Lett 203:59–82
Kjarsgaard IH (1998) Rare earth elements in sövitic carbonatites and their mineral phases. J Petrol 39:2105–2121
Kjarsgaard BA, Hamilton DL (1989) The genesis of carbonatites by liquid immiscibility. In: Bell K (ed) Carbonatites—genesis and evolution. Unwin Hyman, London, pp 388–404
Kjarsgaard B, Peterson T (1991) Nephelinite-carbonatite liquid immiscibility at Shombole volcano, East Africa: petrographic and experimental evidence. Mineral Petrol 43(4):293–314
Komnenic A (2013) Mining research online article: China growing uneasy over Greenland's rare earth ambitions. www.mining.com. Accessed 9 Aug 2013
Korja A, Heikkinen P, Aaro S (2001) Crustal structure of the northern Baltic Sea palaeorift. Tectonophysics 331:341–358
Kresten P (1979) The Alnö complex: discussion of the main features, bibliography and excursion guide. Nordic Carbonatite Symposium, Alnö
Kresten P (1980) The Alnö complex: tectonics of dyke emplacement. Lithos 13:153–158
Kresten P (1986) The Alnö alkaline area. 7th IAGOD Symposium Excursion Guide No. 9/10. Swed Geol Surv 67:20–22
Kresten P (1990) Alnöområdet. In: Lundqvist T, Gee D, Kumpulainen R, Karis L, Kresten P (eds) Beskrivning till berggrundskartan över Västernorrlands län. Sveriges geologiska undersökmingar, ser Ba, 31, pp 238–278
Kyser TK (1986) Stable isotope variations in the mantle. Rev Mineral 16:141–164
Lee WJ, Wyllie PJ (1994) Experimental data bearing on liquid immiscibility, crystal fractionation, and the origin of calciocarbonatites and natrocarbonatites. Int Geol Rev 36:797–819
Lee WJ, Wyllie PJ (1998) Processes of crustal carbonatite formation by liquid immiscibility and differentiation, elucidated by model systems. J Petrol 39:2005–2013
Lifton J (2013) Technology metals research online article: the future markets for the rare technology metals. www.techmetalsresearch.com. Accessed 16 Jul 2013
Lottermoser BG (1990) Rare earth element mineralisation within the Mt. Weld carbonatite laterite, Western Australia. Lithos 24:151–167
Loubet M, Bernat M, Javoy M, Allègre CJ (1972) Rare earth contents in carbonatites. Earth Planet Sci Lett 14:226–232
Lundqvist T (1979) The Precambrian of Sweden. Swed Geol Surv, Serie C, 768
Lundqvist T, Gee DD, Kumpulainen R, Karis L, Kresten P (1990) Beskrivning till berggrundskartan över Västernorrlands län. Swed Geol Surv, Ba31., 429 pp
Marks MAW, Shilling J, Coulson IM, Wenzel T, Markl G (2008) The alkaline-peralkaline Tamazeght complex, High Atlas Mountains, Morocco: mineral chemistry and petrological constraints for derivation from a compositionally heterogeneous mantle source. J Petrol 49:1097–1131

Mearns E-W (1986) Sm–Nd ages for Norwegian garnet peridotite. Lithos 19:269–278
Melezhik VA, Fallick AE, Smirnov YP, Yakovlev YN (2003) Fractionation of carbon and oxygen isotopes in 13C-rich Palaeoproterozoic dolostones in the transition from medium-grade to high-grade greenschist facies: a case study from the Kola Superdeep Drillhole. J Geol Soc 160:71–82
Menzies MA, Wass SY (1983) CO_2 and LREE-rich mantle below eastern Australia: a REE and isotopic study of alkaline magmas and apatite-rich mantle xenoliths from the Southern Highlands Province, Australia. Earth Planet Sci Lett 65:287–302
Mitchell RH (2005) Carbonatites and carbonatites and carbonatites. Can Mineral 43:2049–2068
Mitchell RH (2008) Petrology of hypabyssal kimberlites: relevance to primary magma compositions. J Volcanol Geotherm Res 174:1–8
Möller P, Morteani G, Schley F (1980) Discussion of REE distribution patterns of carbonatites and alkalic rocks. Lithos 13:171–179
Morogan M, Lindblom S (1995) Volatiles associated with the alkaline-carbonatite magmatism at Alnö, Sweden: a study of fluid and solid inclusions in minerals from the Långarsholmen ring complex. Contrib Mineral Petrol 122:262–274
Morogan V, Woolley AR (1988) Fenitisation at the Alnö carbonatite complex, Sweden: distribution, mineralogy and genesis. Contrib Mineral Petrol 100:169–182
Moss RL, Tzimas E, Kara H, Willis P, Kooroshy J (2011) Critical metals in strategic energy technologies. European Commission Joint Research Centre: Scientific and Technical Reports, Zurich. (161)
Negishi M (2012) Reuters online article: Japan, Kazakhstan to develop rare earth metals. www.reuters.com. Accessed 29 Apr 2012
Nelson DR, Chivas AR, Chappell BW, McCulloch MT (1988) Geochemical and isotopic systematics in carbonatites and implications for the evolution of ocean-island sources. Geochim Cosmochim Acta 52:1–17
Ng E (2012) South China morning post online article: rare earth prices to stay high for years. www.scmp.com. Accessed 15 Aug 2012
Olafson M, Eggler DE (1983) Phase relations of amphibole, amphibole-carbonate, and phlogopite-carbonate peridotite: petrologic constraints on the asthenosphere. Earth Planet Sci Lett 64:305–315
Parente M, Frijia G, Di Lucia M (2007) Carbon-isotope stratigraphy of Cenomanian-Turonian platform carbonates from the southern Apennines (Italy): a chemostratigraphic approach to the problem of correlation between shallow-water and deep-water successions. J Geol Soc Lond 164:609–620
Patterson M, Francis D, McCandless T (2009) Kimberlites: magmas of mixtures? Lithos 112:191–200
Pineau F, Javoy M, Allegre CJ (1973) Etude systématique des isotopes de l'oxygen, du carbon ey du strontium dans les carbonatites. Geochim Cosmochim Acta 37:2363–2377
Rankin AH (1977) Fluid inclusion evidence for the formation conditions of apatite from the Tororo carbonatite complex of eastern Uganda. Mineral Mag 41:155–164
Roopnarain S (2013) Petrogenesis of carbonatites in the Alnö Complex, Central Sweden. Master thesis, Uppsala University, 108

Rosén K (1994) Studies on countermeasures after radioactive depositions in Nordic agriculture. In: Dahlgaard H (ed) Nordic radioecology: the transfer of radionuclides through Nordic ecosystems to man. Studies in Environmental Science 62, pp 239–260

Russell JK, Porritt LA, Lavallée Y, Dingwell DB (2012) Kimberlite ascent by assimilation-fuelled buoyancy. Nature 481:352–357

Savin SM, Epstein S (1970) The oxygen and hydrogen isotope geochemistry of ocean sediments and shales. Geochim Cosmochim Acta 34:43–63

Schleicher H, Keller J, Kramm U (1990) Isotope studies on alkaline volcanics and carbonatites in the Kaiserstuhl, Federal Republic of Germany. Lithos 26:21–36

Schmincke HU (2004) Volcanism. Springer Verlag, Berlin

Skelton A, Vourinen JH, Arghe F, Fallick A (2007) Fluid-rock interaction at a carbonatite-gneiss contact, Alnö, Sweden. Contrib Mineral Petrol 154(1):75–90

Sneddon C, Howarth RB, Norgaard RB (2006) Sustainable development in a post-Brundtland world. Ecol Econ 57:253–268

Sobolev AV, Chaussidon M (1996) H_2O concentrations in primary melts from supra-subduction zones and mid-ocean ridges: implications for H_2O storage and recycling in the mantle. Earth Planet Sci Lett 137:45–55

Sparks RSJ, Brown RJ, Field M, Gilbertson MA (2007) Kimberlite ascent and eruption. Nature 447:53–57

Stoppa F, Woolley AR (1997) The Italian carbonatites: field occurrence, petrology and regional significance. Mineral Petrol 59:43–67

Strauss CA, Truter FC (1950) The alkali complex at Spitskop, Sekukuniland, Eastern Transvaal. Trans Geol Soc S Afr LIII:81–125 (Plates XIII–XXIII)

Sun S-S, McDonough WF (1989) Chemical and isotopic systematics of oceanic basalts: implications for mantle composition and processes. Geol Soc Lond Spec Publ 42:313–345

Taylor HP, Frechen J, Degens ET (1967) Oxygen and carbon isotope studies of carbonatites from the Laacher See District, West Germany and the Alnö District, Sweden. Geochim Cosmochim Acta 31:407–430

van Balen RT, Heeremans M (1998) Middle Proterozoic–early Palaeozoic evolution of central Baltoscandian intracratonic basins: evidence for asthenospheric diapirs. Tectonophysics 300:131–142

Verhulst A, Balaganskaya E, Kirnarsky Y, Demaiffe D (2000) Petrological and geochemical (trace elements and Sr–Nd isotopes) characteristics of the Paleozoic Kovdor ultramafic, alkaline and carbonatite intrusion (Kola Peninsula, NW Russia). Lithos 51:1–25

Viladkar SG, Pawaskar PB (1989) Rare earth element abundances in carbonatites and fenites of the Newania complex, Rajasthan, India. Bull Geol Surv Finl 61:113–122

von Eckermann H (1948) The alkaline district of Alnö Island. Sver Geol Unders Ca 36:176

von Eckermann H (1958) The alkaline and carbonatitic dikes of the Alnö formation on the mainland north-west of Alnö Island. K Sven Vetenskapsakad Handl 7:1–64

von Eckermann H (1966) Progress of research on the Alnö carbonatite. In: Tuttle OF, Giltins J (eds) Carbonatites. Interscience, Publishers, Wiley, pp 3–31

Vuorinen JH (2005) The Alnö alkaline and carbonatitic complex, east central Sweden a petrogenetic study. PhD Thesis, Stockholm University, 130

Vuorinen JH, Hålenius U (2005) Nb–Zr and LREE-rich titanite from the Alnö alkaline complex: crystal chemistry and its importance as a petrogenetic indicator. Lithos 83:128–142

Vuorinen JH, Skelton ADL (2004) Origin of silicate minerals in carbonatites from Alnö Island, Sweden: magmatic crystallisation or wall rock assimilation? Terra Nova 16:210–215

Wagner C, Mokhtari A, Deloule E, Chabaux F (2003) Carbonatite and alkaline magmatism in Taourirt (Morocco): petrological, geochemical and Sr-Nd isotope characteristics. J Petrol 44(5):937–965

Wall F (2013) Rare earth elements. In: Gunn AG (ed) Critical metals handbook. Wiley-Blackwell, Chicester, p 456

Wyllie PJ, Huang WL (1975) Peridotite, kimberlite and carbonatite explained in the system $CaO–MgO–SiO_2–CO_2$. Geology 3:621–624

Zaitsev AN, Bell K (1995) Sr and Nd isotope data of apatite, calcite and dolomite as indicators of source, and the relationship of phoscorites and carbonatites from the Kovdor massif, Kola Peninsula, Russia. Contrib Mineral Petrol 121:324–335, 92–314

Zaitsev AN, Wall F, Le Bas MJ (1998) REE-Sr–Ba minerals from the Khibina carbonatites, Kola Peninsula, Russia: their mineralogy, paragenesis and evolution. Mineral Mag 62:225–250

Excursion Guide

4

Abstract

This chapter offers a series of organised excursions on the island of Alnö and to several locations north of Alnö, including the Sälkär skerries and the Söråker intrusion. The excursions will bring the visitor to the geologically most important localities of the Alnö igneous complex and several sites of additional interest regarding the botany, pre-history and economic potential of Alnö Island. The chapter encourages the visitor to act responsibly in respect to local customs and sampling ethics.

In this section we offer a number of guided tours to some of the best outcrops on and around Alnö Island and the recommended excursion localities are marked on Fig. 4.1.

The local population is largely aware of the geological wonders of Alnö and is usually very friendly and accommodating, but we advise that you inform owners when entering their premises. Please note that sampling is not permitted at the marked geological localities (blue signs). Sampling at many localities in this guide requires a permit from Länsstyrelsen in Västernorrland (www.lansstyrelsen.se/vasternorrland). Illegal sampling is highly inappropriate in our view, as subsequent visitor will pay the price. Access to some areas (e.g. the islands north of Alnö) may be seasonally restricted, due to e.g. bird nesting.

Please observe good parking manners and follow traffic signs even if they seem to be "homemade". The residents will be grateful. Minor tarmac or gravel roads are

P. Kresten and V. R. Troll, *The Alnö Carbonatite Complex, Central Sweden*, GeoGuide, https://doi.org/10.1007/978-3-319-90224-1_4

Fig. 4.1 Excursion localities within the main Alnö complex (map from Google maps)

often too narrow to allow two vehicles to pass each other. Special "meeting places" on such minor roads are marked by a white "M" on blue ground—to be used by the vehicle nearest to the sign. These "meeting places" are highly unsuitable for parking. Also note that roads with blue signs are public roads, while those with yellow signs are private roads. When driving on the latter, extra discretion is appropriate.

Regarding accommodation on the island, there is an affordable hotel with a hostel component at Stornäset ("Stornäsets Pensionat och Vandrarhem"), with details on the Internet (www. stornäset.com).

The excursions are planned to start from Vi village, the largest settlement on Alnö, which is located near the bridge head that brings visitors from the mainland to Alnö Island (Fig. 1.4).

Route 1: The North Coast

Drive from Vi towards the North, passing Alnö church (Alnö kyrka). There, a large blue sign documents the geological sites that are protected by law (Fig. 4.2). Continue towards the North, until you reach the first geological locality near

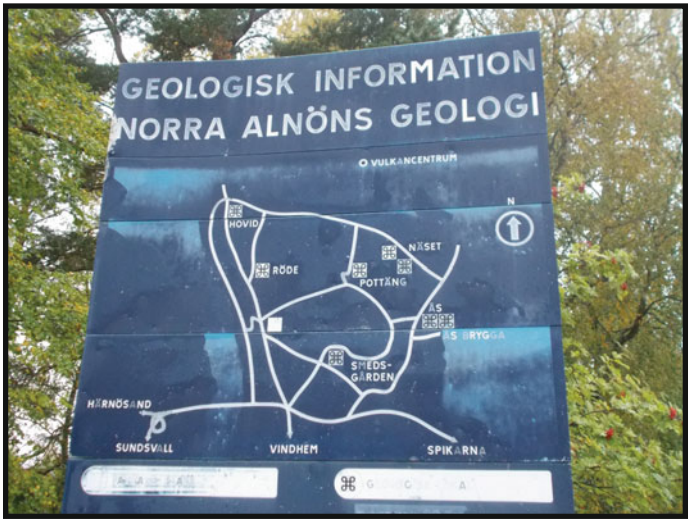

Fig. 4.2 Geological sign near Alnö kyrka (Alnö church), outlining key localities of geological interest

Fig. 4.3 Stop 1 at a protected 'Geological Locality'

Hovid, marked by a blue road sign on the left hand side of the road (Fig. 4.3). Park here to inspect alnöite breccia in a road section. We advise to wear high visibility vests when operating along road sections here on Alnö.

4.1 Alnöite Breccia at Hovid

N62°28'20.1"/E017°22'37.5"

Here an about 20 m wide alnöite breccia is exposed in a road-cutting. According to magnetometric measurements, the outcrop exposed represents a local widening (a "blow" in kimberlite terminology) of a dyke-like intrusion. The dyke apparently tapers off within 30 m to both the north and the south (Fig. 4.4). The alnöite contains larger crystals of mica (phlogopite), amphibole (black, good cleavage) and some chrome diopside (grass-green) and megacrysts (xenocrysts, in part) of titanian pargasite, diopside, titanomagnetite and almandine garnet are found. The greenish groundmass is dominated by mica, calcite, serpentine, and titanomagnetite. The rock is a breccia, i.e., it is very rich in fragments. Many of the fragments are granites, gneisses, dolerites or sövites (coarse carbonatites) from the surroundings. In addition, we find granulites (plagioclase, pyroxene, amphibole, garnet) and eclogites (garnet, pyroxene). These rocks represent a vertical section of the Earth's crust down to about 25 km. Fragments of more or less fenitized granites and migmatites, diabase and rocks resembling "sövite pegmatite" are frequent.

The contact to the wall-rocks is best displayed towards the south-west. At the contact, the veined gneisses have been converted into a brick-red fine-grained rock with occasional bluish stringers of alkali amphiboles. The process, called fenitization (see Chap. 1), is caused by influx of alkaline solutions, converting the wall-rock into a rock rich in feldspar, but poor in, or devoid of, quartz. The breccia is intersected by small dykes of beforsite and silicocarbonatite.

When finished at Locality 1, follow the main road towards the northern coast, i.e., turn right at the upcoming cross roads. Drive for only a few kilometers until you see another blue sign for 'Geologisk Lokal'. Park on the opposite side of the road just in front of the large rocks that block this small uphill road. Walk uphill for about 100 m. The outcrop is on your left hand side, but can be rather overgrown in summer (Fig. 4.5). The small road has been privatized and the owners do not want a lot of traffic in their backyard.

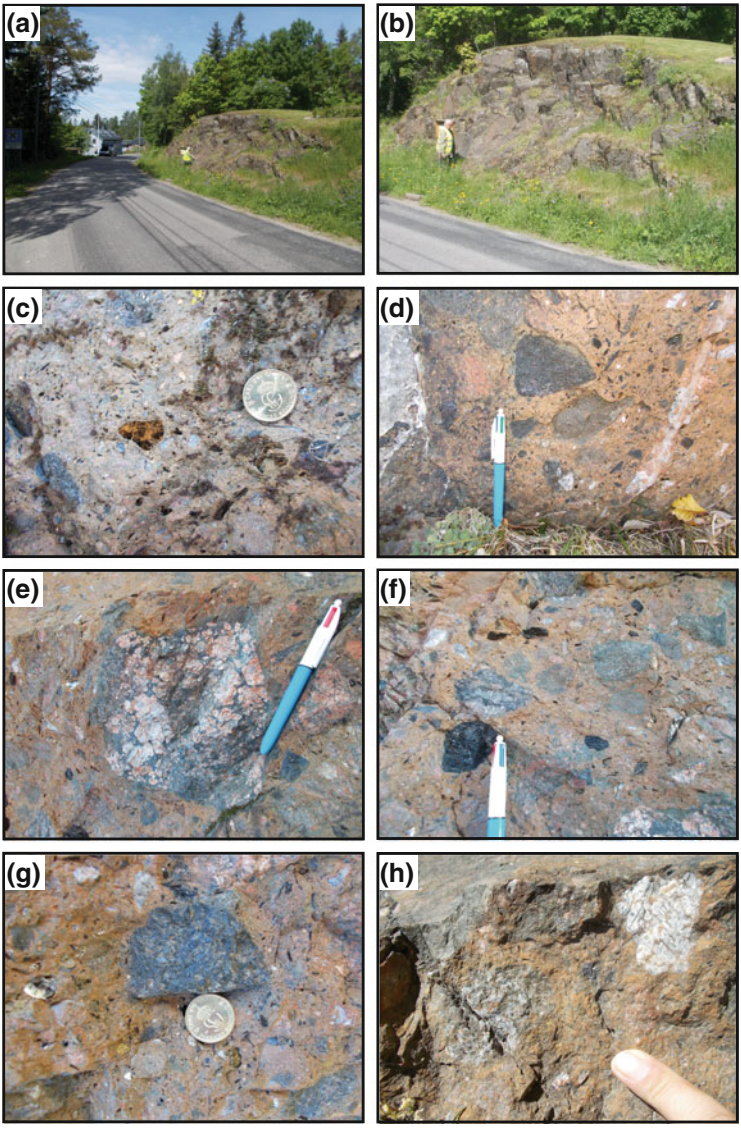

Fig. 4.4 Alnöite breccia at Hovid. The alnöite is crowded with xenoliths of various origins (see text for details)

4.2 Road-Cutting North of Hartung (close to the Coastal Road)

N62°28'08.5"/E017°25'37.9"

This site has fallen in disarray, in part because of the road blockage. Here, gradations from weakly to more strongly fenitized migmatite are observed. With increasing fenitization, the structure of the migmatite disappears. Alkali amphibole (richterite) is found in low-grade fenites, as well as aegirine (tiny black needles, often growing along cracks). At the southernmost part of the outcrop, near a small red barn, a small outcrop exposes the zone of crushing, often found at the boundaries between quartz-bearing and quartz-free fenites.

Intersecting the northern outcrop, a dyke of melanite-nephelinite is seen, with phenocrysts of nepheline (white) and melanite garnet (shiny, black) in a hydrated and carbonated, fine-grained matrix (Fig. 4.5). When the vegetation permits, several small dykes of carbonatite are found here also, as well as a phonolitic dyke.

Return to your vehicle and continue on the main coastal road. Turn left from the main road just after the Hörningsholm village sign. Follow the track (Pottängsvägen) for a short drive until the track takes a sharp left swing just before the coast. Park the car here.

4.3 Hörningsholm, close to the Beach; Sövite Pegmatite

N62°28'10.8"/E017°26'44.1"

Before entering this private property, please take contact with the residents. In the meadow immediately to your south, several small outcrops (a few meters across) of "sövite pegmatite" are found. These display coarse-grained intergrowth of calcite and lamellar pyroxene (aegirine augite), with some mica, titanomagnetite and apatite (Fig. 4.6). The large crystals and feather-type features imply rapid growth conditions or speedy cooling, perhaps on the order of days to weeks considering some of the available experimental data. The texture closely resembles the spinifex texture frequently found in komatiites as well as in some Iron Age (iron-rich) bloomery slags.

When finished, return to the main coastal road and continue toward the East. After a short drive on the coastal road, turn left again, just opposite an animal pension, and follow the small road (passing a car mechanic workshop) towards the coast. Park some 400–500 m further down on the track at a parking space on the left (usually the last bit of this track is closed off). Walk from here for ca 150 m to

Fig. 4.5 Near Hartung, along blocked road. Here, gradations from weakly to more strongly fenitized migmatite are observed. At the southernmost part of the outcrop, near a small red barn, a small outcrop exposes the zone of crushing, often found at the boundaries between quartz-bearing and quartz-free fenites. Intersecting the northern outcrop, a dyke of melanite-nephelinite is seen (**b**, **c**), with phenocrysts of nepheline (white) and melanite garnet (shiny, black) in a hydrated and carbonated, fine-grained matrix

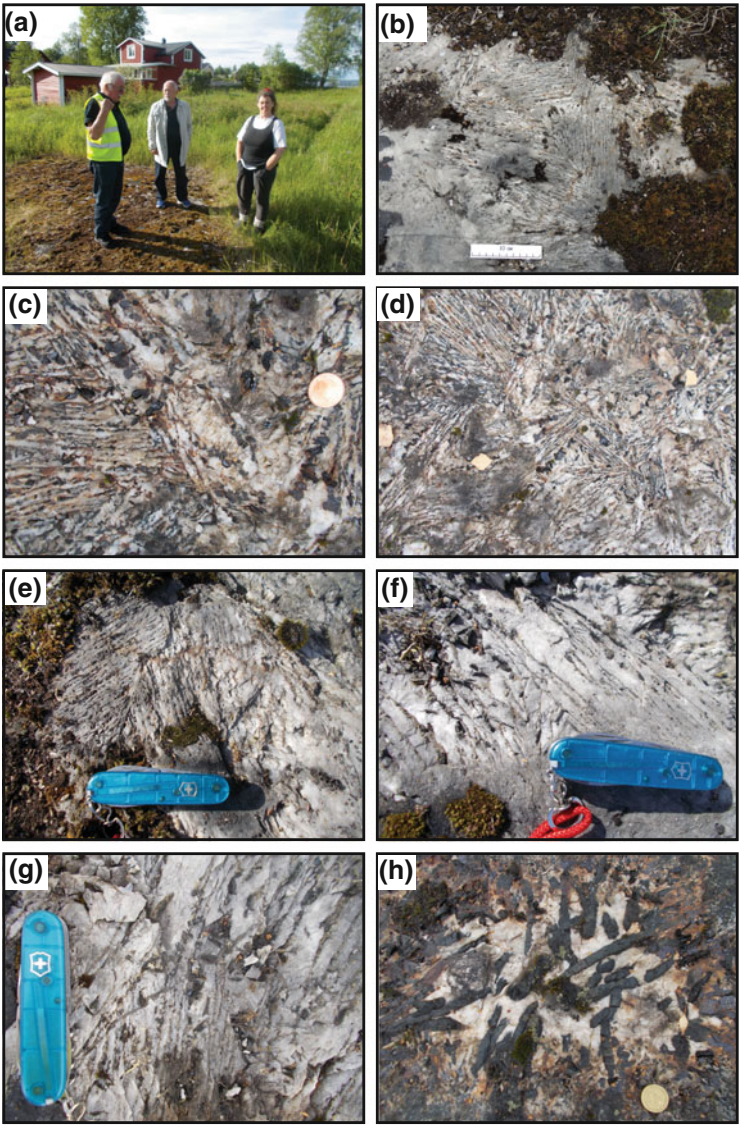

Fig. 4.6 Hörningsholm. Sövite pegmatite with coarse-grained intergrowth of calcite and lamellar pyroxene (aegirine augite), with some mica, titanomagnetite and apatite

the end of the gravel road, and toward a little shed. The outcrop can be found right in front of the shed.

4.4 Outcrops near Coast East of Hörningsholm; Intrusive Mélange

N62°28'05.5"/E017°27'34.5"

A complicated mélange of rock types containing fenites, ijolites, nepheline syenites, pyroxenite and sövite is exposed here. This outcrop forms part of the Northern Ring Complex that is frequently intruded by younger intrusive rocks of the Southern Ring centre (Fig. 4.7).

Specifically, outcrops of banded and sheared sövite, presumably indicating flow patterns, are seen in front of the shed and also contain strung out, dark pyroxenite (some of the pyroxenite portions are rich in titanomagnetite and/or apatite). Locally some syenitic rocks occur as do some fine-grained, reddish-brown dykelets. This outcrop presents strong evidence for the mixed occurrence of silicate magma (pyroxenite) with carbonatite magma (sövite), and implies that both were liquid simultaneously when migrating into the current position. A few steps further towards the shore, in fact almost at the shore and behind a second small shed, banded melteigite (a melanocratic member of the ijolite series) is exposed that is cross-cut by nepheline syenite. Small dykes of sövite cross-cut both (Fig. 4.8). In addition, loose boulders of sövite are present in the area here, which carry well-crystallized diopside, titanomagnetite and dysanalyte (black cubes).

Return to the main road and continue towards the East. After a short drive you will meet another blue sign for 'Geologiska Local'. Park here.

4.5 The "Boliden Quarry" near Hörningsholm

N62°27'42.9"/E017°27'26.0"

Abandoned small quarry in juvite, a leucocratic variety of nepheline syenite with $K_2O > Na_2O$ (Fig. 4.9). Here, the juvite is medium- to fine-grained, with nepheline (greyish on weathered surface) and orthoclase feldspar (reddish). Included are fragments of coarse-grained ijolite (nepheline, pyroxene). The outcrop is cross-cut by carbonatite and lamprophyre dykes.

The locality is the so-called Boliden quarry. The Boliden mining company was testing whether or not the rock here was suitable for aluminum production. This idea failed, however, due to elevated iron contents in the nepheline caused by minute inclusions of pyroxene.

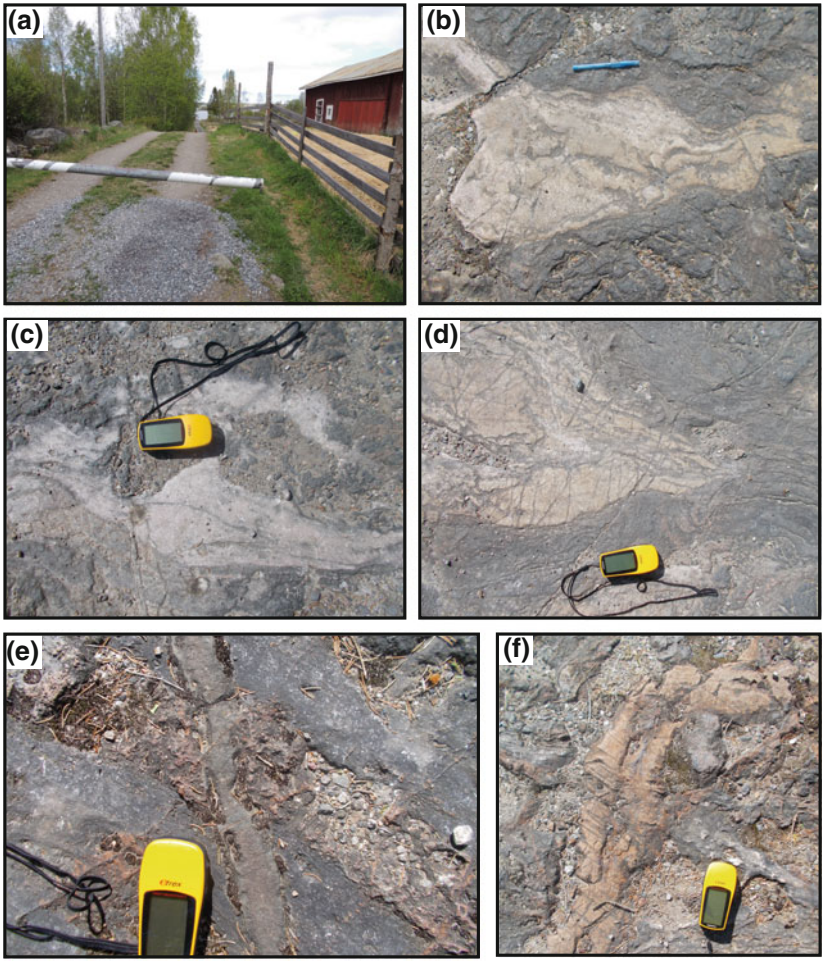

Fig. 4.7 East of Hörningsholm. An intrusive mélange of fenites, ijolites, nepheline syenites, pyroxenite and sövite is exposed here (see text for details)

A little further along the road towards Stornäset (towards the East), about 200 m from the quarry, yellow cancrinite is found in loose boulders and outcrops on the right hand side of the road, e.g. just before the third telephone pole. Cancrinite is a

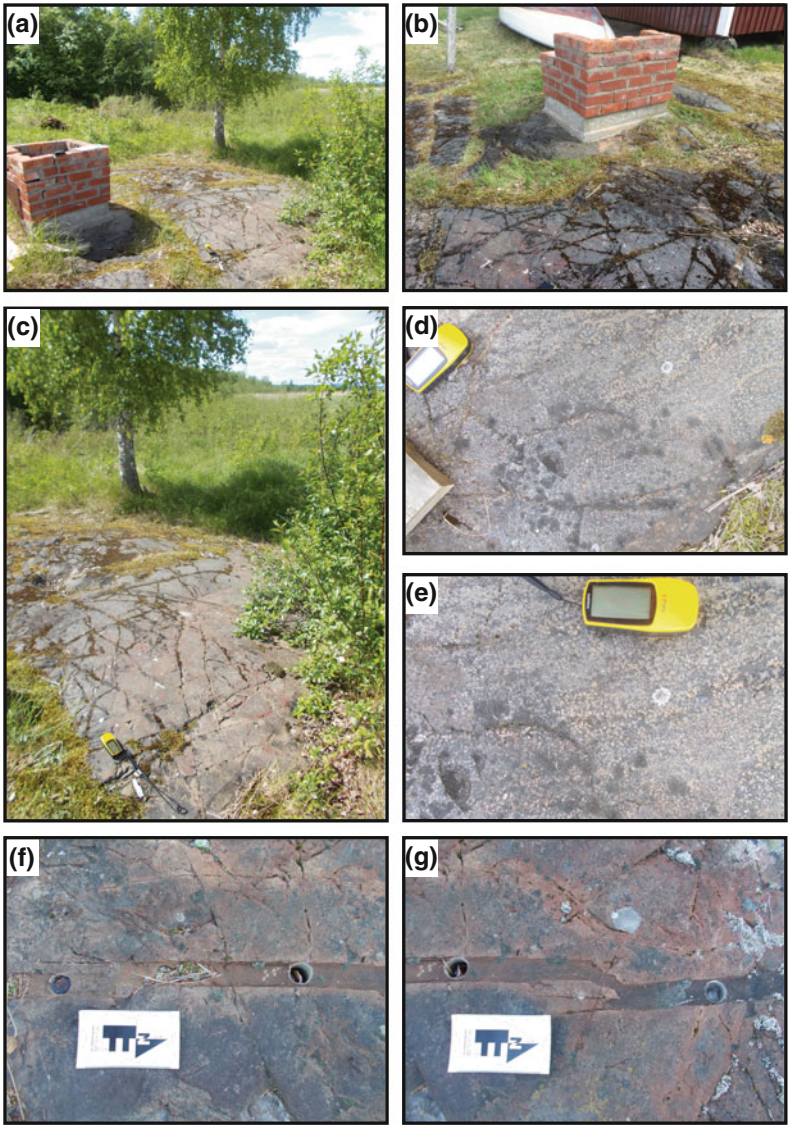

Fig. 4.8 East of Hörningsholm. Flow-banded melteigite is cut here by nepheline syenite. A fine grained small dyke with a “jump” is close by and is a victim of enthusiastic research efforts

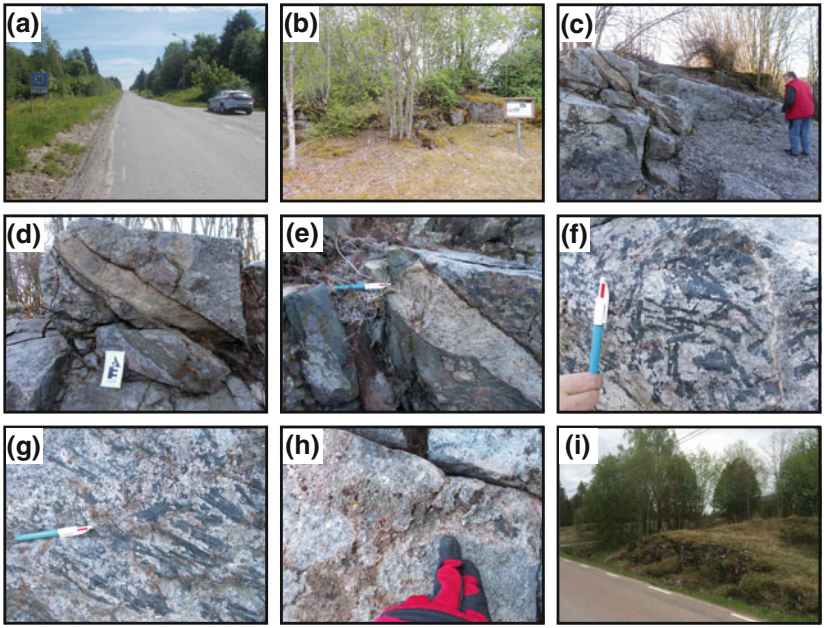

Fig. 4.9 Boliden quarry. Predominantly juvite (**a**–**c**) with fragments of coarse ijolite (**f**–**g**). Cross-cutting carbonatite and lamprophyre dykes (**d**–**e**) and possibly gas vugs (**h**) are seen here too. A little further along the road cancrinite used to be available in outcrop (**i**), but is increasingly hard to find as the site is well known amongst local mineral collectors

sulphur coloured alteration product of nepheline and is found together with nepheline, feldspar, and pyroxene in a rather coarse nepheline syenite.

Return to the car and continue along the main coastal road to the next locality, which is marked by the next blue geology sign ("Geologisk Lokal"), and which is found only a short drive further.

4.6 Type Locality of Alnöite at Näset

N62°27'32.3"/E017°27'58.8"

Unfortunately, this locality is badly overgrown with at times high vegetation. In the remaining exposures, alnöite is found in a dyke-like mass, carrying large phenocrysts of phlogopite in a fine-grained darkish matrix. This is the type locality for

alnöite, i.e., the sites where the rock was first found (Hisinger 1808) and described (Törnebohm 1883). The alnöite dyke is about 16 m wide, rather coarse-grained at the east end of the exposure, but is becoming more fine-grained and calcic towards the west (Fig. 4.10). Rounded brownish grains of olivine (fatty lustre), occasional green pyroxenes and bluish black magnetite occur also. The groundmass is composed mainly of mica, melilite, and calcite. In addition, some inclusions of olivine-rich rocks occur (often altered into mica), and are probably derived from the Earth's upper mantle (i.e., from depths below 30 km).

The rock shows some resemblance to the host rock for diamonds, the famous kimberlite. Both rocks are derived from great depths, about 110–160 km. The alnöites, however, seem to have paused within the Earth's crust, while kimberlites intruded without any interruption. The adaptation of alnöites to lower pressures and temperatures is the reason why they are not diamondiferous, and why included mantle fragments are usually heavily altered.

Across the road, at the parking lot, we find outcrops of ijolite but unfortunately, the exposure here is not very good (Fig. 4.10a). This alkaline plutonic rock is composed of nepheline (light) and pyroxene (dark), with occasional needles of light-coloured wollastonite that are characterised by a silky shine.

Continue on the main road for a few kilometers until the road makes a broad turn to the right. Turn left right here in the bend toward Stornäset and drive towards the Jetty at the coast to park.

4.7 The Jetty at Stornäset

N62°27'42.2"/E017°29'02.5"

At the jetty, boulders of various granites and migmatites and some boulders of alnöite rocks are found. From here, walk along the shore from the jetty eastwards, and several outcrops with migmatite and fenites are seen, cross-cut by flow-layered sövites (Fig. 4.11) and alkaline dykes that can show intricate patterns (Fig. 4.11f–h). Farthest to the east, after walking for some 200–300 m, massive syenitic high-grade fenite is found.

Note along the shore, a sövite intrusion with flow banding and drill holes can be inspected (Fig. 4.12), which is one of the sites in Andersson et al. (2016) that were used to determine how the sövite sheets were originally emplaced. The study concluded that flow patterns may form late in the lifetime of a sheet intrusion when the magma pressure wanes and the walls close in again, as opposed to being of primary flow fabric sensu stricto. According to the authors, these holes are about to be refilled in the near future. Note, when returning towards the main road, the Stornäset Nature

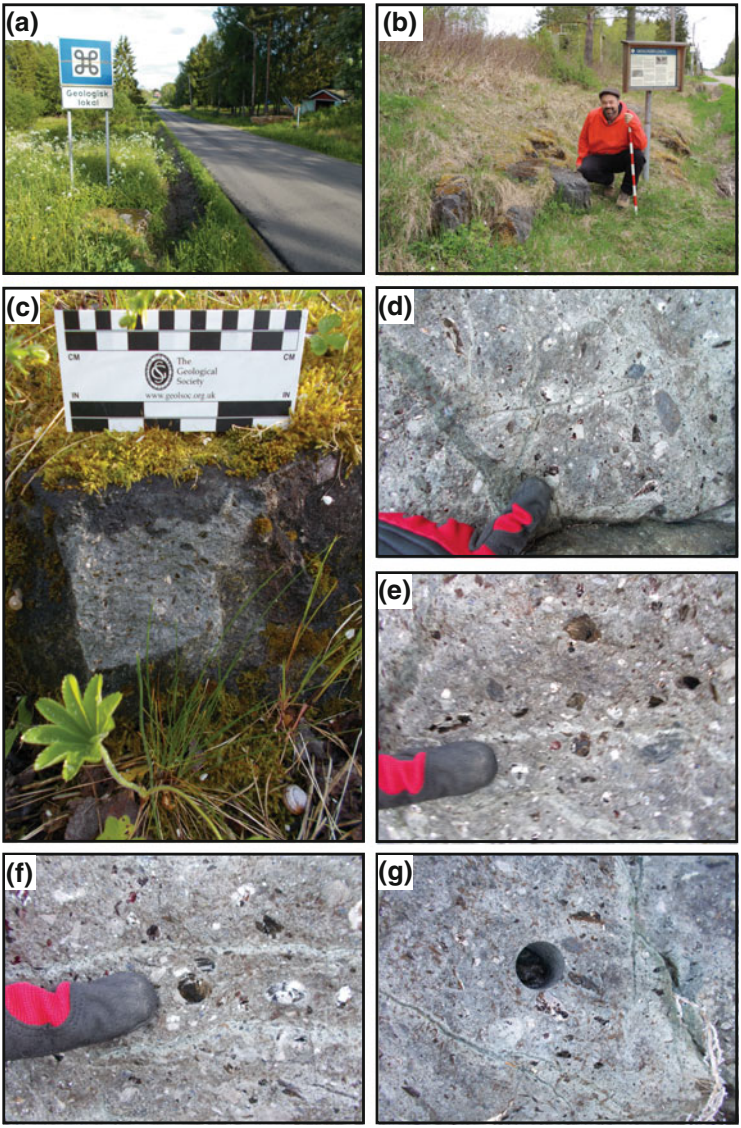

Fig. 4.10 Näset. This is the official alnöite-type locality, but the outcrop is (by now) rather small. Note the large phlogopite crystals and the locally developed flow banding. Xenoliths and schlieren of variable composition are not uncommon

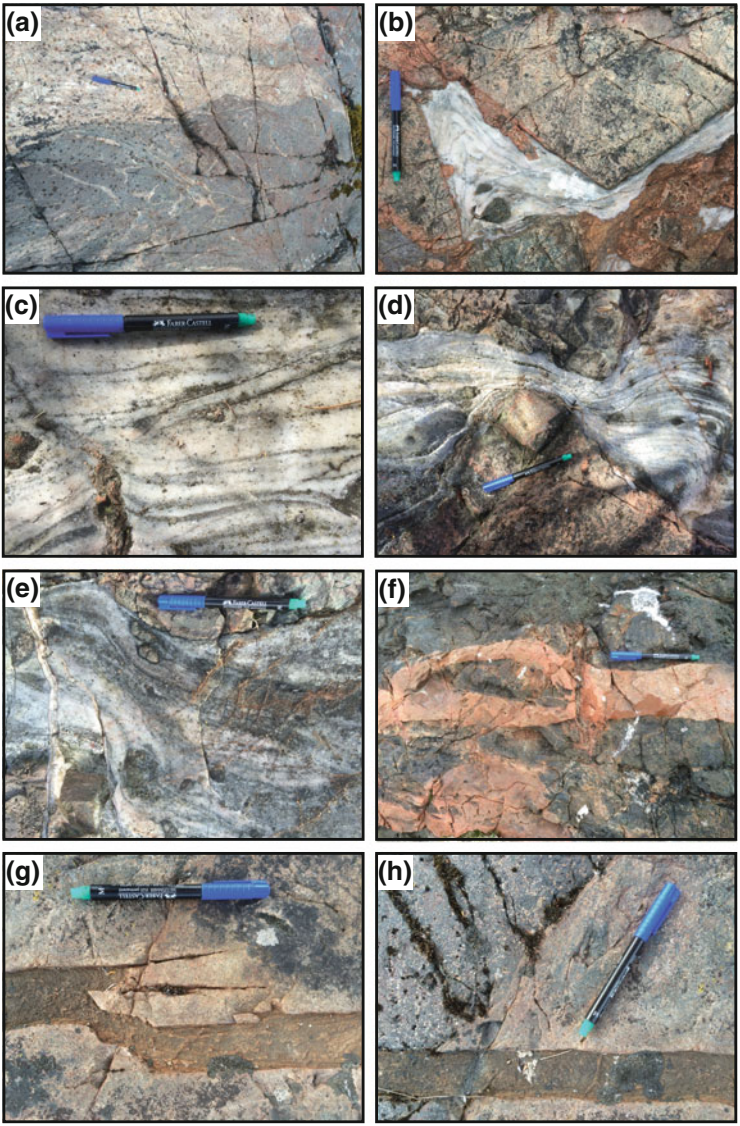

Fig. 4.11 Stornäset. Here several outcrops with migmatite and fenites are seen, cross-cut by flow-layered sövites and small carbonatite dykes. The later dykes can show intricate patterns. Farthest to the east massive syenitic high-grade fenite is found

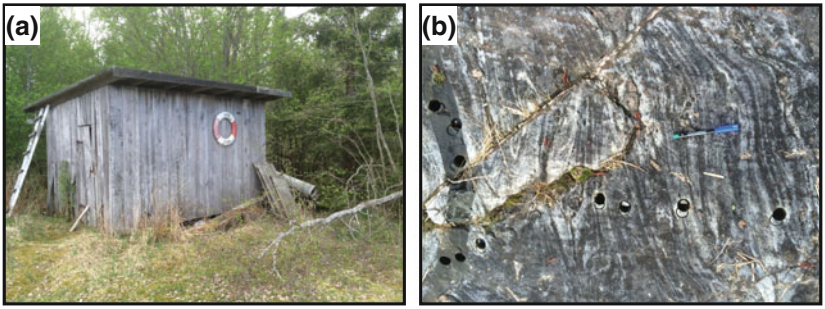

Fig. 4.12 At the coast near Stornäset, close to a small broad shed, you will find drill holes in sövite originating from a study by Andersson et al. (2016) (see text for details)

Reserve can be accessed using a path that is starting near the sports ground just a little beyond the bend in the main road (see information board). If you are keen to explore the plant and animal life of the region also, we recommend this hike (Fig. 4.13).

4.8 Stornäset Nature Reserve

The reserve covers an area of 107 hectares along the northern shore of Alnö including the north-eastern promontory of the island. Probably the finest site for migrating birds in Västernorrland County, the reserve was founded in 1968 and was further enlarged in 2016. It is intended to preserve breeding grounds for nesting birds. Accordingly, within the reserve there is a bird protection area where access is strictly forbidden during the time from April 1st to October 10th. This is because the principal bird migration seasons are during May, and from mid-July to beginning of October. Most birds stay only a little while on their way to, or from Central and Southern Europe to northern Sweden, Finland, or Russia.

Follow the track to another parking space after about 500 m. After another 500 m you will find a camp site with view points. A BBQ setup is present there, as well a simple toilet facility.

Pintail, Shoveler, Garganey, Great Crested Grebe, Mute Swan and Whooper Swan are frequently encountered, as are Grey Plover, Golden Plover, Ruff and Reeve, (Spotted) Redshank, Turnstone, and Dunlin. Other species occasionally present include Snow Bunting, Scarlet Grosbeak, Bluethroat, and Yellow Wagtail. Among birds of prey, you may encounter Rough-legged Buzzard, Hen Harrier, Merlin, or Goshawk. More rare guests include Heron, Great Snipe, Curlew Sandpiper, Red-necked Phalarope, or Shelduck.

Fig. 4.13 Stornäset nature reserve is well worth a visit if you are interested in flora and fauna of the region (see text for details). Images courtesy of J. Granbo

There is also much to see for the visitor interested in botany. Firstly one encounters a forest dominated by alder (*Alnus* sp.), with herbs such as wolf's bane (*Aconitum lycoctonum*), hedge woundwort (*Stachys sylvatica*) or marsh cinquefoil (*Comarum palustre*). Thereafter there are shrubs of willow (*Salix* sp.) and birch (*Betula sp.*) with bog-myrtle (*Myrica gale*), as well as grey (*Alnus incana*) and black (*A. glutinosa*) alder.

Within the zone flooded by high-water (Fig. 4.13), we find sea arrow grass (*Triglochin maritime*), black grass (*Juncus gerardii*), creeping bentgrass (*Agrostis stolonifera*), as well as red fescue (*Festuca rubra*). Towards the beach, one can identify slender spike-rush (*Eleocharis uniglumis*), clustered sedge (*Carex glareosa*), narrow small-reed (*Calamagrostis stricta*), sea milkwort (*Glaux maritime*), Mackenzie's carex (*Carex mackenziei*) or marsh arrow grass (*Triglochin palustris*). Below medium water level, we have water horsetail (*Equisetum fluviatile*), mare's tail (*Hippuris vulgaris*), marsh bed-straw (*Galium palustre*), tufted loosestrife (*Lysimachia thyrsiflora*), soft-stem bedrush (*Schoenoplectus tabernaemontani*), common (*Eleocharis palustris*) and slender (*E. uniglumis*) spike-rush and of course the common reed (*Phragmites australis*).

End of route 1.

Route 2: The Southern Route

Leave the roundabout north of Vi in easterly direction (first exit). After about 900 m turn left, entering the road towards Stornäset. Then, turn left again at the sign "Nedergård". After 750 m you find a fenced area (formerly Alnö mechanical factory, AMV) that is the next locality. The gates are usually open during work hours.

4.9 Abandoned Sövite Quarry at Smedsgården

N62°26'31.0"/E017°26'03.3"

Inside the fencing of the former Alnö mechanical manufactory (AMV), at the northern end, fenites (cut by a magnetite dyke), wollastonite-rich rocks, sövite with few fragments and some dykes of brick-red trachyte are exposed (Fig. 4.14). The fenites at the left hand side of the outcrop contain a rather narrow dyke almost entirely composed of magnetite and grade into a wollastonite-rich contact lithology nearer to a sharp sövite dyke contact (Fig. 4.14). The sövite shows distinct flow banding that is semi-parallel with the exposed contact. The sövite intrusion strikes approximately NE-SW and it dips away from the southern ring complex

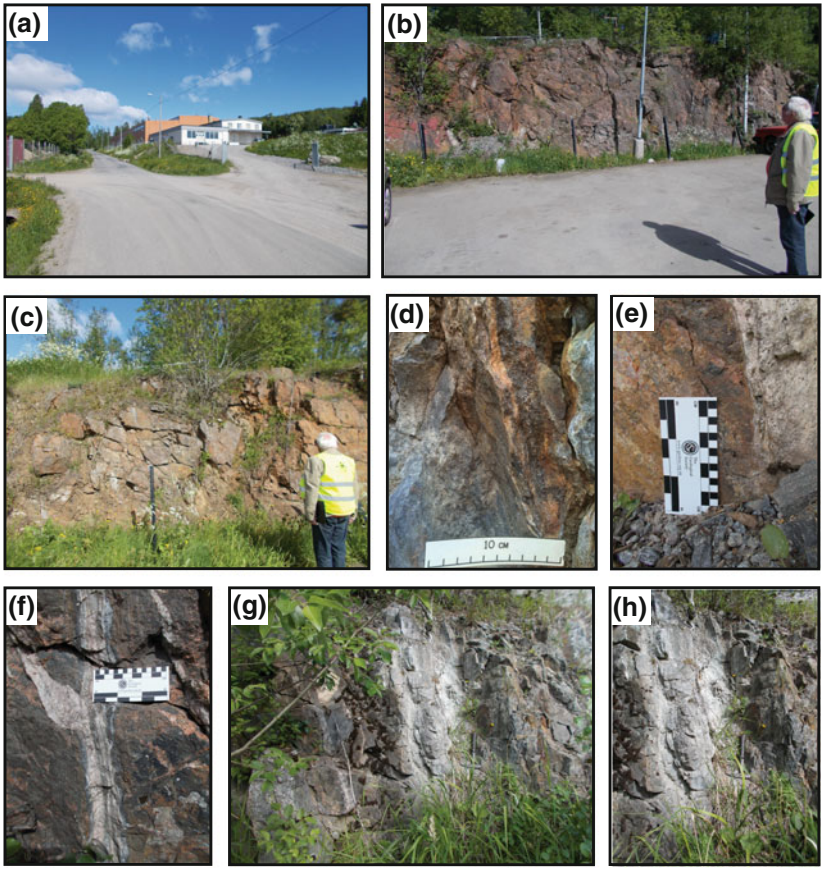

Fig. 4.14 Smedsgården quarry: Country rock exposure and contact zone. At the northern end, fenites (**b**, **c**) are cut by a magnetite dyke (**d**). Wollastonite-rich rocks (**e**–**h**) follow and grade into intrusive sövite

(Fig. 4.15). This outcrop here may thus represent an outer edge of a ring-dyke like intrusion along the southern end of the main complex.

Leave the AMV area and turn right (uphill). Take the next turn to the right also and soon after at a T-junction, go to the right again. Follow this road for about 750 m and stop on the right hand side at a small Nature Reserve that is dedicated to

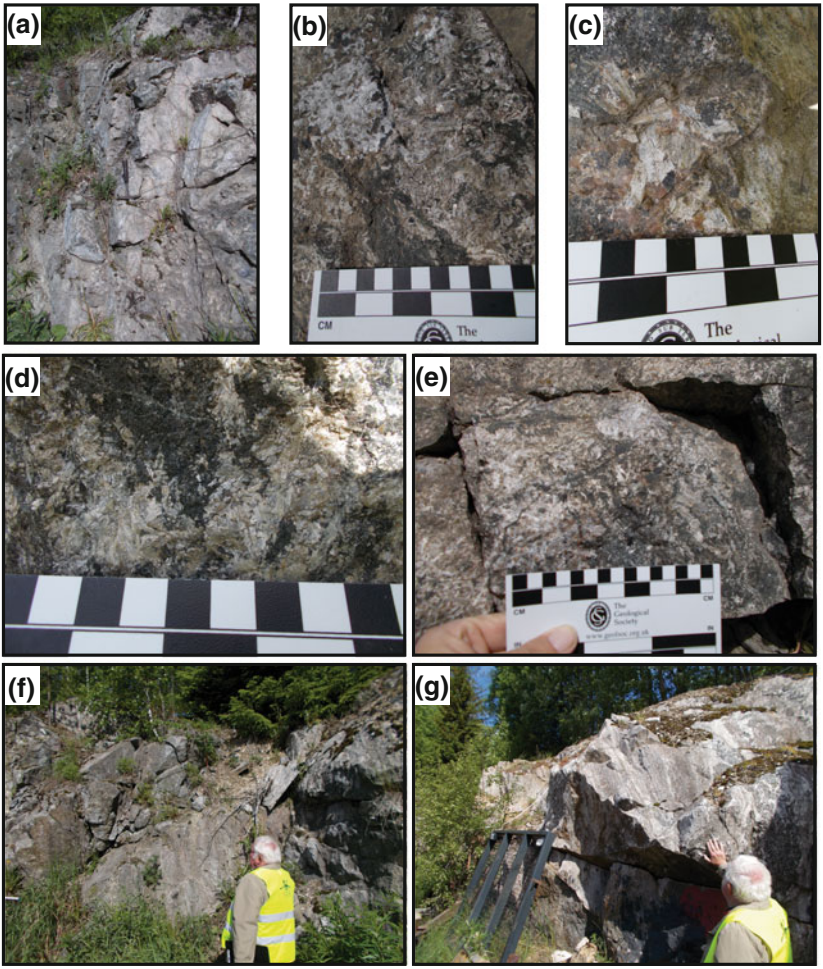

Fig. 4.15 Smedsgården quarry: Intrusive sövite sheet with wollastonite-rich contact zone and intense semi-vertical flow banding. This sövite sheet intrusion forms part of the proposed ring-dyke system at the southern end of the main ring-complex

the plant life on Alnö. Plants thrive on the special soils that form due to the unusual nature and composition of the bedrock that is naturally rich in K and P and many vital other nutrients.

4.10 Smedsgården Nature Reserve

N62°26'36.2"/E017°26'34.4"

The Nature Reserve here covers an area of 5.3 hectares (about 13.1 acres), and apparently very little has changed inside the reserve for more than 250 years. This fact, plus the local geology—nepheline syenites veined by sövites—have caused the special flora of the reserve. The section closest to the road is subjected to scything, while the other two sections are grazed by sheep. Within the reserve, there are two Iron Age grave mounds, a sheep stable and two barns (Fig. 4.16). Within the reserve, please do not damage the vegetation, e.g., plucking or digging up of plants is forbidden by law as is to break twigs or damage trees and shrubs in any way. Also, please do not light a fire.

During spring, the area is dotted with Cowslip primrose (*Primula veris*). Other flowers include Fumewort (*Corydalis intermedia*) and Least gagea (*Gagea minima*) in the depressions, the Hill violet (*Viola collina*, a.k.a. "Sundsvall violet") and Rock violet (*Viola rupestris ssp. rupestris*) around outcrops, and Spring whitlow grass (*Erophila verna*), Woodland draba (*Draba nemorosa*) and the Strict forget-me-not (*Myosotis stricta*), among others, on the outcrops (Fig. 4.16).

Later during the year, commonly end June, the reserve shows itself from its most magnificent side, with the following plants: Maiden pink (*Dianthus deltoides*), Lady's bedstraw (*Galium verum*), Nottingham catchfly (*Silene nutans*), Hoary plantain (*Plantago media*), Spotted cat's ear (*Hypochoeris maculata*), Meadow rue (*Thalictrum simplex*), Field garlic (*Allium oleraceum*), Wood avens (*Geum urbanum*), Basil thyme (*Satureja acinos*), Black mullein (*Verbascum nigrum*), and Common harebell (*Campanula rotundifolia*).

Somewhat rarer species include Paira sedge (*Carex pairaei*), Vernal sedge (*Carex caryophyllea*), Common quaking grass (*Briza media*) and the multiflowered buttercup (*Ranunculus polyanthemos*). In the scythed area, wild basil (*Satureja vulgaris*) flowers around end July—beginning of August.

Owing to the special geology of northern Alnö, very rare hybrids are found. The fern Wall-rue (*Asplenium ruta-muraria*) grows exclusively on calcareous rocks (or on mortar), while the Northern spleenwood (*Asplenium septentrionale*) shuns limestone. Rare hybrid forms between these two ferns have been found at the contacts between sövites and silicate rocks.

If you are keen, a small optional geology walk is possible here also. Just opposite the Nature Reserve entrance, a track leads into the forest. After some 200 m, a small path goes off to the right and leads to an abandoned sövite quarry.

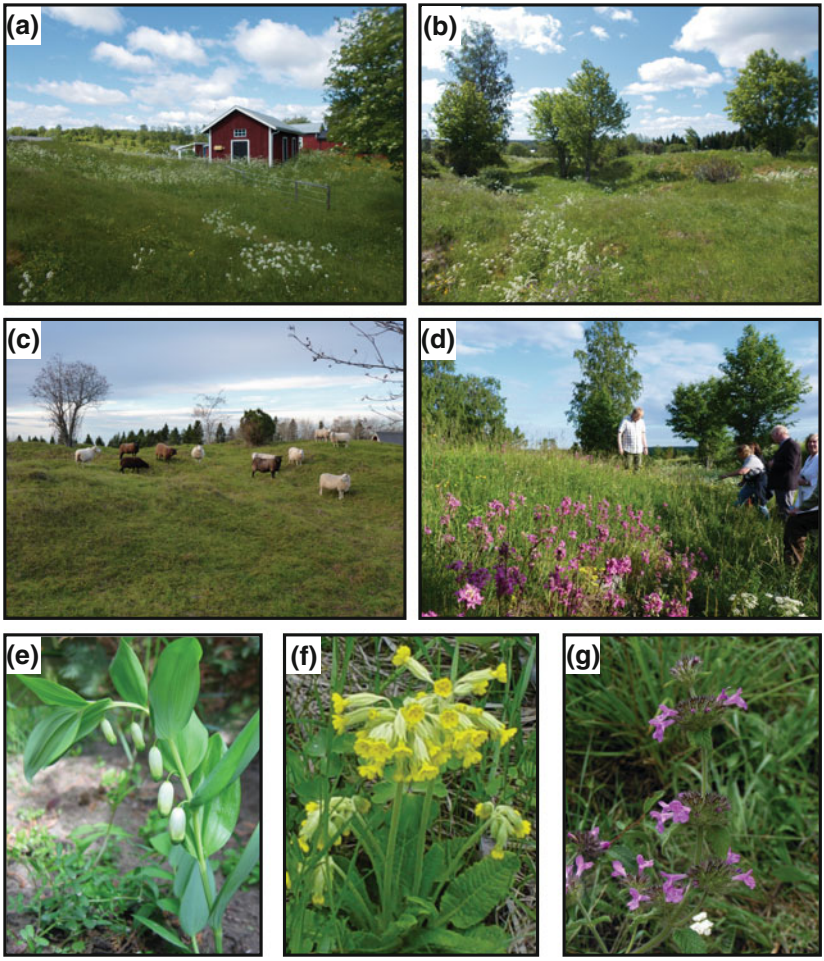

Fig. 4.16 **a**–**d**, Botany Nature Reserve near Smedsgården, **e** Solomon's seals, **f** cowslip, **g** wild basil. Images **c** and **d** from John Granbo, images **e**–**g** from wikimedia.org

Along the path, some small outcrops of ijolite occur. Unfortunately, the old quarry is now fenced in and carries seasonal water. You may not be able to enter it for a detailed inspection if you visit at an unfortunate time.

In the old quarry, various sövite varieties have been observed, which are commonly banded. The sövites of the southern wall carry abundant pyrochlore (fersmitic). This mineral is strongly radioactive and you probably want to wear gloves when dealing with the rocks here.

Return to your vehicle and continue along the road in easterly direction until you reach the village of "Släda". You may park on the dirt track at the entrance area to Stavsätt farm opposite the village sign and decorative mail boxes. As the outcrops are in direct vicinity of the houses, we recommend that you inform the inhabitants that you are there.

4.11 Old Iron Mine at Stavsätt Farm in Släda

N62°26'38.1"/E017°27'10.7"

Here, in front of the Stavsätt farm partly overgrown outcrops of former iron minings can be inspected. The mineralization occurs in serpentinized pyroxenite (jacupirangite), veined by sövites in east-westerly directions. Local banding in the pyroxenite is visible. Beautiful and cm-seized octahedrons of titanomagnetite can be found here as well as small baddeleyite crystals of collector quality. The magnetite occurs often at the boundary between pyroxenite and sövite (Fig. 4.17), while the baddeleyite occurs dominantly in fracture fills.

Iron ores were discovered on Alnö in 1670 and a number of minor old mines were operated in the area between Ås, Släda and Stavsätt (Lundbohm 1899). These usually reside in pyroxenites or jacupirangites. Gangue minerals include serpentinised olivine, apatite and biotite. At the beginning, the iron ore was used at Galtströms bruk, along the Bothnian shore south of Alnö. Later on, the ores were shipped to the iron works of Graninge, Gnarp and especially Åvike, where they were mixed with iron ore from Utö (an island south-east of Stockholm). The Alnö iron ores had in general relative high contents of titanium and sometimes phosphorous. According to von Eckermann (1948), the maximum iron content at Stavsätt is 39%. Note very small-scale mining for magnetite also occurred elsewhere, e.g. in the sövite at Hörningsholm (Route 3).

After this locality, drive to Ås village and soon after passing through Ås village, turn sharp right. Just a minute later, turn sharp left into a well laid out forest track. Drive for a few hundred meters before you reach the next stop, which is a protected site and is marked by a blue sign for 'Geologisk lokal'. Park here.

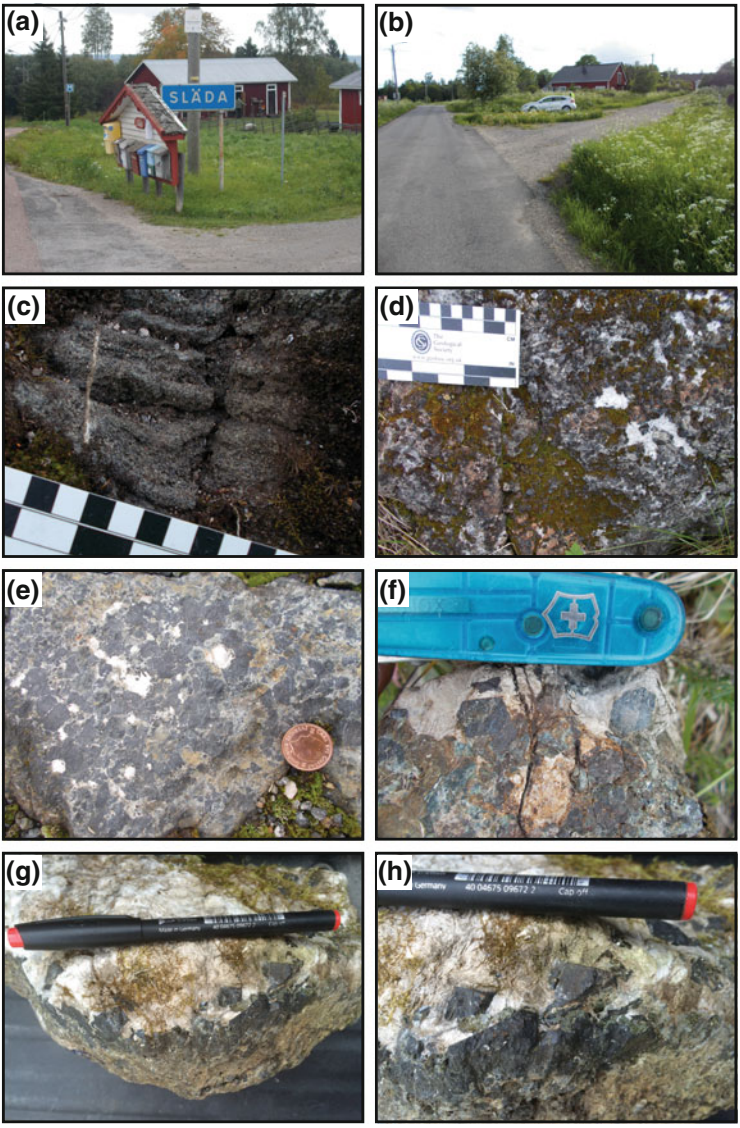

Fig. 4.17 **a**, **b** At Stavsätt in Släda, you will find an old mining site that was previously exploited for iron due to a high content in magnetite. It is said that Harry von Eckermann was frequently staying at Släda farm during his fieldwork visits. **c**, **d** Pyroxenite types at Släda. **e**–**h** Magnetite at Släda

4.12 Old Quarry Outcrop along Ås Forest Road; Naturminnet Ås

N62°26'38.8"/E017°28'17.3"

Large outcrop of melanocratic nepheline syenites (called malignite) and ijolite. The rocks here are very coarse grained (Fig. 4.18). At this locality, building stone has been quarried. The dominant rock type here is nepheline syenite, made up of nepheline (grey, glassy, and fractured), potassium feldspar (reddish with cleavage) and some acicular pyroxene crystals (black or greenish black). In some parts of the outcrop, ijolite occurs too (nepheline and pyroxene, but no feldspar) as well as alkaline pyroxenite (mainly pyroxene). In addition, fine-grained dykes dominated by potassium feldspar occur. These are similar to the 'borengite' of the Röde locality (see route 3). Note, nepheline syenite and ijolite are the most common alkaline plutonic rocks within the Alnö intrusion.

When finished, walk down the forest track for a short while until you see the shore (people living there do object to car traffic). Along the path leading down to the shore, small outcrops of pyroxenite can be seen. Once you reach the small T-junction at the bottom of the forest road, turn left and after only a few meters inspect some exposures in front of a private house (Fig. 4.19).

4.13 Rheomorphic Fenite near Ås Jetty

N62°26'33.1"/E017°28'36.0"

Within the Alnö Complex, rheomorphism has been taken place on a grand scale. This outcrop of high-grade fenites illustrates the process on a small scale. The fenites have in part become mobile, with clearly intrusive leucocratic mobilisates intruding veined gneiss and more low-grade fenites, while leaving pyroxene-rich layers behind. A small but nice outcrop of leucocratic high-grade fenites occurs here, with potassium feldspar as the dominant mineral. The fenites show crystal size variations of several cm and some crystals reach above 3 cm across. Occasionally, thin layers of pyroxene, likely aegirine, are seen (Fig. 4.19). The intrusive ('rheomorphic') behaviour of the fenite here is indicated by fragments of veined gneiss (greywacke type) in the fenite, as well as by apparent flow laminations, underlining that mobilization of once reacted fenite materials did likely occur within the Alnö complex.

Opposite locality 4.13, a small path leads down to the beach and to Ås jetty, which is our next stop.

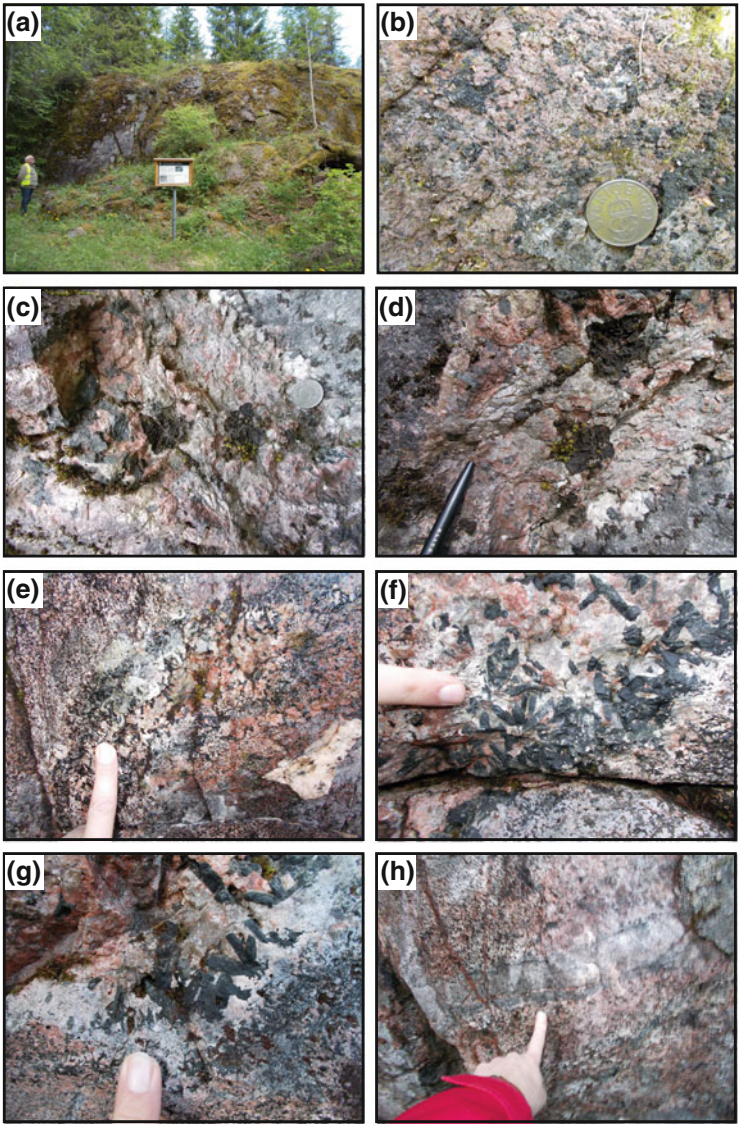

Fig. 4.18 Ås—forest road; nepheline syenite and ijolite, locally with pegmatite pods and rafts of coarser (cumulate) materials. (**f**, **g**) Note the large pyroxene needles in the pegmatite facies

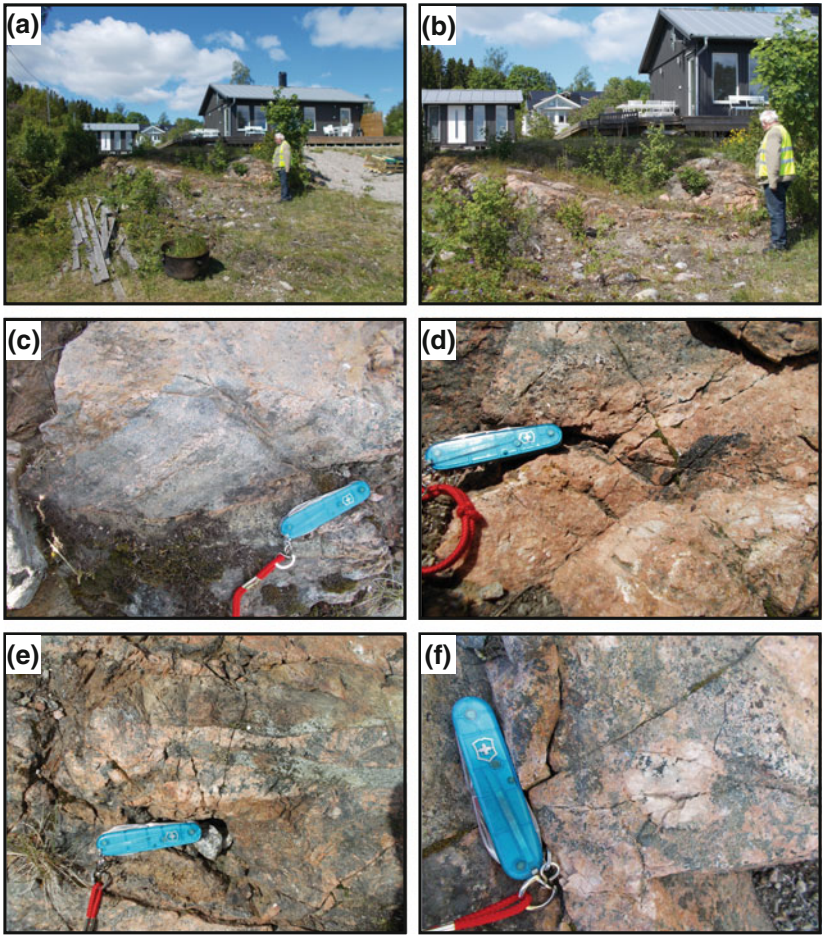

Fig. 4.19 Rheomorphic fenite is exposed near Ås jetty and shows potassium feldspar as well as bands of augite. Fragments of veined country rock gneiss are also present

4.14 Boulders at Ås Jetty

N62°26'38.4"/E017°28'40.6"

Ås jetty was constructed to load ships with iron ore sourced from many small quarries on Alnö (e.g.at Släda) to supply the Åvike iron works a little to the North

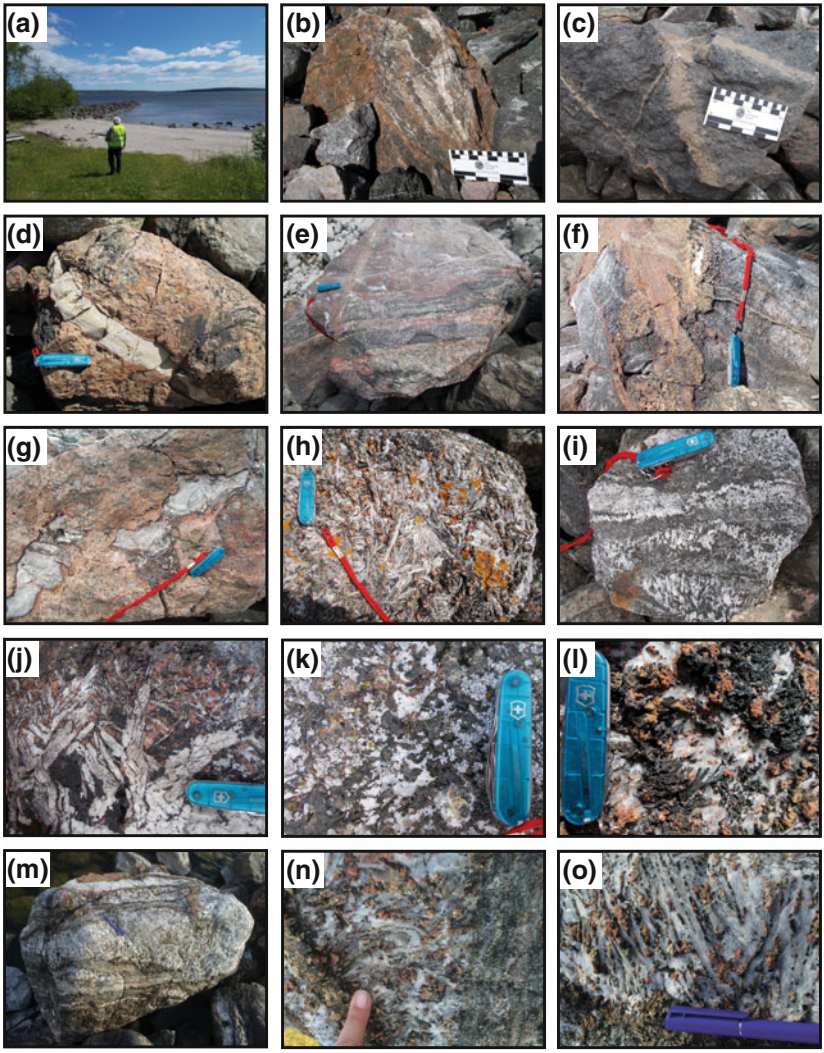

Fig. 4.20 Boulders at Ås jetty (see text for details)

of Alnö. The jetty is made with boulders and blocks of Northern Alnö and represents a catalogue of rocks from the igneous complex (Fig. 4.20).

The blue-grey magnetite was the main source of iron during the jetty's active time (1754–1884). In the 1880s, however, technical developments allowed smeltering of Kiruna-type ore, which made Fe-mining here at Alnö no longer economical.

At the base of the jetty, blocks of black alkali pyroxenite (jacupirangite) can be found with distinct and very common Ti-magnetite, but also some nepheline, apatite and melanite crystals. Further out on the jetty are lovely blocks of sövite pegmatite which display black and white colour mosaics with reddish variations in some places and a particularly beautiful example is found at the farthest tip of the jetty. The jetty was declared a 'protected site' in 1976 as it carries relevance to the geology of the island.

Moreover, along the beach here, larger blocks of biotite sövite can be inspected which often contain larger inclusions (xenolith) of rocks the sövite magmas picked up '*en route*' to the surface. Along the shore in both directions, rare boulders of kimberlitic rocks maybe found too, which are characterized by the large amounts of olivine phenocrysts. In addition to sövite and kimberlite, boulders of nepheline syenite and ijolite are present.

The outcrops on the rocky promontory south of the jetty show strongly fenitized rocks, cross-cut by sövites, carbonatites and phonolites. In the small bay to the south of this outcrop, a man-sized boulder of kimberlitic alnöite carrying ultramafic nodules can be inspected. The kimberlitic alnöites of the area (including the mainland north of Alnö) have been investigated for their diamond potential, but no secure occurrence has so far been confirmed for Alnö, despite intense efforts by mining companies and academic geologists alike (see also Chap. 2).

An alnöite intrusion can be inspected at low water two coves further south from the jetty and shows larger micas in a fine-grained bluish-black matrix (Fig. 4.21). Small carbonatite sheet intrusions are found here as well (Fig. 4.21g, h), making for a nice in situ rock assemblage of alnöite, sövite, and alkaline dykes, representing some of the crucial rock types of the Alnö igneous complex.

After finishing at the jetty and the little bays here, walk back to your vehicle and return to the main road. Once you leave the forest track, turn left (to the south) onto the main road. Just a short drive further, in a major bend along the road, we will reach the next locality. It is best to park on a little dirt track to the left, some 20–30 m before the road bend with the outcrop (Fig. 4.22).

4.15 Sövite Sheet Intrusion in Ijolite Country Rock

N62°26'29.1"/E017°27'57.9"

Please watch the traffic here and use safety vests as the outcrop is right in the bend and oncoming traffic may not immediately see you when working at this outcrop.

A banded (flow textured) sövite sheet intrudes silicate rock (ijolite), which can be seen on either side of the sövite intrusion (Fig. 4.22). The sövite carries ample fragments of bedrock lithologies as well as igneous xenoliths from earlier

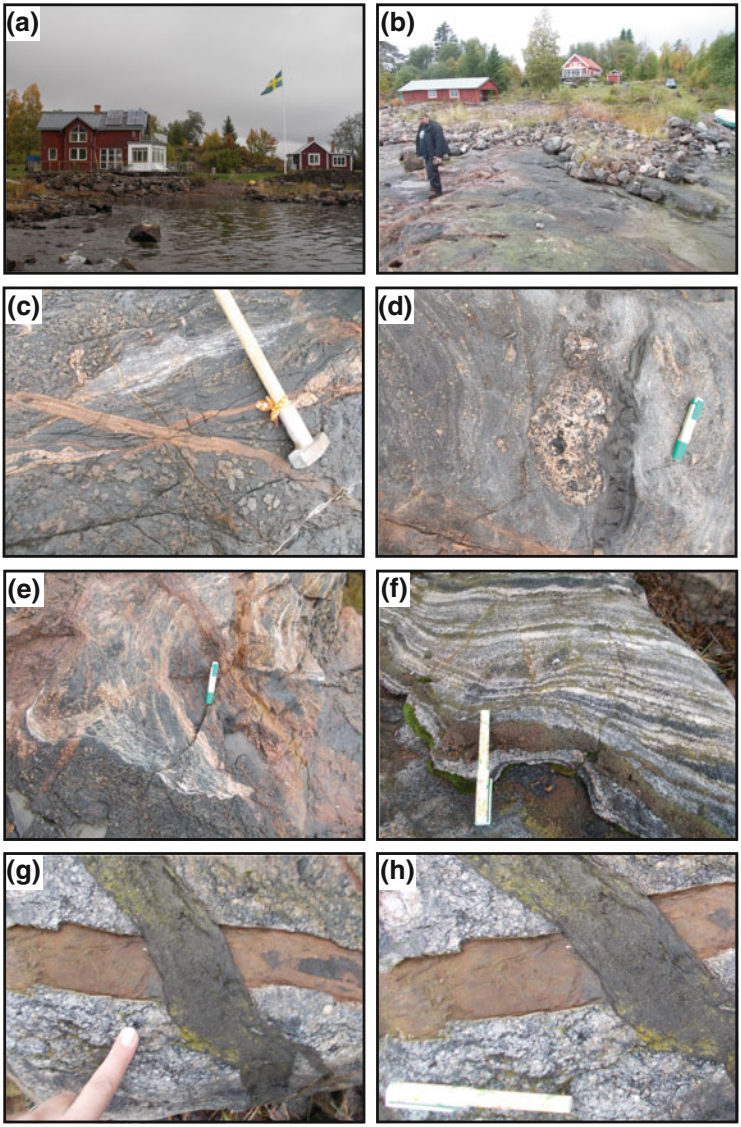

Fig. 4.21 Alnöite sheet intrusion near Ås jetty shows the large phlogopite crystals typical for alnöite. Sövite and alkaline silicate veins and dykes are also exposed at this site

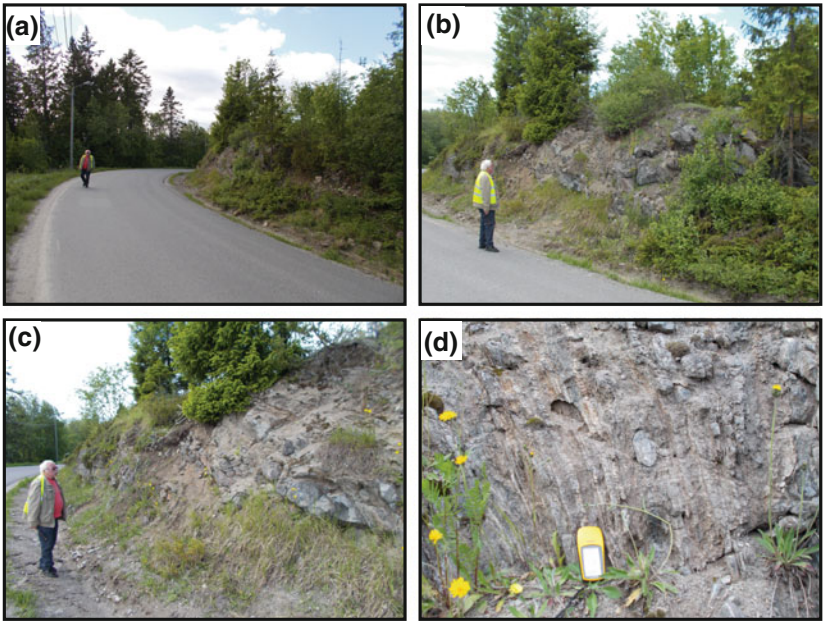

Fig. 4.22 Sövite sheet intrusion along main road at locality Fig. 4.15. The sövite is rich in foreign inclusions here (xenolith) and shows marked flow banding

magmatic activity at Alnö, implying significant magma-host rock interaction below the currently exposed intrusion level.

End of route 2.

Route 3: Central Northern Alnö

Drive to Alnö Church (Alnö kyrka), which you passed previously on route 1. Park where safe and convenient.

4.16 Old Alnö Church

N62°26'52.9"/E017°24'27.5"

The Alnö old church was built around AD 1200 (Fig. 4.23); but most of the beautiful murals are from the 15th century. As the population increased, a new church was built

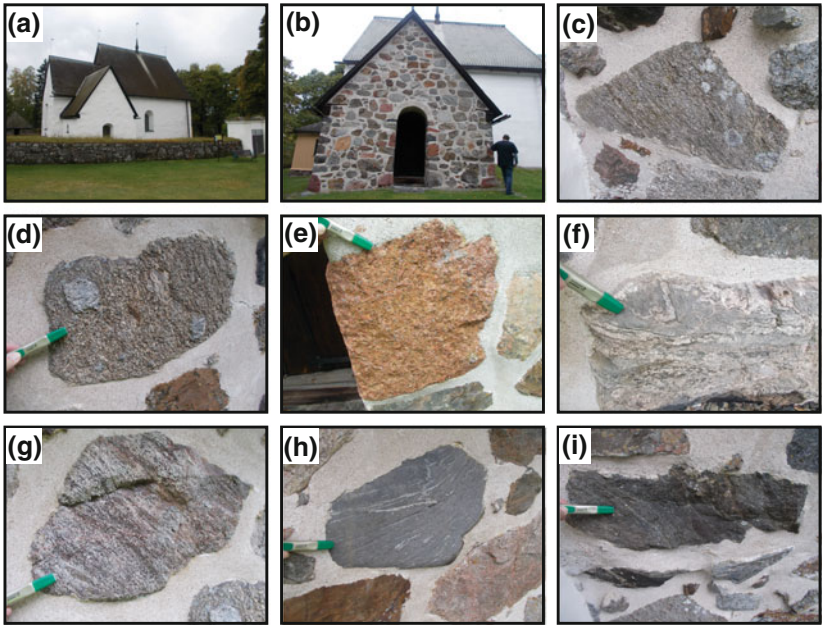

Fig. 4.23 Gamla Alnö kyrka (the old church) shows a variety of regional rock types (granites, gneisses, shales) that mainly derive from blocks and boulders that came to Alnö in the glacial drift (see Chap. 1 for details on regional geology)

in 1865. It burnt down only a few years later, and the old church came into use again. The famous Swedish Art Nouveau architect Ferdinand Boberg designed another new church that was finally consecrated in 1896 (Fig. 4.24).

From the old church, the baptismal basin was installed in the new church (Fig. 4.24e). The basin is at least 50 years older than the old church according to dendrochronology. It had been carved from fir- and pine-wood. It is illustrating the battle between the heathen faith and christianity, and emphasizes the importance of baptism. The basin was dated to the middle of the 1100th century. It is a unique cultural artefact not only for Scandinavia but for the whole of Europe. It has been exposed abroad in several occasions, e.g., at the Louvre in Paris in 1963.

The upper part, formed like a wooden storage bowl, depicts figures with glories or wings, probably Christ himself and the archangels, in a background of loops possibly reflecting the rich vegetation in paradise. Among the loops, human heads seem to represent people that have found salvation due to baptism. The pattern

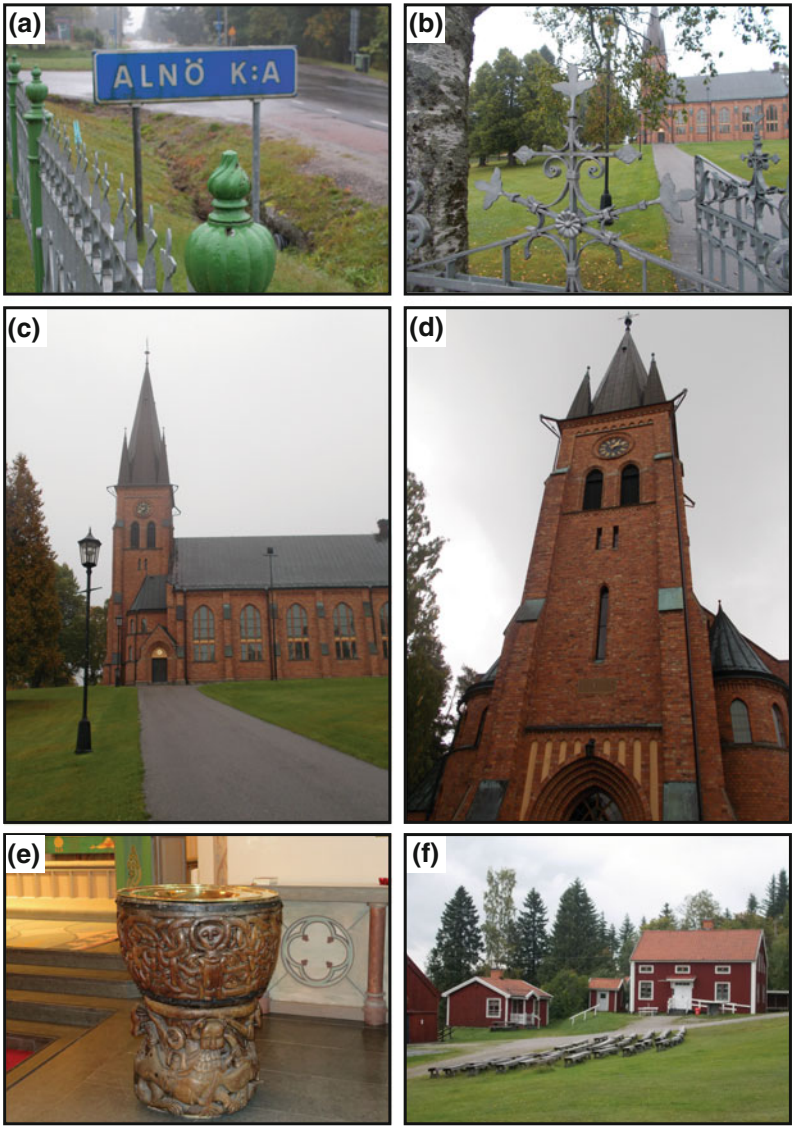

Fig. 4.24 Alnö church was built in the late 19th century and was designed by the famous Swedish architect F. Boberg. The new church hosts a 11th century baptism font (Photo courtesy of J. Granbo). Nearby, the local hometown society (**f**) runs a centre with cafe and a series of events in summer, which are well worth a visit if you happen to visit at the right time. They also offer a selection of Alnö rocks to look at and to familiarize oneself with the exceptional bedrock geology of the island

does resemble those found in Norway, suggesting that Christianity arrived from there. Monks from the British Isles may have come to Alnö via Nidaros (Trondheim).

The carvings of the foot depicts the battle between paganism and Christianity, but in a surprisingly oriental style. Tied-up lions are the beasts that represent the powers of darkness and evil. During pagan times, children that were born sick or malformed were left to the beasts of the wilderness. By contrast, the carvings of the Alnö baptismal basin emphasizes the importance of baptism for all children to prevent them getting seized by the devil.

In the rear of the old church a selection of regional rock types can be seen (granites, gneisses and shales), most of which seem to be derived from glacial erratics though and are not directly from Alnö (Fig. 4.23).

From Alnö church, drive north to Båräng. There turn left into Nackavägen and follow the road until you see a blue sign for "Geologisk Lokal". Park on the left hand side of the road. We recommend that you wear a safety vest when operating near a road.

4.17 The "Borengite" at Röde

N62°27'39.9"/E017°23'57.2"

This road-cutting is of locally fenitized migmatite intersected by various trachytic dykes. This is the type locality of "borengite", a dyke rock with a fluorite-rich potassic trachyte composition. At the centre of the road cutting, we find the so-called 'borengite', a dyke that is one of the most potassium-rich rocks known. The rock consists mainly of alkali-feldspar. It is brownish red, with greenish blue spots that contain mainly fluorite. In its central parts, the dyke is more coarse-grained, while the margins are fine-grained chilled contacts. The borengite is among the earlier dykes that preceded the main intrusions of alkaline rocks and carbonatites (Fig. 4.25). The rock has been named after the local village of Båräng by von Eckermann (1960). The name has not found widespread international recognition, and the rock would classify as an alkaline trachyte when using modern nomenclature.

The road cutting also shows some carbonatite dykes, as well as cracks filled with coarse calcite. The wall-rock is a veined gneiss (migmatite) that has reacted along cracks with the alkali- and carbonate-rich solutions that emanated during the intrusion of the Alnö rocks and shows various degrees of 'fenitization', first described at the type locality Fen (Telemark, Norway).

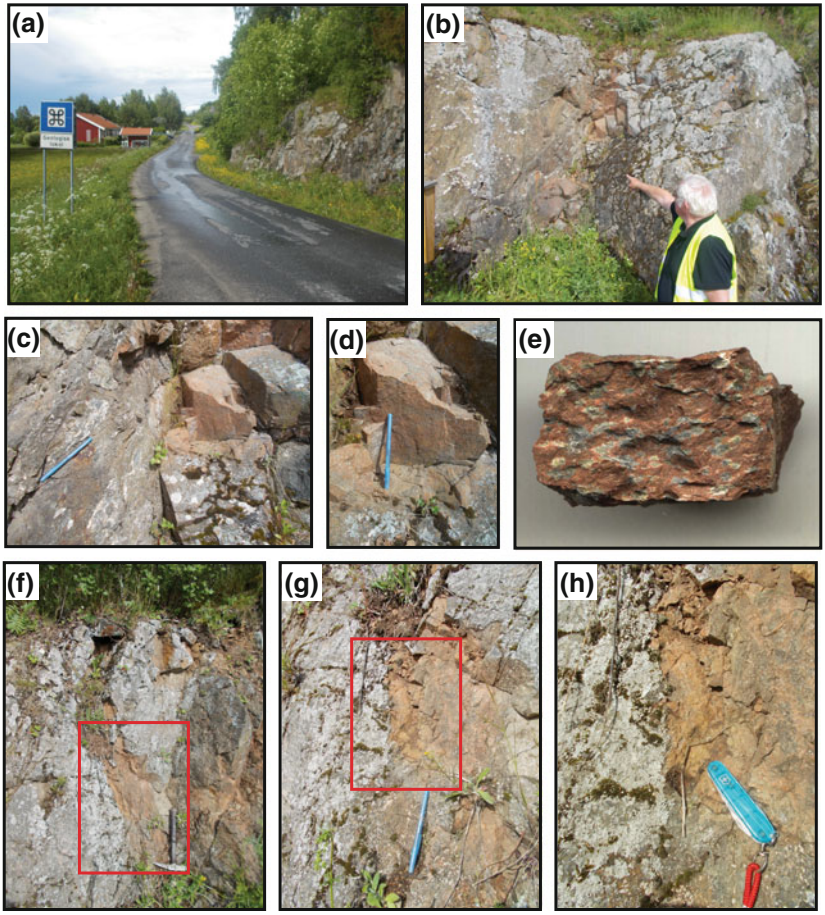

Fig. 4.25 Borengite near Röde. This road-cutting of locally fenitized migmatite intersected by various dykes of "borengite", a dyke rock with a fluorite-rich potassic trachyte composition (see text for details). Image **h** is a zoom in of images **f** and **g**

Notably, during the late 1960s sövite was quarried near Båräng and for use as a fertilizer (due to high Ca, K, P). However, the discovery that the rock was highly radioactive (high U, Th) soon stopped this effort.

Fig. 4.26 An Iron Age burial mound near the "borengite" locality. Alnö, although smaller at the time, was already a major Iron Age cultural center, and Iron Age burial mounds and grave fields are common on the island

Note the Iron Age burial mound in the field just north of the outcrop (Fig. 4.26). Return to the main road and drive to the north. Just at the next take-off to the right ("Gistavägen"), there is the biggest Iron Age burial mound on the whole island, called "Värdeshögen" (Fig. 4.27). Park here.

4.18 Iron Age Burial Mound and Grave-Field

(N62°27'39.7"/E017°23'31.3")

In 1684, it was partly excavated and it was noted that the mound contained "a brass urn with cremated bones". If this report is correct, the "brass" would most likely be bronze, indicating the grave of a religious leader.

From the adjacent mound, "a horse skeleton and various armour, including a stirrup" has been extracted during an excavation. The gilded stirrup originates from the 16th century and displays oriental decorations. It is now at the Historical Museum in Stockholm and it remains enigmatic how such relatively young items ended up in a prehistoric grave and "grave robbing" may need to be envisaged.

Continue the small road further, and across the junction ahead, you find an Iron Age grave field on the left hand side of the road (Fig. 4.28). Weapons are rare grave gifts, more often glass beads, bone combs, bronze brooches have been found, as well as iron nails and rivets. In several graves, bear claws were found, probably the remnants of bear skins.

That Alnö had been a religious centre during Iron Age is indicated by the names of settlements: "Vi" is derived from "vigja", indicating that a place had been hallowed to some god. "Hof" (like "Hofvid") indicates the site of a temple.

Fig. 4.27 "Värdeshögen", the largest Iron Age burial mounds of the island is found close to the main road leading to the north shore (Stop Fig. 4.18)

There are few finds from the Stone Age at Alnö, indicating that the island was already inhabited prior to the Iron Age, although it was smaller then (the present isostatic land rise is about 8 mm/year). Near Hovid, a Bronze Age mound was excavated in the 1930s. The mound is now gone; below it was a stone cist with remnants of human bones; no grave gifts were found, however.

Drive back to Alnövägen and turn to the south (left). Just before the new church, turn left at the sign "Hörningsholm". A little later, turn left toward Hartung (Hartungvägen). Note, Hartungvägen is a private road and it is a "*Cul de Sac*".

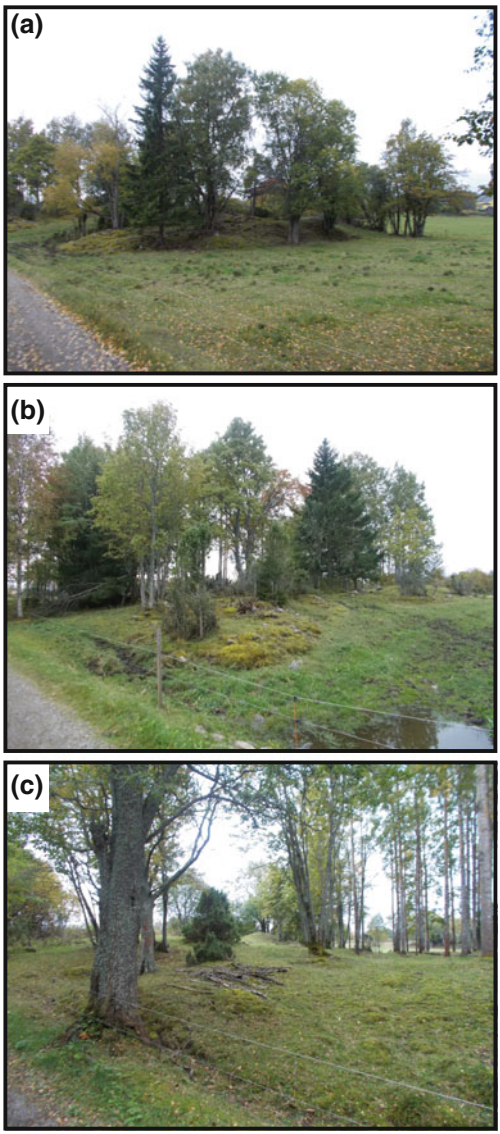

Fig. 4.28 Iron Age grave-field near locality Fig. 4.18 (see text for details). Glass beads, bronze brooches, iron nails, and bear claws were found among the grave gifts

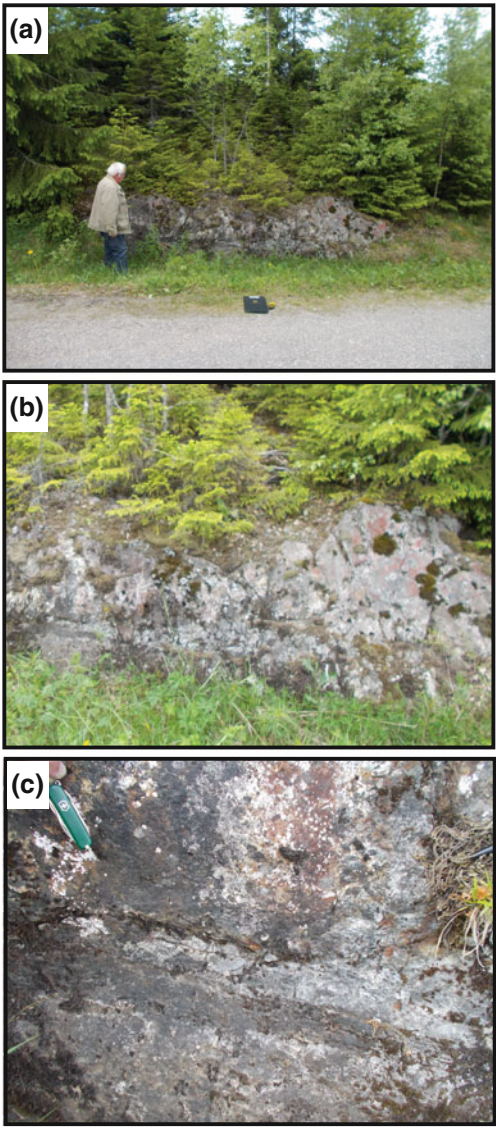

Fig. 4.29 Outcrop along Hartungsvägen shows ijolite/melteigite, which has been broken up into large angular fragment and the interstices are filled with nepheline-syenitic material. Needles of aegirine augite, aggregates of melanite garnet and spots of pyrrhotite are seen

4.19 Road-Cutting North of Hartung (Along Hartungsvägen)

N62°27'47.8"/E017°25'49.6"

The outcrop shows ijolite/melteigite, which has been broken up into large angular fragments. The interstices are filled with nepheline-syenitic material. Field and petrographic evidence suggests that the nepheline-syenitic material might represent the product of in situ differentiation. Needles of aegirine augite, aggregates of melanite garnet and spots of pyrrhotite are also observed (Fig. 4.29). Note, several drill holes are seen here at the outcrop, which are strongly weathered by now and which go back to a palaeomagnetic study carried out in the mid-80s, i.e. the weathering represents a time span of some 35 years.

Continue on Hartungvägen northward. At the end of the drivable road (blocked by rocks), park the car near the rock blocks and walk behind the shed of a larger farm on the right hand side. Please ask for permission when entering the farmstead. The farmer is very friendly and is aware of the geological relevance of his backyard!

4.20 Farm North of Hartung: Banded Fenite with Migmatite Domains

N62°28′07.4″/E017°25′43.9″

Here a larger outcrop of fenite can be inspected, but parts of the outcropping rock are overgrown with dark lichen. The fenite here displays relict gneiss textures as well as ductile deformation features (Fig. 4.30). In part, the outcrop is made of areas that are still quartz bearing migmatite, while other domains are fenite (i.e. quartz has been removed by reaction), suggesting that the various stages of fenitization are on superb display here (Fig. 4.30c–h).

Drive back to main road and turn left to Pottäng. Drive through the hamlet of Pottäng and follow the road downhill. In a sharp bend of the road, turn right to inspect the Pottäng quarry site. Please note that you are entering private property. If you meet people there, please ask for permission.

4.21 Pottäng Old Barite Quarry

(N62°27'33.1"/E017°26'25.4")

Also, several abandoned barite quarries (e.g. this one here near Pottäng) are present, which were mined during WWII. Barite is a source of Ba and Sr, which

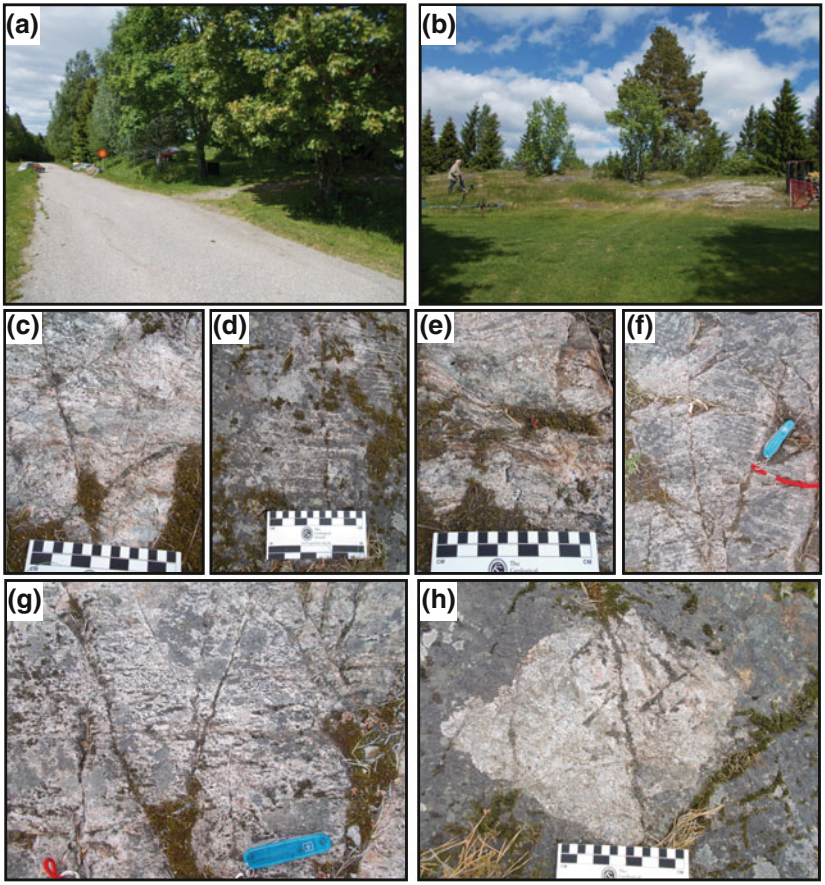

Fig. 4.30 Outcrop behind farm at the end of Hartungsvägen. Variably fenitized migmatites can be inspected here

was used in signal flares to create a certain colour of light to convey various pieces of information over long distances. The Pottäng is now fenced off and is not safe to visit (Fig. 4.31). The tailings that can still be found near these old quarry contain barite, fluorite, calcite, pyrite and goethite.

Route 3 ends here and we recommend to start route 4 in the morning instead of after e.g. having completed route 3, as it will possibly be a little late for the 'boat trip' we offer below.

End of route 3.

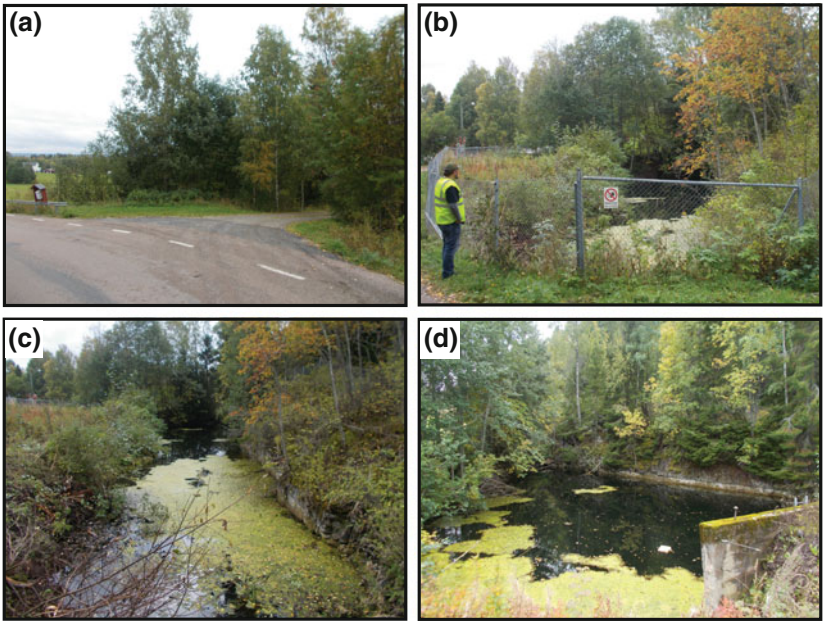

Fig. 4.31 Old barite quarry at Pottäng. Being on private property, please contact the owner. For your own safety and comfort please do stay outside the fencing

Route 4: The Islands North of Alnö

The small islands north of Alnö are well worth a visit, but a rowing boat is required. Unfortunately, there is no boat rental on the island. You will have to ask someone local if you can borrow or rent a boat, or alternatively bring an inflatable rubber boat. Even a simple boat might do as the water depth in most near-coastal areas here is below 2 m. Please wear safety vests, however (Fig. 4.32).

Row your boat from e.g. Stornäset (see Route 1) to the NW-point of Långharsholmen (Fig. 4.33). At the landing site on Långharsholmen is a metal ring to fix your boat near the Nature Reserve sign that briefly explains the flora of the island (Fig. 4.34).

Fig. 4.32 A rowing boat is required to reach the small islets North of Alnö

Fig. 4.33 Map for route 4, the boat trip to the little islands North of Alnö (satellite image from Google maps)

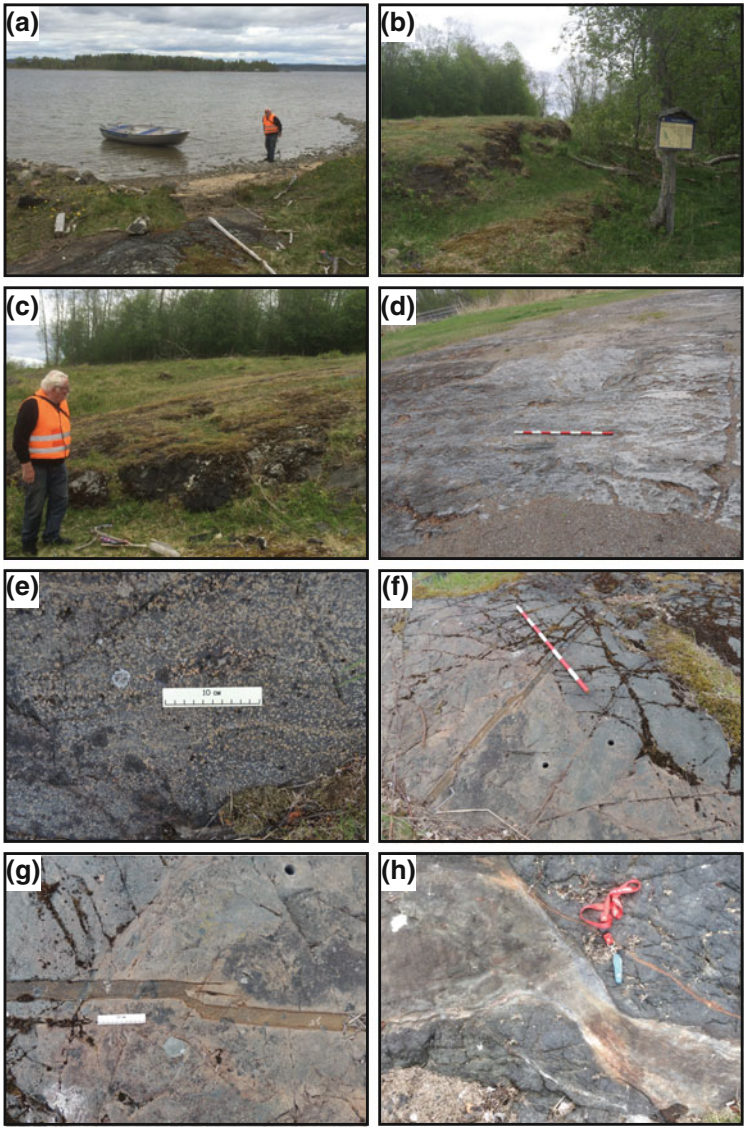

Fig. 4.34 The landing site on Långharsholmen offers an introduction to the flora and fauna of the islet and some good rock exposures of plutonic silicate intrusives and carbonatite dykelets

4.22 Långharsholmen Nature Reserve

N62°28'09.8"/E017°28'03.7"

Depending upon prevailing winds and the water level, migrating birds alternate between Långharsholmen, Hörningsholmen, and the Nature Reserve at Stornäset. Within the reserve, it is forbidden to damage land, the plants, or deadwood. Also, you may not disturb animal life or drive a motor vehicle. Dogs have to be kept on the leash. Grey Plower, Bar-tailed Godwit, Spotted Redshank, Little Stint, Temminck's Stint, Pintail, Shoveler, and Pochard are among birds visiting the Reserve.

The island has traditionally been used for grazing and scything. Even today, cattle are transported by ferry from Stornäset. This open landscape is home to a variety of flowers. In the pasture, we find Maiden pink (*Dianthus deltoides*), Wallpepper (*Sedum acre*), Field gentian (*Gentiana campestris*), or Thyme-leaf sandwort (*Arenaria serpyllifolia*), to name only a few species. In more moist conditions, we find Meadow pea (*Lathyrus pratensis*), Marsh pea (*L. palustris*), Felwort (*Gentiana amarella*), and Common buttercup (*Ranunculus acris*).

Moreover, Fairy flax (*Linum catharticum*), Dwarf milkwort (*Polygala amarella*), Hairlike sedge (*Carex capillaris*) and Common quaking grass (*Briza media*) are found, which are all indicators of calcareous soil.

In the forested parts, mainly made up of Grey alder (*Alnus incana*) and Bird cherry/Hagberry (*Prunus padus*), we also find Wood cranesbill (*Geranium sylvaticum*), Wolf's bane (*Aconitum lycoctonum*), Meadowsweet (*Filipendula ulmaria*) and, in the moister parts, Moschatel (*Adoxa moschatellina*).

Meadows along the beach carry Black grass (*Juncus gerardii*), Narrow small-reed (*Calamagrostis stricta*), and Red fescue (*Festuca rubra*). Further towards the sea, we find Slender spike-rush (*Eleocharis uniglumis*), and Water sedge (*Carex aquatilis*). Below mean water level, we find Water horsetail (*Equisetum fluviatile*), Mare's tail (*Hippuris vulgaris*) as well as Common and Slender spike rush (*Eleocharis palustris, E. uniglumis*).

The information panel also reminds us about the present isostatic land uplift amounting to 80 cm per hundred years (0.8 cm/yr). The uplift is the consequence of the several kilometers thick ice sheet during the Ice Ages that had pushed down the surface of the Earth and has since disappeared. The iron ring in the outcrop nearby was used for tying down one's boat near the shore about one hundred years ago.

In respect to rock exposures here at the landing sites, we find dark pyroxenite dominated outcrops with banded sövite intruded by younger sövite (pure white) and ijolite (Fig. 4.34). Outcrops along the shore to the south show pyroxenite, sometimes altered to vibetoide (pyroxene + amphibole) or into rocks composed entirely of mica. Some pyroxenite outcrops show laminar flow textures, with alternating layers of coarse- and fine-grained material.

A short walk to the north of the landing place reveals, a cupola-shaped intrusion of medium-grained ijolite.

4.23 Långharsholmen Island

N62°28'13.9"/E017°28'05.2"

A key locality for understanding the geology of the northern area (Fig. 4.33). Here, a banded sövite-pyroxenite suite is intruded by a younger ijolite (Fig. 4.35) forming a copula-shaped intrusion. Within the main intrusion to the south, ijolites are older than the sövites and are intruded by them, as well as by nepheline syenites. Accordingly, here we have field evidence that indicates the Northern Ring Complex, to predate the main complex at Alnö Island.

From here, you can either continue by boat or on foot to Stugholmen (stop 24 in Fig. 4.33. The water between the islands is very shallow at highest water mark, but falls dry when water level is low (Fig. 4.36). Walk across the sandy flats towards the coastal outcrop on the western shore of Stugholmen skerries i.e. to the North of your position (Fig. 4.37).

4.24 Skerries North-West of Långharsholmen Island

N62°28'26.0"/E017°27'58.2"

On the way, pass a beautiful outcrops with flow-banded sövite with boudinage of relatively competent pyroxenite, commonly altered (Fig. 4.37).

Continue towards Stugholmen (Swedish "stuga" = cottage, "holmen" = the islet) and walk to the outcrop along the shore farthest to the west of the cottage.

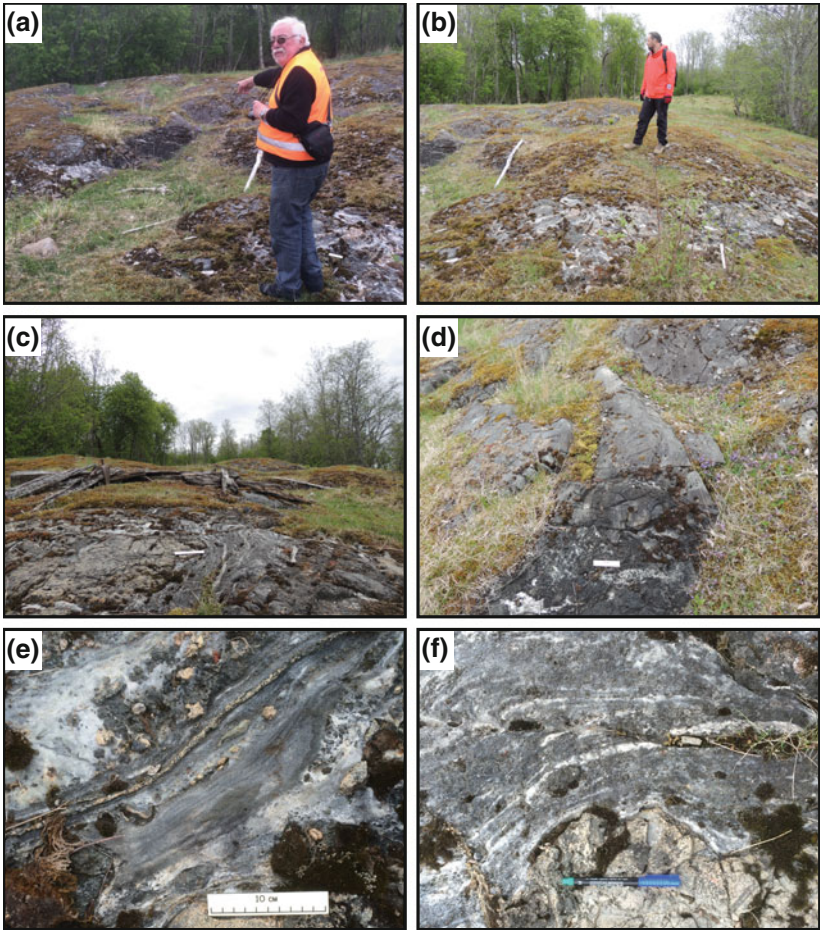

Fig. 4.35 Contact between sövite and later intrusion of ijolite can be inspected on small "whaleback" cupola (a, b), indicating the older age of the Northern Ring complex

4.25 Stugholmen (a.k.a. Finnbergens Skär)

N62°28′28.5″/E017°28′05.4″

Flow-banded sövite and some layers of pyroxenite. Within the sövite, "blebs" or "bubbles" occur that resemble sövite pegmatites. However, these "bubbles" appear

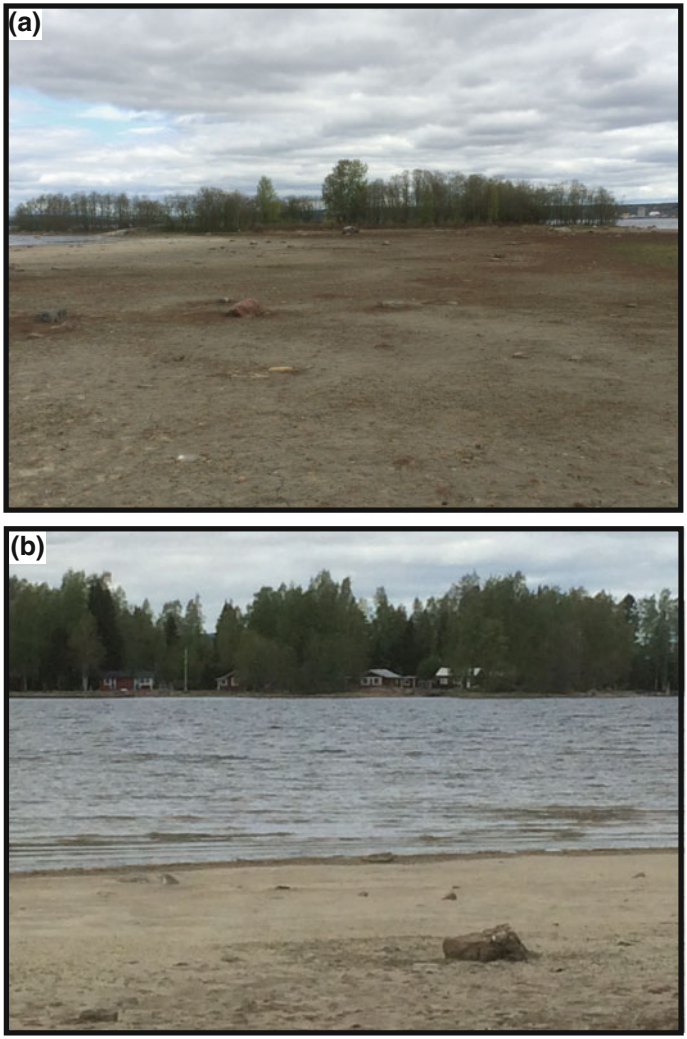

Fig. 4.36 Walk on sandy ground to the next outcrop, which is on Stugholmen, a little north of your current position

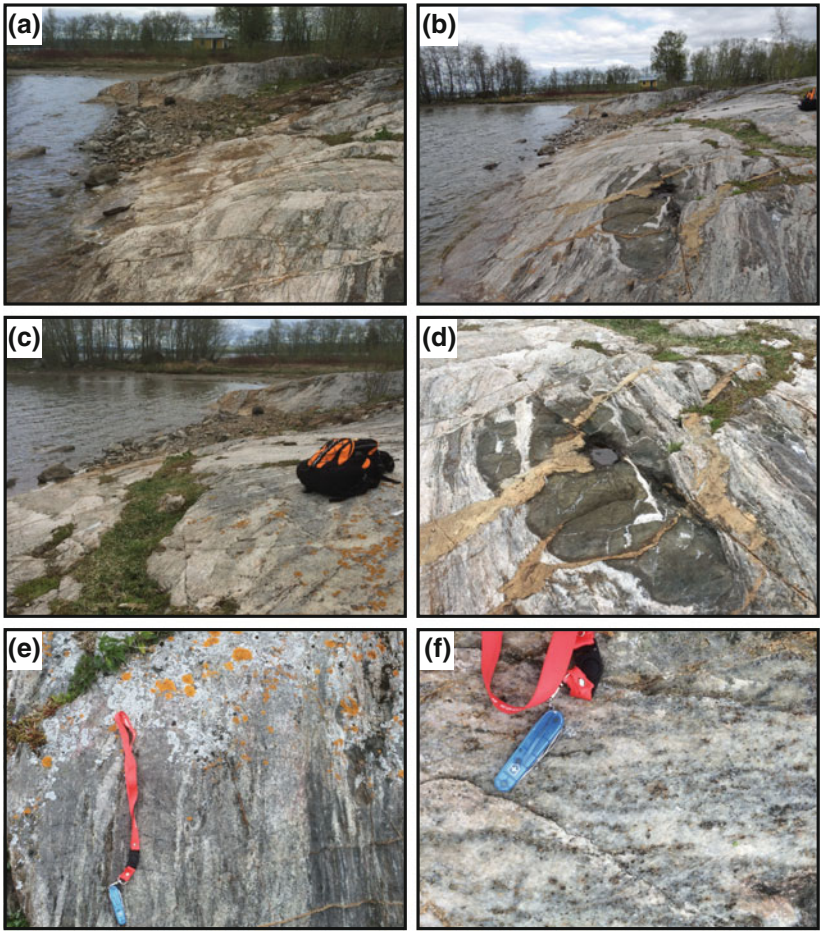

Fig. 4.37 Stugholmen outcrops at locality 24 in Fig 4.33. Flow-banded sövite with various mafic inclusions can be inspected here. From here walk toward the cottage (stuga) for more sövite exposures

to have formed by recrystallization of sövite, most likely during hydrothermal conditions. Calcite had grown radially from a central nucleus, pushing the melanocratic minerals (mainly pyroxene) to the borders of the "bubbles". Various stages of this process can be seen (Fig. 4.38).

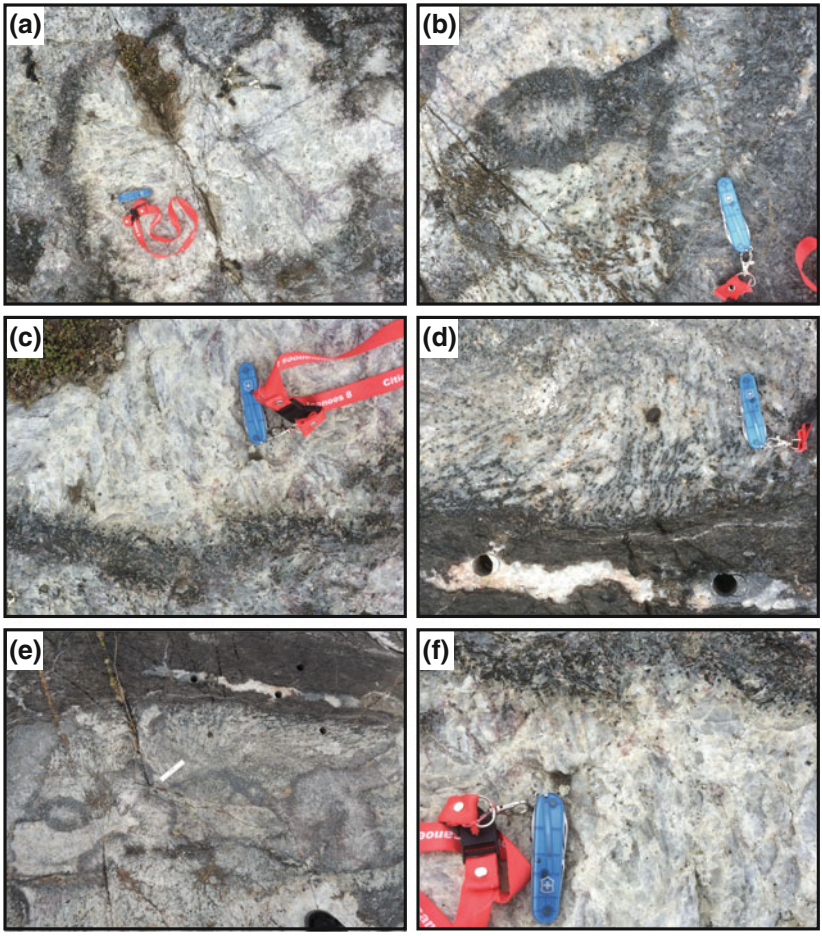

Fig. 4.38 On Stugholmen coarsely crystalline sövite pegmatite is exposed (see text for details)

4.26 North of cottage on Stugholmen

N62°28'30.7"/E017°27'57.6"

Walking along the northern shore towards the cottage, you may find local boulders of sövites may contain perovskite minerals (brownish to black cubes). North of the

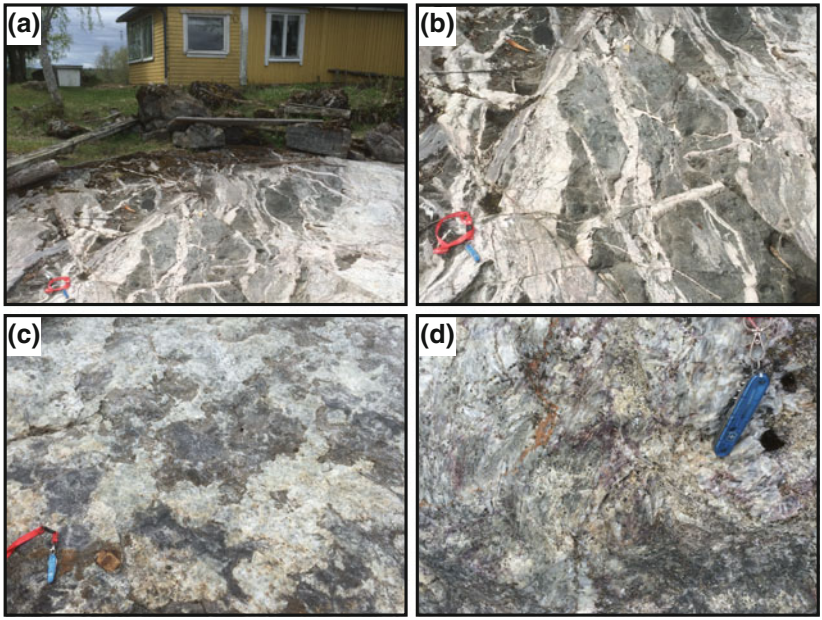

Fig. 4.39 On Stugholmen heavily veined and partly re-crystallized sövite is seen at the landing site behind the cottage

cottage (Fig. 4.39), at the anchoring site, again flow-banded sövite with pyroxenite is exposed. On closer inspection, you may find greenish stringers rich in apatite containing highly radioactive fersmite.

From here, return to your boat and make your way to the Sälkär skerries (stop 27 in Fig. 4.33).

4.27 Sälskär Skerries

Västra Sälskär N62°28'36.1"/E017°27'02.4"
Östra Sälskär N62°28'34.6"/E017°27'06.7"

Between the two skerries there is a large boulder of the Sälskär breccia (Fig. 4.40), with smaller boulders being found mainly on the western skerry. The Sälskär breccias is composed of agglutinated concretional lapilli of melilitite. The lapilli range in size between barely one millimetre to about 4 cm, around cores of olivine

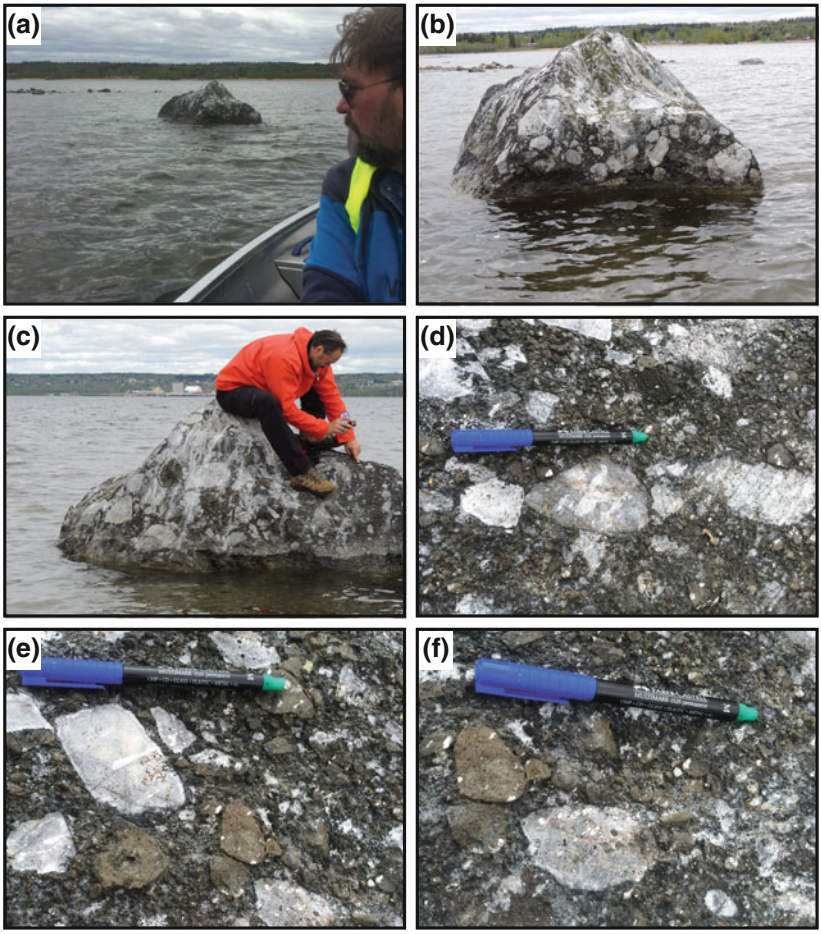

Fig. 4.40 Boulders of Sälskär breccia are found between and on the two Sälskär skerries. The breccia was first described by H.von Eckermann and indicates a carbonatite vent in this area (see text for details)

or magnetite. The breccias also contains fragments of sövite originating from to the Northern Ring Complex (i.e., carrying perovskite-type minerals). The matrix of the breccias is classified as carbonatite, with calcite, apatite, mica, and pyrochlore. The matrix constitutes 10–20 vol.% of the rock (Fig. 4.40). The boulders were apparently shifted into this position by sea ice in the 1930s and were reported by

locals to Harry von Eckermann, who first investigated them. The rock is characteristic of a vent-fill in diatreme-type conduits and the rocks marks the likely existence of such a vent here (Fig. 4.40).

The Sälskär breccias would then represent a funnel-shaped carbonatite explosive vent, according to magnetometry measuring about 1.5 × 2 km at the surface, tapering downwards, with a depth exceeding 700 m. During a very dry summer in 1976, when it was possible to walk to the skerries, Peter Kresten found an apparent contact between the breccias and a fine-grained melilitite. The latter showed a distinct erosion pattern (like sand-blasting) at the contact.

On the western skerry next to the large isolated breccia boulder (Fig. 4.41), flow-layered sövite (carrying perovskite) alternating with pyroxenite is found, the latter is sometimes boudinaged.

End of route 4.

Route 5: Söråker

In addition to outcrops on Alnö or in the direct vicinity of Alnö, one outcrop beyond Alnö Island is recommended showing the Söråker intrusion on the mainland north of Alnö (Fig. 4.42). To get there drive north on the E4 from Sundsvall and leave the E4 at exit 235 towards Söråker. Drive towards Söråker and after a few kilometers, turn right towards "Strand". At the next T-junction, drive on "Söråkersgatan" down to the sea, passing the Pacwire factory. Then, follow "Båthamnsgatan" along the shore. After 350 m, stop at a bicycle track (left hand). On the slope, several boulders of uncompahgrite are found. After another 70 m, there is a rather low outcrop on the left hand side of the road, in front of a larger private house, just before "Nya Söråkersgatan".

4.28 The Söråker Intrusion

N62°30'04.5"/E017°30'00.2"

The Söråker intrusion is a satellite intrusion to the Alnö main complex and it is likely an early manifestation of magmatism in the area. If this is correct, then a N-S migration of igneous activity within the Alnö-complex may be indicated: Söråker—Northern Ring Complex—main intrusion on Alnö Island. However, this supposition will have to wait future radiometric dating to be finally confirmed.

The characteristic plutonic rock here is uncompahgrite which consists of coarse melilite with diopsidic pyroxene, pyrrhotite, melanite garnet, and apatite (Fig. 4.43). Locally, sövite pockets are present also (Fig. 4.44). The uncompahgrite is

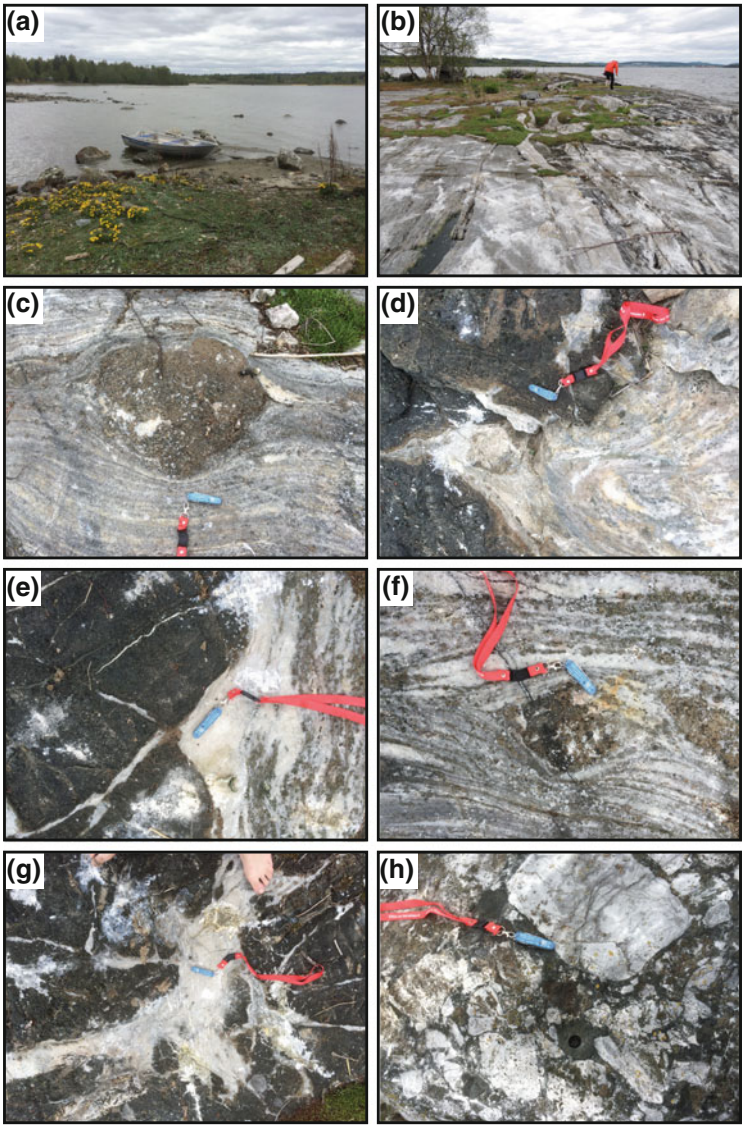

Fig. 4.41 The Sälskär skerries (locality 27 in Fig. 4.33), show sövite with inclusions (**d**-**h**) and boulders of Sälskär breccia (**h**)

Fig. 4.42 Drive from Alnö to Söråker to inspect the Söråker intrusion (locality 4.28)

undersaturated in silica, but strictly speaking not alkaline, although small pockets with nepheline-bearing material have been observed. In the Söråker area, only scarce outcrops of sövite are found, showing peculiar sövite types (calcite, idiomorphic melanite garnet, and apatite) or fine-grained rocks entirely composed of phlogopite and garnet. A characteristic feature is that Söråker garnets have relatively high zirconium contents (i.e., the kimzeyite molecule), distinguishing them from all other garnets found in the Alnö-Sundsvall area. If you intend to take a sample, the slope at the newly cleared bicycle track is recommended (Fig. 4.44).

Farther to the south-east, some outcrops of fenite exist if you are interested and have the time. Also, along the shore, boulders of apatite- and wollastonite-rich rocks as well as alnöite boulders and boulders of fenites can be found.

End of route 5.

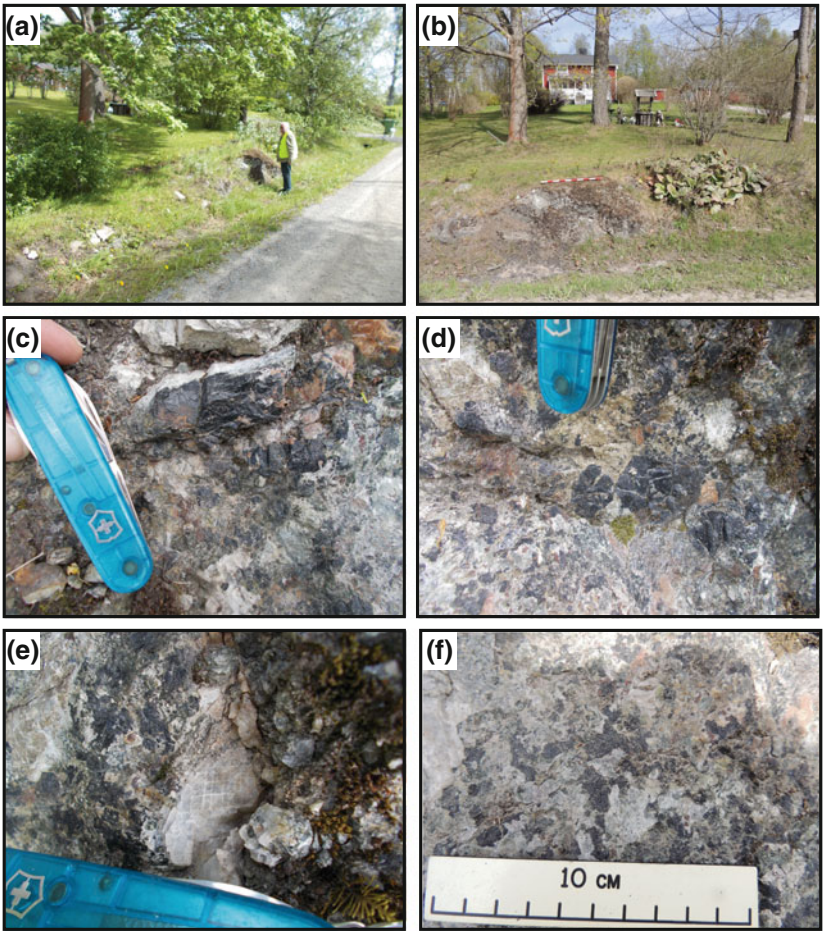

Fig. 4.43 Söråker intrusion on the mainland NE of Alnö Island. The characteristic plutonic rock here is uncompahgrite, which consists of coarse melilite with diopsidic pyroxene, pyrrhotite, melanite garnet, and apatite. Locally, pockets of sövite are present

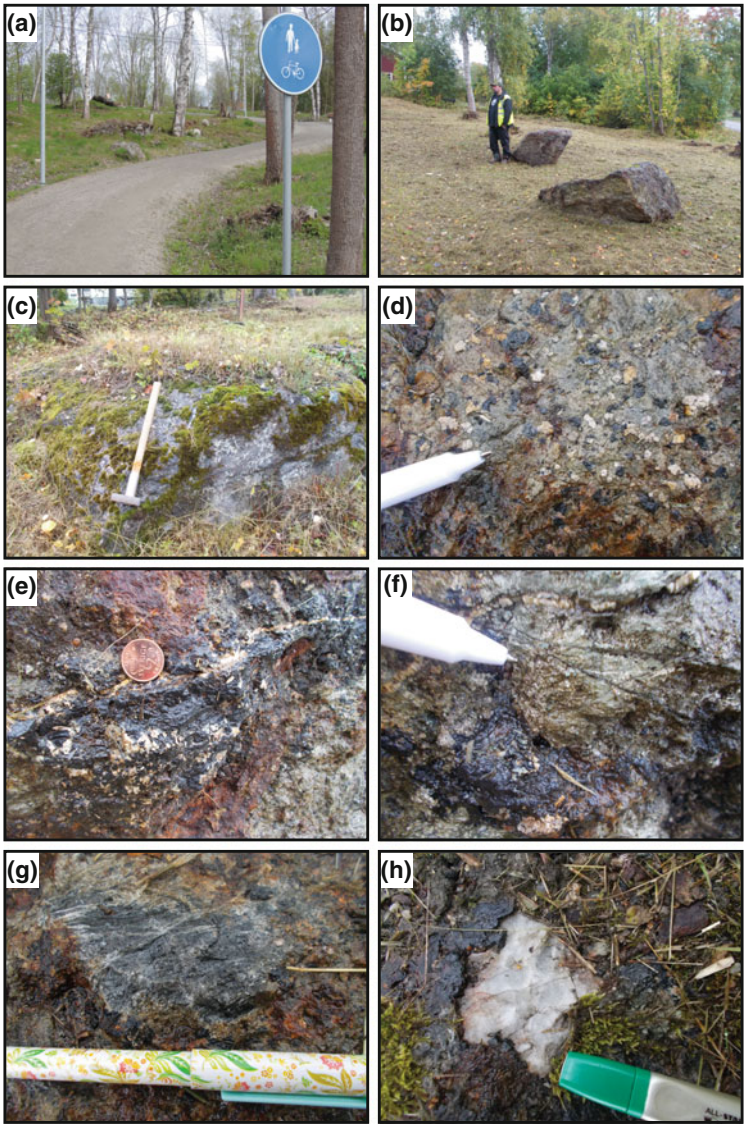

Fig. 4.44 Some small outcrops and a series of local boulders in the new bicycle track give some further insight. Here coarse plutonic assemblages of nepheline (**d**), garnet (**e**), wollastonite (**f**, **g**) and calcite (**h**) are exposed

References

Andersson M, Almqvist B, Burchardt S, Troll V, Malehmir A, Snowball I and Kübler L (2016) Magma transport in sheet intrusions of the Alnö carbonatite complex, central Sweden. Sci Rep 6: 27635

Hisinger W (1808) Samling till en mineralogisk geografi öfver Sverige. H. A Nordström, Stockholm

Lundbohm H (1899) Berggrunden inom Vesternorrlands Län. Sver Geol Unders C 177, 26 31, 47 48

Törnebohm AE (1883) Mikroskopiska bergartsstudier; XVIII Melilitbasalt från Alnö. GFF 76:240–251

von Eckermann H., (1960) Borengite. A new ultra potassic rock from Alnö island. Arkiv Mineral. Geol. 2(39):519–528

von Eckermann H (1948) The alkaline district of Alnö Island. Sver Geol Unders Ca 36:176

Appendix

Table A.1 Examples of dated carbonatite ring-complexes

Complex	Location	Characteristics	References
Alnö	Sweden	The Alnö complex has been dated at circa 546–584 Ma and has a circular shape with a diameter of about 4 km	(Downes et al. 2005; Brueckner and Rex 1980)
Alto Paranaïba Province	Brazil	The complexes in Paranaiba province were emplaced between 79 Ma and 88 Ma. These carbonatites occur as massive cores (plugs, stocks) usually displaying oval to circular outlines	(Gomes et al. 1990; Eby and Mariano 1992)
Amambay Alkaline Province (Cerro Sarambí, Cerro Chiriguelo)	Paraguay	Amambay Alkaline Province was emplaced between 111 and 126 Ma and is located in the northeastern region of Eastern Paraguay at the border with Brazil (South Mato Grosso State) and is made up of elliptical carbonatite-ring complexes (Cerro Sarambí and Cerro Chiriguelo). This magmatic activity is believed to have formed during the initial stages of rifting between Africa and South America in Early Cretaceous times	(Commin-Chiaramonti et al. 1999; Gomes et al. 2011)
Amba Dongar	India	The Amba Dongar intruded the Bagh limestones and sandstones of Cretaceous age, as well as the Deccan basalts and the Precambrian Dharwar basement circa 68 Ma ago and forms concentric ring dikes of calcite carbonatite and carbonatite breccias	(Simonetti et al. 1995; Kumar et al. 1996; Ray 2003; Ray and Shukla 2004)
Bingo complex	Democratic Republic of Congo	The Bingo complex has an age of approximately 516 Ma and shows a vague horse-shoe shape open to the south. It is an intrusive complex of carbonatite, ijolite and nepheline syenite	(Woolley et al. 1995)

(continued)

P. Kresten and V. R. Troll, *The Alnö Carbonatite Complex, Central Sweden*, GeoGuide, https://doi.org/10.1007/978-3-319-90224-1

Table A.1 (continued)

Complex	Location	Characteristics	References
		of about 6 × 4 km emplaced into Precambrian orthogneisses	
Chilwa Island carbonatite complex	Malawi	The Chilwa Island carbonatite complex has been intruded at ca 120 Ma and has an oval vent (230 × 260 m) containing calcitic and dolomitic carbonatite and breccia, rimmed by zones of fenitized country rocks	(Simonetti and Bell 1994; Eby et al. 1995)
Dicker Willem	Southwest Namibia	The 5 km^2 Dicker Willem complex, of Eocene age (49 Ma), is a circular subvolcanic intrusion consisting almost exclusively of carbonatite. Rock types range from early nepheline sövites through sövite and dolomite alvikite to late-stage ferroan carbonatites. The complex is emplaced into high-grade gneisses of the Mid-Proterozoic Namaqua Province	(Reid and Cooper 1992; Cooper and Reid 1998)
Fen	Telemark, SE Norway	The Fen complex intruded Proterozoic gneisses and has a Cambrian age (540–560 Ma). It has a circular shape and is the type locality for fenite. In the Fen complex peralkaline calcite carbonatite (pyroxene sövite) is associated with nepheline syenite, alkali pyroxenite and rocks of the melteigite-ijolite-urtite series	(Kresten and Morogan 1986; Andersen and Taylor 1988; Andersen 1989)
Fuerteventura	Spain	The emplacement at 25 Ma, was related to an extensional tectonic event. The Fuerteventura carbonatites, form three semi-circular plutonic ultra-alkaline complexes in the Esquinzo, Ajuy-Solapa and Punta del Peñón Blanco areas. The basal complex of Fuerteventura also contains ultra-alkaline pyroxenite, syenites and carbonatite dykes. Carbonatite dykes have also been found in the metamorphic aureoles and in anatexite	(Demény et al. 2004; Ahijado et al. 2005; Casillas et al. 2011)

(continued)

Table A.1 (continued)

Complex	Location	Characteristics	References
Goudini complex	South Africa	The Goudini carbonatite complex has been dated to an age of 1190 Ma and is oval in outline, approximately 5.5 × 4.5 km in size, Goudini represents an eroded volcano structure containing pyroclastic rocks and lavas. It has an overall concentric shape	(Harmer and Gittins 1997; Verwoerd 2008)
Lueshe complex	Democratic Republic of Congo	The Lueshe carbonatite complex shows an age of about 516 Ma and has a oval shape, about 3 × 2 km in size. It is located in the NE of the Democratic Republic of Congo. This complex is an alkaline plutonic massif emplaced in a metamorphozed basement consisting of micaschists, quartzites and amphibolites of Burundian age	(Meyer and Béthune 1960; Maravic and Morteani 1980; Maravic et al. 1989; Nasraoui et al. 2000)
Oka carbonatite complex	Quebec, Canada	The Oka complex has been dated at circa 110 Ma and is a double-ring structure with an oval outline, 7 × 2.5 km, with the major axis trending northwest. It is intrusive into a Precambrian inlier which consists of gneisses and anorthosites of the Grenville structural province. The oval-shaped carbonatite core is enclosed by crescentic tabular masses and a ring-dyke of ultramafic alkalic rocks	(Treiman and Essene 1985; Shafiqullah et al. 1970; Wen et al. 1987; Cox et al. 2006)
Panda Hill complex	Tanzania	The Panda Hill carbonatite complex has been dated at 116 Ma and is situated near the southwestern flank of the Rukwa Trough in southwestern Tanzania. It comprises a carbonatite body, a fenite aureole and feldspathic agglomerate and breccia. The complex is about 2.5 km in diameter and consists of an outer ring and a central plug	(Basu and Mayila 1986; Bell and Blenkinsop 1987)
Phalaborwa (Palabora) complex	South Africa	The Phalaborwa complex has been dated at an age of 2047 Ma and intruded an Archaean terrain of granites, gneisses, quartzites, granulites, amphibolites, and talc and serpentine schists. The main complex is an elongate irregularly-shaped pipe-like body with a known vertical extent, based on gravity data, of ~5 km	(Eriksson 1984 Groves and Vielreicher 2001)

(continued)

Table A.1 (continued)

Complex	Location	Characteristics	References
Salmagorskii ring igneous complex	Kola Peninsula, NW Russia	The age of the Salmagorskii intrusion is estimated to be 375 Ma. The Salmagorskii Ring complex forms a concentrically zoned, pipe-like intrusion in which ultramafic rocks (dunite or clinopyroxenite) occupy the central parts of the complex and melilitolites and foidolites surround the former	(Korobeinikov et al. 1998)
Salpeterkop	South Africa	An age of 66 Ma has been estimated for the Salpeterkop complex. It forms part of a dome with radial fractures extending to a distance of at least 16 km and forms an almost perfectly circular outline. The main rock types are carbonatite, trachyte and olivine melilitite.	(Verwoerd 1990; Verwoerd et al. 1995)
Sokli carbonatite complex	Eastern Lapland, Finland	The carbonatite body has been dated to 380–360 Ma and is a circular, cone-shaped structure and covers an area of about 20 km^2. The complex consists mainly of sövite and is surrounded by a fenitized aureole	(Paarma 1970; Vartiainen and Paarma 1979; Kramm et al. 1993)
Spitskop complex	South Africa	Spitskop Complex is of Proterozoic age (1400–1200 Ma) and represents a classic alkaline ring complex, some 5 km across, composed of successive intrusions of pyroxenite, ijolite, nepheline syenite, and carbonatite	(Harmer 1999; Ionov and Harmer 2002)
Sukulu, Tororo, Bukusu, Napak, and Toror	Uganda	The Sukulu carbonatite complex has been dated at 45 Ma and is the most southerly of a line of Tertiary carbonatites in southeast Uganda, i.e. Tororo, Bukusu, Napak and Toror. It forms a circular group of hills, some 4 km across, and comprises carbonatite, ijolite and an aureole of fenites	(King 1965; Bell and Powell 1970; Ting et al. 1994)
Sung Valley Alkaline-carbonatite complex	Shillong Plateau, NE India	An age of 115 Ma has been obtained from the Sung Valley carbonatite complex and has been dated to the youngest member of the complex. The complex occurs as small dykes, veins and oval shaped intrusive carbonatite bodies	(Gupta and Sen 1988; Srivastava et al. 2005)

(continued)

Table A.1 (continued)

Complex	Location	Characteristics	References
Tchivira Catanda, Monte Verde-Sulima, Coola, Bailundo, Longojo, Virulundo, and Lupongola complexes	Angola	The Early Cretaceous (138–130 Ma) carbonatites and associated alkaline rocks of Angola belong to the Paraná-Angola-Etendeka Province and occur as ring complexes and other central-type intrusions along northeast trending tectonic lineaments, parallel to the trend of coeval Namibian alkaline complexes. The Tchivira Complex is a ring structure more than 12 km in diameter, centred approximately on the Tchivira peak (2365 m)	(Issa-Filho et al. 1991; Alberti et al. 1999; Melgarejo et al. 2012)
Tundulu	Malawi	The Tundulu carbonatite complex in southeastern Malawi was intruded during the late Jurassic to early Cretaceous over three episodes. The carbonatite comprises three ring structures, each belonging to a separate intrusive phase. The entire complex has a diameter of about 2 km	(Ngwenya 1994)

Table A.2 X-ray diffraction patterns of "type I knopite", Holmquist's original collection. Guinier-Hägg camera, monochromatic Cu Kα radiation

PJH-1	PJH-2	PJH-3	PJH-4	PJH-5	I	Phase, *d* (I)
		4.94	4.944	4.934	1	ti 4.93 (3)
				4.813	3	
				4.535	1	
	3.534	3.523	3.524	3.522	10	an 3.52 (10)
		3.298		3.3	8	
			3.241	3.248	2	ti 3.233 (10)
	3.034	3.034				
		2.999	2.999	3	2	ti 2.989 (9)
		2.955		2.958	1	
2.74	2.741					il 2.74 (10)
2.717	2.718		2.724			pv 2.719 (4)
	2.699					pv 2.701(10)
		2.613	2.613	2.615	5	
				2.596	1	ti 2.595 (9)
				2.533	2	il 2.54 (9)
			2.432	2.436	1	an 2.431 (1)
			2.381	2.383	1	an 2.378 (2)
			2.335	2.334	2	an 2.332 (1)
	2.311					pv 2.313 (1)
			2.285	2.296	1	ti 2.273 (3)
	2.227					pv .217(1),il
	2.203					pv 2.201 (4)
	2.127					ti 2.101 (2)
				2.05	3	ti 2.058 (4)
	1.912					pv 1.911 (5)
			1.896	1.896	2	an 1.892 (3)
			1.875			il 1.86 (9)
				1.77	2	il 1.72 (10)
			1.703	1.702	1	an 1.700 (2)
			1.67	1.669	2	an 1.667 (2)
			1.645			i 1.643 (4)
				1.614	1	il 1.63 (5)

(1) and 12 weak reflections between d = 1.580 and 1.027 Å.
(2) and 6 weak reflections between d = 1.495 and 1.168 Å.
(3) and 8 weak reflections between d = 1.512 and 1.266 Å.
an = anatase ASTM 21-1272, il = ilmenite ASTM 3-0781, pv = perovskite ASTM 22-153, ti = titanite ASTM 11-142.

References

Ahijado A, Casillas R, Nagy G, Fernández C (2005) Sr-rich minerals in a carbonatite skarn, Fuerteventura, Canary Islands (Spain). Mineral Petrol 84:107–127

Alberti A, Castorina F, Censi P, Comin-Chiaramonti P, Gomes CB (1999) Geochemical characteristics of Cretaceous carbonatites from Angola. J Afr Earth Sci 29:735–759

Andersen T, Taylor PN (1988) Pb isotope geochemistry of the Fen carbonatite complex, S.E. Norway: age and petrogenetic implications. Geochimica et Cosmochimica Acta 52:209–215

Andersen T (1989) Carbonatite-related contact metasomatism in the Fen complex, Norway: effects and petrogenetic implications. Mineral Mag 53:395–414

Basu NK, Mayila A (1986) Petrographic and chemical characteristics of Panda Hill carbonatite complex, Tanzania. J S Afr Earth Sci 5:589–598

Bell K, Blenkinsop J (1987) Nd and Sr isotopic compositions of East African carbonatites: implications for mantle heterogeneity. Geology 15:99–102

Bell K, Powell JL (1970) Strontium isotopic studies of Alkalic rocks: the alkalic complexes of Eastern Uganda. Geol Soc Am Bull 81:3481–3490

Brueckner HK, Rex DC (1980) K–Ar and Rb–Sr geochronology and Sr isotopic study of the Alnö alkaline complex, northeastern Sweden. Lithos 13:111–119

Casillas R, Demény A, Nagy G, Ahijado A, Fernández C (2011) Metacarbonatites in the Basal Complex of Fuerteventura (Canary Islands). The role of fluid/rock interactions during contact metamorphism and anatexis. Lithos 125:503–520

Conmin-Chiaramonti P, Cundari A, DeGraff JM, Gomes CB, Piccirillo EM (1999) Early Cretaceous-Tertiary magmatism in Eastern Paraguay (western Praná basin): geological, geophysical and geochemical relationships. J Geodyn 28:375–391

Cooper AF, Reid DL (1998) Nepheline Sövites as parental magmas in carbonatite complexes: evidence from Dicker Willem, Southwest Namibia. J Petrol 39:2123–2136

Cox RA, Wilton DHC (2006) U–Pb dating of perovskite by LA-ICP-MS: An example from the Oka carbonatite, Quebec, Canada. Chem Geol 235:21–32

Demény A, Vennemann TW, Ahijado A, Casillas R (2004) Oxygen isotope thermometry in carbonatites, Fuerteventura, Canary Islands, Spain. Mineral Petrol 80:155–172

Downes H, Balaganskaya E, Beard A, Liferovich R, Demaiffe D (2005) Petrogenetic processes in the ultramafic, alkaline and carbonatitic magmatism in the Kola Alkaline Province: a review. Lithos 85:48–75

Eby GN, Mariano AN (1992) Geology and geochronology of carbonatites and associated alkaline rocks peripheral to the Paraná Basin, Brazil-Paraguay. J S Am Earth Sci 6:207–216

Eby GN et al (1995) Geochronology and cooling history of the northern part of the Chilwa Alkaline Province, Malawi. J Afr Earth Sci 20:275–288

Eriksson SC (1984) Age of carbonatite and phoscorite magmatism of the Phalaborwa complex (South Africa). Isotope Geosci 2:291–299

Gomes CB, Ruberti E, Morbidelli L (1990) Carbonatite complexes from Brazil: a review. J S Am Earth Sci 3:51–63

Gomes CB, Velázquez VF, Azzone RG, Paula GS (2011) Alkaline magmatism in the Amambay area, NE Paraguay: the Cerro Sarambí complex. J S Am Earth Sci 32:75–95

Groves D, Vielreicher NM (2001) The Phalaborwa (Palabora) carbonatite-hosted magnetitecopper sulfide deposit, South Africa: an end-member of the iron-oxide copper-gold-rare earth element deposit group? Mineralium Deposita 36:189–194

Gupta RP, Sen AK (1988) Imprints of the Ninety-East Ridge in the Shillong Plateau, Indian Shield. Tectonophysics 154:335–341

Harmer RE (1999) The petrogenetic association of carbonatite and alkaline magmatism: constraints from the Spitskop complex, South Africa. J Petrol 40:525–548

Harmer RE, Gittins J (1997) The origin of dolomitic carbonatites: field and experimental constraints. J Afr Earth Sci 25:5–28

Ionov D, Harmer RE (2002) Trace element distribution in calcite-dolomite carbonatites from Spitskop: inferences for differentiation of carbonatite magmas and the origin of carbonates in mantle xenoliths. Earth Planet Sci Lett 198:495–510

Issa-Filho A, Dos Santos ABRMD, Riffel BF, Lapido-Loureiro FEV, McReath I (1991) Aspects of the geology, petrology and chemistry of some Angolan carbonatites. J Geochem Explor 40:205–226

King BC (1965) Petrogenesis of the Alkaline igneous rock suites of the volcanic and intrusive centres of eastern Uganda. J Petrol 6:67–100

Korobeinikov AN et al (1998) Geology and copper sulphide mineralization of the Salmagorskii Ring Igneous complex, Kola Peninsula, NW Russia. J Petrol 39:2033–2041

Kresten P, Morogan V (1986) Fenitization at the Fen complex, southern Norway. Lithos 19:27–42

Kumar D, Mamallan R, Dqivedy KK (1996) Carbonatite magmatism in northeast India. J Southeast Asian Earth Sci 13:145–158

Maravic H, Morteani G (1980) Petrology and geochemistry of the carbonatite and syenite complex of Lueshe (N.E. Zaire). Lithos 13:159–170

Maravic H, Morteani G, Roethe G (1989) The cancrinite-syenite/carbonatite complex of Lueshe, Kivu/NE-Zaire: petrographic and geochemical studies and its economic significance. J Afr Earth Sci 9:341–355

Melgarejo JC, Costanzo A, Bambi ACJM, Goncalves AO, Neto AB (2012) Subsolidus processes as a key factor on the distribution of Nb species in plutonic carbonatites: the Tchivira case. Lithos, Angola. https://doi.org/10.1016/j.lithos.2012.06.024. in press

Meyer A, de Béthune P (1960) The Lueshe carbonatite (Kivu, Belgian Congo). International Geological Congress, XXI Session, Norden (Part XIII, Petrographic Provinces, Igneous and Metamorphic Rocks), pp 304–309

Nasraoui M, Toulkeridis T, Clauser N, Bilal E (2000) Differentiated hydrothermal and meteoric alterations of the Lueshe carbonatite complex (Democratic Republic of Congo) identified by a REE study combined with a sequential acid-leaching experiment. Chem Geol 165:109–132

Ngwenya BT (1994) Hydrothermal rare earth mineralization in carbonatites of the Tundulu complex, Malawi: processes at fluid/rock interface. Geochimica et Cosmochimica Acta 58:2061–2072

Paarma H (1970) A new find of carbonatite in the north Finland, the Sokli plug in Savukoski. Lithos 3:129–133

Ray JS, Shukla PN (2004) Trace element geochemistry of Amba Dongar carbonatite. Earth Planet Sci 113:519–531

Ray JS (2003) Evolution of Amba Dongar carbonatite complex: Constraints from 40Ar–39Ar chronologies of the Inner Basalt and an alkaline plug. Int Geol Rev 45:857–862

Reid DL, Cooper AF (1992) Oxygen and carbon isotope patterns in the Dicker Willem carbonatite complex, southern Namibia. Chem Geol (Isotope Geosci Section) 94:293–305

Shafiqullah M, Tupper WM, Cole TJS (1970) K–Ar age of the carbonatite complex, Oka, Quebec. Can Mineral 10:541–552

Simonetti A, Bell K (1994) Isotopic and geochemical investigation of the Chilwa Island carbonatite complex, Malawi: evidence for a depleted mantle source region, liquid immiscibility, and open-system behaviour. J Petrol 35:1597–1621

Simonetti A, Bell K, Viladkar SG (1995) Isotopic data from the Amba Dongar Carbonatite complex, west-central India: evidence for an enriched mantle source. Chem Geol (Isotope Geosci Section) 122:185–198

Srivastava RK, Heaman LM, Sinha AK, Shihua S (2005) Emplacement age and isotope geochemistry of Sung Valley Alkaline-carbonatite complex, Shillong Plateau, northeastern India: implications for primary carbonate melt and genesis of the associated silicate rocks. Lithos 81:33–54

Ting W, Rankin AH, Woolley AR (1994) Petrogenetic significance of solid carbonate inclusions in apatite of the Sukulu carbonatite, Uganda. Lithos 31:177–187

Treiman AH, Essene EJ (1985) The Oka carbonatite complex, Quebec: geology and evidence for silicate-carbonate liquid immiscibility. Am Mineral 70:1101–1113

Vartiainen H, Paarma H (1979) Geological characteristics of the Sokli Carbonatite complex, Finland. Econ Geol 74:1296–1306

Verwoerd WJ (2008) The Goudini carbonatite complex, South Africa: are-appraisal. Can Mineral 46:825–830

Verwoerd WJ (1990) The Salpeterkop ring structure, Cape Province, South Africa. Tectonophysics 171:275–285

Verwoerd WJ, Vilkoen EA, Chevallier L (1995) Rare metal mineralization at the Salpeterkop carbonatite complex, Western Cape Province, South Africa. J Afr Earth Sci 21:171–186

Wen J, Bell K, Blenkisop J (1987) Nd and Sr isotope systematics of the Oka complex, Quebec, and their bearing on the evolution of the sub-continental upper mantle. Contrib Mineral Petrol 97:433–437

Woolley AR, Williams CT, Wall F, Garcia D, Moute J (1995) The Bingo carbonatite-ijolitenepheline syenite complex, Zaire: geology, petrography, mineralogy and petrochemistry. J Afr Earth Sci 21:329–348

Glossary

Accretionary lapilli are like volcanic hailstones that form by the addition of concentric layers of ash around a central nucleus (e.g. a crystallized mineral).

Alkaline rocks are rocks in which the chemical content of the alkaline elements (potassium, sodium and calcium oxide) is greater than the atomic amount of aluminium (e.g. high A/CNK ratio), leading to the formation of alkaline minerals.

Alnöite is an intrusive ultramafic, igneous rock, distinctive in possessing primary calcite, melilite, phlogopite, pyroxene, and olivine.

Alnöite breccia is an alnöite dyke or pipe rock with abundant xenoliths of various types.

Alvikite is a fine-grained calcite carbonatite dyke.

Anorogenic magmatism is the formation, intrusion or eruption of magmas in settings other than convergent plate margins and orogeny.

Aphanitic describes a fine-grained igneous rock that has such a compact texture that the constituent minerals cannot be resolved with the naked eye.

Autolith is a fragment of a previously crystallized portion of rock enclosed in the same magma from which it formerly solidified.

Aureole is a region in which country rocks surrounding an igneous intrusion have been recrystallized or otherwise reacted in response to the heat and fluids supplied by the intrusion.

P. Kresten and V. R. Troll, *The Alnö Carbonatite Complex, Central Sweden*, GeoGuide, https://doi.org/10.1007/978-3-319-90224-1

Banded structure describes a rock texture characterized by an arrangement of usually different minerals or mineral proportions in layers that appear as bands in outcrop or thin section.

Beforsite is a carbonatite dyke rock dominated by dolomite.

Borengite is an alkaline trachyte that may comprise alkali-feldspar and occasional fluorite. It is one of the most potassium-rich rocks that are known.

Botryoidal texture is derived from Greek and is one in which a mineral or rock has a globular external form resembling a bunch of grapes. This is a common form for hematite, goethite, smithsonite, fluorite and malachite.

Boulder is a large block of rock that typically has been smoothened by erosion or glacial action.

Caldera volcano is a large cauldron-like volcanic depression that forms following the evacuation of a magma chamber/reservoir.

Carbonatite is an intrusive or extrusive igneous rock defined by mineralogical composition to consist of $\geq 50\%$ of carbonate minerals. It is relatively rare amongst igneous rocks in general.

Coarse grained rocks have a grain size of >5 mm across.

Cone sheet(s) are a type of high-level igneous sheet intrusion found in partly eroded central volcanic complexes. Cone sheets or cone sheet swarms, typically show the overall geometry of an "inverted cone" (i.e. they are "inward dipping").

Continental crust is the solid outermost layer of the Earth that forms the major continental masses. It is lying above the upper mantle and is up to ~ 70 km thick.

Dip and strike refers to the orientation or attitude of a geological feature. The strike line of a bed fault, or other planar feature, represents the intersection of that feature with a horizontal plane. The dip gives the steepest angle of descent of a tilted bed or intrusion relative to a horizontal plane, and is given in degree (0°–90°) as well as with a direction (N, S, E, W) in which the bed is dipping downwards.

Dolerite (also called "diabase") is a fine grained dyke or sill of basaltic composition.

Dunite is an igneous plutonic rock, of ultramafic composition (>90% olivine), with coarse-grained texture. It can contain up to $\sim 10\%$ of orthopyroxene or clinopyroxene.

Dyke a subvertical sheet intrusion of magma or sediment usually >45° in dip

Eruptive vent is a volcanic conduit through which lava erupts or erupted onto the Earth's surface.

Fenite is a rock that formed from a metasomatic alteration associated particularly in the aureoles around alkaline or carbonatite intrusions. The ultimate results of fenitization are rocks rich in alkali feldspars.

Fine-grained describes a rock with average grain size ≤ 1 mm (see also coarse-grained).

Gneiss is a rock type formed by high-grade regional metamorphic processes from pre-existing formations that were originally either igneous or sedimentary in nature.

Granite is a felsic intrusive igneous rock that is granular in texture and is usually coarse-grained. It usually carries feldspars mica and quartz.

Greywacke is an immature sediment characterized by poorly sorted angular grains of quartz feldspar, and small rock fragments (lithics) set in a clay-rich matrix

Harzburgite is a mantle-type rock made of dominantly olivine and orthopyroxene. It belongs to the peridotite group of rocks.

Ijolite is an alkaline igneous rock consisting of nepheline and clinopyroxene (augite). Ijolite is often part of anorogenic alkaline igneous complexes and is frequently associated with carbonatites.

Intrusion refers either to the forcing of molten rock into an earlier rock formation or to the rock mass produced by an intrusive process.

Jacupirangite is an alkaline pyroxenite made of the characteristic minerals of titanian augite nepheline, magnetite and melanite garnet.

Kimberlite is an ultramafic K-rich igneous rock which may contain diamond. Its most abundant mineral is olivine. Other minerals include chrome pyrope Cr-diopside, picroilmenite, chromite and phlogopite.

Lapilli are rounded droplets of molten lava ejected during a volcanic eruption. By definition they range from 2 to 64 mm in diameter.

Mafic (mafic = magnesium and iron) is a compositional term that describes magma rocks or minerals that hold high proportions of magnesium and iron. If a rock is labeled "mafic", it usually involves high proportions of the ferromagnesian minerals olivine, pyroxene, biotite, hornblende and low concentrations of feldspar and quartz.

Magma is a mixture of molten rock, volatiles and crystals that is found beneath the surface of the Earth.

Magma chamber or reservoir is a large pool of liquid rock with various amounts of crystals found beneath the surface of the Earth. There, magma may reside temporarily on its way from the upper mantle to the Earth's surface or can solidify to form a pluton.

Magnetic anomaly is a local variation in the Earth's magnetic field resulting from the magnetism of the rocks below. Magmatic rocks often contain the magnetic minerals magnetite, maghemite, ilmenite or pyrrhotite and can therefore show a magnetic anomaly.

Major elements are those elements that are present highly abundant in a rock. About ten major elements compose 95% of the Earth's crust. They are Si, Al, Ca, Mg, Na, K, Ti, Fe, Mn and P.

Mantle is a layer inside a terrestrial planet and some other rocky planetary bodies. The mantle lies between the core and the crust and is made of peridotite-type rocks in case of planet Earth. Frequently a "fertile" lower mantle is distinguished from a "depleted" upper mantle in respect to previous melting events, whereby "depleted" implies that melt was already produced and lost at a previous stage.

Matrix (or groundmass) of a rock is the fine-grained mass of material wherein larger grains crystals or clasts are embedded.

Medium-grained describes a rock with grain sizes between 1 and 5 mm.

Melilitite is a fine-grained dyke rock with predominant (at Alnö >70 vol.%) melilite.

Melilitolite is a coarse-grained mafic plutonic rock containing more than 10% modal melilite and where melilite is more abundant than feldspathoids.

Melteigite is a melanocratic member of the ijolite series and contains between 10 and 30% nepheline and a high proportion of mafic minerals.

Metasediment is a sedimentary rock that has been altered by metamorphism due to e.g. burial and heating or due to reheating close to later magmatic intrusions.

Migmatite is a high grade metamorphic rock that is a mixture of metamorphic and an igneous rock as it contains formerly melted portions.

Minor elements or trace elements are present in a rock at concentrations <1000 ppm (or 0.1 wt%).

Ouachitites are dense dark-coloured ultra-mafic rocks which usually show prominent biotite and abundant augite.

Outcrop is a visible exposure of bedrock or lithified ancient sediment now available on the surface of the Earth.

Paragenesis describes the concept of an equilibrium assemblage of mineral phases that occur in a rock.

Pegmatite is a holocrystalline intrusive igneous rock, usually composed of large interlocking crystals which formed rapidly under fluid-rich conditions.

Petrogenesis describes the combined processes that gave rise to the origin of an igneous or metamorphic rock.

Peridotite is a dense ultramafic, coarse-grained igneous rock consisting mostly of olivine, and pyroxene. Usually, it has less than 45% silica. Peridotite is the most common rock type of the Earth's mantle.

Plastic deformation (or ductile deformation) refers to changes in the shape or size of an object that are occurring at a temperature were the deformed material is no longer brittle. This deformation is usually irreversible.

Plutonic rocks are solidified from a molten rock below the surface of the Earth. They tend to be coarser grained than many eruptive rocks.

Porphyrite is a quartz-free porphyry (crystal-rich rock) whose feldspar is plagioclase or K/Na-feldspar. It may contain matrix quartz, however.

Porphyry is a rock that carries phenocrysts in a fine-grained matrix.

Pyroxenite is an ultramafic igneous rock consisting primarily of minerals from the pyroxene group such as augite, diopside, hypersthene, bronzite or enstatite.

Radial dyke is a vertical to subvertical sheet intrusion which emanates from a central volcanic plug or complex.

Rare earth elements (REE) are a set of seventeen chemical elements in the periodic table specifically the fifteen lanthanides, as well as scandium and yttrium and are widely used in petrogenetic assessment of rocks and minerals. They are frequently divided into light REE (LREE) and heavy REE (HREE).

Recrystallization (solid-state) is a metamorphic process that occurs under temperature and pressure where atoms of a mineral are reorganized by diffusion and/or dislocation glide to produce a new crystal arrangement and association.

Rheomorphism is a metamorphic (or better: metasomatic) process of rock liquefaction (note: not melting) resulting in its flowing or intruding into surrounding rocks. For high-grade fenites, being mainly composed of alkali feldspar and pyroxene, the rock will split into a mobilisate (mainly feldspar) and a restite (mainly pyroxene).

Ring dyke is an intrusive sheet-like igneous body that is circular oval or arcuate in plan and has steep contacts, usually with an overall 'bell-jar' shaped geometry. Ring dykes often enclose sunken caldera blocks.

Satellite intrusion is an off-centre or peripheral intrusion to a larger magmatic complex.

Scintillometer is an instrument used to records radioactivity using photoelectric effects caused in a Na(Tl)-iodide crystal.

Scyelite is a hornblende-rich picrite that can also carry mica.

Sericitisation is the process or state of alteration by which feldspar is converted into sericite (i.e light mica of muscovite and/or paragonite type).

Shear fracture are the cracks in rock materials resulting from shear forces that exceeded the cohesive strength of the rock in that plane.

Silicate rock is a rock formed mainly from silicate minerals.

Silico-carbonatite are carbonatites rocks with 50–70% carbonate minerals and 50–30% silicate minerals.

Sövite is a coarse-grained variety (or facies) of carbonatite usually an intrusive, igneous rock made of >50% carbonate minerals.

Strike line of a bed fault, or other planar feature, is a line representing the intersection of that feature with a horizontal plane (see also dip and strike).

Syenite is a coarse-grained alkaline intrusive (plutonic) igneous rock with a general composition similar to that of granite but deficient in quartz (<5%) and with low contents of intermediate plagioclase.

Trace elements (see "minor elements").

Trachyte is an intermediate volcanic igneous rock with an aphanitic to porphyritic texture and an overall alkaline composition. It is the volcanic equivalent of syenite.

Ultramafic is a term that describes an igneous and meta-igneous rock with a low silica content ≤ 45 wt.% and usually ≥ 90 wt.% of mafic minerals. Generally an ultramafic rock has >18% MgO and is high in FeO, but low in potassium.

Ultramafic nodule is a usually rounded lump of ultramafic rock found in mafic igneous rocks. They are commonly derived from the mantle or lower crust.

Urtite is a coarse-grained igneous rock consisting of nepheline (about 85% of the rock) plus ferromagnesian minerals such as aegirine, aegirine-augite, and possibly soda-iron amphibole.

Volcanic breccia is a volcanic rock composed of broken fragments of minerals or rock cemented together by a fine-grained matrix that can be similar to or different from the composition of the fragments. Volcanic breccias are frequently associated with volcanic vents.

Wehrlite is an ultramafic mantle rock that is composed of olivine and clinopyroxene. It is a subdivision of the compositional spectrum of peridotites.

Xenocryst from ancient Greek "foreign crystal".

Xenolith from ancient Greek "foreign rock". A rock fragment which becomes incorporated in an igneous rock during magmatic evolution and which has not been, or only partly been, digested by the host magma. See also "xenocryst".